HYDRODYNAMICS OF VEGETATIVE CHANNEL WITH DOWNWARD SEEPAGE

A Thesis submitted

In partial fulfillment of the requirements for the degree of

Doctor of Philosophy

Submitted by

Thokchom Bebina Devi

(126104013)

DEPARTMENT OF CIVIL ENGINEERING

INDIAN INSTITUTE OF TECHNOLOGY GUWAHATI,

GUWAHATI-781039, ASSAM

AUGUST, 2016

Declaration of Authorship

I, Thokchom Bebina Devi, declare that this thesis "HYDRODYNAMICS OF VEGETATIVE CHANNEL WITH DOWNWARD SEEPAGE" and the work presented in it are my own and has been generated by me as the result of my own original research

I confirm that:

1. This work was done wholly or mainly while in candidature for a research degree at this University;

2. Where any part of this thesis has previously been submitted for a degree or any other qualification at this University or any other institution, this has been clearly stated;

3. Where I have consulted the published work of others, this is always clearly attributed;

4. Where I have quoted from the work of others, the source is always given. With the exception of such quotations, this thesis is entirely my own work;

5. I have acknowledged all main sources of help;

6. Where the thesis is based on work done by myself jointly with others, I have made clear exactly what was done by others and what I have contributed myself;

Signed: ……

Date: ……

Department of Civil Engineering
Indian Institute of Technology Guwahati
Guwahati-781039, Assam, India

Dr. Bimlesh Kumar
Associate Professor
bimk@iitg.ernet.in
0361-258 2420

Prof. Subashisa Dutta
subashisa@iitg.ernet.in
0361-258 2415

CERTIFICATE

This is to certify that the thesis entitled **Hydrodynamics of Vegetative Channel with Downward Seepage** submitted by Thokchom Bebina Devi to the Department of Civil Engineering, Indian Institute of Technology Guwahati, is a record of bonafide research work under our supervision and is worthy of consideration for the award of the degree of Doctor of Philosophy of the Institute.

Date:
Place: Guwahati

Dr. Bimlesh Kumar

Prof. Subashisa Dutta

List of Publications

Journals

Accepted

Devi, T. B., & Kumar, B. (2016). Experimentation on submerged flow over flexible vegetation patches with downward seepage. *Ecological Engineering*, *91*, 158-168.

Devi, T. B., Daga, R., Mahto, S. K., & Kumar, B. (2016). Drag and turbulent characteristics of mobile bed Channel with mixed vegetation densities under downward seepage. *ASME Journal of Fluids Engineering*, *138*(7), 071104.

Devi, T. B., & Kumar, B. (2015). Turbulent flow statistics of vegetative channel with seepage. *Journal of Applied Geophysics*, *123*, 267-276.

Devi, T. B., & Kumar, B. (2016). Channel Hydrodynamics of Submerged, Flexible Vegetation with Seepage. *Journal of Hydraulic Engineering*, *142 (11)*, 04016053.

Devi, T.B., Sharma,A., & Kumar, B. (2016). Turbulent characteristics of vegetated channel with downward seepage. *ASME Journal of Fluids Engineering*, *138 (12)*, 121102.

Devi, T. B., & Kumar, B. (2016). Flow characteristics in an alluvial channel covered partially with submerged vegetation. *Ecological Engineering*, *94*, 478-492.

Devi, T. B., Sharma, A., & Kumar, B. (2016). Studies on emergent flow over vegetative channel bed with downward seepage. *Hydrological Sciences Journal*, doi: 10.1080 / 02626667. 2016. 1230673

Shivpure, V., Devi, T. B., & Kumar, B. (2015). Analysing turbulence characteristics of flow over submerged flexible vegetated channel. *ISH Journal of Hydraulic Engineering*, *21*(3), 265-275.

Shivpure, V., Devi, T. B., & Kumar, B. (2016). Turbulent characteristics of densely flexible submerged vegetated channel. *ISH Journal of Hydraulic Engineering*, *22*(2), 220-226.

Devi,T.B. & Kumar, B. (2016) Flow characteristics in a fully covered submerged natural vegetation with downward seepage. *Canadian Journal of Civil Engineering* (Accepted)

Under review

Devi, T.B., Sharma, A., & Kumar, B. Hydrodynamics of channel with partly emergent vegetation. *Hydrological Sciences Journal* (Under revision)

Conferences

Thokchom Bebina Devi, Bimlesh Kumar and S. Dutta- Analysis of Flow Predictors in Rigid Vegetated Channel, *National Conference on Sustainable Water Resources Planning, managment and Impact of Climate Change*, April 5th -6th , 2013, Birla Institute of Technology and Science-Pilani, Hyderabad Campus, Hyderabad, India.

Thokchom Bebina Devi and Bimlesh Kumar- Near Bed hydrodynamics of Vegetative Channel with Seepage, *National Conference On Water and its Sustainability in mining and Other Environment: Vision 2050* on March 28th -29th, 2014, Department of Civil Engineering, Indian School of Mines, Dhanbad.

Thokchom Bebina Devi and Bimlesh Kumar- Flow Analysis around Submerged vegetation, *IAHR World Congress 2015*, The Hague, 28th June to 3rd July 2015

Thokchom Bebina Devi and Bimlesh Kumar - An experimental study on the flow characteristics in a mixed vegetation patches with downward seepage, International Conference on Emerging Trends in Science and Engineering Research, NIT Manipur, 2nd -4th December 2015.

Thokchom Bebina Devi, Anurag Sharma, Sumit Kumar Mahto, Rishabh Daga and Bimlesh Kumar- Flow Characteristics in a vegetative channel with downward seepage, *20th International Conference on Hydraulics, Water Resources and River Engineering, Hydro-2015*, IIT Roorkee, 17th to 19th December, 2015.

Thokchom Bebina Devi, and Bimlesh Kumar - A study on the flow characteristics in a finite vegetation patch with downward seepage, *River Flow2016-8th International Conference on Fluvial Hydraulics*, 12th -15th July, 2016, St.Louis.

Thokchom Bebina Devi, and Bimlesh Kumar -A Study on the Flow Characteristics in a Partially covered natural vegetation with Downward Seepage, *20th Congress of the IAHR APD 2016*, 27th -31st August 2016, Colombo, Sri Lanka.

Acknowledgements

Completion of this Doctoral Dissertation has been a truly life-changing experience for me and it would not have been possible to do without the support and guidance that I received from many people.

First of all, I would like to thank my supervisor, **Dr. Bimlesh Kumar**, for his guidance, motivation and kind advice throughout my PhD research studies. You have been a tremendous mentor for me. The unconditional support given by Sir has always made me to clarify my doubts despite his busy schedules and I consider it as a great privilege to do my doctoral programme under his guidance and to learn from his research expertise. During my research period, he gave me intellectual freedom in my work, engaging me in new ideas, and demanding a high quality of work in all my endeavors. One simply could not wish for a better or friendlier supervisor. I could not have imagined having a better advisor and mentor for my Ph.D. study.

I would also like to give my sincere thanks to my co-supervisor, **Prof. Subashisa Dutta** for his constant support, availability and constructive suggestions which helped me in accomplishing the work presented in this thesis. He offered so much advice and guided me in the right direction.

I would like to acknowledge **Department of Civil Engineering** at IIT Guwahati for giving me the opportunity to pursue my PhD and do my research work. My PhD experience benefitted greatly from the courses I took during my course work period.

Besides my advisor, I would like to thank my thesis committee: **Prof. Rajiv Kumar Bhattacharjya, Dr. Sreeja P., Dr. Hrishikesh P. Gadgil, Dr. Ajay Kalamdhad, Dr. Nanda Kishore, Dr.Rishikesh Bharti and Dr. Suresh Kartha** for their insightful comments, encouragement and guidance through this process; your discussion, ideas, and feedback have been absolutely invaluable.

Before starting my research, it was my first step to be in well verse with the sophisticated instruments that would be needed in my research. I would like to express my gratitude towards **Dr.Vishal Deshpande** and **Mahesh Patel** for introducing me to the instruments required for my research work. And Special thanks to **Mahesh Patel** for encouraging me and for helping me out at the starting of my research when my mind got blank and I didn't even know how to start taking the measurements also.

Next, I would like to thank Bazal Daa (**Bazal Hoque**) for helping me in my experimentation work. There is no word to explain myself how lucky I am to get an elder brother like you. You got every solution for every problem. You could easily solve any kind of confusion or problem. The helping hand you extend is nowhere to be found.

My sincere gratitude to my two B.Tech juniors, **Rishabh Daga** and **Sumit Kumar Mahto** for being there always to help me out. Both of your sincerity and seriousness towards work and always active mode really motivated me a lot when I felt so down. Without your support and help, I would not have achieved this far. My best wishes are with you two. Besides, I would also like to thank **Varsha Shivapure**, **Anurag Sharma**, **Rutuja Chavan**, **Rakesh Ranjan, Sainath Panigrahi, Arvind Kumar** and **Jaideep Sherahwat** for giving me their time and helping me in my experiments. Additionally, the help extended by summer interns, **Karishma Choudhury, Mrigakshee Sharma** and **Nupur Kalita** cannot be left unmentioned.

To my closer friends, **Sophia Leichombam, Rubina Thoudam, Ngangkham Devarani and Sanasam Sunderlal**, I express my gratitude for their unconditional friendship, support and patience throughout these years. I would also like to thank **Dr.Thiyam Tamphasana Devi, Amrita Khwairakpam** and **Shantirani Senjam** for giving support in this journey.

I am really indebted to my family, my lovely parents; **Nimaichand** and **Mukharasana**, and to my two lovely brothers; **Karnajit** and **Kelinjit** for their unending support, love and encouragement and without which I would not have come this far.

I would like to give sincere thanks to **Dipankar Singh** for staying by my side and giving me emotional support and helping me in completing this research.

I would like to acknowledge **Ministry of Earth Sciences**, **Government of India** for sponsoring the project titled 'Resistance Characteristics of mobile bed Vegetation (MoES/PAMC/H&C I 26 I 20 13-PC-ll)'

Above all, I owe it all to **Almighty God** for granting me the wisdom, health and strength to undertake this research task and enabling me to its completion.

Abstract

The presence of vegetation in an open channel can significantly affect the hydrodynamic behaviour of the flow and consequently sediment transport by obstructing the flow and changing the flow characteristics. Understanding the hydraulics of flow over vegetation is very important to support the management of fluvial processes. The present research work experimentally investigates the flow over flexible vegetation. Experimental data collected in a straight flume having a bed covered by grass-like vegetation have been used to analyze different flow characteristics for flexible submerged elements. Experiments were conducted for both artificial as well as natural vegetation. An important parameter of sand bed channels, downward seepage, was considered in the present work on vegetated channel. Two different seepage percentages, 10% and 15%, were considered for exploring the change in flow characteristics with respect to no seepage case.

Vegetation height is an important parameter in influencing the flow characteristics in a vegetated channel flows where velocity is reduced near the top of the vegetation. Velocity profiles show the presence of an inflection point near the top of the vegetation where maximum Reynolds stress is achieved. Results show that velocity measured at upstream vegetation section is always higher than the downstream section even with the application of downward seepage. The maximum value of Reynolds stress occurs near the top of the vegetation. When the flow enters the vegetation section, the local effect of the presence of vegetation on sediment transport is more at the upstream vegetation section and then decreases which is shown by higher Reynolds stress at the upstream as compared to downstream vegetation section highlighting the importance of vegetation in providing as an erosion control. The velocity profiles measured in the unobstructed region of uniform pattern is higher as compared to the velocity measured in line with the vegetation stems of staggered pattern. Downward seepage increases the velocity, Reynolds stress and turbulent intensities. It can be inferred from moment analysis results that the downward seepage increases the flux transport in downward direction and diffusion in the streamwise direction which is shown by the governance of sweep event over ejection event from quadrant analysis. Turbulent Kinetic Energy (TKE) budget is also evaluated. Turbulent diffusion or transport is one of the essential components of TKE budget. Turbulent diffusion transports the energy near the vegetation edge

towards the free-surface as well toward the vegetation zone. The transport towards the vegetation zone increases with the downward seepage while it decreases in the upper free surfaces.

Vegetation density is one of the important parameters that affect the flow resistance. The present study shows that higher vegetation density when placed at the downstream side leads to a reduction in velocity, Reynolds stress and turbulent intensities. Downward seepage decreases the effect of drag offered by the vegetation stems. Smaller vegetation spacing (or higher vegetation density) provides more resistance to flow because of which lower velocity is achieved. The length scale and time scale increases with increase in percentage of seepage.

For a channel covered partially with vegetation, an increase in the flow characteristics such as velocity, Reynolds stress and turbulent intensities are observed in the unvegetated region as the flow goes downstream. The maximum depth of erosion with downward seepage is more than for the case of no seepage and erosion increases as the flow goes downstream.

Contents

List of Figures

List of tables

List of symbols

σ_g	Gradation coefficient
ϕ	Angle of repose
E'	Voltage generated in a conductor (volt)
u_c	Velocity of the conductor (ms^{-1})
ε_Y	Yalin's critical condition of bed movement
γ_s	Submerged specific weight of the grains (Nm^{-3})
ρ	Mass density of the fluid (kgm^{-3})
τ^*	Critical Shields stress (Nm^{-2})
γ	Specific weight of water (Nm^{-3})
u_c^*	Critical shear velocity (ms^{-1})
u^*	Shear velocity (ms^{-1})
σ_u	Streamwise Turbulent Intensity (x-direction) (ms^{-1})
σ_w	Vertical Turbulent Intensity (z-direction) (ms^{-1})
H'	Hyperbolic hole region
$I_{i,H'}$	Indicator function
$S_{i,H'}$	Fractional contribution of Reynolds stress
ε	Energy dissipation ($J\ kg^{-1}s^{-1}$)
p'	Pressure fluctuations (Nm^{-2})
k_w	Wave number (m^{-1})
u^+	Non-dimensional velocity
z^+	Non-dimensional vertical height
Δz	Depth of the virtual bed level (m)
z_o	Depth of the zero velocity level (m)

$\tau_{xz}(=-\overline{u'w'})$	Time averaged Reynolds stress (Nm^{-2})
u', v', w'	Velocity fluctuations in x, y and z directions (ms^{-1})
$(\overline{u'u'})^{0.5}, (\overline{v'v'})^{0.5}, (\overline{w'w'})^{0.5}$	rms value of u', v' and w' (ms^{-1})
A	Observation area (m^2)
a	Projected plant area per unit volume (m^{-1})
ADV	Acoustic Doppler Velocimeter
A_p	Area of pipe (m^2)
B	Magnetic field (T)
C	Kolmogorov's constant
C_d	Coefficient of discharge
C_D	Drag coefficient
d_{50}	Median diameter (mm)
d_v	Diameter of vegetation (m)
E	Streamwise modulus of elasticity (Nm^{-2})
E_L	Eulerian integral length scale (m)
E_T	Eulerian integral time scale (s)
f	Frequency (Hz)
f_{Fx}	Form drag force (N)
F_{ii}	Velocity power spectra function
f_{kw}	TKE flux in vertical direction (m^3s^{-3})
Fr	Flow Froude number
f_{Vx}	Viscous drag force (N)
g	Acceleration due to gravity (ms^{-2})
H	Flow depth at incipient motion condition (m)
h_d	Average deflected height of vegetation (m)
h_n	Flow depth measured over the rectangular notch (m)
h_v	Actual height of vegetation (m)
I	Moment of inertia (m^4)
I_e	Energy gradient

k	Total kinetic energy (m^2s^{-2})
k	von Karman constant
L	Length of the conductor (m)
L_n	Length of the rectangular notch (m)
m	Total number of detachments
M	Vegetation density
M_{12} and M_{21}	Advection of Reynolds stress in Streamwise and vertical directions
M_{30} and M_{03}	Flux of Reynolds stress in Streamwise and vertical directions
N	Total number of samples
p_d	Pressure diffusion (m^2s^{-3})
P_D	Non-dimensional pressure diffusion
p_s	Shear production (m^2s^{-3})
P_s	Non-dimensional shear production
p_w	Wake production (m^2s^{-3})
P_w	Non-dimensional wake production
Q	Main Channel discharge (m^3s^{-1})
q_s	Seepage discharge (m^3s^{-1})
$R(t)$	Auto correlation function
R^*	Boundary Reynolds number
Re	Flow Reynolds number
S	Bed slope
SNR	Signal to Noise ratio
S_{uu}	Spectral density function for u' (m^3s^{-2})
s_v	Spacing of vegetation (m)
t	Observation time (s)
T	Total sampling time of velocity pulse (s)
TKE	Turbulent Kinetic Energy
t_t	Turbulent diffusive transport (m^2s^{-3})

T_t	Non-dimensional turbulent diffusive transport
u, v, w	Instantaneous velocities in x, y and z directions (ms^{-1})
U,V,W	Time averaged velocities in x, y and z directions (ms^{-1})
z	Any vertical distance (m)

1 Introduction

1.1 Overview

The flow conditions are extremely complex where flow passes through aquatic riparian vegetation. Vegetation affects fluvial processes and is key in current river management and river hydraulics. Advances in understanding the behavior of flow over vegetation allow us to improve both the knowledge of flow-velocity profiles and flow resistance and the design of vegetated channels (Tsujimoto 1999). The presence of vegetation is one of the factors that change the mean and turbulent flow field in a channel (Nepf, 2012a).

The impact of vegetation on the flow conditions can be discussed in two different views. Aquatic vegetation in conveyance channels increases the flow resistance thereby reducing the conveyance capacity and was traditionally regarded as a nuisance and hence it was removed from channels to increase the passage of flow (Kouwen, 1992; Wu *et al*, 1999). Aquatic vegetation grown in riverine and wetland environments plays a critical role in ecosystem services (Corenblit *et al*, 2007). It not only provides food sources and habitat for some economically important fish (Edgar 1990, Kemp *et al* 2000), but also directly regulates the concentrations of oxygen, carbon and nutrients by uptake and biological transformation (Carpenter and Lodge, 1986; Wang *et al*, 2010; Pierobon *et al*, 2013). The presence of aquatic vegetation also alters the natural flow structure (Nepf 1999, Neumeier and Amos, 2006; Chen and Kao, 2011; Meire *et al* 2014), and thus influences the transportation and diffusion of sediment and pollutants indirectly (Kadlec, 1995; Okamoto *et al*, 2012). The vegetation along the riverbed plays an important role on the hydrodynamic behavior, on the ecological equilibrium and on the characteristics of the river (Wilcock *et al*, 1999; Mars *et al*, 1999; Lee and Shih, 2004; Pollen and Simon, 2005; Turker *et al*, 2006, Zhu *et al* 2016). The presence of vegetation canopies in rivers has recently been regarded as one of the key measures for water management and river environment, and therefore, it is necessary to study the flow structures in a vegetative channel (Poggi *et al*, 2004; Ghisalberti and Nepf, 2006;Tanino and Nepf, 2008). In addition, vegetation is known to increase bank stability, reduce erosion, provide habitat

for aquatic life, attenuate floods, increase aesthetic values and filter pollutants. Recently, efforts are being taken up for river restoration, re-naturalization and rehabilitation of watersheds and watercourses in which growing of vegetation is the first and foremost step (Kothyari *et al*, 2009a). Therefore, a proper understanding of the interaction between the flow, sediment and vegetation is required for understanding the problem. Based on the flow conditions and vegetation characteristics, aquatic vegetation can be grouped in two classes- (i) submerged and emergent vegetations and (ii) rigid and flexible vegetations.

1.2 Types of vegetation

In describing the flow characteristics in a vegetated channel, it is important to have a clear idea regarding the types of vegetation. Aquatic vegetation has been classified as submerged, emergent, rigid and flexible vegetation (Figure 1.1). As the name suggests, submerged vegetation refers to the type of vegetation in which the flow depth is more than the height of the vegetation while emergent vegetation is the opposite of submerged vegetation where the vegetation height is more than the flow depth. The difference between rigid and flexible can be made as flexible vegetation is the one in which the height of the vegetation changes according to the flow conditions while the height of the rigid vegetation remains the same for whatsoever flow conditions exist. In comparison to studies related to rigid vegetation types, there have been a fewer number of investigations on flow in channels with flexible vegetation (Wilson *et al*, 2003). Submerged canopies can have a positive impact on water quality by removing Phosphates and Nitrates poured into the rivers (Velasco *et al*, 2003). For both submerged and emergent configurations, the case of flexible elements has to be distinguished from that of rigid elements. From the application point of view, the grass-like vegetation can be considered flexible and, because of its small average height, it is usually completely submerged. Shrubby vegetation is, instead, rigid and could assume both the emergent and the submerged configuration; a flood flowing in a channel can completely bend the rigid vegetation, often breaking and lying it down on the bed (Ferro, 2006). For rigid elements, the hydraulic behavior of the bed roughness is similar to that of a fixed bed formed by elements of known geometry (hemispheres, cubes, gravels, etc.) in large-roughness conditions

(Kowobari *et al*, 1972; Shen, 1973; Petryk and Bosmajian, 1975; Ferro and Giordano, 1990, 1992; Baiamonte and Ferro, 1997; Armanini and Righetti, 1998; Stone and Shen, 2002).

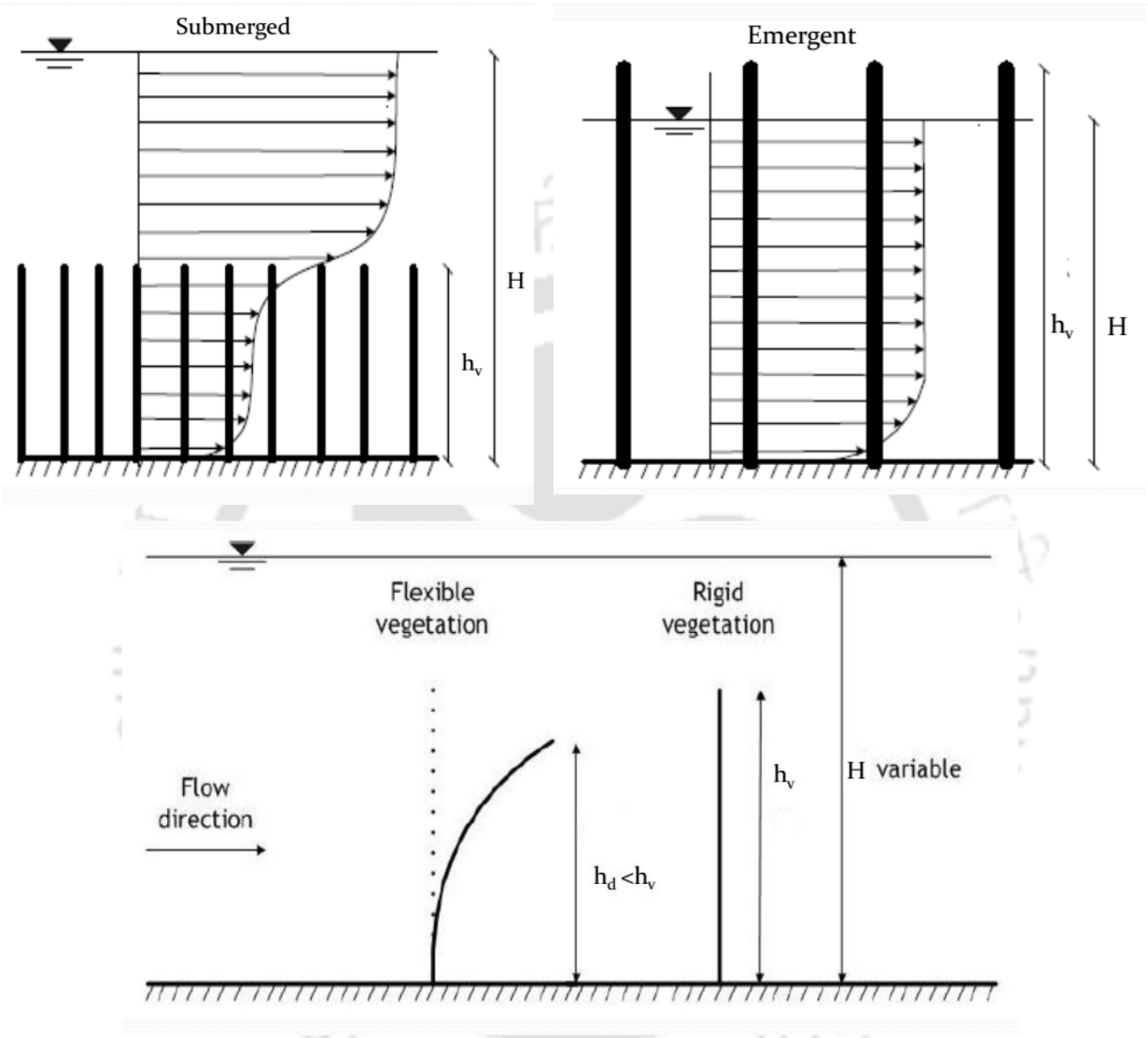

Figure 1.1 Different types of vegetation: Submerged, Emergent, Flexible and Rigid

Determination of flow within a vegetated open channel is a very complicated problem. This problem becomes more complicated when the boundary roughness changes from time to time with the stage of growth of vegetation. The flexible elements can assume different configurations (Kouwen *et al*, 1969; Gourlay, 1970; Kowobari *et al*, 1972) due to both the hydrodynamic action of the flow and the bending stiffness *EI*, where *E* is the streamwise modulus of elasticity of the

vegetation element and *I* is the moment of inertia of the cross section of the element itself. Three different configurations have been experimentally observed for the flexible elements (Kouwen *et al*, 1969; Gourlay, 1970):

- Elements that are *erect* and do not change their position in time;
- Elements that are subjected to a *waving motion* and, thus, change their position in time;
- Elements that assume permanently a *prone position*.

1.3 State of the art

In the earliest studies on vegetation, the investigation of the role of vegetation in rivers was directed towards the interactions between plants and hydrodynamics. The analysis of the resistance due to vegetation was largely faced, in particular on the determination of the contribution of herbaceous and algal vegetation to flow resistance (Kouwen, 1988), a question that is still unanswered (Nikora, 2010). In the last years, several investigations have tackled the problem of the resistance exerted by bushes (Järvelä, 2004; Righetti and Armanini, 2002) or, in general, by submerged vegetation (Baptist *et al*, 2007; Stephan and Gutknecht, 2002). Another fundamental aspect is represented by the influence of rigid and emergent plants on flow resistance (Ishikawa *et al*, 2000; James *et al*, 2004; Kothyari *et al*, 2009b; Tanino and Nepf, 2008). The relationship between turbulence and drag resistance is one of the most complex issues concerning the plant-flow interactions. Because of its complexity, the research is now moving toward a deeper analysis of the turbulence structure and diffusive transport processes through plants (Ghisalberti and Nepf, 2009; Li and Shen, 1973; López and García, 2001; Nepf and Ghisalberti, 2008; Nepf, 1999; Takemura and Tanaka, 2007). These studies include sediment transport processes (mostly suspended load transport), diffusion and dispersion of passive and reactive scalars and its implications for water quality problems and for transport processes in rivers.

Laboratory observations of the effects of artificial vegetation with rigid stems (e.g., Nepf, 1999; Fairbanks, 1998) and flexible stems (e.g., Ikeda and Kanazawa, 1996; Nepf and Vivoni, 2000; Wilson *et al*, 2003; Ghisalberti and Nepf, 2002, 2006) on the steady flow and unsteady turbulent flow structures have led to a deeper understanding of the transport and mixing of sediments and

other scalars related to ecosystem health. Wilson *et al* (2003) presented detail scaling of the biomechanical properties of the plants and explore the effects of two forms of flexible vegetation on the turbulence structures. Fairbanks (1998) identified the importance of the horseshoe vortex in understanding the local scour patterns. Different materials have been used for imitating aquatic vegetation such as wooden cylindrical dowels or rods (Stone and Shen, 2002; Liu *et al*, 2008; Poggi *et al*, 2004), flexible strips or blades (Nepf and Vivoni, 2000; Chen *et al*, 2011) and natural vegetation (Järvelä, 2002; Stephan and Gutknecht, 2002; Carollo *et al*, 2005). Previous researchers carried out a large number of investigations on experiments using artificial and natural vegetation in flume (Stephan and Gutknecht, 2002; Järvelä, 2002; Righetti and Armanini, 2002), on analytical approaches for vertical velocity profile (Klopstra *et al*, 1997; Huthoff *et al*, 2007; Yang and Choi, 2010), on turbulence characterization for submerged rods and vegetation (Nepf and Vivoni, 2000; López and García, 2001) and on numerical approaches (Kutija and Hong, 1996; Darby, 1999; Simoes and Wang, 1997). In the last decade the characterization of not only the mean flow but also of the turbulence structure in a vegetated open channel flows has received a lot of attention. Understanding of the turbulence structure of rough flows with plants as roughness elements has been initiated from the studies of atmospheric flows over canopies (Finnigan, 1979; Gao and Shaw, 1988; Raupach *et al*, 1991). Some research efforts attempt to describe the turbulence structure in vegetated open-channel flows (Tsujimoto *et al*, 1992; Nepf, 1999; López and García, 2001; Shi *et al*, 1996).

Kouwen *et al* (1969) presented velocity profiles observed in a laboratory flume planted with strips of styrene which simulated the vegetation and found out that the velocity profile above the vegetation layer follows logarithmic law. However, inside the vegetation layer the velocity is constant.

Temple (1982) suggested a two layered velocity profile for vegetated open channels. For depth of flow less than the bending height of vegetation, velocity distribution is almost constant and depends only on vegetation density and channel bed slope. But when the depth of flow increases such that the submerged condition occurs, velocity profile is dependent on momentum transfer in the form of turbulent shear.

Anwar (1996) conducted a series of experiments in shallow coastal water to estimate the effects of flow uncertainties on the mean velocity distribution. The mean velocity profiles were measured during the accelerating and decelerating phases of the tidal coastal flows. The measured velocity profiles have three distinct regions, i.e., (i) inner region (adjacent to bed) (ii) outer region and (iii) overlap region. Velocity profiles in outer and overlap regions obey the log law and defect law, respectively.

Sumer *et al* (1996) measured velocity profile inside and outside the sheet flow layer of movable bed in a tilting flume with four different types of sediments of varying sizes. Measured velocity profiles are found to follow logarithmic law near the bed, outside the sheet flow layer. However, inside the sheet flow layer, power law is satisfied.

Ikeda and Kanazawa (1996) conducted seven experimental runs to study the three dimensional organized vortices above the flexible vegetation. The velocity profile shows an inflection point near the top of the vegetation and the flow becomes unstable and leads to the formation of three dimensional vortices. The streamwise and vertical turbulence intensities have their maximum value at the top of the vegetation and it decreases towards the free surface and the bottom. The Reynolds stress increases linearly from the free surface to the top of the vegetation. The organized vortices consist of two counter-rotating vortices in the horizontal and lateral directions in which the lateral scale is nearly equal to the streamwise scale. The shape of the organized vortices is elliptical and the vortices are inclined downward to the front.

Wu *et al* (1999) investigated the variation of vegetative roughness coefficient with the flow depth. It is observed that the roughness coefficient reduces with increasing flow depth under the unsubmerged condition. For fully submerged condition, the vegetative roughness coefficient tends to increase at low flow depths but then decrease to an asymptotic constant as the water level increases. A simplified model based on force equilibrium was developed to evaluate the drag coefficient of the vegetal element after which Mannings equation was employed to convert the drag coefficient into roughness coefficient.

Nepf and Vivoni (2000) explored the transition between submerged and emergent vegetation regimes from the experiments conducted in an open channel flume with model vegetation taking momentum sources, turbulence and exchange dynamics into consideration. The flow within the canopy in submerged case is divided into two distinct zones- upper canopy called the vertical exchange zone and lower canopy called the longitudinal exchange zone while in emergent case only the longitudinal exchange zone is present. The drag coefficient increases towards the bed which reflects the importance of viscous effects.

Stephan and Gutknecht (2002) carried out laboratory experiments using three different types of aquatic vegetation. The zero plane displacement increases with increase in the length of the stems of the plants but not in the same ratio. The turbulent intensity decreases with decrease in the relative submergence for flow of small relative submergence.

Carollo *et al* (2002) conducted a series of experiments in a laboratory flume to study the influence of flexible vegetation concentration and depth/vegetation height ratio on the velocity profile from the velocity measurements obtained by a two-dimensional Acoustic Doppler Velocimeter. The experimental profiles are identified with three zones; Zone I inside the vegetation, characterized by very small velocities; Zone II in which the logarithm velocity profile can be fitted to the measured velocities (logarithm zone); Zone III characterized by positive vertical velocity gradients, progressively decreasing to zero near the free surface, where the velocity profile become vertical (free-stream zone). With the decrease in stem concentration the velocity inside the vegetation increases but the velocity above the vegetation decreases, the thickness of the free-stream zone decreases and the curvature of the velocity profile inside and above the vegetation decreases.

Järvelä (2002) studied the flow resistance of various combinations of natural grasses, sedges and willows in a laboratory flume and found that friction factor decreases with Reynolds number in all the test series except in the test series of leafless willows on bare bottom soil where friction factor is more or less independent of Reynolds number. For leafless willows on bare soil, friction factor

increases almost linearly with flow depth and independently with flow velocity while velocity has a considerable effect of friction factor.

Velasco *et al* (2003) conducted a series of laboratory experiments in a 20m long, 1m wide and 0.9m deep concrete flume using plastic plants seeded in a gravel bed. The flow resistance due to different densities of flexible vegetation was characterized and distinguished the different flow regimes below and above the vegetation. For totally prone vegetation condition the friction factor decreases for different plant densities and their values decrease to a nearly asymptotic value which is equivalent to that of the non-vegetated case.

Musleh and Cruise (2006) investigated the functional relationships of resistance in wide flood plains with rigid unsubmerged vegetation. Drag Coefficient and Manning's coefficient show an increasing linear relationship with flow depth but Friction factor increases in a slightly non-linear fashion with the flow depth. Friction factor decreases in a highly non-linear manner with increasing flow velocity. Friction factor is more sensitive towards changes in rod diameter and lateral spacing than streamwise spacing.

Liu *et al* (2008) conducted laboratory experiments to develop velocity and turbulence intensity profiles to observe the changes in flow characteristics as water flows through a vegetation array simulated by rigid acrylic dowels. A velocity spike followed by an inflection point that led to a region of lower velocity is observed for both submerged and emergent conditions. The turbulent intensity remains constant for the entire flow depth for emergent condition but it has a peak at the top of the array for submerged condition and decreases at the bed and free surface.

Nepf and Ghisalberti (2008) reviewed recent work on flow and transport in channels with submerged vegetation, including discussions of turbulence structure, mean velocity profiles, and dispersion. For submerged canopies of sufficient density, the dominant characteristic of the flow is the generation of a shear-layer at the top of the canopy. The shear-layer generates coherent vortices by Kelvin-Helmholtz (KH) instability. For flexible canopies, the passage of the KH vortices generates a progressive wave along the canopy interface, termed as *monami*. The KH

vortices formed at the top of the canopy penetrate a certain distance into the canopy. This penetration scale segregates the canopy into an upper layer of rapid transport and a lower layer of slow transport. Flushing of the upper canopy is enhanced by the energetic shear-scale vortices. In the lower layer, turbulence is limited to length-scales set by the stem geometry, and the resulting transport is significantly slower than that of the upper layer.

Nezu and Sanjou (2008) discussed the turbulence structures and coherent large-scale eddies in the vegetated canopy open-channel flows. Large scale coherent eddies of sweeps and ejections are formed near the vegetation edge which is shown by an inflection point in the mean velocity profile. The whole flow region is divided into three zones: the emergent zone, the mixing-layer zone and the log-law one. It is found that ejections and sweeps govern the turbulence structure and coherent motions in aquatic flows. The Reynolds stress attains a maximum value at the vegetation edge and the penetration of Reynolds stress or momentum exchange increases with decrease in vegetation density.

Righetti (2008) addressed the problem of the resistance due to vegetation in an open channel flow, characterized by partially and fully submerged vegetation formed by colonies of bushes. The flow is characterized by significant spatial variations of velocity between vertical profiles that make the traditional approach based on time averaging of turbulent fluctuations inconvenient. Velocity measurements were completed together with the measurements of drag exerted on the flow by bushes at different flow depths. The experimental data shows that the contribution of form-induced stresses to the momentum balance cannot be neglected. The mean velocity profiles and the spatially averaged turbulent intensity profiles allow inferring that the vegetation density is a driving parameter for the development of a mixing layer at the canopy top in the case of submerged vegetation.

Yagci and Kabdasli (2008) revealed that flow downstream of a vegetation element is significantly retarded and the velocity profile no longer follows a logarithmic law. Experimentally obtained time-averaged velocity data show that sub-canopy flow occurs downstream of vegetation in the region close to the bed for the three types of vegetation tested, but with increasing compactness of

vegetation the strength of the sub-canopy flow increases. On the other hand, with increasing compactness of vegetation, relatively lower and in some cases negative time-averaged velocity values are observed in the area close to water surface downstream of the vegetation. Another aspect is that in the event of a flood the presence of vegetation with a compact foliage and branch structure reduces streamwise mean velocity. However, this situation also leads to a decrease of conveyance and thus elevated water depth values should be expected.

Cheng (2011) proposed a representative roughness height for quantifying the effect of submerged vegetation on flow resistance in the surface layer. The proposed roughness height is characterized by its proportionality to both stem diameter and vegetation concentration and performs better than other length scales in collapsing resistance data collected under a wide range of vegetation conditions. An approach was then developed for estimate of the average flow velocity and thus resistance coefficients for both cases of rigid and flexible vegetation. The analysis shows that the friction factor defined for the surface layer above the vegetation slightly increases with increasing relative roughness height, the latter being taken as the ratio of the roughness height to the surface layer thickness.

Siniscalchi et al (2011) investigated the effects of a finite-size vegetation patch on flow turbulence, variations in drag forces experienced by individual plants within the patch, and flow-drag interrelations. The results show zones of increased turbulent energy close to the leading edge and along the patch canopy top, where turbulence shear production is enhanced. Zones of negative Reynolds stresses are found inside the patch and they reflect the influence of plant morphology, which affects the shape of the streamwise velocity profile and associated turbulent fluxes. Modifications to the power spectral densities of velocity by the plants indicate the emergence of two plant-induced mechanisms of energy production, which are most likely related to the wake turbulence and shear layer turbulence. Drag fluctuations appear to be correlated with the velocity field, with this correlation being especially profound at the highest-studied flow rate.

Okamoto and Nezu (2013) revealed the development process for large-scale coherent structures within vegetation patches of a limited length. Turbulence measurements were intensively

conducted in open-channel flows with submerged vegetation using Particle Image Velocimetry (PIV). To examine the transition from boundary-layer flow upstream of the vegetation patch to a mixing-layer-type flow within the patch, velocity profiles were measured at 33 positions in a streamwise direction. A phenomenological model for the development process in the vegetation flow was developed. The entire flow region can be classified into four zones: (i) the smooth bed zone, (ii) the diverging flow zone, (iii) the developing zone and (iv) the fully-developed zone.

Termini (2015) analyzed the influence of flow submergence and stem's concentration on vegetation behaviour and mean flow conveyance. Velocity profiles can be better schematized by a composition of two parts of constant velocity (respectively inside and above the vegetation) separated by a confined intermediate region (mixing layer) containing the inflection point. It has been assessed that the thickness of the mixing layer increases as the momentum thickness increases. On the other hand, the momentum thickness linearly increases as the flow submergence increases. An increase in stems' concentration determines a decrease in the mixing layer thickness and a flattening of the velocity profile inside it.

Zhang et al (2015a) conducted laboratory experiments using two types of submerged, flexible vegetation, *V. natans* and *P.malaianus* to investigate the influence of plant morphology on flow structure. The decrease in the frontal area in the lower part of canopy leads to the occurrence of counter velocity gradient and a local velocity maximum occurs within the canopy layer. The Reynolds stress reaches its maximum value at the canopy interface and has negative values at a region where counter velocity gradient occurs within the canopy. Turbulent Kinetic Energy (*TKE*) peaks at the top of the canopy and decays downward into the canopy gradually. Smaller frontal area leads to more flow deflection beneath the canopy and hence acceleration over the top of the canopy decreases. The mean velocity gradient around its top of canopy or the Reynolds stress, *TKE* at the canopy interface are smaller for smaller frontal area canopy.

Kubrak et al (2015) carried out a study based on laboratory measurements of water velocity distributions in a straight rectangular flume with stiff and flexible stems and plastic imitations of the Canadian waterweed. The study addresses the problem of determination of the energy and

momentum coefficients for flows through a vegetated channel. These coefficients were applied to express the fluid kinetic energy and momentum equations as functions of a mean velocity. The coefficients were established for the vegetation layer, surface layer and the whole flow area. The results indicate that the energy and momentum coefficients increase significantly with water depth and the number of stems per unit channel area.

The river bed condition also plays an important role in influencing the flow characteristics in a natural channel. Natural streams often comprise of permeable beds in the form of sand particles and gravels. An essential and well-known feature of permeable boundaries is that mass and momentum transfer takes place across the interface between the fluid and porous media. Water percolates in the form of seepage through boundaries of alluvial channels, rivers and streams due to porosity of the granular material and difference in water level in the stream and ground water table. With the level of the free surface in a river being different from the adjoining groundwater table, two typical seepage flows (suction and injection) may occur through the river boundary. In the case of suction or downward seepage, water seeps out of the river; while with injection or upward seepage, the river receives additional water. Interactions between flow in the main stream and the ambient groundwater, or hyporheic exchanges, are important because of their role in controlling the transport of contaminants and maintaining a healthy stream ecosystem (Brunke and Gonser, 1997; Jones and Mulholland, 2000). Tanji and Kielen (2002) estimated that seepage losses in semi-arid regions can account for 20–50% of the total flow volume in unlined earthen canals. Kinzli *et al.* (2010) and Martin and Gates (2014) measured loss of water around 40% and 15% because of downward seepage. Australian National Committee on Irrigation and Drainage (ANCID, 2006) found that 10-30% of water is lost in the form of downward seepage from alluvial channel. The presence of seepage flow can affect an additional hydrodynamic force on the sediment which will affect the process of sediment transport such as sediment entrainment and formation of bed features. Willets and Drossos (1975) noted that a water intake, when drawing faster moving water towards the sediment bed, can increase the local bed shear stresses resulting in bed erosion around the intake structure. More complex situations occur in the coastal environments, for example in swash zone, where seepage varies both temporally and spatially (Turner, 1995). The hydrodynamic process in such a physical system may result in changes to the

structural features of the flow, implying modification to flow-resistance, sediment entrainment characteristics and morphology of the streambed as compared to that with an impermeable boundary, as is often encountered in a laboratory study. Knowledge of flows over permeable boundaries clearly is not only useful for fundamental research, but also has practical importance in engineering applications. Despite the important influence of seepage on many aspects of practical engineering, relevant information in this area remains scarce. Hence, in order to have a deep understanding about the seepage effects on the channel stability, and to make use of proper equations in the alluvial channel design, it is essential to perform the experiments in the laboratory to understand the problem.

Waters and Rao (1971) studied the hydrodynamic effect of seepage on bed particles. They measured the drag and lift forces on the plastic spheres and found that: (1) injection decreases the drag regardless of the position of sediment particle and (2) seepage increases or decreases the lift acting on a particle on a plane bed (like the natural sediments in rivers). Judging from the viewpoint of drag forces, injection inhibits the motion of a bed particle while suction enhances its motion. From the viewpoint of lift forces, injection inhibits the motion of a plane bed particle and the opposite result holds for the case of suction.

Willetts and Drossos (1975) through their experimental study in a narrow flume with small downward seepage zone observed that downward seepage produces a localized scour hole in the downward seepage zone and grains move at a faster rate in the downward seepage zone than elsewhere in the flume.

Maclean and Willetts (1986) measured the bed shear stress with and without downward seepage by observing the initiation of motion of the indicator grains. They observed that the shear stresses increase with the presence of downward seepage.

Nakagawa *et al* (1988) investigated the effect of seepage on sediment pick-up rates. They found that the changes induced by seepage occur mainly with the pick-up rate rather than the step length related to the motion of sediment particles. The bed load transport model previously established

was thus modified to include the effect of seepage, showing that the bed load transport rate is enhanced by upward seepage and reduced by downward seepage.

Maclean (1991) analyzed the effect of suction on sediment transport and found that suction enhances the sediment transport rate and increased shear stress values are observed in the suction zone.

Prinos (1995) solved the Reynolds-averaged Navier-Stokes equations and studied the effect of downward seepage on the boundary shear stress. The bed shear stress increases with increasing downward seepage rate in the seepage zone. For downward seepage velocity of 9% of the mean channel velocity, the increase in bed shear stress with downward seepage is about eight times to that of the bed shear stress without downward seepage.

Rao and Sitaram (1999) investigated the seepage effects on incipient motion of sand-bed particles. They found that seepage through a sand-bed in a downward direction (suction) reduces the stability of particles and it can even initiate their movement. The bed erosion is increased with the increased rates of suction. However the seepage in an upward direction (injection) increases the stability of bed particles and does not aid in initiating their movement.

Krogstad and Kourakine (2000) investigated localized upward seepage effects on the turbulence structure in a boundary layer. It was observed in their experimental results that as the incoming flow entered the upward seepage region, the bed shear stress is significantly reduced.

Chen and Chiew (2004) experimentally investigated the effect of downward seepage on bed shear stresses in open-channel flow. They observed that the conventional law of the wall is not applicable to open channel flow subjected to downward seepage. Velocity increases in the near-bed region and decreases near the water surface. This resulted in a more uniform velocity distribution. Further, it was also observed that the origin displacement, slip velocity and shear velocity increase with increase in relative downward seepage.

Rao and Sreenivasulu (2009) studied the importance of seepage in the design of channels and revealed that seepage either in "upward" or "downward" can change the resistance as well as mobility of sediment particles. Therefore, it is concluded that the effect of seepage must be considered in canal design. Experimental studies show that suction reduces the stability of the bed particles and initiates their mobility whereas injection increases the stability of the bed particles and reduces their mobility.

Rao *et al* (2011) carried out experiments relevant to the regime behavior of an alluvial channel affected by seepage. Consideration of seepage in flow analysis of regime channel alters its stability. Regime theory was used to define the regression equations for a channel's dimension under stable conditions. Bivariate and trivariate regression relationships were developed for an alluvial channel design under seepage.

Sreenivasulu *et al* (2011) pointed out that in the presence of downward seepage stream power varies non-linearly in the channel and it decreases in the downstream direction. Higher stream power prevails on the upstream end of the channel with downward seepage. Deposition is observed at the downstream end of the flume. They recommended that the effects of downward seepage should be considered in channel design.

Cao and Chiew (2013) conducted laboratory experiments to investigate the influence of suction on sediment transport in closed conduit flows. A conceptual model was set up to analyze suction effects on particle mobility by considering the near-bed velocities based on the theoretical analyses of the forces acting on a spherical particle. The experimental results show that the bed load transport rate increases with suction rate. The results obtained from the numerical simulations also confirm that the near-bed velocities increase with suction.

Deshpande and Kumar (2016a) conducted an experimental study on alluvial channel and found that at high bed shear stress in alluvial channels, made of the non-cohesive material, sediment transport occurs as sheet flow layer of high sediment concentration. The sediment transport in the form of sheet flow is observed when suction is applied to the non-transporting channels designed

on incipient motion condition. The erosion of the channel banks contributes to the sheet flow because of the increased channel bed shear stress. An empirical relation for the thickness of sheet flow layer was developed which includes suction as independent parameter along with others.

1.4 Need for research

Almost all the investigations which focus on flow field and flow resistance, however, have neglected the downward seepage related with mobile beds. The open question is whether to neglect the contribution due to downward seepage is a correct assumption, since in non-vegetated beds the same assumption would be considered a rough approximation. Although the flow characteristics in vegetated channel raise the interest of the researcher community, the hydrodynamics of vegetated channel with downward seepage is not approached. After extensive review of various literature, it is felt necessary to have a detailed and comprehensive research in the laboratory to evaluate the different flow characteristics of vegetated open cannel. It may be concluded that, sand-bed channels are losing a substantial part of the usable water through seepage. Seepage loss not only depletes water resources but also alters the hydrodynamic behavior of the channel. Therefore, seepage loss should be considered while designing a channel section. The hydraulic designers are still lacking of a rational method to determine the hydrodynamics in vegetated riverbeds with downward seepage. Because of practical difficulties in obtaining sufficiently accurate and comprehensive data in actual field experiments, well designed laboratory studies are preferred as a truthful method to provide information concerning details of the hydraulic parameters. Such information is important in application and development of numerical models that can help to predict flow characteristics in vegetated open channel. In the present work, an experimental study on the flow characteristics in a vegetated channel affected with downward seepage is necessary for proper understanding of the problem.

1.5 Objectives

The purpose of this research is to study seepage effects on open-channel flows covered with vegetation. The flow structure in vegetated flows with seepage was investigated by conducting physical experiments. The main objectives of the present study are outlined below:

1.5.1 Flow characteristics in a channel covered with uniformly distributed vegetation

- Study on the dependency of relative submergence
- Study on the effect of vegetation spacing
- Study on the effect of pattern of placing vegetation
- Study on the change in the flow characteristics along the flow direction
- Study on the effect of downward seepage

1.5.2 Effect of mixed vegetation densities on flow structure

- explore the flow characteristics when sparse vegetation density patches are present at the upstream half of the test section and dense vegetation density patches are at the downstream half of the test section
- study the flow characteristics when dense vegetation density patches are present at the upstream half of the test section and sparse vegetation density patches are at the downstream half of the test section
- investigate the streamwise change in the flow characteristics
- study on the effect of downward seepage

1.5.3 Hydrodynamics of seepage affected channel with vegetation bundles

- study the influence of vegetation spacing
- study the change in flow characteristics along the flow direction
- study on the effect of downward seepage

1.5.4 Experimental study of flow through natural vegetation

- explore the flow characteristics when submerged natural vegetation are covered fully for the entire test section
- study the flow characteristics when natural vegetation are covered partially
- investigate the streamwise change in the flow characteristics
- study on the effect of downward seepage

A schematic view of the objectives outlined in the present research work is shown below:

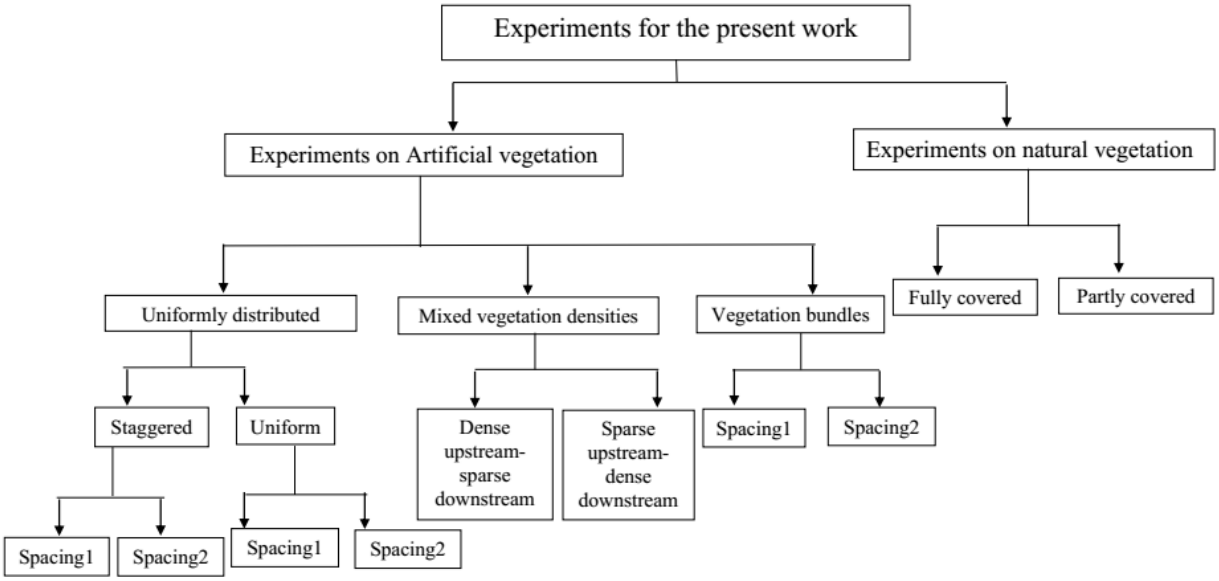

Figure 1.2 Experimental programme in the present research work

1.6 Thesis Organization

The thesis is comprised of seven chapters. A brief introduction of each chapter is described below:

Chapter 1 presents an introduction of the research with the review of literature of various pioneering investigators in the field of vegetated open channels. It highlights various experimental investigations performed using various types of vegetation. The flow conditions in a channel covered with vegetation are stated. It also discusses the investigations on the effect of downward seepage. After a critical review, various objectives of the present study are outlined in this chapter.

Chapter 2 describes experimental program which includes experimental channel design, design and placement of various vegetation elements, experimental procedure for different seepage percentage. Development of the flume is described. Bed material and various instrument used in the experimental study to collect data are presented. Detailed procedure of the data collection and its processing with the results is given.

Chapter 3 presents experimental results pertaining to different vegetation characteristics such as height, vegetation spacing and pattern of placing vegetation. The change in different flow characteristics because of the application of downward seepage is studied. Besides velocity profiles, Reynolds stress and turbulent intensities, moment analysis, quadrant analysis and Energy budget are calculated. Importance of using vegetation as one of the erosion control measures is highlighted.

Chapter 4 explores the flow characteristics in a vegetated channel where two different vegetation densities are mixed in a vegetation patch. The effect of downward seepage is observed. The change in flow characteristics along the flow direction is noted and important results are presented. The calculation of drag coefficient is shown and its change with downward seepage is noted. Important results are drawn with the introduction of mixed vegetation densities.

Chapter 5 also shows the effect of vegetation spacing and downward seepage using another kind of vegetation, by using vegetation bundle. The chapter also studies the change in flow condition as the flow goes downstream. Drag coefficient is also determined for both the spacing and for different seepage cases.

Chapter 6 investigates the flow characteristics using natural vegetation. The chapter highlights the flow characteristics for two different cases: (i) when the vegetation is fully covered for the entire test section and (ii) when the vegetation is partly for half width of the test section. Drag coefficient is calculated. Length and time scales are determined in this chapter. Sediment transport conditions for partly covered vegetation is given.

Chapter 7 presents important findings of the research work for all the experimental conditions. Scope for the future research work is also presented after the section conclusion. Various references that have been reviewed for the present thesis work are listed at the end of the dissertation.

2 Experimentation

2.1 Overview

The objective of the present chapter is to describe the equipment and laboratory methods used for conducting experiments in the present study. Experiments have been designed to make maximum use of the equipment available while minimizing problems such as channel wall effects. All relevant material relating to the methods of operation of this equipment will also be introduced in this chapter. This chapter first describes the apparatus that was available before describing the manner in which it was used for gaining various results. The end of the chapter describes in detail the different series of experiments that were planned and carried out during the course of the research.

2.2 Apparatus and Methods

2.2.1 The Flume

Experiments were conducted in a tilting flume of 20 m long, 1 m wide and 0.72 m deep (Figures 2.1 and 2.2). A tank of dimensions 2.8 m long, 1.5 m wide and 1.5 m deep was provided at the upstream of the flume to straighten the flow prior to its introduction in to the flume. Two metres of upstream length of the main channel bed was made non-porous and the remaining length of the channel was made porous by covering a fine mesh (0.1 mm).This mesh arrangement was supported by steel tube structure of 0.22 m height which was placed on the bottom of the bed. Bottom pressure chamber (15.20 m in length, 1 m wide and 0.22 m deep) was formed by the area between the bottom of the channel and the fine mesh. Sand was placed on the fine mesh in order to prevent its entrance into the bottom chamber. This pressure chamber was used to remove the water from the main channel through the sand bed in perpendicular direction. In order to prevent highly turbulent flow from entering the channel, wooden baffles were installed at the upstream collection tank and the flow was smoothened for a length of 2 m at upstream.

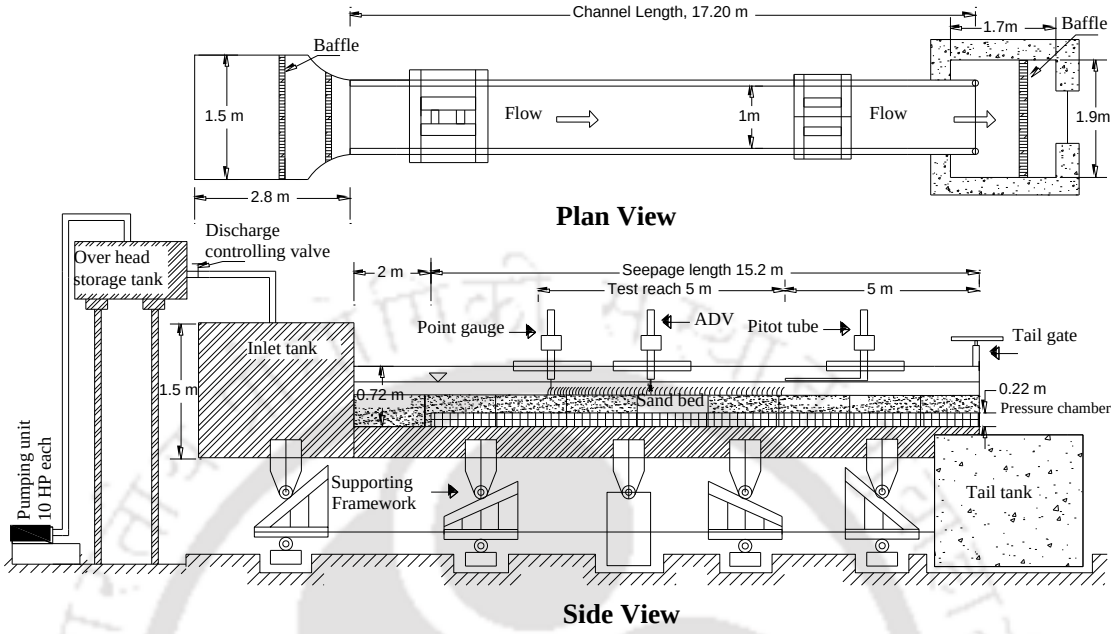

Figure 2.1 Schematic diagram of the experimental flume set-up

Figure 2.2 Photograph of the tilting flume

2.2.2 Test section

Flow in the test section of the flume is significantly affected by the entrance and exit conditions. Strong circulations are present in the flow if it is delivered to the flume directly by means of pipes. In order to avoid the strong circulations present in the flow due to pipes, water was first collected into upstream collection tank of the flume. The level of water rose gradually in the upstream collection tank prior to its introduction into the channel. To ensure the smooth entrance of flow into the channel, couple of baffles was installed in the upstream collection tank just upstream of the channel entrance. Free overfall of flow from the tailgate causes acceleration of flow in the near-bed region just upstream of the tailgate. To minimize the effects of flow entrance and exit conditions in the channel, the test section in the present experiments was considered as a 5 m length in the middle of the flume (4.5 m to 9.5 m from tail gate as shown in Figure 2.1). The flume was long enough to achieve fully developed flow conditions for all the experiments.

2.2.3 Bed material

Carefully sieved river sand of median size (d_{50}) 0.418 mm was used for experiments. Particle size distribution for given sand can be said as uniform if the value of σ_g is less than 1.4 (Marsh *et al*, 2004).

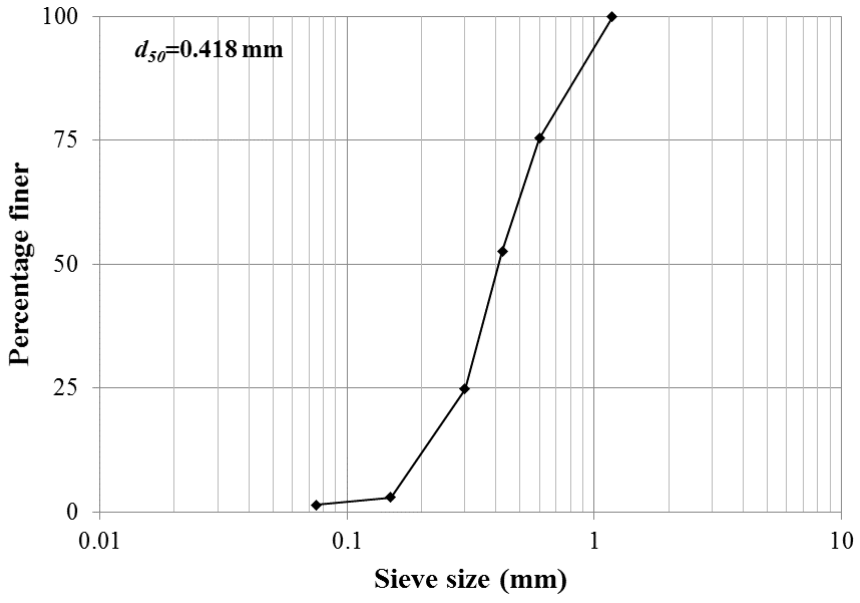

Figure 2.3 Sand size distribution curve

The values of gradation coefficient (σ_g) and angle of repose (ϕ) for the particular sand are 1.17 and 32.55^0. The sand size distribution curve for the particular sand is shown in Figure 2.3.

2.2.4 Flow discharge in the main channel

The discharge in the main channel was measured volumetrically with the help of a rectangular notch provided at the downstream of the flume (Figure 2.4).

Coefficient of discharge was calculated using the equation given below:

$$Q = \frac{2}{3} C_d L_n \sqrt{2g} \left(h_n\right)^{3/2} \qquad (2.1)$$

Figure 2.4 Measurement of flow discharge in the main channel

Coefficient of discharge for the rectangular notch is shown in Figure 2.5 and the value was found to be 0.82.

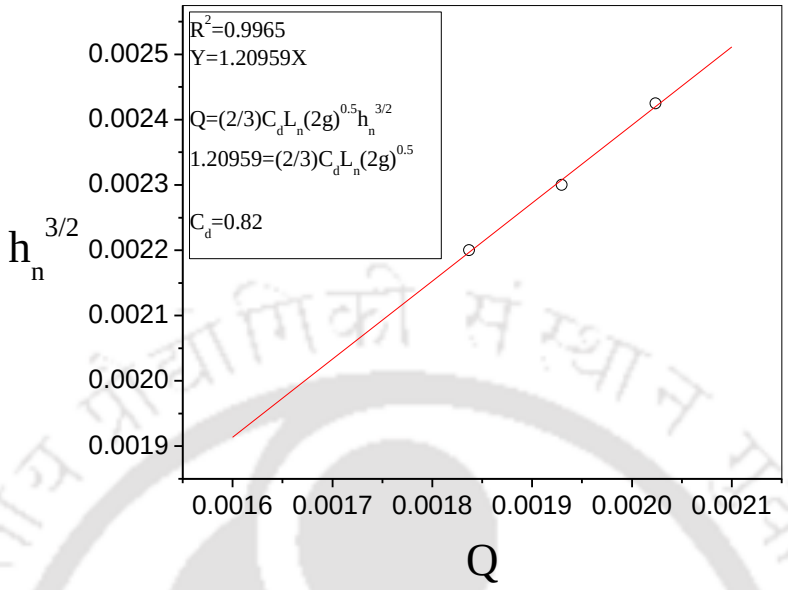

Figure 2.5 Calculation of coefficient of discharge for the rectangular notch

2.2.5 Seepage discharge

The seepage discharge coming from the seepage chamber was measured with the help of a pair of electromagnetic flow meters installed at the downstream of the flume. The flow meters were connected through the pipes to the seepage chamber. The flow meters worked on the principle of Faradays law of electromagnetic induction. According to this principle, when a conductive medium passed through a magnetic field *B*, a voltage, E' was generated which was proportional to the velocity of the conductor, u_c , the density of the magnetic field, *B*, and the length of the conductor, *L*. In a flow meter, a current was applied to wire coils on the meter body to generate a magnetic field. The liquid flowing through the pipe acted as the conductor and induced a voltage which was proportional to the average flow velocity. The induced voltage was detected by sensing electrodes mounted in the flow meter body and sent to a transmitter which calculates the volumetric flow rate based on the pipe dimensions. Mathematically, Faraday's law can be stated as

$$E' \propto u_c.B.L \tag{2.2}$$

Figure 2.6 Electromagnetic flow meters for measuring seepage discharge

The flow meters had a control valve and a digital display which was used for applying desired percentage of seepage discharge (Figure 2.6). The seepage discharge can be estimated using the relation given below:

$$q_s = A_p u_c \tag{2.3}$$

where q_s is the seepage discharge in m^3/s, A_p is the area of pipe in m^2 and u_c is the fluid velocity through the flow meter.

2.2.6 Flow velocity

For investigating the turbulent properties of the flow, instantaneous velocities were measured. Velocity measurements were performed using a four beam down looking Vectrino+ Acoustic Doppler Velocimeter (ADV) probe manufactured by Nortek (Figure 2.7). The instrument allowed data collection at a higher sampling rate up to 200 Hz. The Vectrino uses the Doppler Effect to

measure the velocity. The Doppler Effect is the change in frequency of a wave (or other periodic event) for an observer moving relative to its source. The pitch of a sound is different when a vehicle sounding a siren approaches, passes and recedes from an observer. Compared to the emitted frequency, the received frequency is higher during the approach, identical at the instant of passing by, and lower during the recession. The change in the pitch will give an idea of how fast the vehicle is moving. The ADV used this principle to measure the velocity of water in three dimensions. The device sent out a beam of acoustic pulses at a fixed frequency from a transmitter probe. These waves bounced off of moving particulate matter in the water and three receiving probes "listened" for the change in frequency of the returned sound. The returned sound was not reflected from water. As a pulse was sent out into the flow, it intercepted ambient scatter like microbubble and suspended particle as a target. The target scattered the incident pulse in all directions, some being sent in the direction of the receiver. As far as the receiving transducer was concerned, the target had generated (by reflection) an acoustic signal that propagated from the target in a sampling volume. The ADV then calculated the velocity of the water in the *x*, *y*, and *z* directions. Additionally, the ADV allowed the measurement of the distance of the central transmitter from the boundary. The instrument collected data in a cylindrical remote sampling volume of user adjustable height located 5 cm below the central transmitter.

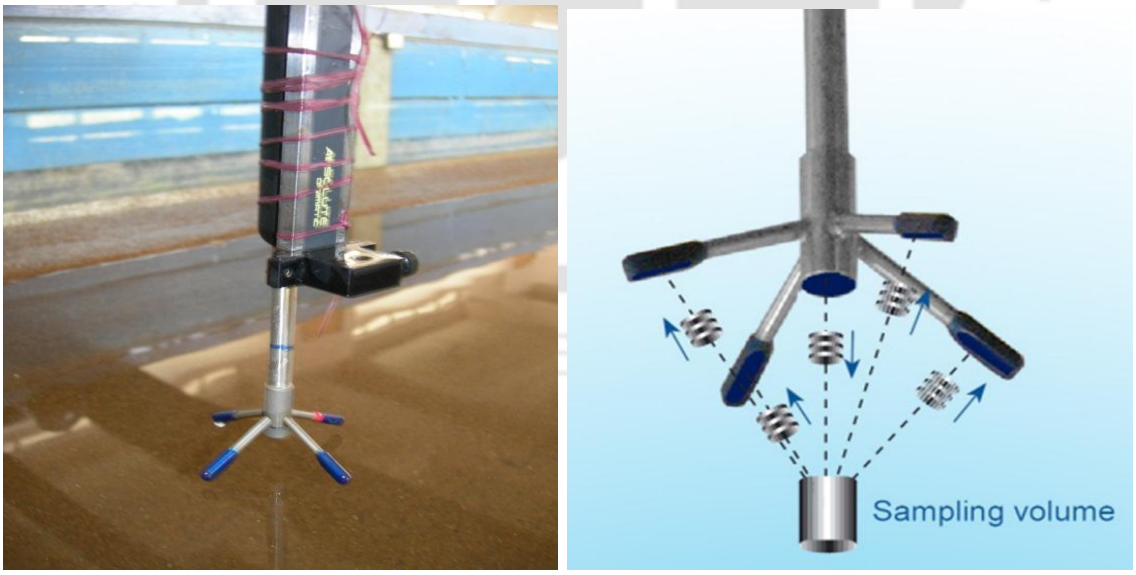

Figure 2.7 Acoustic Doppler Velocimeter for measuring instantaneous velocities

A software called Vectrino^{+} developed by Nortek was used for collecting the instantaneous velocities in the computer system. The height of the sampling volume was set at 4 mm when the measurement location was away from the bed and 1 mm when very near to the bed so that the sampling volume did not touch the particles on the bed surface. The time duration for data acquisition was 5 minutes where 40,000 samples were collected. Special care was taken to collect data with correlation >70% and signal to noise ratio (SNR) >15. Very near to the bed, slight deviation (± 5%) in the correlation was observed. In order to check the uncertainty associated with the ADV data, 16 pulses of 40000 samples for duration of 5 minutes each were collected at a location 3 mm above the bed level.

The velocity data measured by the ADV included spikes because of interference between transmitted and received signals. These data were needed to be post processed or filtered. Acceleration thresholding method (Goring and Nikora, 2002; Dey *et al*, 2012) was used for removing the spikes in the velocity data (Figure 2.8). Threshold values (1-1.5) were selected by trial and error in such a way that the power spectra for streamwise velocity in the inertial subrange yielded a satisfactory fit with Kolmogorov "-5/3 scaling law" in the inertial subrange. It is observed from Figure 2.9 that power spectra for filtered velocity pulses was in good agreement with the Kolmogorov's −5/3 law in the inertial subrange. For both no seepage as well as seepage cases, it is observed that power spectra for both no seepage and seepage runs are similar which suggests that spectra are not adversely affected by the application of seepage.

In Table 2.1, U, V and W are the time averaged velocities in streamwise, spanwise and vertical direction, u', v', and w' are the fluctuations of instantaneous streamwise velocity u, spanwise velocity v and vertical velocity w, respectively, $(u'u')^{0.5}$ is the root-mean-square (rms) of u', $(v'v')^{0.5}$ is the rms of v' and $(w'w')^{0.5}$ is the rms of w'. The time averaged velocities were estimated from the measured instantaneous velocities as given below:

$$U = \frac{1}{n}\sum_{i=1}^{n} u_i$$
$$V = \frac{1}{n}\sum_{i=1}^{n} v_i \qquad (2.4)$$
$$W = \frac{1}{n}\sum_{i=1}^{n} w_i$$

where *n* is the total number of samples.

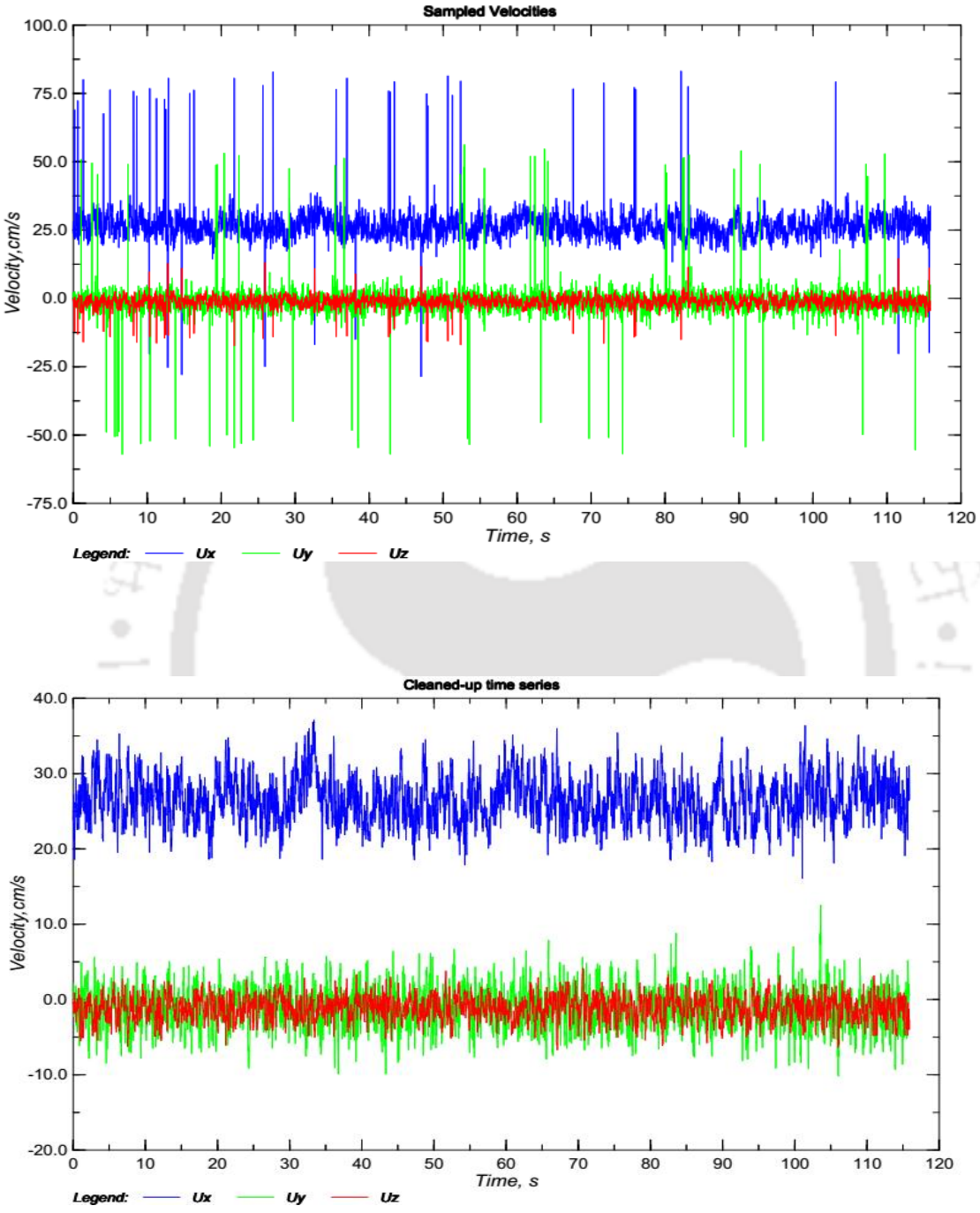

Figure 2.8 Removal of spikes in the sampled velocities data by acceleration thresholding method

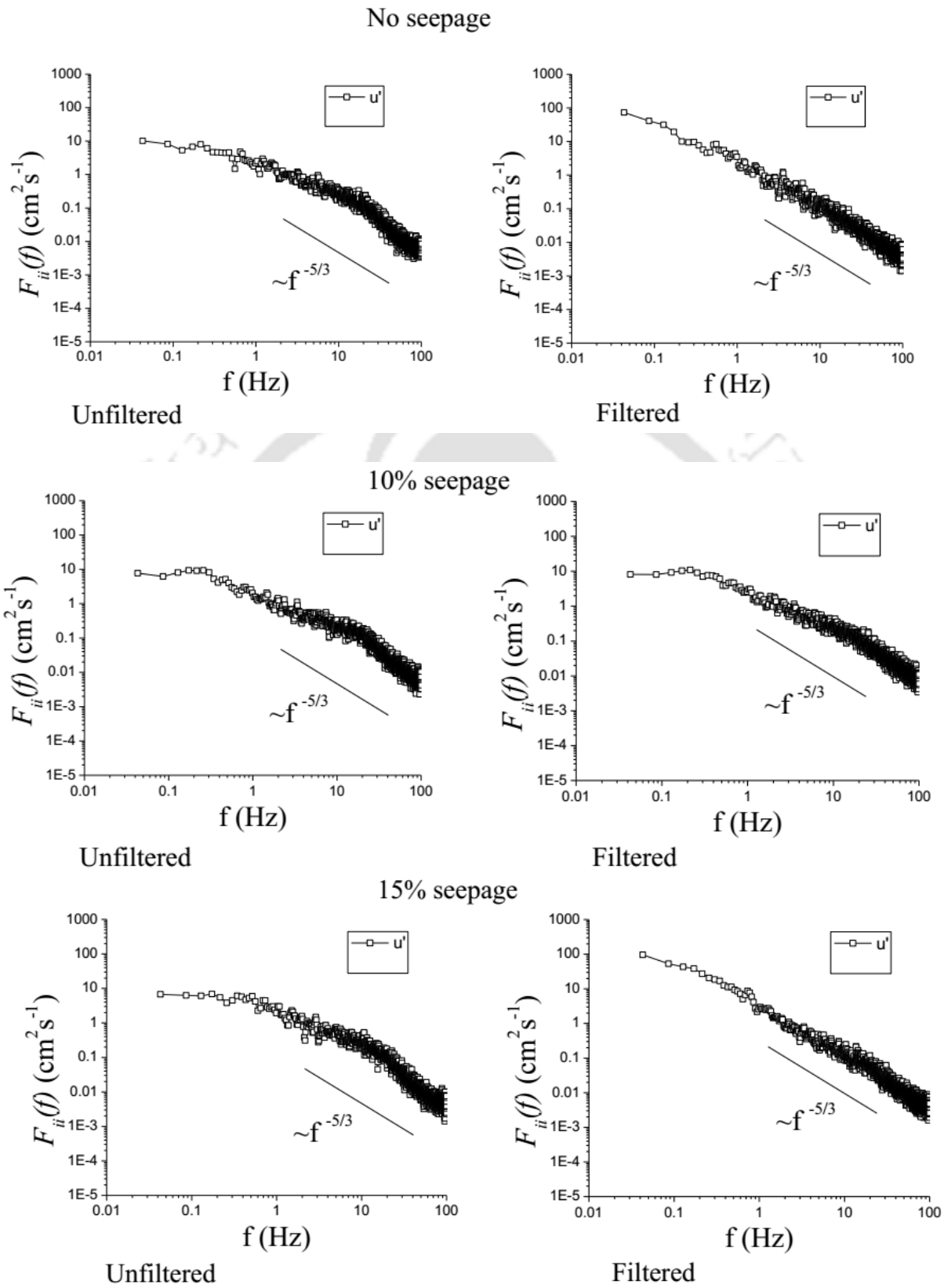

Figure 2.9 Velocity power spectra showing the fit of Kolmogorov's -5/3 scaling law

Table 2.1 Uncertainty associated with ADV data

	U (m/s)	V (m/s)	W (m/s)	$(\overline{u'u'})^{0.5}$ (m/s)	$(\overline{v'v'})^{0.5}$ (m/s)	$(\overline{w'w'})^{0.5}$ (m/s)
Standard deviation	4.34×10^{-3}	9.74×10^{-4}	4.24×10^{-4}	1.09×10^{-3}	9.04×10^{-4}	3.14×10^{-4}
Uncertainty %	0.31	0.07	0.03	0.06	0.07	0.03

2.2.7 Flow depth

The flow depth in the channel was measured with the help of a digital point gauge attached to a moving trolley (Figure 2.10). This was a direct indicating gauge which eliminated observation errors due to vernier and scale reading. It could be set to zero anywhere in the operating range to permit easy relative level checking. The liquid crystal display was easy to read and had a resolution of ±0.01mm. A quick-release mechanism permitted rapid changes of position. The depth of flow was defined as a difference between the water surface level and the bed level.

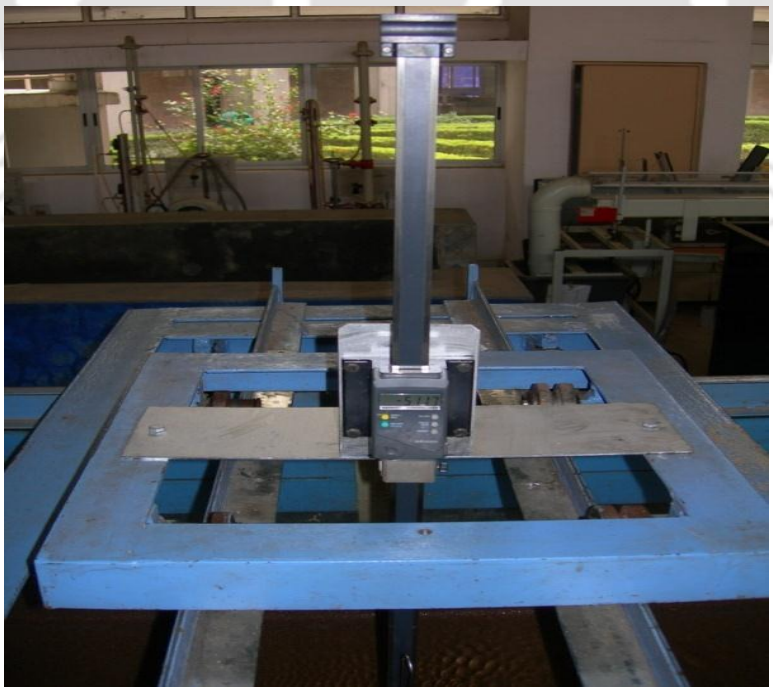

Figure 2.10 Digital Point gauge for measuring flow depth

2.2.8 Water surface elevation

Water surface slope in experiments was measured using a Pitot-static tube connected to a digital manometer which was further attached to a moving trolley. The digital manometer was powered by two batteries of 12 Volts each connected in series. The outer tube consisting of static pressure holes when connected to digital manometer gave the piezometric height at that point. Water surface slope was measured by moving the trolley in the streamwise direction. Pitot-static tube and digital manometer arrangement are shown in Figure (Figure 2.11).

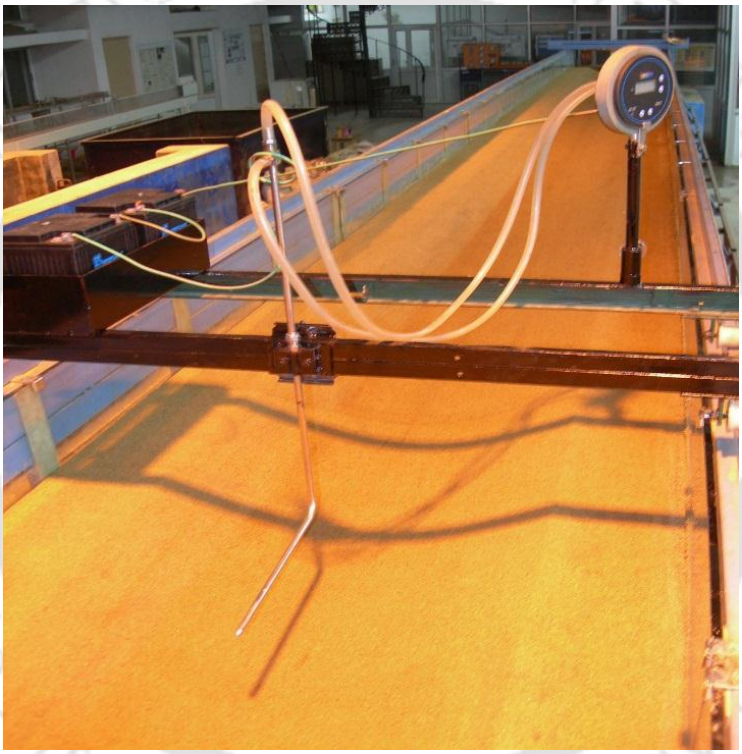

Figure 2.11 Pitot tube and digital manometer assembly for measuring water surface slope

2.2.9 Bed slope

Bed slope of the flume was measured with the help of Total Station. A Total Station was a modern electronic device that combined the ability to simultaneously measure a position horizontally and vertically. It had two components, a machine mounted on a static tripod, and a 'target' prism on a metal staff, which was moved around the site. The machine part of the Total Station had a lens

somewhat like a telescopic rifle-sight with cross-hairs which were focused on the prism. The whole instrument revolved horizontally and the lens swiveled vertically too. The Total Station was partly based on a principle used in traditional theodolites, where angles were calculated from vertical and horizontal 360-degree scales. It combined these with a device known as an Electronic Distance Measurer or EDM.

2.2.10 Temperature and Kinematic Viscosity

Average temperature of water during an experiment was recorded by Vectrino+ ADV which had a temperature sensor (thermistor), located inside the probe head. The corresponding value of kinematic viscosity (cm^2/s) was determined from standard tables.

2.2.11 Fixing of Flow depth

Large number of investigations (Jarvela, 2004; Poggi *et al*, 2004; Ghisalberti and Nepf, 2006; Liu *et al*, 2008) have been done on flow and transport phenomenon with different types of submerged vegetation but did not clearly specify the criteria for choosing the main channel flow depth. Literature on flexible vegetation (Nepf and Vivoni, 2000; Wilson *et al*, 2003; Huai *et al*, 2009) seems to suggest the ratio of flow depth to the height of submerged vegetation in the range of 1.2 to 4. Keeping the large variation existed in the literature for determining the submerged vegetation height, present work derived the main channel flow depth based on the unique relationship among uniform sand size, flow depth and discharge as per standard Shields curve or incipient motion condition.

An incipient motion criterion is generally considered for designing stable or threshold channel. Thus, in the present study the incipient motion or threshold channel criteria was used for defining the flow depth for a particular sand diameter, d_{50} =0.418 mm. Yalin's incipient motion criteria (1972) was used for the present study and it was achieved at a flow depth (H) of 12 cm when measured at the centre of the test section and discharge (Q) of 0.0326 m^3/s after verifying with the help of Shields diagram.

Yalin (1972) proposed a term 'ε_Y' in which its value determines the critical condition of bed movement. ε_Y is given by

$$\varepsilon_Y = \left(\frac{m}{At}\right)\sqrt{\frac{\rho d_{50}^{\ 5}}{\gamma_s}} \qquad (2.5)$$

where m is the number of detachments, A is the observation area, t is the time, d_{50} is the median diameter of grains, γ_s is the submerged specific weight of the grains and ρ is the mass density of the fluid. Theoretically the value of ε_Y should be zero but for practical purposes, Miller (1977) recommended a value of 10^{-6}. During experiment, it had been tried to keep the value of ε_Y as close as possible to the recommended value. Table 2.2 shows the different parameters achieved at incipient motion condition.

Table 2.2 Flow conditions at incipient motion condition

Incipient Motion run	d_{50} (mm)	***H*** (m)	***V*** (m/s)	***Q*** (m^3/s)	***Re***	***Fr***	R_*	τ_*
	0.418	0.12	0.27	0.0326	1.3×10^5	0.25	6.5432	0.0323

2.2.12 Vegetation characteristics

2.2.12.1 Vegetation material

Flexible rubber cylinders of two different diameters, 10 mm and 5 mm, were used for simulating vegetation. Oryza sativa stems were used for simulating natural vegetation cover.

2.2.12.2 Vegetation motion

For flexible vegetation, it is important to identify the plant motion. Kouwen and Unny (1973) proposed a term 'aggregate stiffness' which is the product of vegetation density (*M*) and flexural rigidity (*EI*).

MEI is estimated using the equation given below (Kouwen and Li, 1980):

$$MEI = \gamma HS\left[3.4h_v\left(\frac{h_d}{h_v}\right)^{0.63}\right]^4 \qquad (2.6)$$

where γ=specific weight of water, *H*= flow depth at no seepage or incipient motion, *S*= bed slope, h_v= total vegetation height and h_d = average deflected vegetation height. Carollo *et al* (2005) and Okatomo and Nezu (2009) classified the different flow patterns in flexible vegetated channel as erect or rigid, gently swaying or without organized motions, monami or with organized motions and prone. A flexible vegetation shows prone behaviour when the shear velocity is higher than a critical value which is estimated as (Kouwen and Li, 1980):

$$u^*_c = 0.028 + 6.33(MEI)^2 \qquad (2.7)$$

where u^*_c is expressed in m/s and MEI in N/m^2.

In the present study, $u^* < u^*_c$ and hence the vegetation did not show prone configuration. Additionally, *monami* occurs at $\frac{u^*}{u^*_c} \geq 0.75$ whereas swaying occurs at lower friction velocity (Okamoto and Nezu, 2010). The flow pattern in the present study was gently swaying.

2.2.13 Experimental Program

The experimental program consisted of four test series in which three test series were conducted on flow characteristics with artificial vegetation and the remaining on flow characteristics with natural vegetation. The flow depth and flow discharge were kept same for all test series. Different types and characteristics of vegetation were used. Experiments were conducted for no-seepage, 10% seepage and 15% seepage. The arrangement of vegetation for different test series are given below:

2.2.13.1 Uniformly distributed vegetation patches

The vegetation area was modeled using the 10 mm diameter flexible cylinders. The submerged heights of vegetation (h_v) were kept as 8 cm and 6 cm (ratio of flow depth to vegetation height are 1.5 and 2, which lies in the range suggested).

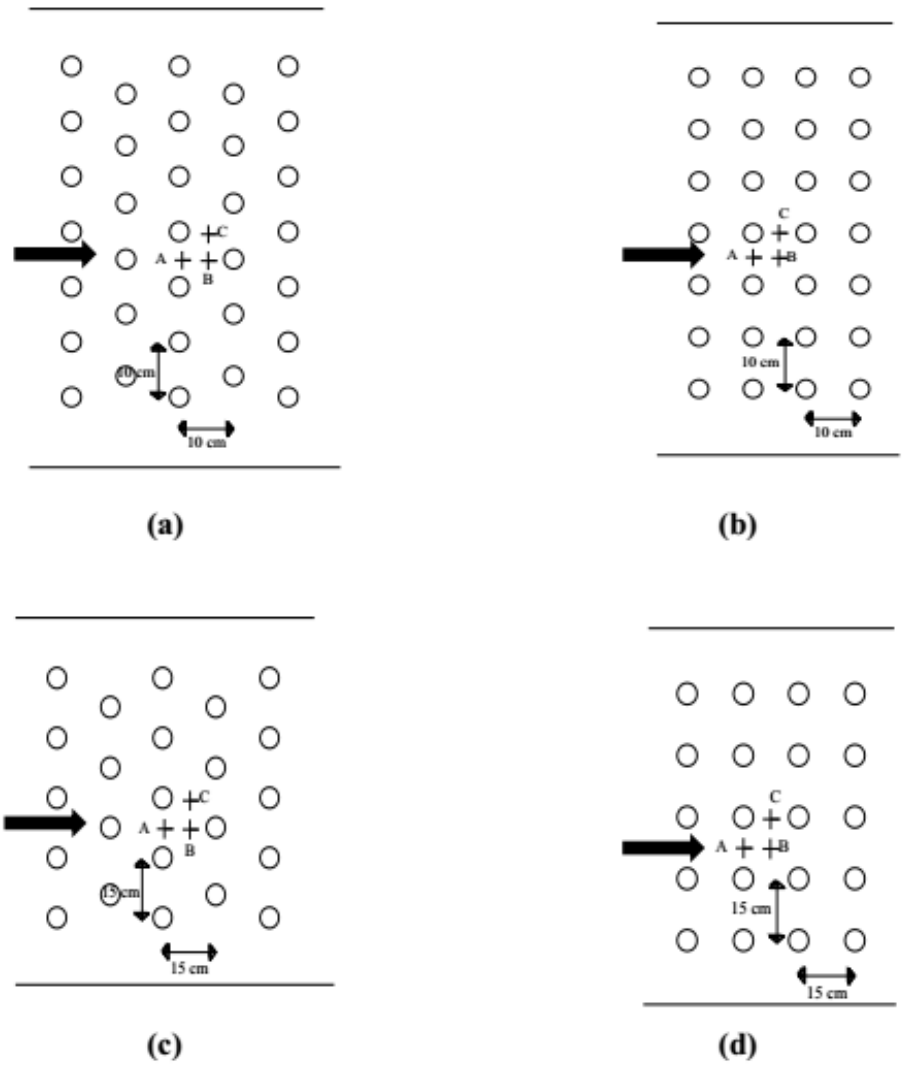

Figure 2.12 Locations of velocity profile measurements (a) Staggered at s_v=10 cm (b) Uniform at s_v=10 cm (c) Staggered at s_v=15 cm (d) Uniform at s_v=10 cm

Figure 2.13 Photographs showing the placing of cylinder stems as artificial vegetation (a) staggered (b) uniform

Two different patterns of placing the vegetation stems were selected for investigating the change in flow characteristics with change in pattern of placing vegetation. The vegetation stems were placed in a staggered pattern as well as uniform pattern at an equal spacing (s_v) of 15 cm and 10 cm. The measurement zones were set at upstream (8.5 m), centre (7m) and downstream (5.5 m) test section. At each measurement zone, a specific measurement location was selected which was same for all the measurement zones so that the effect of downward seepage could be derived (Figure 2.12). Figure 2.13 shows the photographs taken after placing the vegetation stems. The experimental parameters for the particular study on uniformly distributed vegetation stems are shown in table 2.3.

Table 2.3 Experimental conditions for uniformly distributed vegetation stems

No.	h_v (m)	h_d (m)	H (m)	Pattern	d_v (m)	s_v (m)	S	% of seepage
1	0.08	0.04	0.12	Staggered	0.01	0.15	0.0015	0
2	0.08	0.04	0.12	Staggered	0.01	0.15	0.0015	10
3	0.08	0.04	0.12	Staggered	0.01	0.15	0.0015	15
4	0.08	0.04	0.12	Staggered	0.01	0.10	0.0015	0
5	0.08	0.04	0.12	Staggered	0.01	0.10	0.0015	10
6	0.08	0.04	0.12	Staggered	0.01	0.10	0.0015	15
7	0.08	0.04	0.12	Uniform	0.01	0.15	0.0015	0
8	0.08	0.04	0.12	Uniform	0.01	0.15	0.0015	10
9	0.08	0.04	0.12	Uniform	0.01	0.15	0.0015	15
10	0.08	0.04	0.12	Uniform	0.01	0.10	0.0015	0
11	0.08	0.04	0.12	Uniform	0.01	0.10	0.0015	10
12	0.08	0.04	0.12	Uniform	0.01	0.10	0.0015	15
13	0.06	0.031	0.12	Staggered	0.01	0.10	0.0015	0
14	0.06	0.031	0.12	Staggered	0.01	0.10	0.0015	10
15	0.06	0.031	0.12	Staggered	0.01	0.10	0.0015	15

For same channel discharge Q (no seepage) = 0.0326 m^3/s.

2.2.13.2 Mixed vegetation patches

Six runs were carried out for the present study where three runs were conducted when 5 mm d_v and 10 mm d_v were placed at the upstream half section and downstream half section respectively and the remaining three runs vice versa. The vegetation cylinders were placed in staggered pattern and the centre to centre spacing (s_v) were fixed at $10d_v$ (where d_v is in cm) for the entire test section (Figures 2.14 and 2.15) giving rise to different vegetation densities for different vegetation diameter (vegetation density of 10 mm d_v =120 stems/m^2 and vegetation density of 5 mm d_v = 430 stems/m^2). For all the experiments, measurements were taken at three locations, viz. upstream, centre and downstream, along centre line of the vegetation zone or test section (Figure 2.14a and 2.15a). Table 2.4 shows the experimental conditions.

(a)

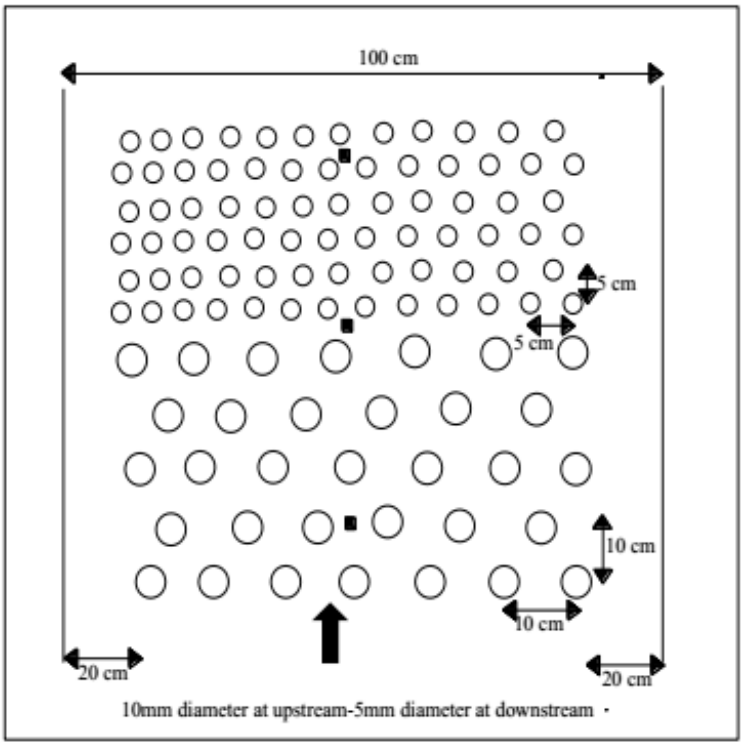

(b)

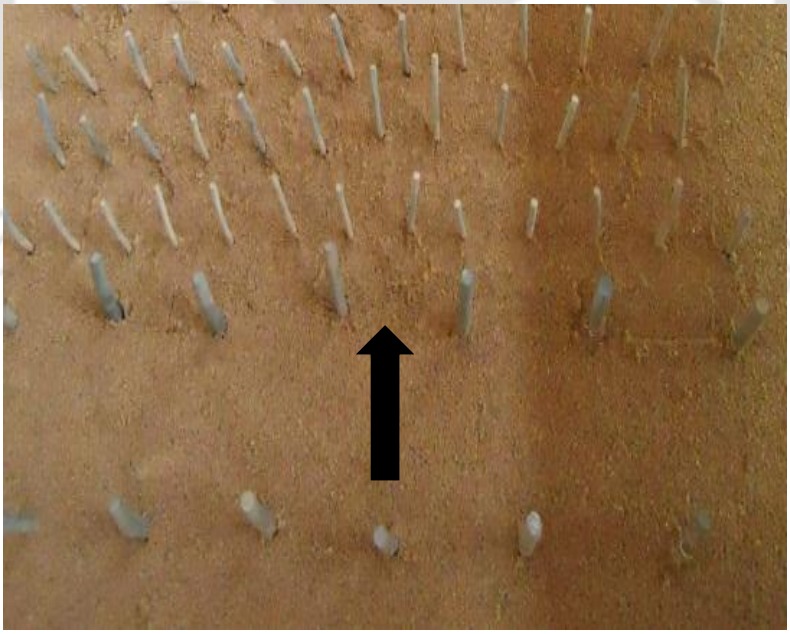

Figure 2.14 Mixed vegetation pattern of placing 10 mm diameter upstream and 5 mm downstream

(a)

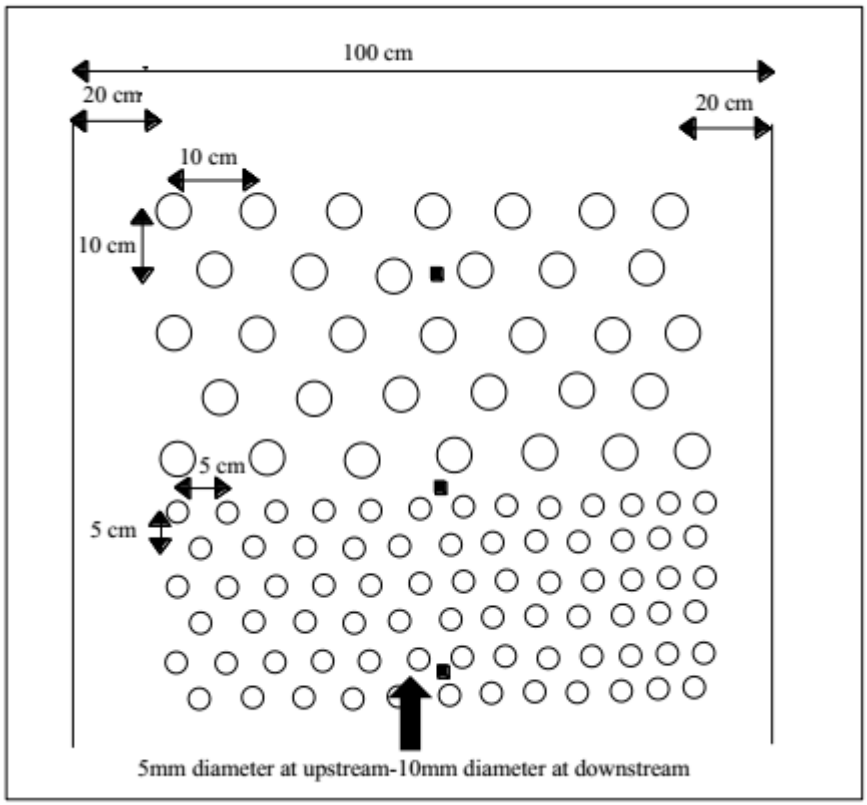

(b)

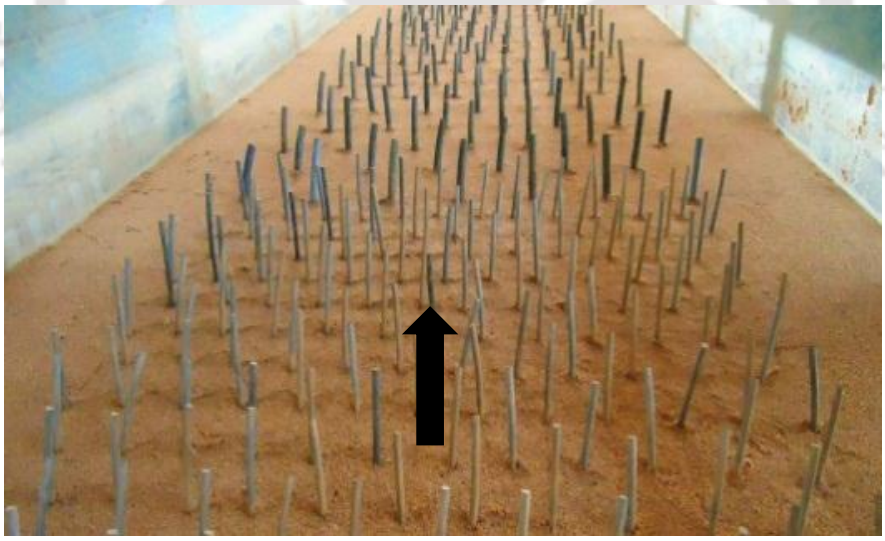

Figure 2.15 Mixed vegetation pattern of placing 5 mm diameter upstream and 10 mm downstream

Table 2.4 Experimental conditions for mixed *vegetation patches*

No.	h_v (m)	h_d (m)	H (m)	**Pattern**	S	**% of seepage**
1	0.06	0.0456	0.12	5mm upstream- 10 mm downstream	0.0015	0
2	0.06	0.0456	0.12	5mm upstream- 10 mm downstream	0.0015	10
3	0.06	0.0456	0.12	5mm upstream- 10 mm downstream	0.0015	15
4	0.06	0.0456	0.12	10mm upstream- 5 mm downstream	0.0015	0
5	0.06	0.0456	0.12	10mm upstream- 5 mm downstream	0.0015	10
6	0.06	0.0456	0.12	10mm upstream- 5 mm downstream	0.0015	15

For same channel discharge Q (no seepage) = 0.0326 m^3/s.

2.2.13.3 Vegetation bundles

Flexible rubber cylinders of diameter (d_v) 4 mm and height (h_v) 4 cm were used for simulating vegetation. Single rubber cylinders were combined to a group of three to imitate a vegetation patch. The vegetation patches were placed in staggered pattern (Figure 2.16). The deflected vegetation height (h_d) lies in 3-3.8 giving an average value of 3.5 cm. Two different centre-centre spacing (s_v) were adopted, 10 cm and 15 cm, in which the vegetation stems were placed equally in both lateral as well as streamwise directions for the entire vegetation zone. For all the experiments, measurements were taken at the upstream (8.5 m), centre (7.0 m) and downstream (5.5 m) vegetation zone or test section (Figure 2.16(a)). The experimental conditions are given in table 2.5.

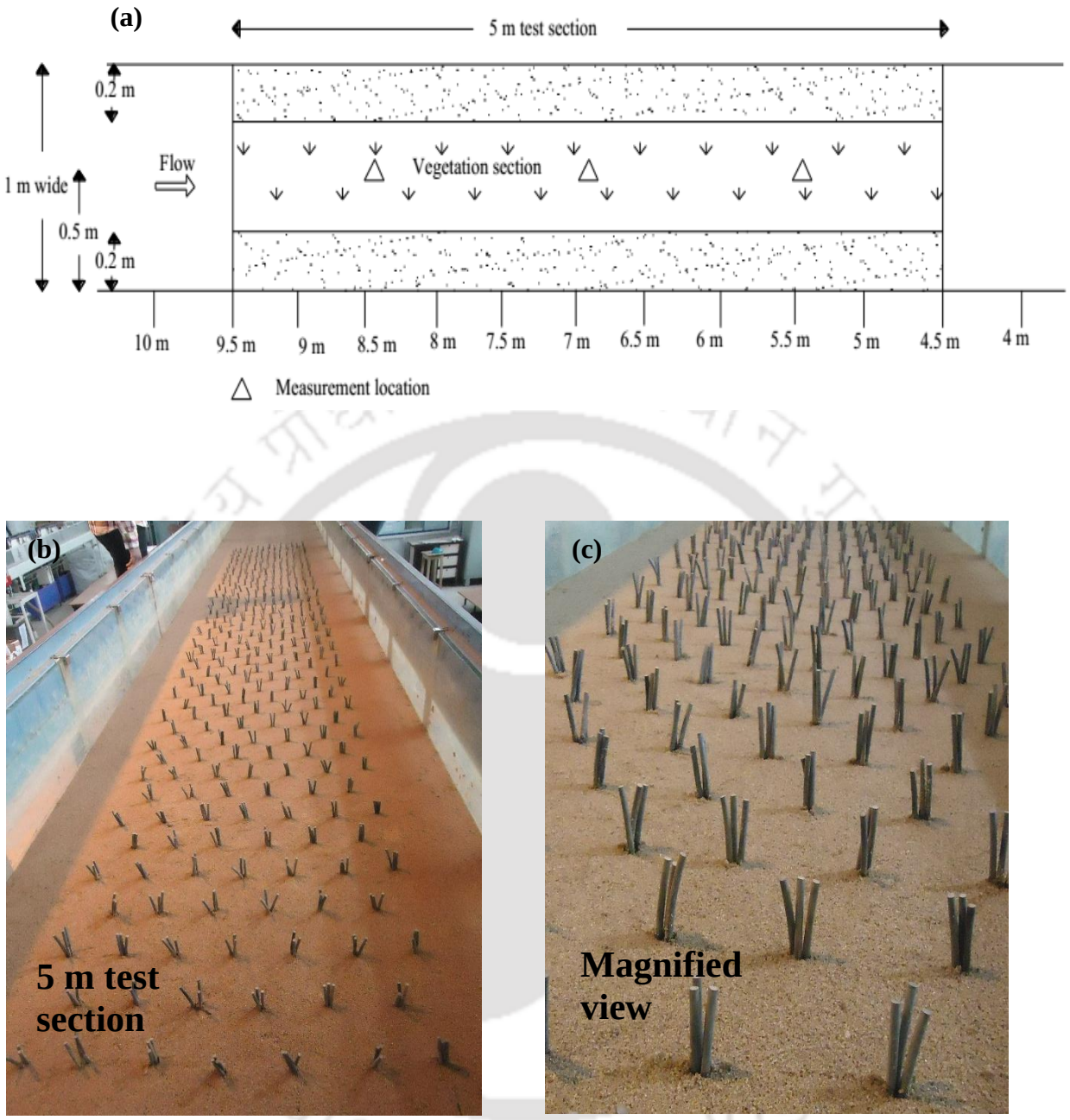

Figure 2.16 Experimental set-up (a) Test section with measurement locations (b) Photograph taken after placing of vegetation patches (c) Magnified view of vegetation patches

Table 2.5 Experimental conditions for vegetation bundles

No.	***H*** (m)	h_v (m)	h_d (m)	***Pattern***	s_v (m)	***S***	***% of seepage***
1	0.12	0.04	0.035	Staggered	0.15	0.0015	0
2	0.12	0.04	0.035	Staggered	0.15	0.0015	10
3	0.12	0.04	0.035	Staggered	0.15	0.0015	15
4	0.12	0.04	0.035	Staggered	0.10	0.0015	0
5	0.12	0.04	0.035	Staggered	0.10	0.0015	10
6	0.12	0.04	0.035	Staggered	0.10	0.0015	15

For same channel discharge Q (no seepage) = 0.0326 m^3/s.

2.2.13.4 Natural vegetation (Fully covered)

The vegetation zone was located in the middle of the flume covering an area of 5m long and 1 m wide (Figure 2.17). The flow depth was kept higher than the height of the vegetation. The height of the vegetation (h_v) was 4 cm and the deflected vegetation height lies in the range of 3-3.5 cm (average deflected vegetation height, h_d =3.25 cm). Natural rice stems (*Oryza sativa*) were planted for the whole test section of the flume at a vegetation density of 560 stems/m^2 to simulate a fully submerged canopy. For all the experiments, measurements were taken at the upstream section, centre of the vegetation section and downstream section for studying the spatial distribution of flow characteristics (Figure 2.17a).

2.2.13.1 Natural vegetation (Partly covered)

The vegetation zone was positioned in the middle of the flume covering an area of 5m long (starting from upstream 9.5 m to 4.5 m as demarcated on the flume) and 0.5 m wide (Figure 2.18). Natural rice stems (*Oryza sativa*) were planted for laterally half of the flume in a staggered pattern for submerged condition at 10 cm centre-centre. Three to four rice stems were bound into a bundle to simulate a vegetation stem of average diameter of around 10 mm (Figure 2.18b). For submerged vegetation, the deflected height of the vegetation (h_d) was found to be in the range of 3.0-3.7 cm (average deflected vegetation height of 3.3 cm).

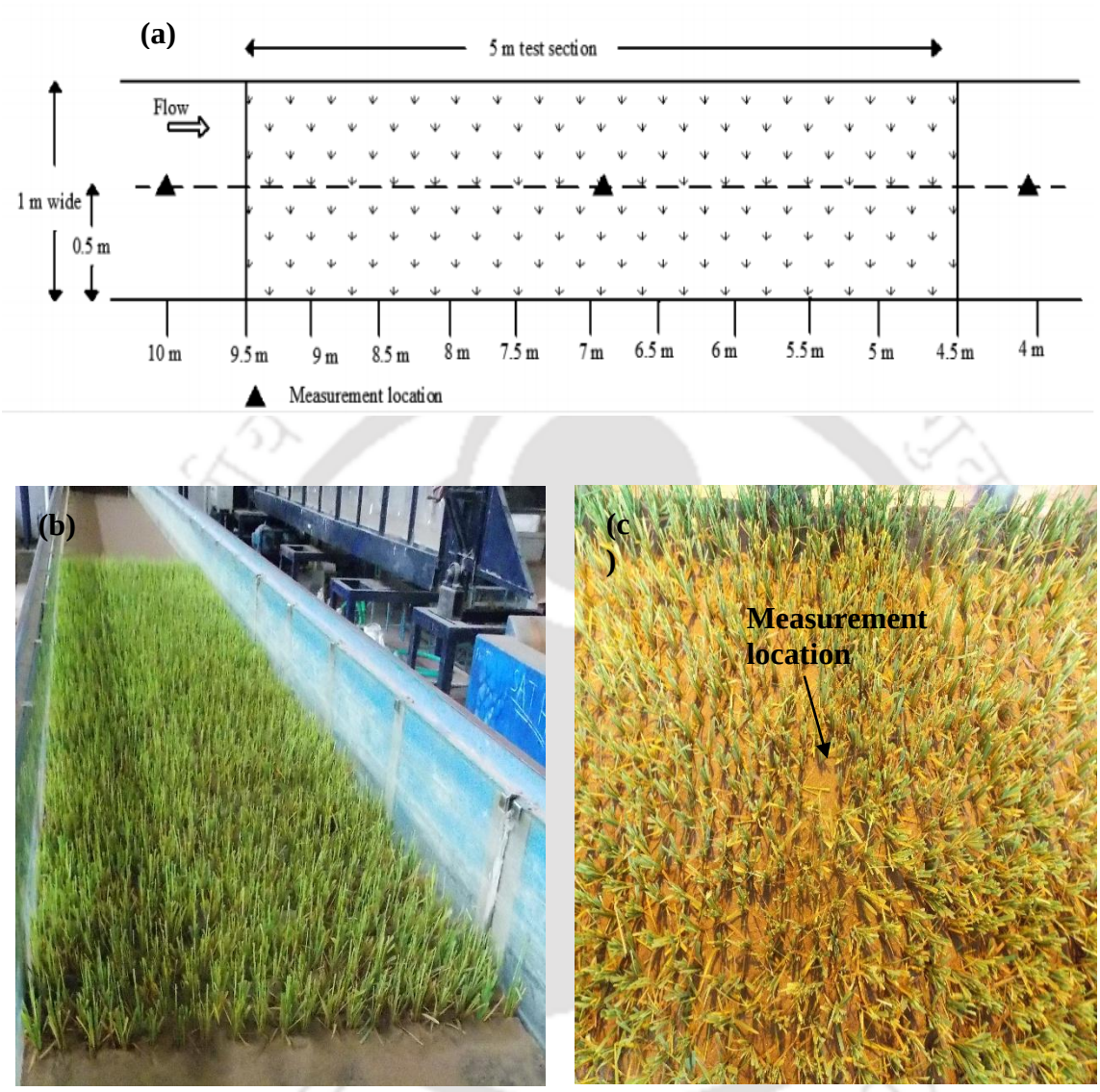

Figure 2.17(a) Plan view of test section (b) Photograph taken after placing vegetation (c) Photograph showing the measurement location

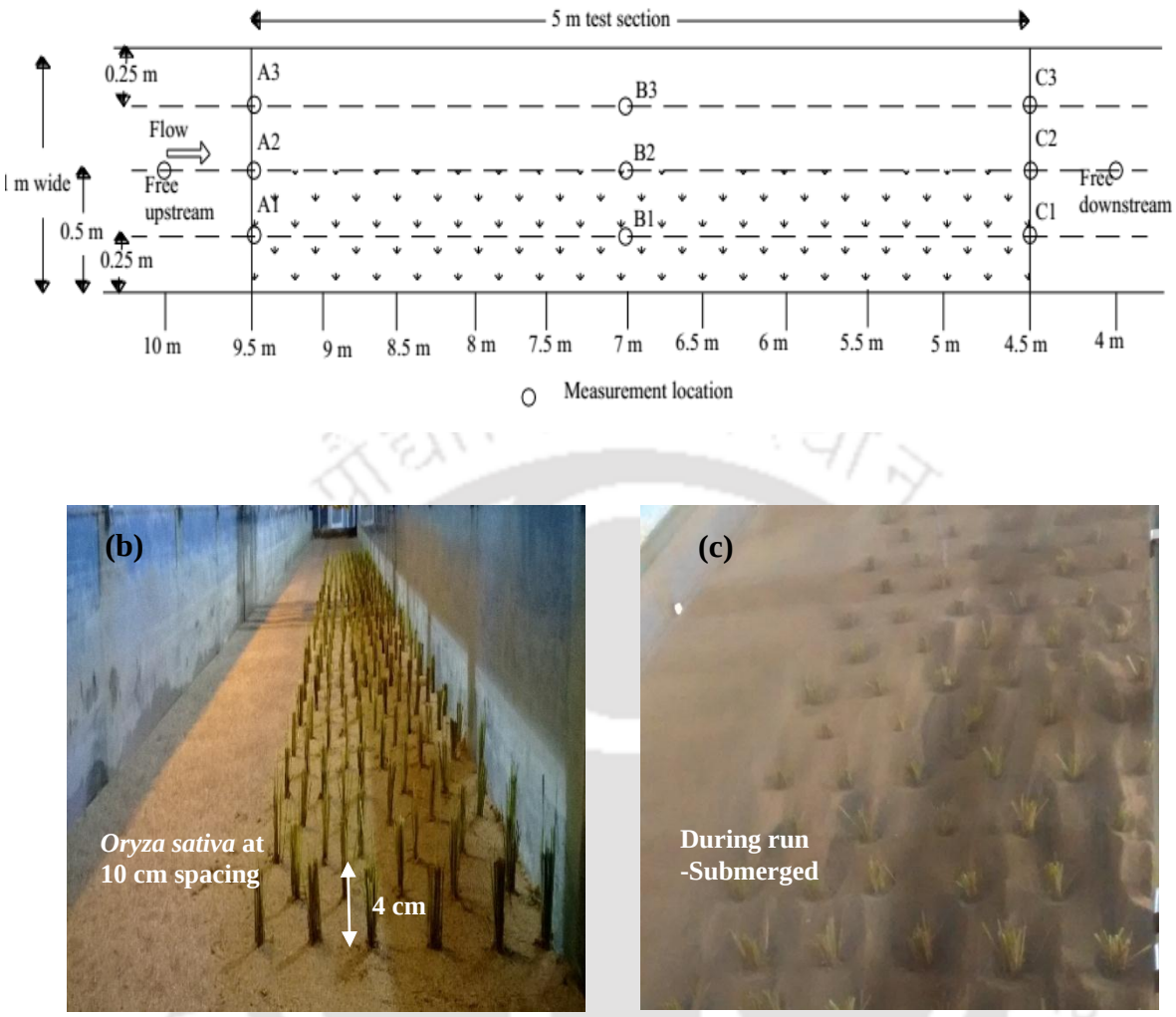

Figure 2.18 (a) Plan view of test section and photographs taken after placing of rice stems (a) before run (b) During run showing the submerged condition

For all the experiments of partially covered, measurements were taken at the vegetation section, interface of the vegetation and plane bed or un-vegetated section and un-vegetated section. For studying the spatial distribution of flow characteristics, 11 measurement locations were decided (Figure 2.18a); free upstream, free downstream, upstream, centre and downstream of vegetation section (A1, B1 and C1), interface section (A2, B2 and C2) and unvegetated section (A3, B3 and C3). Table 2.6 shows different experimental parameters for the study.

Table 2.6 Experimental conditions for natural vegetation cover

No.	***H*** (m)	h_v (m)	h_d (m)	***Pattern***	***S***	***% of seepage***
1	0.12	0.04	0.0325	Fully covered	0.0015	0
2	0.12	0.04	0.0325	Fully covered	0.0015	10
3	0.12	0.04	0.0325	Fully covered	0.0015	15
4	0.12	0.04	0.033	Partly covered	0.0015	0
5	0.12	0.04	0.033	Partly covered	0.0015	10
6	0.12	0.04	0.033	Partly covered	0.0015	15

For same channel discharge Q (no seepage) = 0.0326 m^3/s.

3 Flow characteristics in a channel covered with uniformly distributed vegetation[i,ii]

3.1 Introduction

Turbulent flow of water through vegetation is a very complex phenomenon. Until the 1960's, it was believed that a single resistance coefficient such as Manning's *n* could adequately describe the resistance effects caused by vegetation. Empirical curves were developed that related *n* to the product of the average velocity and the hydraulic radius (Palmer, 1945). It is widely accepted today that a single resistance coefficient cannot adequately describe submerged flow through vegetation. To effectively model flows containing vegetation, we must understand how the presence of vegetation affect the mean velocity profile and the turbulence structure. Vegetation on river beds absorbs pollutants in the channels and provides habitat for aquatic animals. Although river vegetation plays an important role in the river ecosystem, research on aquatic vegetation within the framework of river mechanics has been limited. During the last few decades, there has been a great deal of studies employing various approaches for predicting velocity distribution and turbulence properties, and hence overall hydraulic resistance. A number of these studies attempted to describe the whole velocity profile covering both vegetation canopy and overlying flow regions (Nepf and Ghisalberti, 2008; Katul *et al*, 2002), while other studies have focused on specific segments, e.g., the overlying flow region (Kouwen *et al*, 1969; Stephan and Gutknecht, 2002) or a region within the vegetation (Inoue, 1963). It is therefore useful to conduct further research that will broaden our understanding of the effect of aquatic vegetation on river flow patterns and sediment behavior. Unlike flow characteristics in open channels without vegetation, the flow velocity distribution with vegetation is not subject to the exponential rule, and anisotropy is significant (Wu, 2007). Experiments by Lü (2008) showed that the flow velocity distribution is

[i] Devi, T. B., & Kumar, B. (2015). Turbulent flow statistics of vegetative channel with seepage. *Journal of Applied Geophysics*, *123*, 267-276.

[ii] Devi, T. B., & Kumar, B. (2016). Channel Hydrodynamics of Submerged, Flexible Vegetation with Seepage. *Journal of Hydraulic Engineering*, 04016053.

uniform along the water depth direction in open channels with emergent rigid vegetation. Li and Shen (1973) suggested that the vegetation arrangement on the river bed affects the sediment transport rate. Less sediment is transported when plants are arranged in a staggered pattern, as compared with the traditional parallel pattern. Wang and Wang (2010) found that vegetation increases the deposition of suspended sediment in water. This chapter presents the results of velocity profiles and turbulence characteristics in a uniformly distributed vegetation stems. The change in flow conditions with the application of downward seepage is noted. It discusses the effect of vegetation height, vegetation spacing and pattern of placing the vegetation element on flow characteristics.

3.2 Velocity

The presence of vegetation in a channel affects the flow characteristics. The transition from sand bed to the vegetated bed leads to the development of a new boundary layer. Figure 3.1 below shows the distribution of streamwise component of velocity at the upstream, centre and downstream vegetation sections. For no-seepage case, the velocity profile over flexible vegetation is similar to the profile found out by previous investigators (Righetti, 2008; Chen *et al*, 2011; Li *et al*, 2014). For experiments on plane mobile bed (Chen and Chiew, 2004; Dey and Nath, 2009; Dey *et al*, 2012), the flow velocity is logarithmic while with vegetation, it is a different case where the flow region in the vegetation zone is reduced because of the drag imposed by vegetation.

For each of the velocity distributions, vegetation height is found to influence the flow characteristics, flow velocity is reduced near the vegetation top. The average deflected vegetation height of 0.08 m is 0.04 m and hence an inflection occurs near $z/H \cong 0.33$ and for 0.06 m vegetation height, the average deflected vegetation height is 0.031m ($z/H \cong 0.26$).

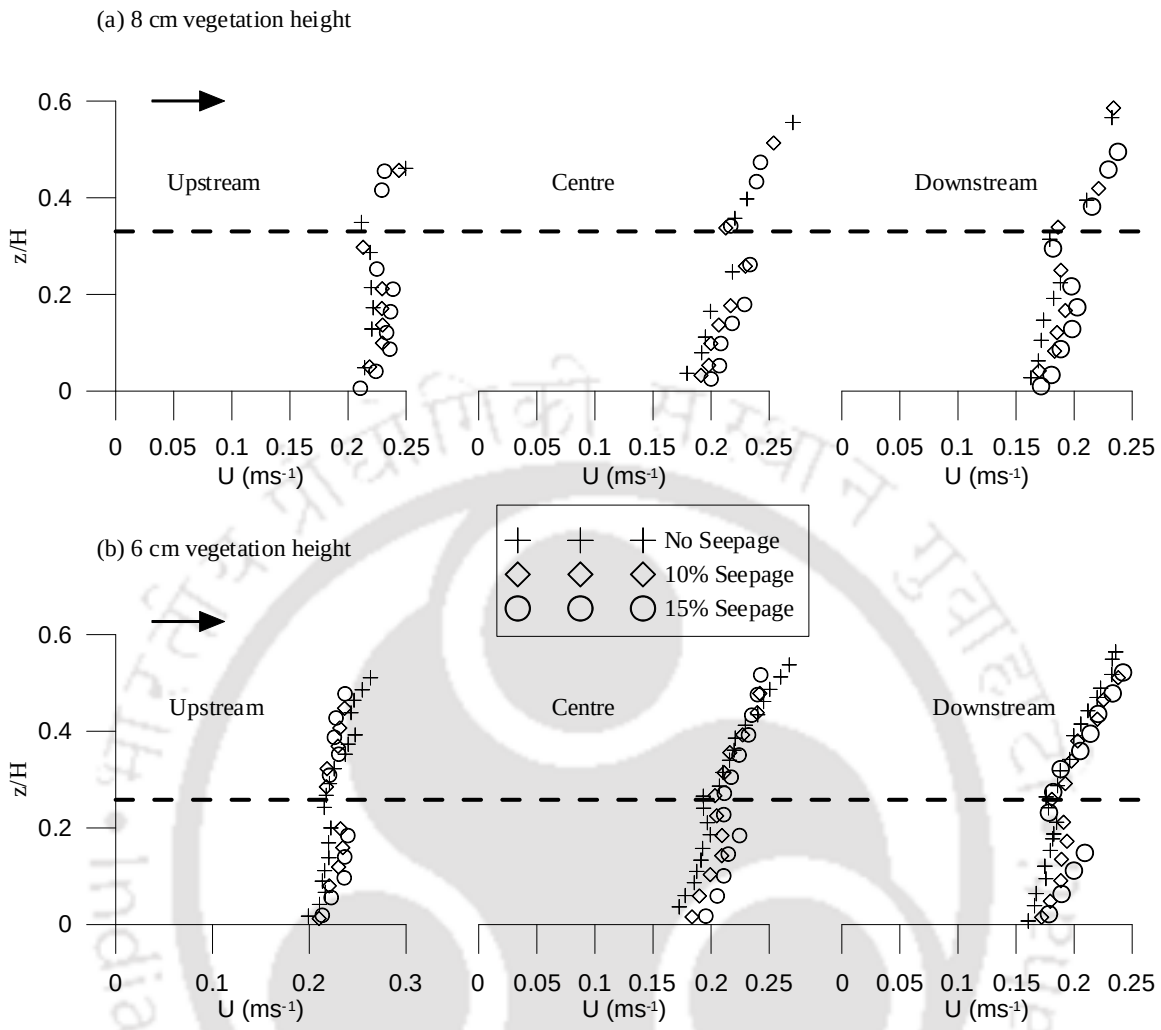

Figure 3.1 Velocity profiles at upstream, centre and downstream for No-seepage, 10% Seepage and 15% seepage (a) 8 cm vegetation height (b) 6 cm vegetation height (Dashed line shows the top of the deflected vegetation height)

As seen from figure 3.1, flow velocity decreases toward the top of the vegetation for no-seepage, 10% seepage and 15% seepage cases. The vegetation stems induce a drag because of which it resists the flow and hence velocity is lower in the lower layer. On observing the streamwise variation of velocity, it is noted that velocity decreases along the channel length. The resistance offered by the vegetation stems increases as the flow goes downstream. After the application of downward seepage, it is found that velocity at the downstream is lower than the upstream which shows that vegetation is still effective in reducing the flow velocity as it goes downstream.

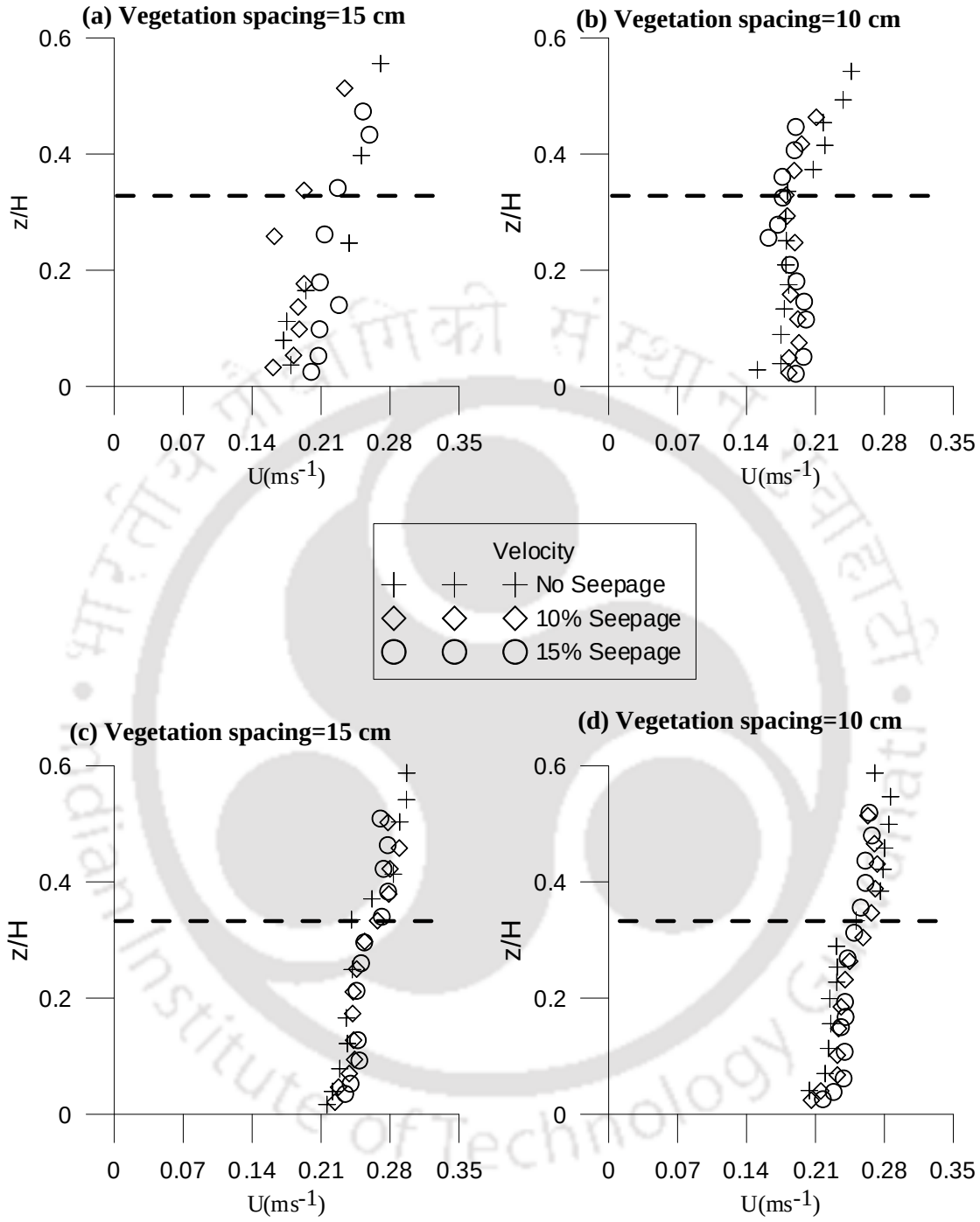

Figure 3.2 Velocity profiles of staggered (a, b) and uniform pattern (c, d) for no-seepage, 10% seepage and 15% seepage (Dashed line shows the top of the vegetation element) for 8 cm vegetation height

On comparing the staggered as well as uniform pattern, at the measurement location, higher velocity is achieved for uniform pattern than staggered pattern (Figure 3.2). For the staggered pattern, there is the presence of vegetation stems in front and behind of A from which the stem induces the drag and hence the velocity is lowered. While for uniform pattern, there is no vegetation stem in front and behind of A and hence the velocity is measured in the unobstructed region. The velocity in the free stream region is higher than the velocity measured in line with the vegetation stems (Liu *et al*, 2008). The effect of vegetation spacing on flow velocity is noted. 15 cm vegetation spacing has higher flow velocity than 10 cm vegetation spacing. Lesser vegetation spacing means more vegetation density leading to more resistance to flow thereby reducing the flow velocity.

The presence of downward seepage brought to a change in flow discharge and momentum transfer and hence the velocity distribution is modified. It is known that when downward seepage occurs in a channel, the velocity profile shifts downwards because of which the velocity near the bed increases. When water is drawn through the bed, it leads to a change in boundary shear stresses. The increase in velocity and bed shear stress leads to more sediment movement near the bed. From the figures 3.1 and 3.2, it can be seen that the presence of seepage leads to an increase in velocity near the bed, when 10% and 15% seepage percentages are applied, as compared to no-seepage case. Irrespective of the vegetation pattern and spacing, a higher velocity zone exists in the lower flow region or the near bed region. Velocity increases on an average value of 8 % with the application of 10% seepage. It is also observed that in the lower flow region the velocity for 15% seepage case is slightly higher, with an average increasing value of 5%, than the velocity for 10% seepage. This shows that the application of downward seepage leads to an increase in the velocity in the vegetation zone.

3.3 Reynolds Stress

Vegetation in the flow is regarded as a type of roughness with a large scale and hence regarded as parts of roughness resistance of riverbeds while the flow above the vegetation is regarded as the flow on the riverbed. It is assumed that the Reynolds Stress ($\tau_{xz} = \overline{u'w'}$) of the flow on the ordinary

bed and at the top of the vegetation follows a linear law having a maximum value at the top of the vegetation.

$$\rho u_*^2 (1-\frac{z}{H}) = -\rho \overline{u'w'}$$

$$(1-\frac{z}{H}) = \frac{-\overline{u'w'}}{u_*^2} \qquad (3.1)$$

For experiments on plane mobile bed (Chen and Chiew, 2004; Dey and Nath, 2009; Dey *et al*, 2012), maximum Reynolds stress occur near the bed highlighting the importance of channel bed in turbulence production but for vegetated flows, the position of maximum Reynolds stress is no longer the channel bed. Because of the difference in velocity just above and below the vegetation layer, momentum exchange takes place at the interface or top of the vegetation which leads to the formation of shear layer. The presence of shear layer leads to the production of oscillations near the vegetation top. These oscillations are responsible for exchange of mass and momentum between the lower or vegetated layer and upper or surface layer. Thus, vertical distribution of Reynolds stresses have been calculated inorder to describe the momentum diffusion mechanism.

Figure 3.3 shows different distributions of Reynolds stress at three different streamwise distances (upstream, centre and downstream) for 8 cm and 6 cm vegetation heights. It is observed that Reynolds stress is increased from the water surface towards the location where vegetation is present and reached a maximum value near the top of the vegetation. After attaining a maximum value near the top of the vegetation, it decreased towards the bed. More turbulence is created by oscillation at the top of the vegetation. This in turn leads to occurrence of more momentum exchange near the top of the vegetation and ultimately results in more Reynolds stress at that location. While in the downside of the vegetated layer the oscillations are obstructed by the vegetation stems. Therefore, the diminishing nature of Reynolds stress is attributed to the fact that the farther the location from the top of the vegetation, the smaller is the oscillations.

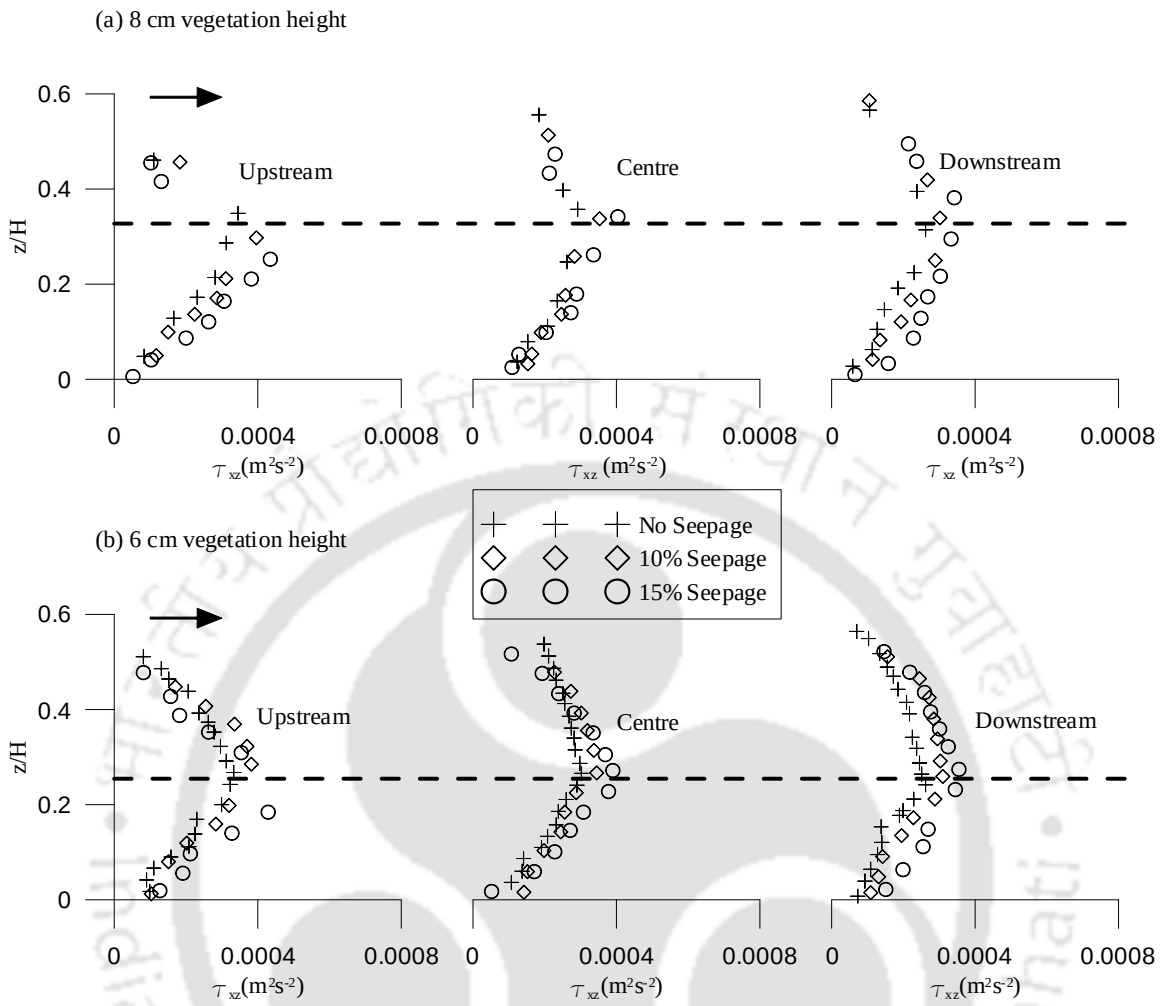

Figure 3.3 Reynolds stress profiles at upstream, centre and downstream for No-seepage, 10% Seepage and 15% seepage (a) 8 cm vegetation height (b) 6 cm vegetation height

It is already found from previous studies that presence of downward seepage increases the bed shear stress thereby increasing the sediment movement or transport. Downward seepage increases the maximum Reynolds stress at no seepage by a percentage increase of 18% (average value for upstream, centre and downstream) for 10% seepage and average of 31% for 15% seepage for 8 cm vegetation height. For 6 cm vegetation height, it is increased by an average value of 16% at 10% seepage and 30% at 15% seepage. The increase in Reynolds stress is attributed to the local effect imposed by the vegetation stems in the occurrence of erosion and deposition around it.

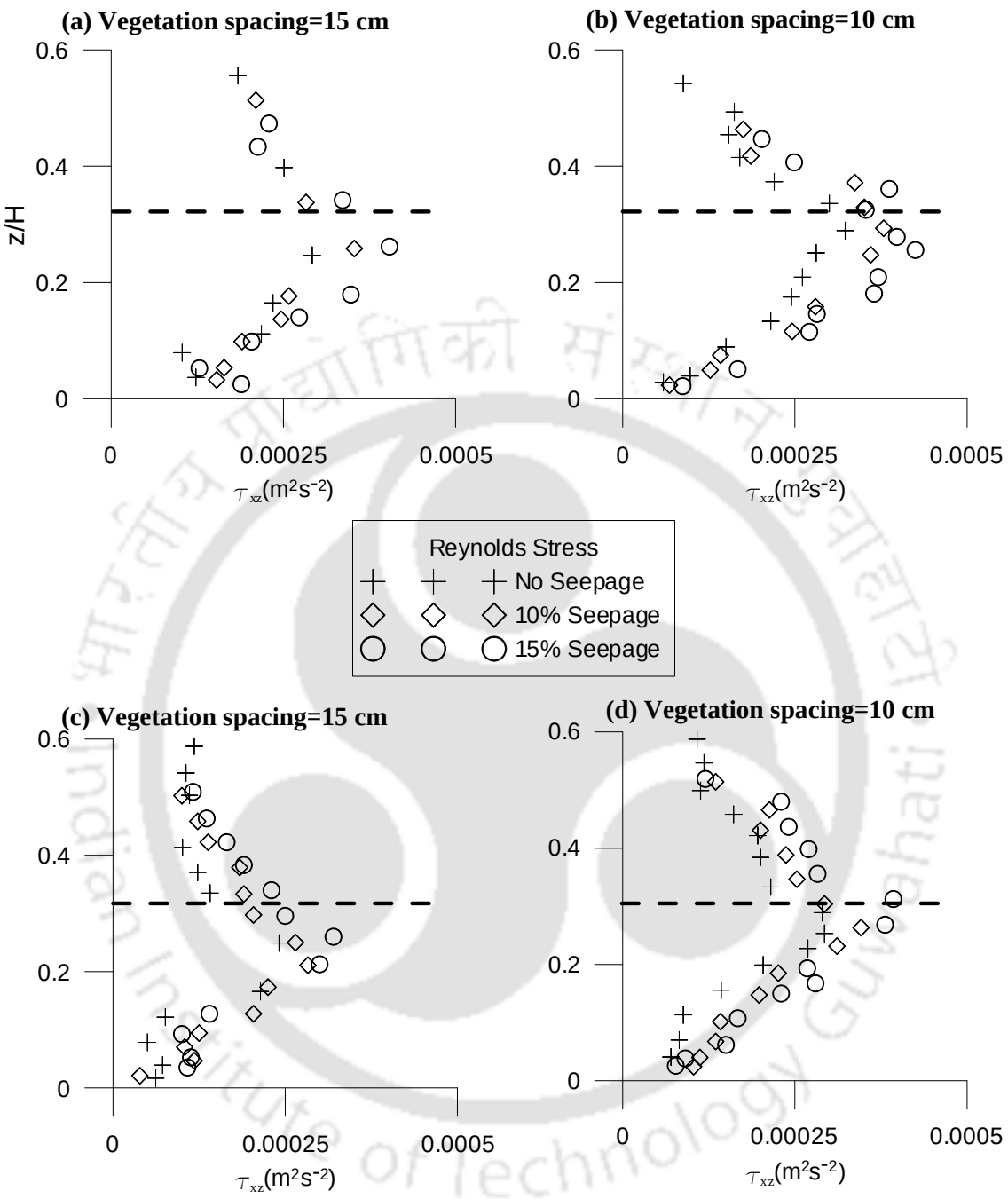

Figure 3.4 Reynolds stress profiles of staggered (a, b) and uniform pattern(c, d) for no-seepage, 10% seepage and 15% seepage

The maximum Reynolds stress, on an average for 8 cm vegetation height and 6 cm vegetation height, at the upstream measurement location are 14% higher than the centre location and 29%

higher than the downstream measurement location (for no seepage). A noteworthy point is that even with the application of downward seepage the maximum Reynolds stress at the upstream is always higher than the downstream measurement location (an average approx. value of 12% for centre location and 15% for downstream location) which signifies the importance of using vegetation as a part of river restoration programme. For both staggered and uniform pattern, 10 cm vegetation spacing has a higher value of Reynolds stress than 15 cm (Figure 3.4). Lesser vegetation spacing or more vegetation density has more resistance to flow leading to more shear in flow. Therefore more Reynolds stress is achieved for 10 cm than 15 cm. For both the pattern and spacing, the maximum Reynolds stress near the vegetation top is increased to an average value of 18% from no-seepage to 10% seepage and 13% from 10% seepage to 15% seepage.

3.4 Turbulence Intensities

Turbulence intensity is generally calculated to obtain information regarding contribution of fluctuating components of velocity to the turbulence production. It is defined as:

$$\sigma_u = \sqrt{\frac{\sum_1^n (u-U)^2}{n-1}} \tag{3.2}$$

$$\sigma_w = \sqrt{\frac{\sum_1^n (w-W)^2}{n-1}} \tag{3.3}$$

where u and w are the instantaneous velocity components in streamwise and vertical directions, U and W are the time-averaged velocity components in streamwise and vertical directions and n is the number of velocity samples recorded. σ_u and σ_w of 8 cm and 6 cm vegetation heights are plotted for no-seepage, 10% seepage and 15% seepage and shown in figure 3.5 below. All the turbulence intensities reach a maximum value near the top of the vegetation which is different from the case of plane mobile bed with no vegetation where the maximum value of turbulent intensities lies near the bed. The flow is highly sheared near the top of the vegetation and hence a maximum value of turbulence intensity is noted. The turbulence intensities at the upstream are greater than downstream and centre because the wake generated because of the oscillations, decrease in the downstream direction.

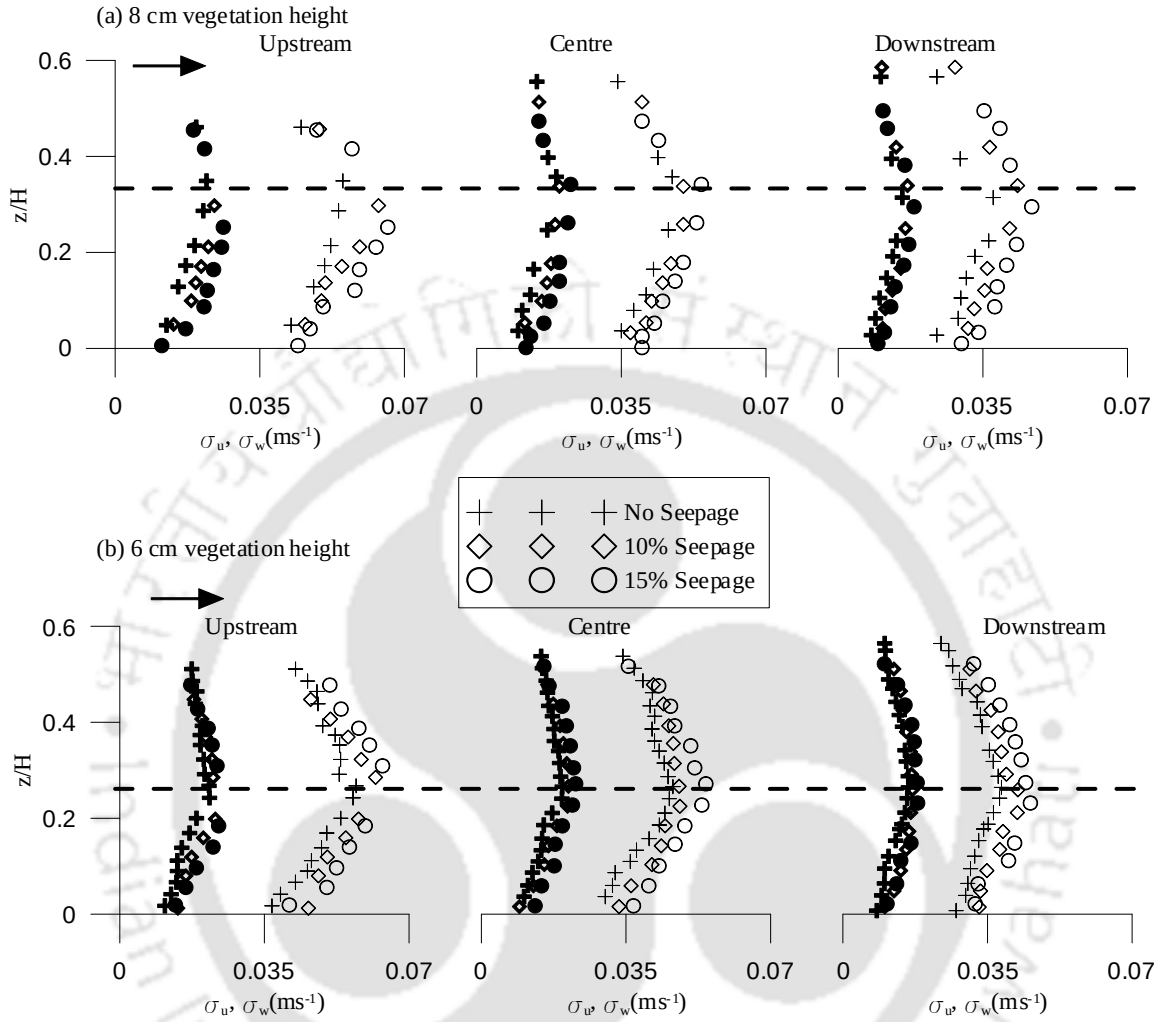

Figure 3.5 Turbulent Intensities in streamwise direction, σ_u (+, ◇ ,○) and vertical direction, σ_w (✚,◆,●) for no-seepage, 10% seepage and 15% seepage cases (a) 8 cm vegetation height (b) 6 cm vegetation height

Vertical turbulence intensities also exhibit similar behaviour as streamwise turbulence intensities but in terms of magnitude vertical turbulence intensities are nearly one-third of the streamwise turbulence intensities. All the profiles show maximum value near the top of the vegetation. The turbulence intensities at the upstream is reduced in the range of 22-31% as the flow reached downstream. From the results of the turbulence intensities, it can be deduced that the intensity of velocity fluctuations occur at the starting portion of the vegetation zone decreases at the ending of

the vegetation zone implying that turbulent fluctuations are reduced because of the presence of vegetation as the flow goes downstream.

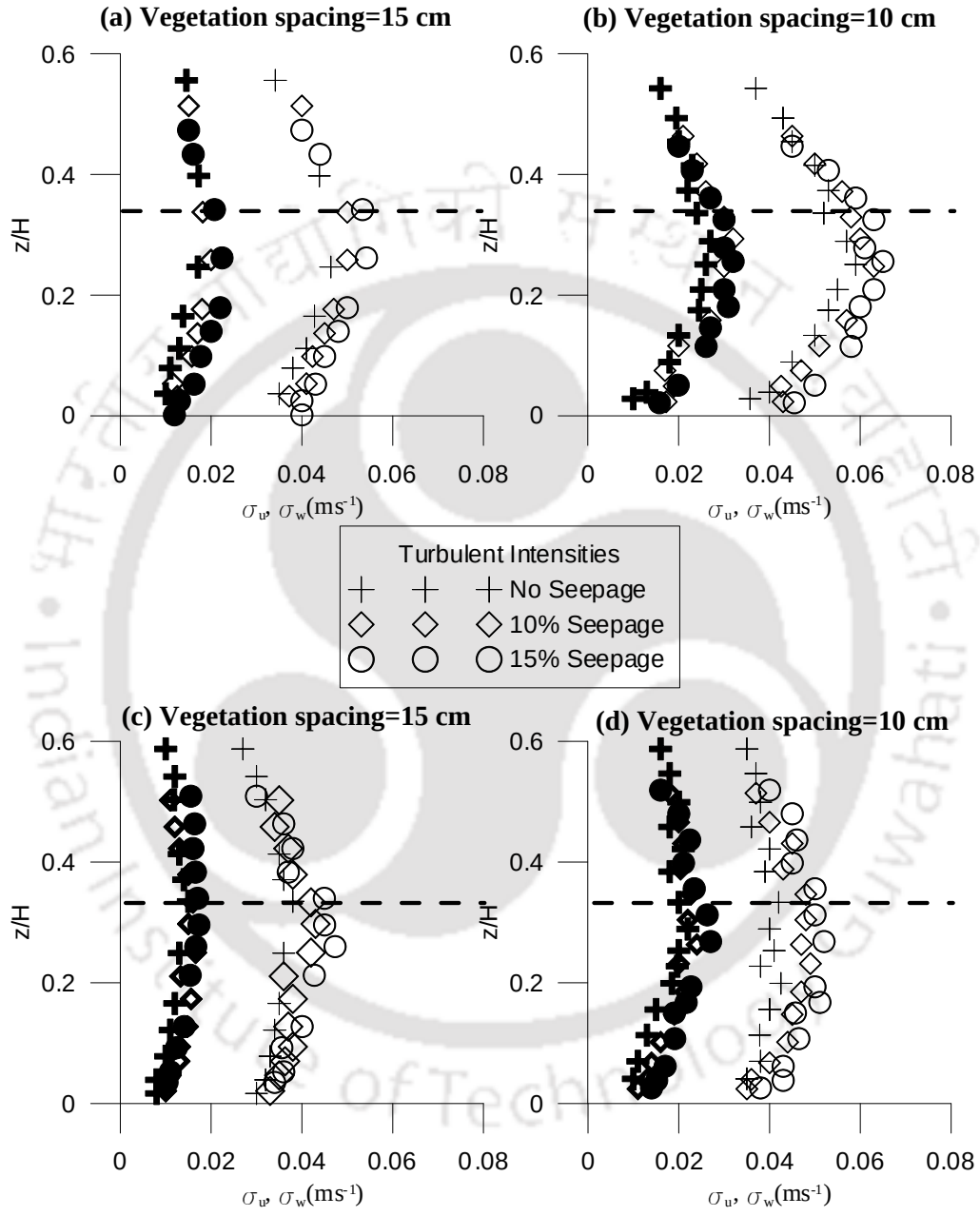

Figure 3.6 Turbulent Intensities in streamwise direction, σ_u (+, ◇ ,○) and vertical direction, σ_w (✚,◆,●) for no-seepage, 10% seepage and 15% seepage cases: staggered (a, b) and uniform pattern(c, d)

Figure 3.6 shows distribution of turbulence intensities of different pattern and spacing at the particular measurement location for no-seepage, 10% seepage and 15% seepage. The profiles show higher value for staggered pattern as compared to uniform pattern. The flow for staggered pattern is measured in line with the vegetation stems which produces drag and opposes the incoming flow resulting in the formation of a shear flow while for uniform pattern, it is measured in the unobstructed region and the flow is not much sheared. Therefore, lower turbulence intensities are achieved for uniform pattern than staggered pattern. . Additionally, it is observed that 15 cm centre-centre spacing has got slightly lower turbulence intensities than 10 cm centre-centre spacing irrespective of the vegetation pattern. The flow is slightly more sheared for 10 cm centre-centre than 15 cm centre-centre which is shown by higher value of Reynolds stress. 15 cm spacing has approximately 15% less intensities values as compared to 10 cm vegetation spacing. The effect of seepage is also studied. As observed, downward seepage increases the shear stress and hence with increase in downward seepage percentage, the flow is more sheared which leads to more turbulence intensities. For 10% and 15% seepage also, turbulence intensities for both the vegetation height are more, achieving an average increase value of 15% for 10% seepage and 25% for 15% seepage as compared to no-seepage case.

3.5 Moment Analysis

The study of the third order correlation of velocity fluctuations are generally carried out to derive virtual information on contribution of velocity fluctuations, in terms of flux and diffusion, to the turbulent coherent structures. The third order correlation is defined by $M_{jk} = \overline{\hat{u}^j \hat{w}^k}$ where j+k=3, $\hat{u} = u' / \left(\overline{u'u'}\right)^{0.5}$ and $\hat{w} = w' / \left(\overline{w'w'}\right)^{0.5}$ (Raupach, 1981). $M_{30}\left(\overline{\hat{u}^3}\right)$, also known as the skewness of u', is the streamwise (streamwise) flux of the streamwise Reynolds stress while the skewness of w', $M_{03}\left(\overline{\hat{w}^3}\right)$, is the vertical flux of the vertical Reynolds stress. $M_{12}(\overline{\hat{u}^1\hat{w}^2})$ and M_{21} $(\overline{\hat{u}^2\hat{w}^1})$ are the diffusion terms defining the diffusions of $\overline{w'w'}$ in x-direction or streamwise direction and $\overline{u'u'}$ in z-direction or vertical direction respectively. Third order correlations of velocity fluctuations (M_{30}, M_{03}, M_{12} *and* M_{21}) for no-seepage, 10% seepage and 15% seepage at upstream, centre and downstream are shown in figure 3.7 and 3.8 below.

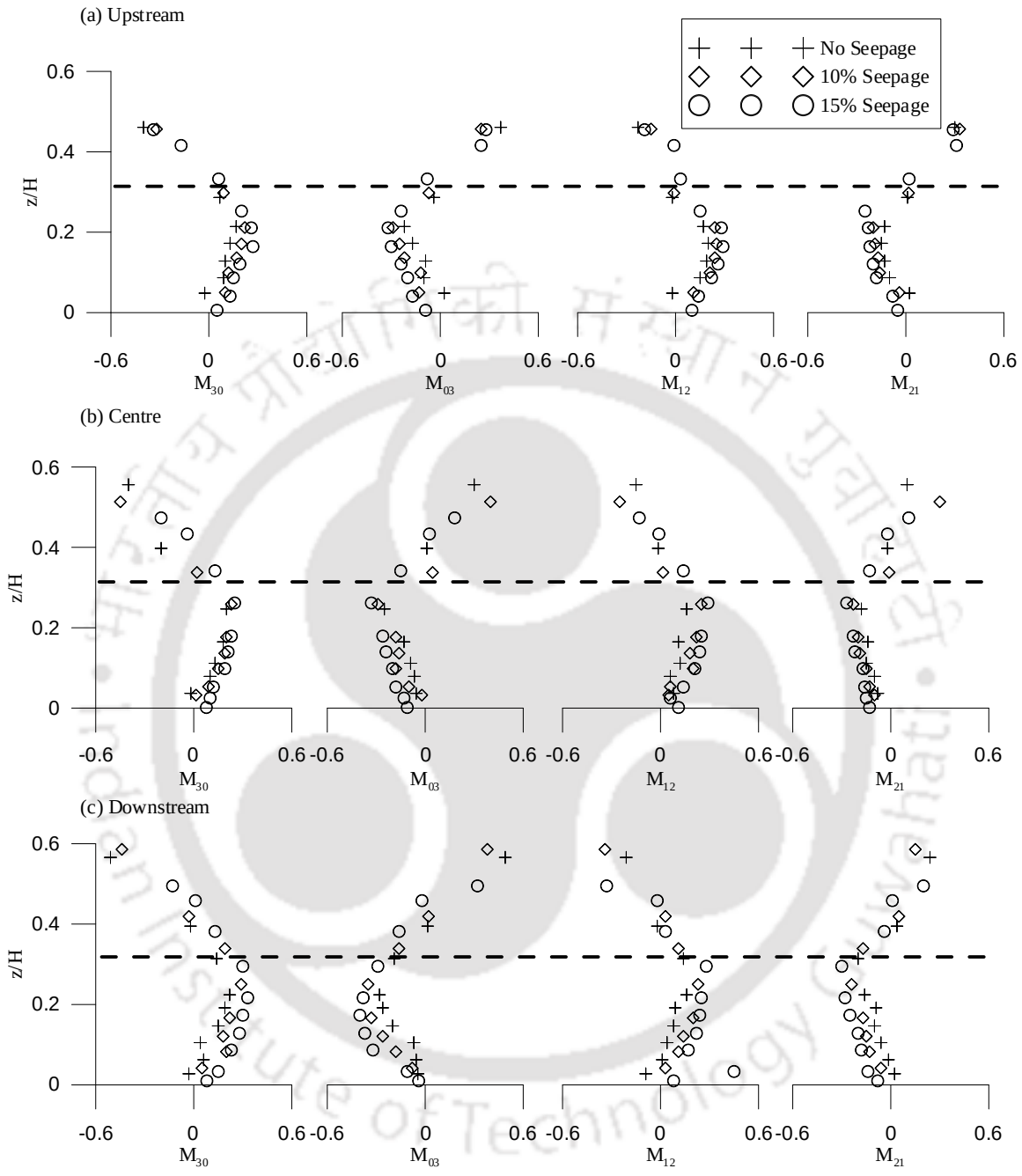

Figure 3.7 Distributions of third-order moments (M_{30}, M_{03}, M_{12} and M_{21}) at upstream, centre and downstream for no-seepage, 10% seepage and 15% seepage for 8 cm vegetation height

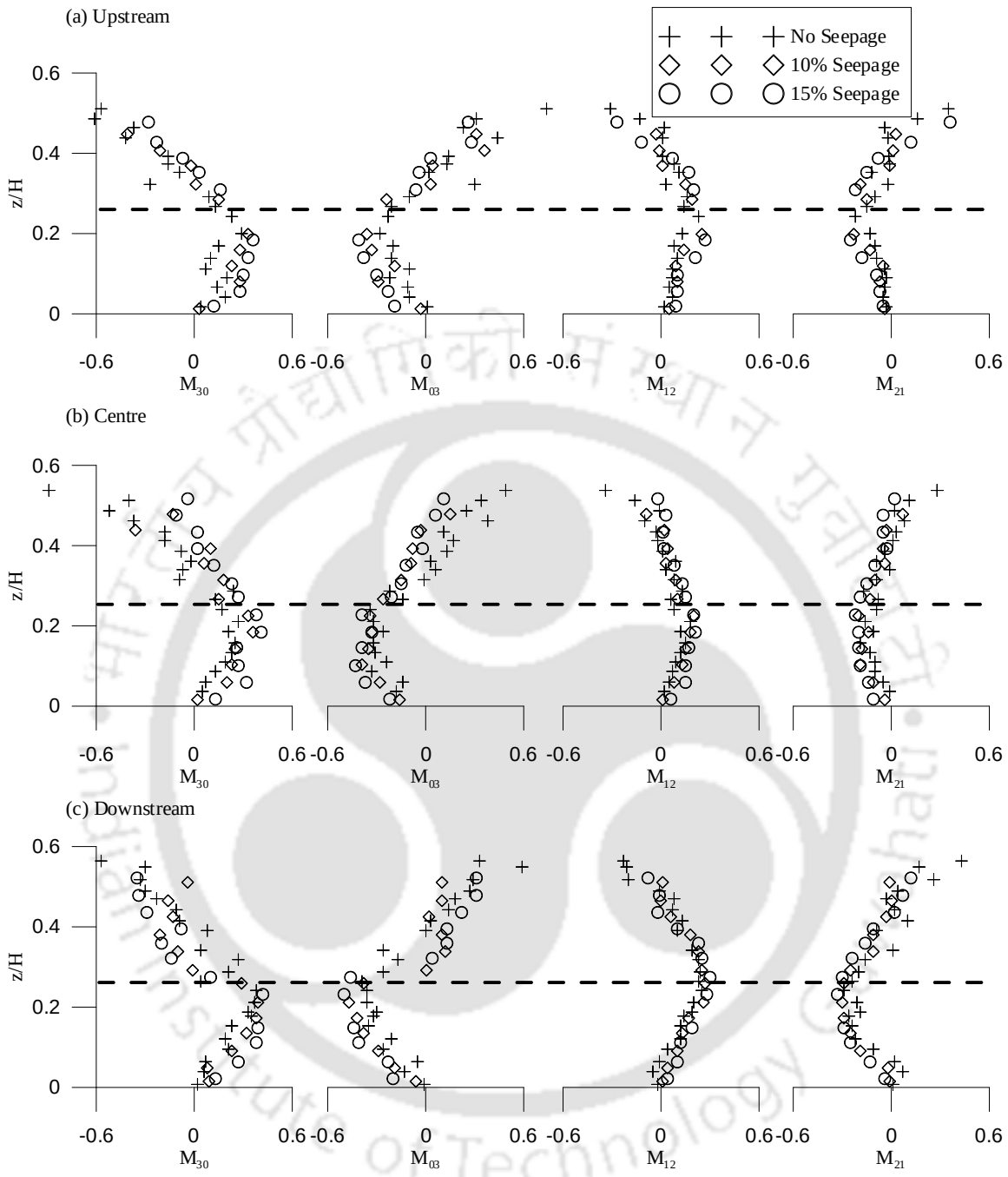

Figure 3.8 Distributions of third-order moments (M_{30}, M_{03}, M_{12} and M_{21}) at upstream, centre and downstream for no-seepage, 10% seepage and 15% seepage for 6 cm vegetation height

Third order moments for plane mobile bed is different from vegetated flows. In the plane mobile-bed flow (Dey *et al*, 2012), M_{30} and M_{12} start with small positive values near the bed, changing

over to negative values for z/H ≥ 0.06 which implies that the bed-load transport influences M_{30} and M_{12} by changing the $\overline{u'u'}$ -flux and the $\overline{w'w'}$ -diffusion to the streamwise direction. At z/H> 0.06, the $\overline{u'u'}$ -flux and the $\overline{w'w'}$ -diffusion occur against the streamwise direction and become pronounced with increasing z/H. M_{03} and M_{21} in mobile-bed flows are negative near the bed (z/H ≤ 0.06) and positive for $z/H > 0.06$ which suggests that the $\overline{w'w'}$ -flux and the $\overline{u'u'}$ -diffusion are in downward direction in the near-bed flow zone for the mobile-bed case. In the present study, M_{30} has maximum positive values near the vegetation top which changes to negative values with increasing depth. This implies that the $\overline{u'u'}$ flux occurs in the flow direction for the vegetation zone which denotes the occurrence of shear layer near the vegetation top (Nezu and Sanjou, 2008; Righetti, 2008). With increase in seepage percentage, there is an increase in the positive values of M_{30} near the bed. In the case of M_{03}, it has negative values near the bed, having maximum negative value near the top of the vegetation. With the application of downward seepage, the negativity of M_{03} increases which is justifiable with the fact that downward flow is occurring because of seepage.

M_{12} and M_{21} define the turbulent advection of the normal Reynolds stresses. M_{12} started to have positive values near the bed and the positive nature increases with increase in downward seepage percentage. M_{21} also has negative values near the bed and increases with increase in seepage percentage. M_{12} being positive near the bed and M_{21} being negative near the bed indicates that the $\overline{w'w'}$ diffusion propagates in the streamwise direction and $\overline{u'u'}$ diffusion occurs in the downward direction respectively. The negative values of M_{03} and M_{21} near the bed infer that inrush of flow is occurring in the region and the flow coming towards the bed is again carried away by the flow in the streamwise direction which is observed from positive values of M_{30} and M_{12}.

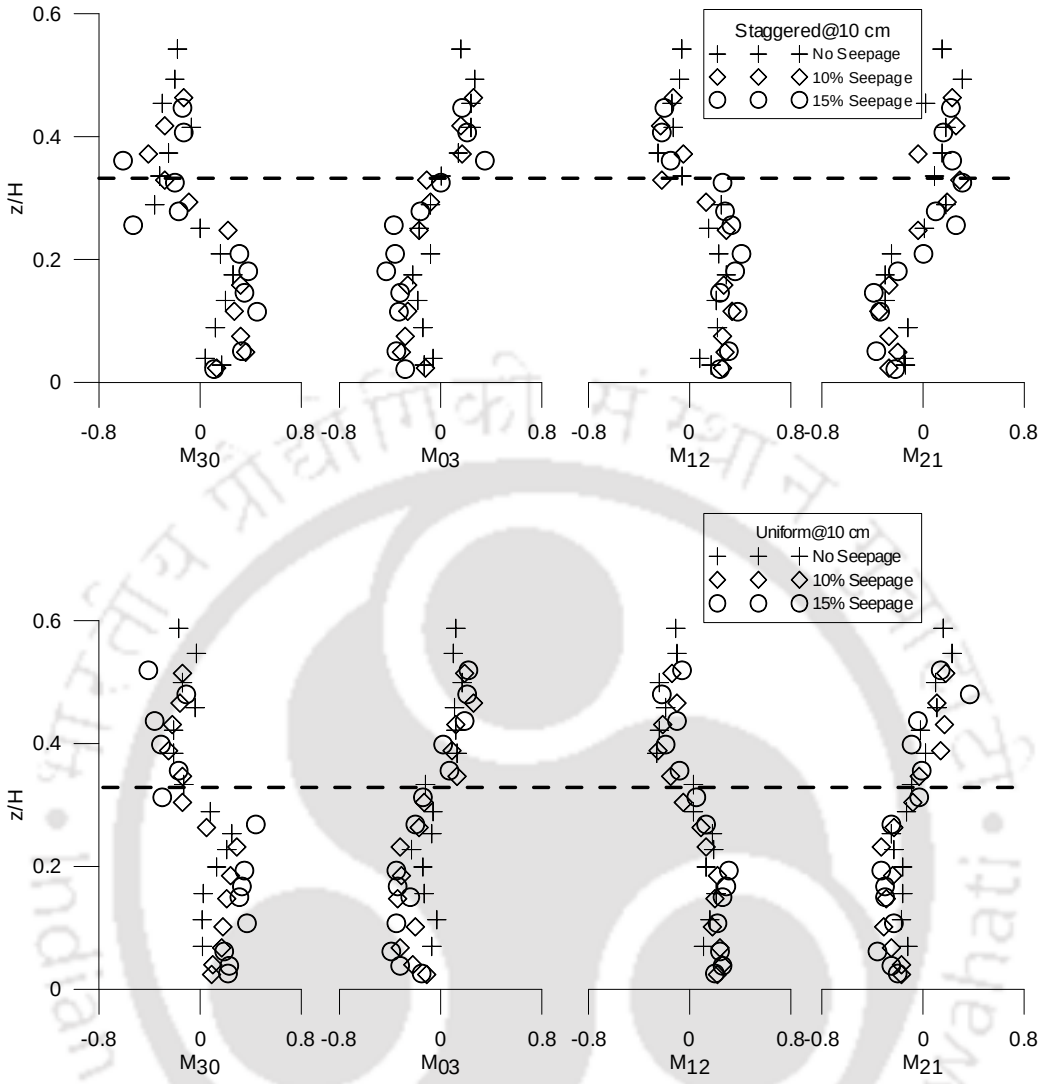

Figure 3.9 M_{30}, M_{03}, M_{12} and M_{21} profiles of staggered pattern and uniform pattern for no-seepage, 10% seepage and 15% seepage

Thus, it can be inferred from the results that the downward seepage appears to decrease the upward flux and the vertical transport of $\overline{u'u'}$ while it increases the streamwise flux and streamwise transport of $\overline{w'w'}$ flux. Irrespective of the vegetation pattern of placement (Figure 3.9), the trend of third order moments remains the same.

3.6 Quadrant Analysis

Organized coherent structures play an important role in mass and momentum exchange and hence these structures need to be identified. Quadrant analysis is carried out to study the contribution of different velocity fluctuations to Reynolds stress at a point. In quadrant analysis, the instantaneous velocity components, u' and w' , are sorted in $u'-w'$ (Lu and Willmarth, 1973). The plane is divided into four quadrants. The four events consist of outward interaction, Q1, $(u'>0, w'>0)$, ejection, Q2, $(u'<0, w'>0)$ inward interaction, Q3, $(u'<0, w'<0)$ and sweep, Q4, $(u'>0, w'<0)$. At any point in a flow, the contribution of different events or quadrants to Reynolds stress is calculated as (Raupach, 1981):

$$\left\langle u'w'_{i,H'}\right\rangle = \lim_{T\to\alpha}\frac{1}{T}\int_0^T u'(t)\,w'(t)\,I_{i,H'}\left[u'(t)\,w'(t)\right]dt \qquad (3.4)$$

The angle brackets show conditional averaging and $I_{i,H'}$ is the indicator function which is defined by:

$$I_{i,H'} = \begin{cases} 1, \textit{if } (u', \mathrm{w}') \text{ is in quadrant i and } \left|u'w'\right| \geq H'\left|\overline{u'w'}\right| \\ 0, \text{otherwise} \end{cases} \qquad (3.5)$$

The stress fraction is calculated as:

$$S_{i,H'} = \left\langle u'w'\right\rangle_{i,H'} \Big/ \overline{u'w'} \qquad (3.6)$$

H' is known as the hyperbolic hole region which is a parameter for investigating the stress contribution from each quadrant to extreme events of Reynolds stress. $H'=0$ means that all the fluctuation components are considered. For some value of H', the fluctuation components falling in the specific region H' are neglected, fluctuations outside the hole region are only considered. Stress contributions to Reynolds stress for different vegetation pattern and spacing corresponding to flow depth for hole size=0 are shown in figure 3.10. The figures are plotted for no-seepage, 10% seepage and 15% seepage at measurement location 'A'. The difference between ejection and sweep is also calculated. The difference between sweep and ejection (*Q4-Q2*) is also calculated where the negative value infers that ejection event is dominant while its positive value implies that sweep action dominates.

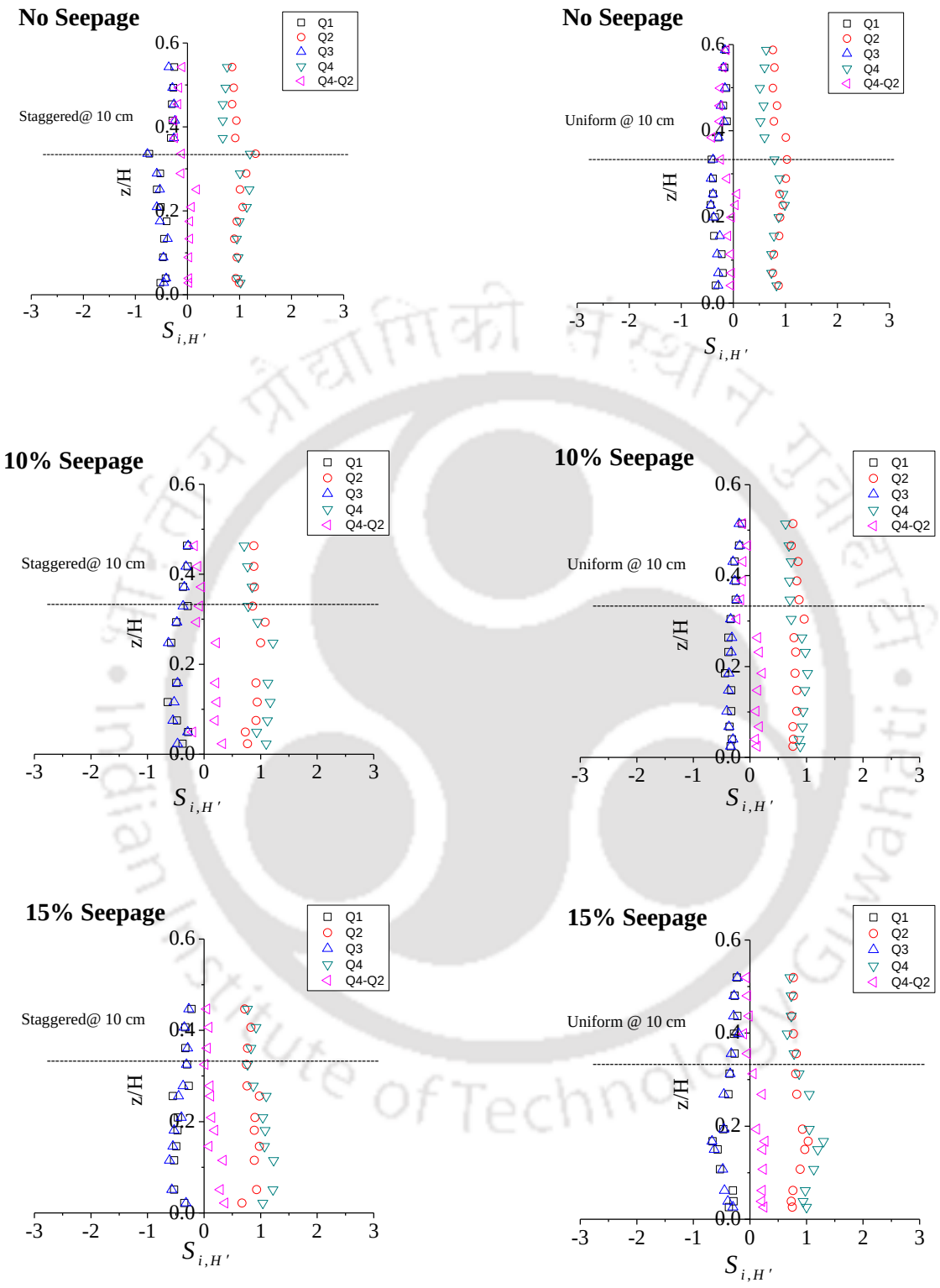

Figure 3.10 Stress fraction contribution from each quadrant at A of staggered pattern and uniform pattern for no-seepage, 10% seepage and 15% seepage ($H' = 0$)

The flow regions dominated by ejection events are analogous with negative values of M_{30} and positive values of M_{03} while sweep events are associated with positive values of M_{30} and M_{03} (Righetti, 2008; Dey and Nath, 2009). In the present observations for staggered pattern it is observed that in the flow region above the vegetation, the flow is dominated by ejection events for no-seepage case but equal contribution of ejection and sweep for lower flow region. With 10% seepage, the difference between ejection and sweep lies closer to zero for upper flow region inferring almost equal contribution of sweep and ejection and the contribution of sweep event is increased. Accordingly with 15% seepage, sweep event has slightly higher contribution comparing to ejection event. It is observed that the application of seepage enhances the sweep event since the flux is occurring in the downward direction. Sweep event dominates the whole flow region for the case of 10 cm centre-centre spacing with 15% seepage. Stress contribution for uniform pattern at no-seepage, 10% seepage and 15% seepage is also presented. For no-seepage the whole flow depth is dominated by ejection event. One of the reasons may be because the flow is not much sheared in the unobstructed region, A, and hence dominated by ejection event only. With the application of seepage, sweep action comes to play a dominant role in the lower flow region, difference between sweep and ejection being higher for increasing seepage percentage.

3.7 Turbulent Kinetic Energy (TKE) Budget

Another objective of the present study is to calculate the components of the turbulent kinetic energy budget. For steady, homogenous flow and by neglecting the viscous diffusion term, the total kinetic energy budget reduces to

$$\frac{\partial k}{\partial t} = p_s + p_w + t_t + p_d + (-\varepsilon) = 0 \qquad (3.7)$$

Where k = total kinetic energy $= \frac{\left(u'^2 + v'^2 + w'^2\right)}{2}$, p_s, is the shear production which is emerged from the turbulent interactions with the mean velocity profile, p_w is the wake production which is the work done by the mean flow against the form drag caused by presence of vegetation, t_t is the turbulent diffusive transport, p_d is the pressure diffusion and ε is the energy dissipation which is regarded as a sink for TKE which damages the turbulent motion and converted into heat.

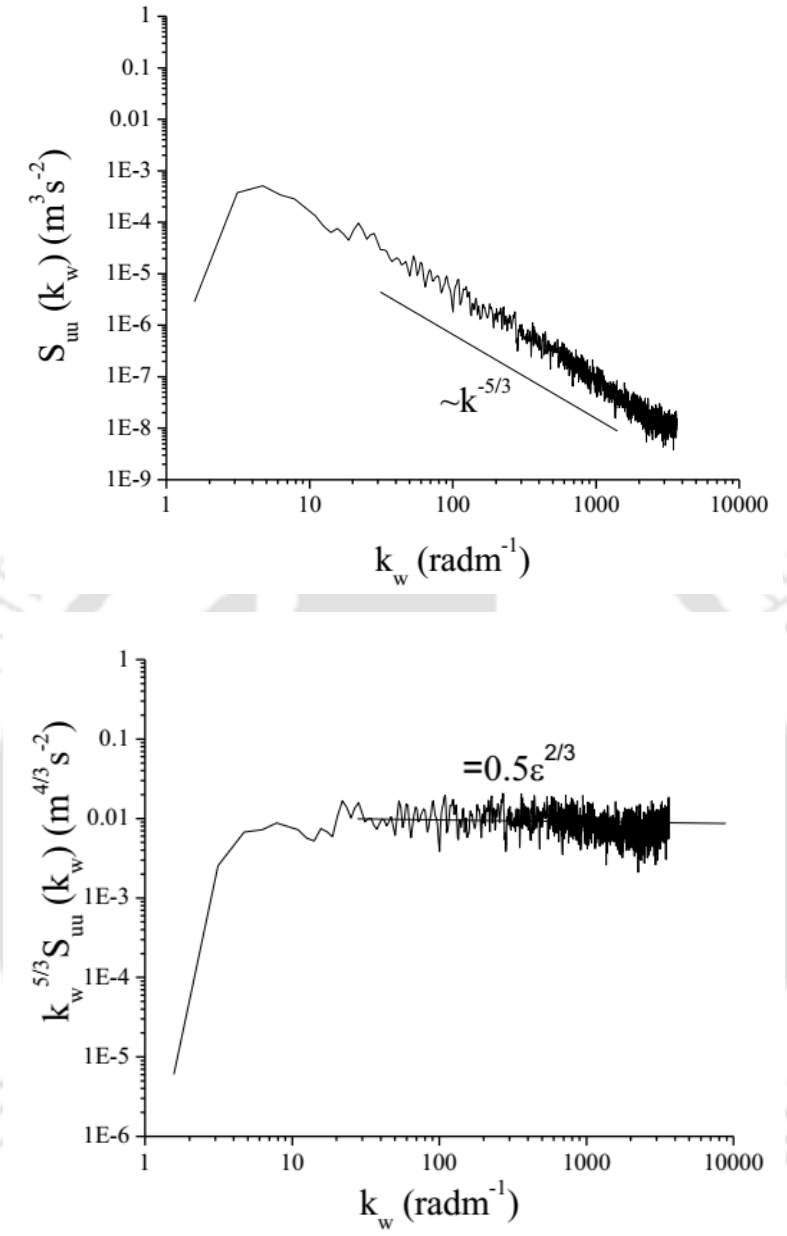

Figure 3.11 Velocity power spectra and estimation of turbulent dissipation rate, ε

Defining the components, equation (3.7) becomes

$$\frac{\partial k}{\partial t} = -\overline{u'w'}\frac{\partial U}{\partial z} + U\left\{\frac{\partial(-\overline{u'w'})}{\partial z} + \frac{u_*^{\,2}}{H - h_d}\right\} + \frac{\partial(-f_{kw})}{\partial z} + \frac{1}{\rho}\frac{\partial(-\overline{p'w'})}{\partial z} + (-\varepsilon) = 0 \qquad (3.8)$$

f_{kw} is the TKE flux in the vertical direction which is calculated as

$$f_{kw} = 0.5(\overline{u'u'w'} + \overline{v'v'w'} + \overline{w'w'w'}) \quad (3.9)$$

The estimation of ε is done by using Kolmogorov's second hypothesis that predicts the following equality describing the true inertial subrange (Pope 2001):

$$k_w^{5/3} S_{uu} = C.\varepsilon^{2/3} \quad (3.10)$$

where k_w is the wave number, S_{uu} the spectral density function for u', and C is the universal Kolmogorov's constant approximately equal to 0.5 (Monin and Yaglom 2007). In Figure 3.11, the spectra S_{uu} (k_w) [= (0.5 u /π) F_{uu} (f)] as a function of k_w [= (2π/ u) f] are drawn using the despiked instantaneous velocity data. The inertial subranges are satisfactorily characterized by Kolmogorov "–5/3 scaling-law". It corresponds to a subrange of k_w where the average value of $k_w^{5/3} S_{uu}$ is relatively constant (that is independent of k_w) as shown in Figure 3.11. Then, ε was estimated from Eq. (3.10). All the components are non-dimensionalised by multiplying each component with h_d/u_*^3 (Nezu and Sanjou, 2008; Dey *et al*, 2012) as P_D, T_t, E, P_s, P_w=(p_d , t_t, ε , p_s, p_w) x h_d/u_*^3.

All the components such as P_s, P_w, T_t and E are computed from velocity measurements and approximation except the pressure transport. The pressure transport is calculated as the residual of the remaining terms i.e.

$$R = P_D = -(P_S + P_W + T_t + (-E)) \quad (3.11)$$

Figures 3.12, 3.13 and 3.14 shows the plot of the different components of TKE budget. For submerged vegetation, there is a strong velocity differential between the vegetation zone and the region above it where there is no vegetation due to which a shear layer is generated near the top of the vegetation.

For all the profiles of P_s, it is observed that maximum value is found near the vegetation top where there is high velocity differential. The normalized values of P_s show no change with change in vegetation pattern and spacing for no-seepage, 10% seepage and 15% seepage (Figure 3.12).

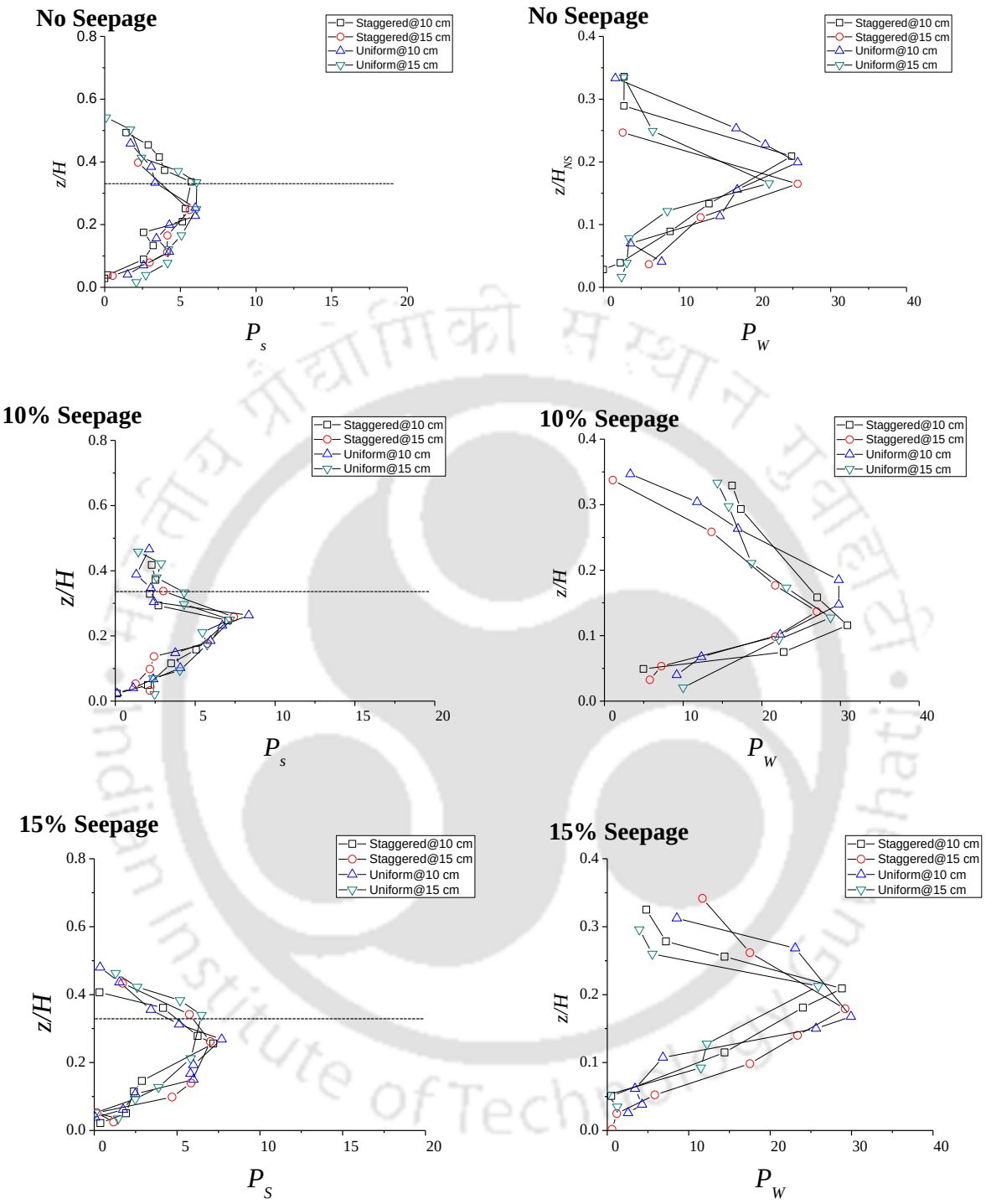

Figure 3.12 Components of the turbulent kinetic energy budget, P_s and P_w, for no-seepage, 10% seepage and 15% seepage at measurement location A

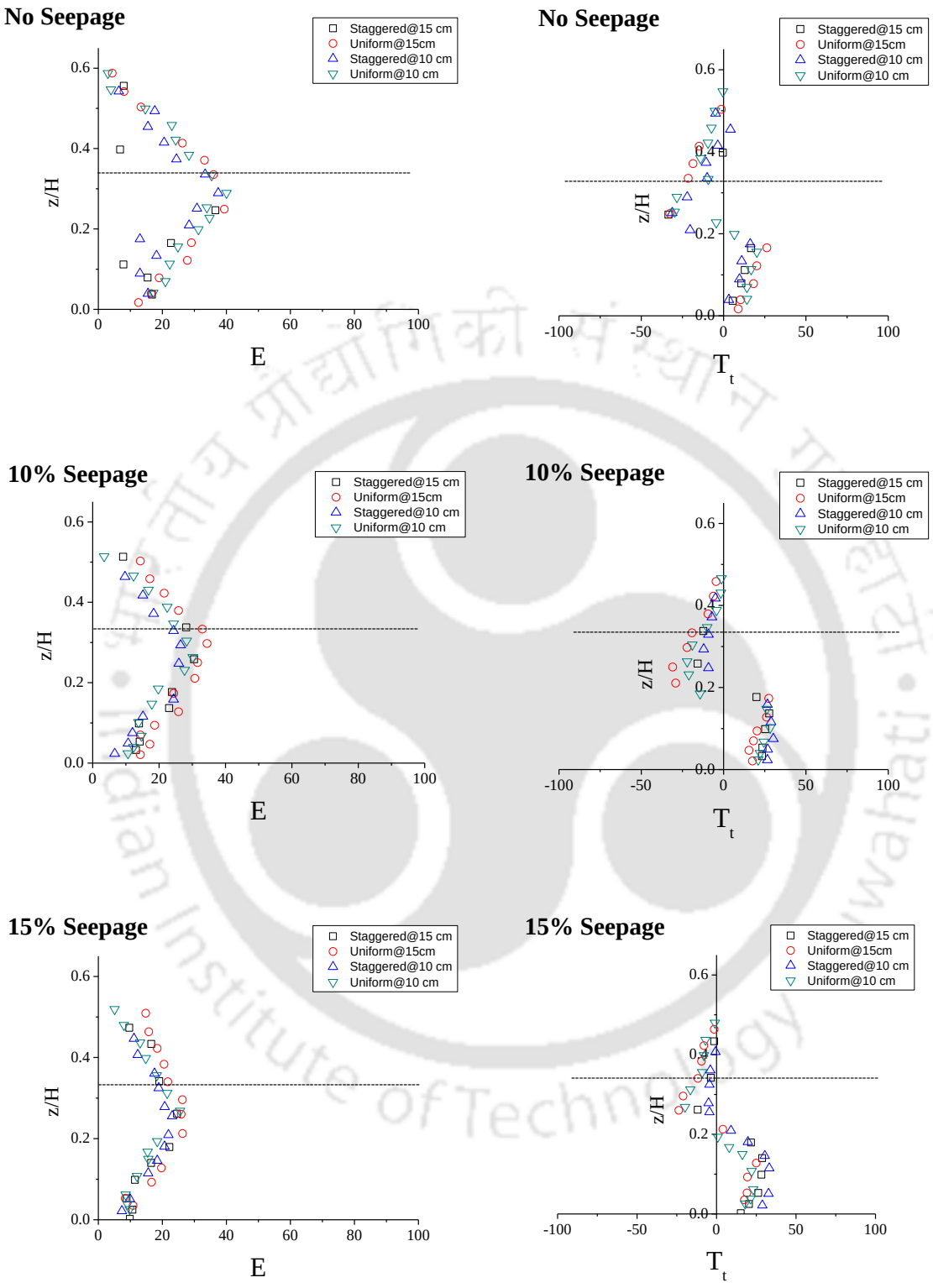

Figure 3.13 Components of the turbulent kinetic energy budget, T_t and E, for no-seepage, 10% seepage and 15% seepage at measurement location A

The wake production, P_w, is analyzed for the vegetation zone only as wake vortices are produced near the vegetation stem only (Nezu and Sanjou, 2008; Nepf and Vivoni, 2000). It is observed that P_w has maximum value near the bed which means that more energy is required for flow to overcome the drag induced by the vegetation stems. P_w also show no change with change in vegetation pattern or spacing for all the three cases of no-seepage, 10% seepage and 15% seepage (Figure 3.12).

For no seepage case, the normalized energy dissipation shows no remarkable change with respect to change in vegetation density and pattern (Figure 3.13). With the application of seepage, the normalized dissipation of staggered pattern at 10 cm vegetation spacing is slightly lower as compared to uniform pattern at 10 cm vegetation spacing.

Turbulent transport or diffusion plays an important role in TKE budget. T_t has negative values in the upper flow region and positive values in the lower vegetation zone (Figure 3.14). This denotes that the turbulent energy near the vegetation edge is transported towards the free region as well as towards the vegetation zone. The energy that is transported towards the vegetation zone is counteracted by the energy dissipation. It may be because of the ejection event that leads to diffusion of energy towards the free or water surface and sweep event that diffuses the energy towards the vegetation edge. With increase in seepage percentage, sweep event dominates, as observed from quadrant analysis, having higher value for lower vegetation spacing. Therefore, turbulent diffusion decreases in the upper flow region and increases in the lower flow region showing the predominance of sweep event. T_t has the most important role in governing the ejection and sweep event which are the key phenomenon for generation of vortices.

The energy transported by the turbulent diffusion is partially counterbalanced by the pressure term which is shown by positive values above the vegetation zone and negative values in the vegetation zone (Figure 3.14). For no-seepage case, there is no notable change in its value with vegetation pattern and spacing while with increase in seepage, the balancing power of P_D increases in the lower vegetation zone and decreases in the upper flow region which is just the opposite of T_t.

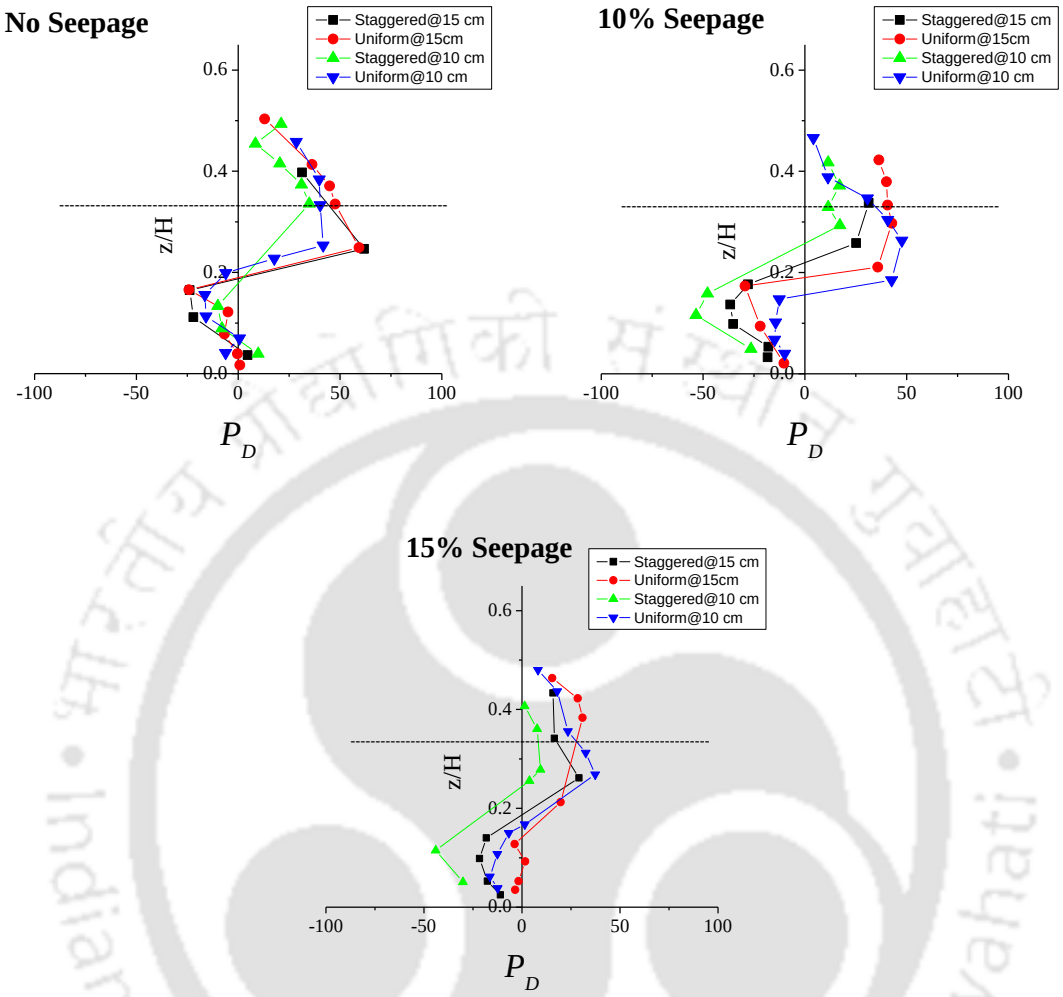

Figure 3.14 Component of the turbulent kinetic energy budget, P_D, for no-seepage, 10% seepage and 15% seepage at measurement location A

3.8 Conclusions

The study presents flume experiments for investigating the flow characteristics in a vegetative channel. The type of vegetation used for the study was flexible vegetation in which flexible vegetation was simulated by flexible rubber cylinders and the flow depth was kept more than the vegetation so that the vegetation was kept fully submerged. The experiments were conducted for no-seepage, 10% seepage and 15% seepage. Different results showing distributions of velocity profiles, Reynolds stress, turbulence intensities and moments are presented for no-seepage, 10%

seepage and 15% seepage at different streamwise distances. From the velocity distributions of 8 cm and 6 cm vegetation heights, it is observed that vegetation height is also an important parameter in vegetated flows. The lowest velocity occurs near the vegetation top. Higher velocity is achieved for uniform pattern which was measured in the unobstructed region comparing to the staggered pattern which was measured in line with the vegetation. The presence of downward seepage modifies the velocity distribution which leads to an increase in velocity in the vegetation zone. However, it is found that vegetation reduces the velocity as the flow goes downstream even at seepage cases. The maximum Reynolds stress at no seepage is increased by a percentage of 18% (average value for upstream, centre and downstream) for 10% seepage and average of 31% for 15% seepage for 8 cm vegetation height. For 6 cm vegetation height, it is increased by an average value of 16% at 10% seepage and 30% at 15% seepage. It is also noted that Reynolds stress decreases along the channel length which implies the importance of using vegetation as river protection measure. The turbulence intensities have a maximum value near the top of the vegetation which is different from the case of plane mobile bed with no vegetation. The turbulence intensities at the upstream is reduced in the range of 22-31% as the flow reached downstream. The presence of vegetation reduces the maximum turbulent fluctuations (range of 22-31%) at the upstream as the flow reaches the downstream measurement location. The positivity of M_{30} and M_{12} increases with increase in seepage percentage implying more transport of $\overline{u'u'}$ flux and $\overline{w'w'}$ diffusion in streamwise direction. With the application of downward seepage, the negativity of M_{03} and M_{21} increases which is justifiable with the fact that downward flow is occurring because of seepage. Downward seepage increases the flux transport in the streamwise direction and downward direction. The contribution of velocity fluctuations to Reynolds stress or bursting phenomenon is studied by carrying out quadrant analysis. Sweep action dominates the whole flow region with the application of downward seepage. The components of the TKE budget are also presented and discussed. Turbulent transport plays one of the most essential components of TKE budget. The negative values and positive values of T_t show that energy at the vegetation edge is transported in the water surface and in the vegetation edge. When downward seepage was applied, the negative value of T_t in the upper flow region is reduced while the positive nature increases in the vegetation zone indicating the dominance of sweep event over ejection event. The turbulent diffusion or transport is counterbalanced by the pressure transport showing by positive values in the upper flow region and negative values in the vegetation zone.

4 Effect of mixed vegetation densities on flow structure[iii]

4.1 Introduction

A large number of researchers have carried out research on resistance characteristics of flows in open channel. Many empirical formulae have already been developed and are now in use. But not a large numbers of works have been done on flow resistance in relatively smooth boundaries of open channel roughened with large roughness elements. Studies on flow resistance caused due to bed forms, vegetation etc. in an open channel flow is helpful to the hydraulic engineers in stage-discharge computation in a channel section, design of channels, sediment analysis etc. Amongst a large number of elements used to roughen the channel sections, vegetation plays a crucial role. Both natural and artificial vegetation can be used in open channel and the channel is called a vegetated channel. As economic development continues to cause deterioration in the state of our environment, there is increasing interest in ecological management. One of the ecological issues associated with river mechanics is the water flow and sediment behavior in the presence of vegetation. The mechanics involving vegetation and sediment is complicated (Stephan and Gutknecht, 2002; Kouwen *et al*, 1981; Tang *et al*, 2007). Vegetation or grasses of different varieties which are mainly used in soil and water conservation works are either planted in the beds of the open channels or they are naturally grown in the open channels. Naturally occurring vegetation varies both in its distribution density and in geometric characteristics. At times, artificial vegetation like polystyrene strips, polyethylene rigid plastic strips (Kouwen *et al*, 1969), flexible plastic strips (Nehal and Ming, 2005), thin wire rods (Fenzl, 1962), aluminium alloy wires (Wessels and Strelkoff, 1968) and wooden circular dowels (Stone and Shen, 2002) are used to simulate vegetation in open channels. Rigid cylinders of circular cross section are also used to simulate plant stems in laboratory studies (Li and Shen, 1973; Jadhav and Buchberger, 1995; López and Gracia, 2001). The existence of vegetation increases the flow resistance, raises the water depth, and promotes the deposition of sediment, and the vegetation may sway with

[iii]Devi, T. B., Daga, R., Mahto, S. K., & Kumar, B. (2016). Drag and turbulent characteristics of mobile bed Channel with mixed vegetation densities under downward seepage. *Journal of Fluids Engineering*, *138*(7), 071104.

the flow pressure, promoting the stirring motion of the flow body, and washing away the sediment around the plant. Flow resistance in open channel flow is very complicated and there are no exact methods to determine it (Järvelä, 2002). The various factors that influence the flow resistance in an open channel are size, shape and irregularity of the channel, channel sinuosity, types of roughness and vegetation including its length, density and stiffness (Chow, 1959). Vegetation that grows in the channel bed and flood plain areas increases the flow resistance and reduces the conveyance. Stem/vegetation drag is one of the important flow resistance parameter in vegetated open channels. Evaluating flow resistance in a straight vegetated channel needs to take into account both the effects of the hydraulic cross section reduction and the dissipative effects due to the presence of the roughness elements (shape, size, arrangement, and concentration of the elements). In fact, both the geometry of the vegetation elements and the turbulence characteristics of the flow affect the hydrodynamic resistance and the size of the wakes generated downstream of the elements themselves (Shen 1973; Ferro and Giordano 1992).

4.2 Velocity Profiles

Figure 4.1 shows different velocity profiles of two different vegetation pattern for no-seepage, 10% and 15% seepage cases. The velocity profiles show reduction in velocity in the lower vegetated region because of the drag imposed by the vegetation stems. For 5mm upstream-10 mm downstream pattern (Figure 4.1a) , the velocities in the centre location is reduced as compared to the upstream location by a value in the range 5-10% while an increase in the downstream velocity, in the range of 10-13%, is achieved as compared to the upstream region. In the case of 10 mm upstream-5mm downstream (Figure 4.1b), the velocity in the centre location is reduced by a value in the range of 9-13% and the velocity in the downstream portion which is concentrated by 5 mm diameter is again reduced by a range of 11-14% as compared to upstream portion. It may because of the reason that less vegetation spacing resists the incoming flow and hence a reduction in velocity is achieved. Previous investigations on the application of downward seepage show that the velocity profile is shifted downwards and hence a higher velocity is achieved in the near bed region (Dey and Nath, 2010; Cao and Chiew, 2013). In the present study, the effect of seepage in a vegetation zone is studied. A higher velocity zone exists in the lower flow region or the near bed region. Velocity increases in the range of 7-10% with the application of 10% seepage. It is also

observed that in the lower flow region the velocity for 15% seepage case is slightly higher, with an increasing value in the range of 3-5%, than the velocity for 10% seepage.

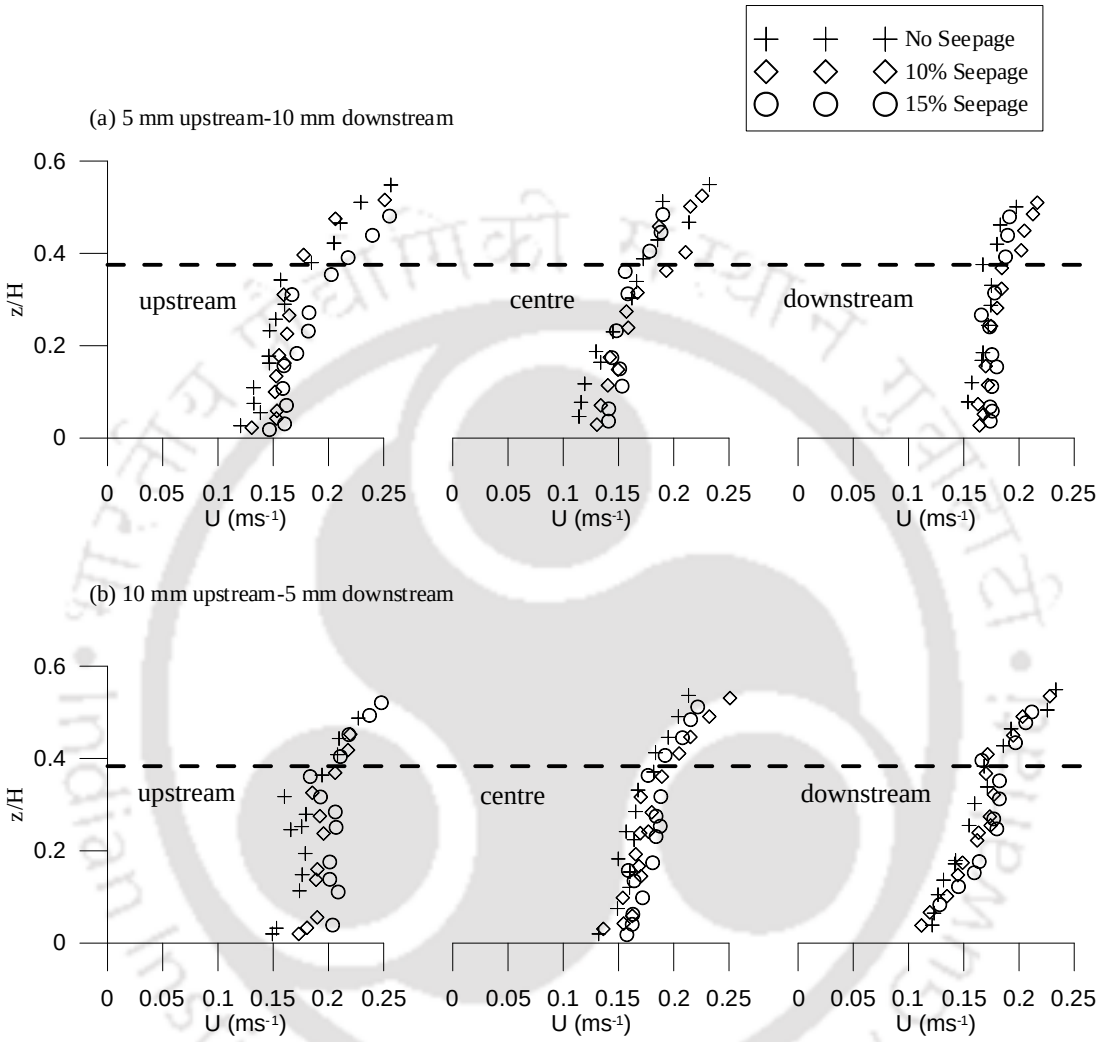

Figure 4.1 Velocity Profiles of different vegetation pattern for no-seepage, 10% seepage and 15% seepage cases (Dashed lines show the top of the vegetation)

4.3 Reynolds stress

For experiments on plane mobile bed (Chen and Chiew, 2004; Dey and Nath, 2009; Dey *et al*, 2012), maximum Reynolds stress occurs near the bed highlighting the importance of channel bed in turbulence production but for vegetated flows, the position of maximum Reynolds stress is no

longer the channel bed. Because of the difference in velocity just above and below the vegetation layer, momentum exchange takes place at the interface or top of the vegetation which leads to the formation of shear layer. The presence of shear layer leads to the production of oscillations near the vegetation top. This oscillation are responsible for exchange of mass and momentum between the lower or vegetated layer and upper or surface layer. Figure 4.2 shows different distributions of Reynolds stress for no-seepage, 10% seepage and 15% seepage with vegetation. It is observed that Reynolds stress is increased from the water surface towards the location where vegetation is present and reached a maximum value near the top of the vegetation. After attaining a maximum value near the top of the vegetation, it decreases towards the bed. The influence of these oscillations divides the flow region into two- upper side and down side. The upper side of the vegetated layer is dominated by the oscillations and more turbulence is created by oscillation at the top of the vegetation. This in turn leads to occurrence of more momentum exchange near the top of the vegetation and ultimately results in more Reynolds stress at that location.

When 5 mm diameter was placed at the upstream and 10 mm at the downstream, the Reynolds stress at the centre location is more as compared to the upstream location with an increase value in the range of 1-4%, which leads to more bed shear stress and sediment transport. As the flow goes downstream, Reynolds stress increases again with a value in the range of 3-9%. An interesting feature is noted for 10 mm upstream- 5 mm downstream where the Reynolds stress is reduced in the range of 4-10% at the downstream portion as compared to upstream location. This means that the vegetation at the downstream portion produces enough drag for reducing the bed shear stress as compared to the upstream case. It is known that the downward seepage increases the shear stress which leads to more sediment transport as compared to no-seepage (Dey and Nath, 2010). In all the profiles, with the increase in seepage percentage, an increase in shear stress is achieved. Since a higher velocity exists in the lower flow region and a decrease in the upper flow region, a higher velocity differential is achieved and because of which a higher Reynolds stress is achieved for higher seepage percentage. The maximum Reynolds stress near the vegetation top is increased to a value of 5-10% from no seepage to 10% seepage and 3-8 % from 10% seepage to 15% seepage.

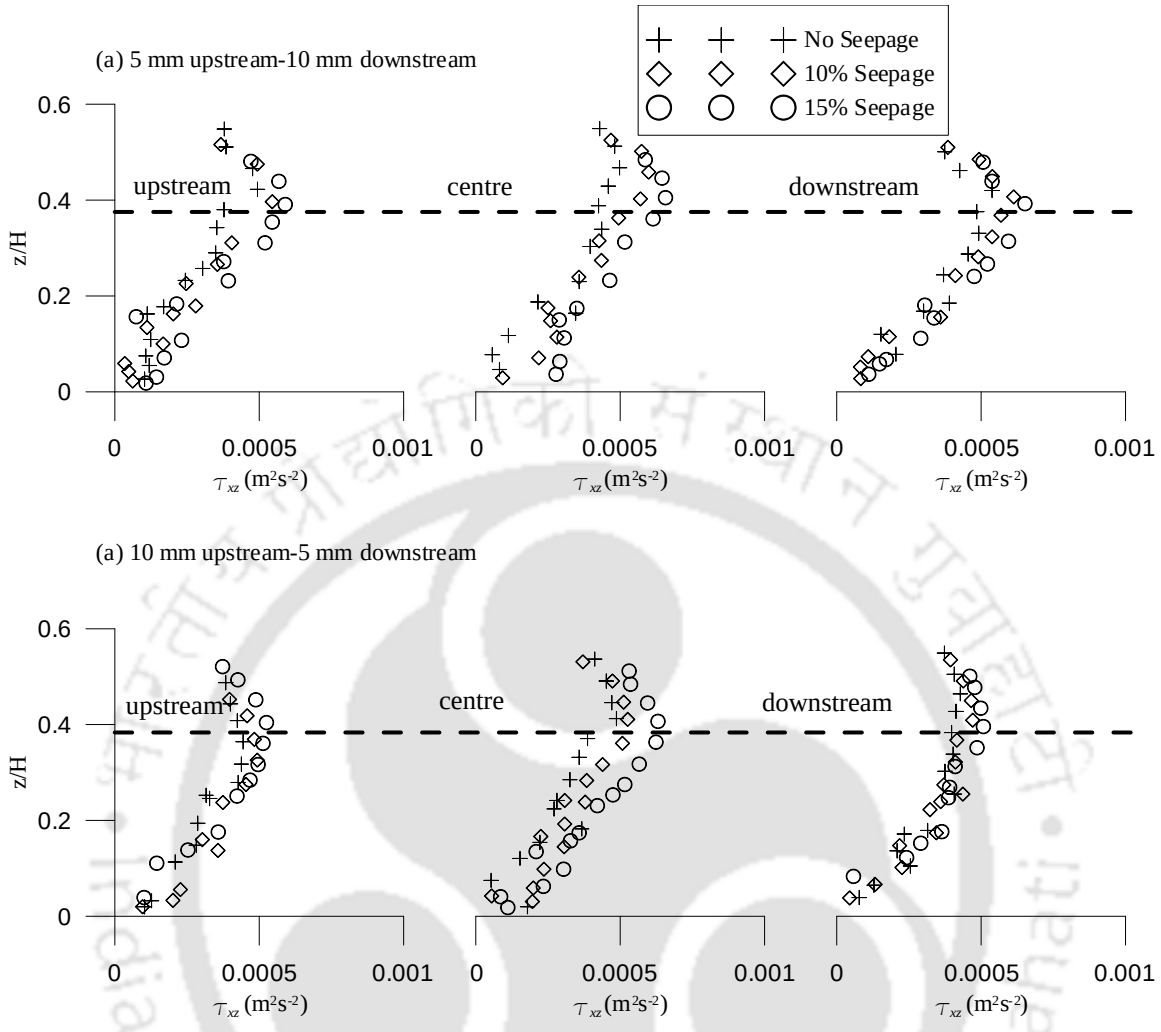

Figure 4.2 Reynolds stress Profiles of different vegetation pattern for no-seepage, 10% seepage and 15% seepage cases (Dashed lines show the top of the vegetation)

4.4 Turbulence Intensities

σ_u and σ_w for no-seepage, 10% seepage and 15% seepage are shown in figure 4.3. Streamwise and vertical turbulence intensities for different vegetation pattern are presented. The effect of seepage application on turbulence intensity can be observed. All the profiles show maximum value near the top of the vegetation element. The presence of the inflection point in the velocity profile and the maximum turbulence intensity lie in close approximation.

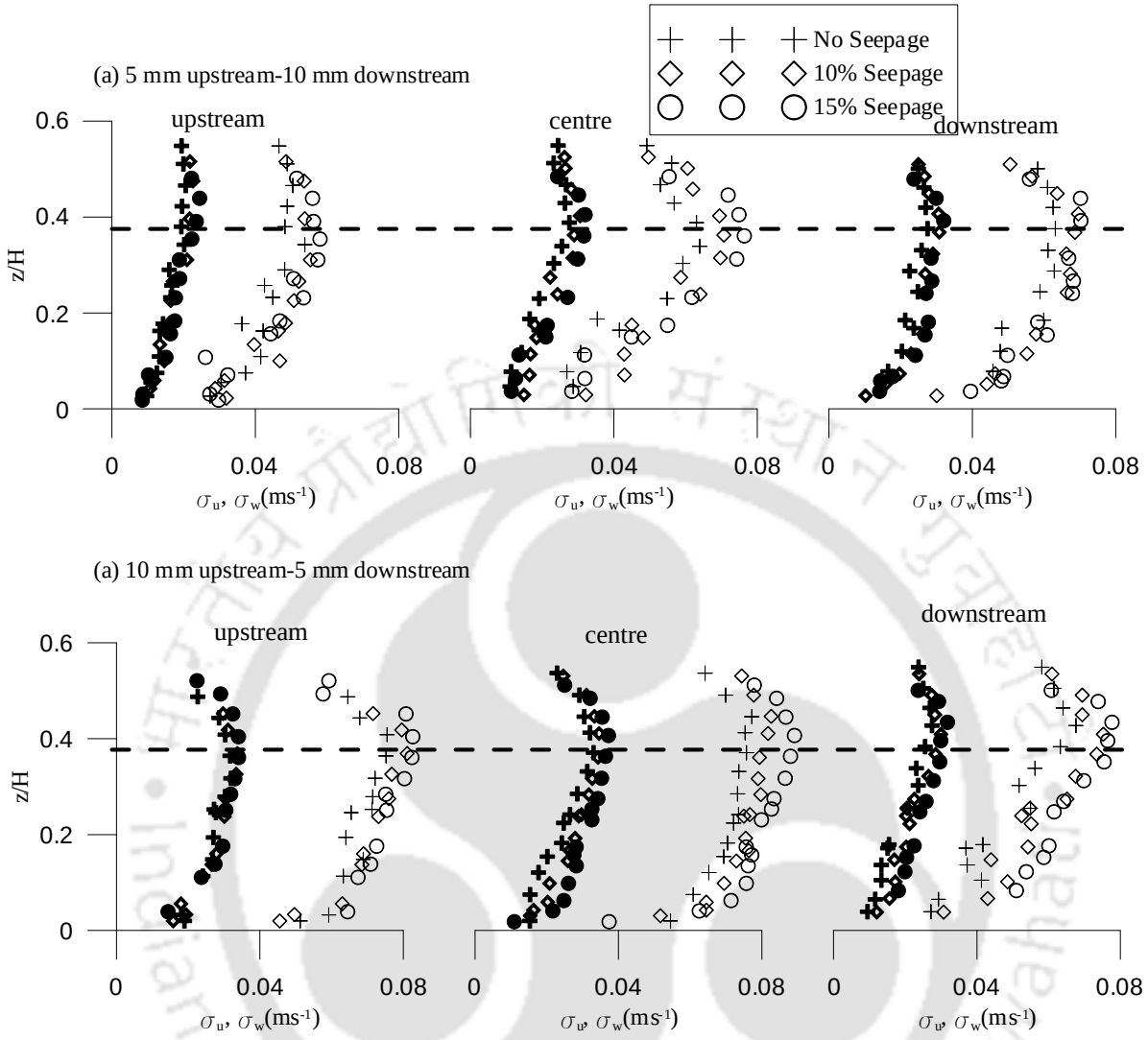

Figure 4.3 Turbulent Intensities in streamwise direction, σ_u (+, ◇ ,○) and vertical direction, σ_w (✚,◆,●) for no-seepage, 10% seepage and 15% seepage cases

For submerged condition, the flow is sheared because of the higher velocity in the upper flow region and lower velocity in the vegetation zone. The shear generated turbulence occurring near the vegetation top increases the vertical as well as streamwise turbulence intensities. As observed, downward seepage increases the shear stress and hence with increase in downward seepage percentage, the flow is more sheared which leads to more turbulence intensities. It is observed in all the profiles that the application of downward seepage increases the turbulence intensities as compared to no-seepage in the range of 6-12% and 3-7% from 10% seepage to 15% seepage cases.

4.5 Moment Analysis

Third order correlations of velocity fluctuations (M_{30}, M_{03}, M_{12} and M_{21}) for no-seepage, 10% seepage and 15% seepage for different vegetation pattern are shown in figures 4.4 and 4.5. For no seepage, M_{30} has positive values near the bed which changes to negative values with increasing depth and the maximum positive occurs below the vegetation. This implies that the $\overline{u'u'}$ flux occurs in the flow direction and the presence of vegetation top obstructs the flux. With the application of seepage, it is known that seepage increases the shear stress which means that more sediment particles get transported in the flow direction. M_{30} achieved a higher positive value near the bed at 10% and 15% seepage percentages as compared to no-seepage case. This means that the transport of flux in the flow direction is more with the application of seepage. In the case of M_{03}, it has negative values near the bed and positive values with increase in depth which indicates that the $\overline{w'w'}$ flux is in downward direction. With the application of downward seepage, the negativity of M_{03} increases which is justifiable with the fact that downward flow is occurring owing to seepage. More negative value is observed below the vegetation zone.

M_{12} and M_{21} define the turbulent advection of the normal Reynolds stresses. For 10% seepage and 15% seepage, these two correlations tend to deviate from zero value. M_{12} started to have positive values near the bed and the positive nature increases with increase in downward seepage percentage. M_{21} also has negative values near the bed and increases with increase in seepage percentage. M_{12} being positive near the bed and M_{21} being negative near the bed indicates that the $\overline{w'w'}$ diffusion propagates in the flow direction and $\overline{u'u'}$ diffusion occurs in the downward direction respectively.

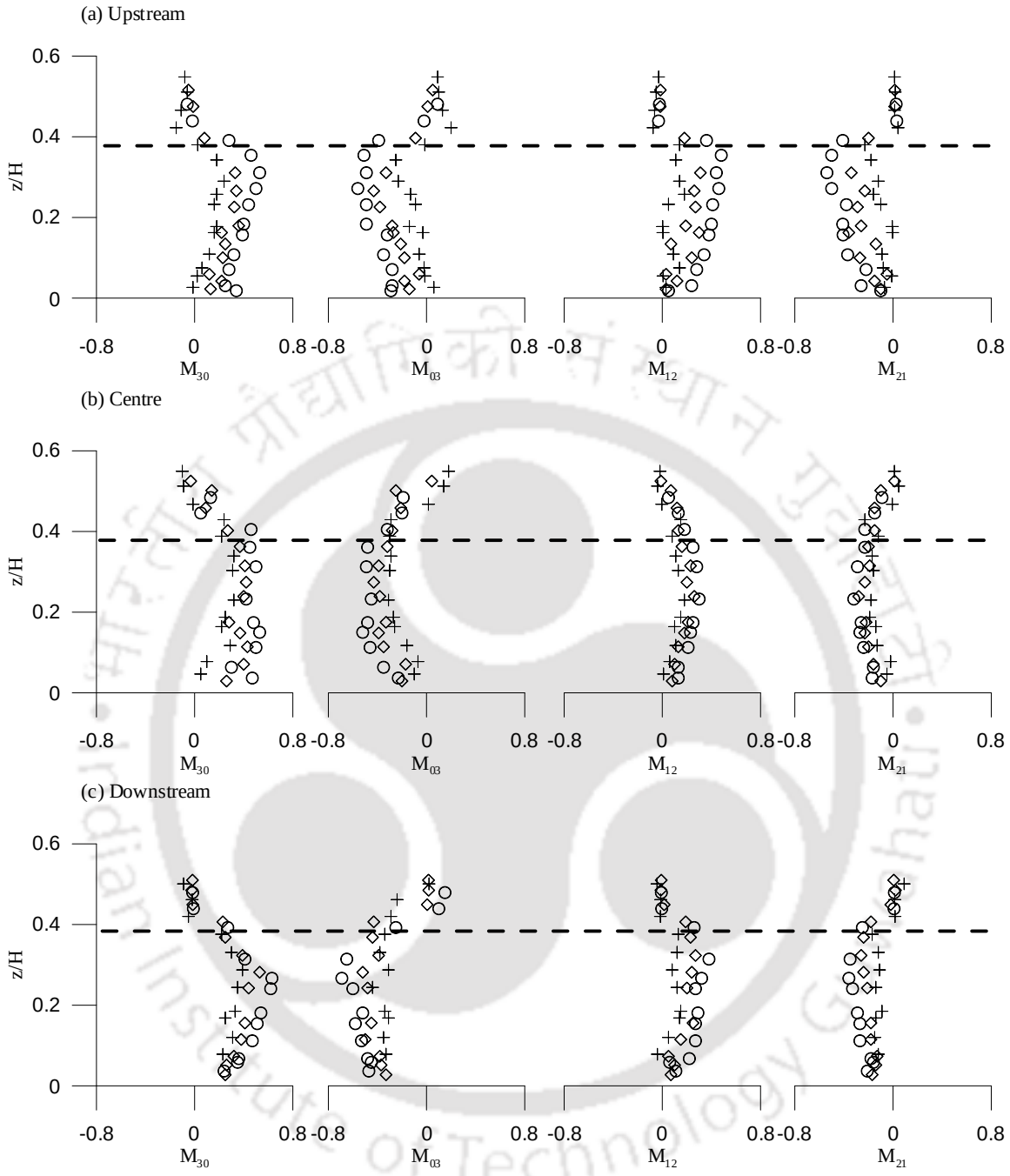

Figure 4.4 Profiles showing third order moments of 5mm diameter upstream-10 mm diameter downstream for no-seepage, 10% seepage and 15% seepage

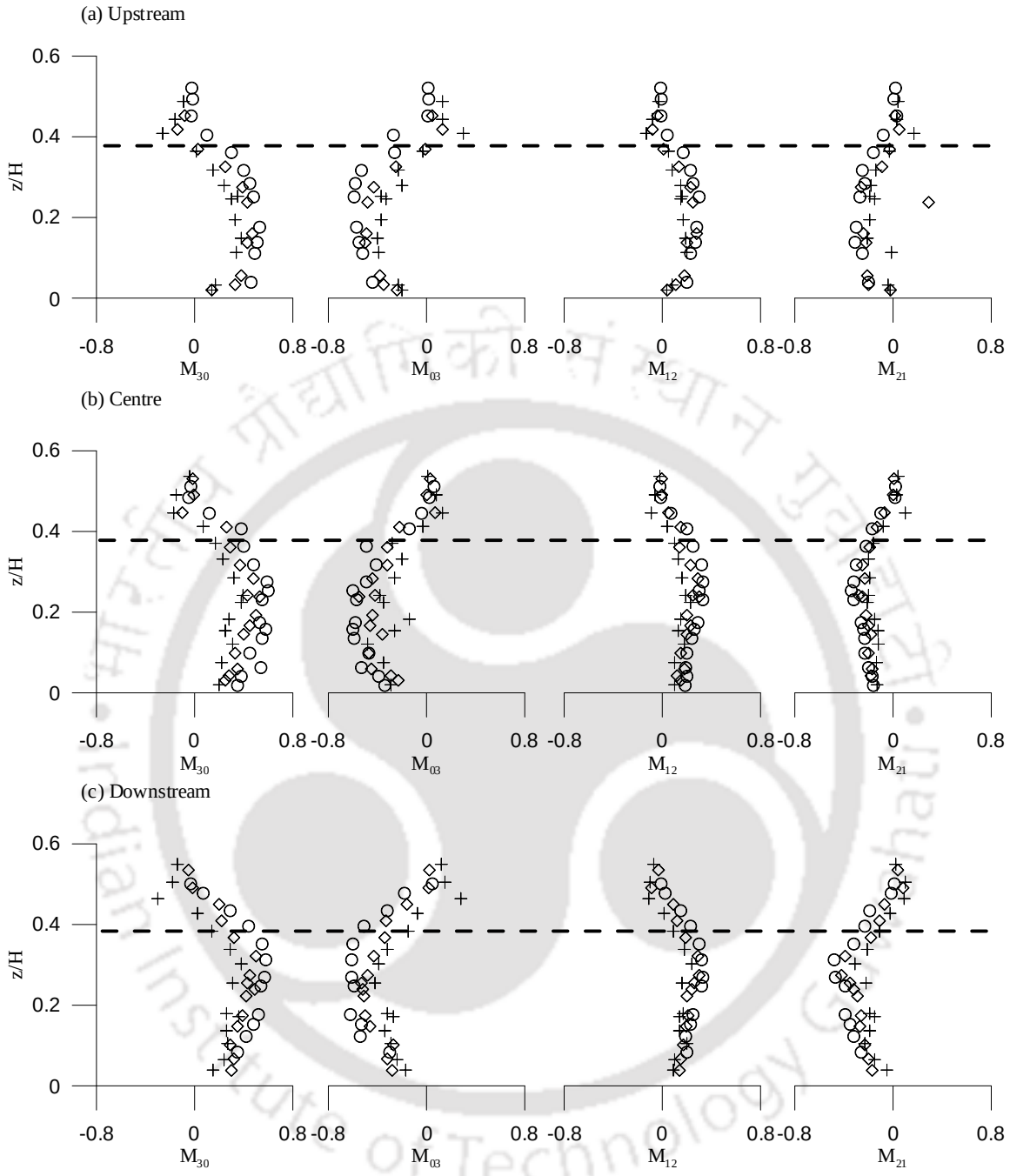

Figure 4.5 Profiles showing third order moments of 10mm diameter upstream-5 mm diameter downstream for no-seepage, 10% seepage and 15% seepage

The negative values of M_{03} and M_{21} near the bed infer that inrush of flow is occurring in the region and the flow coming towards the bed is again carried away by the flow in the flow direction which is observed from positive values of M_{30} and M_{12}.

On observing the change in moment along the streamwise direction for 10mm upstream and 5 mm downstream (Figure 4.4a, 4.4b and 4.4c), the values of moment increases its negativity (M_{03} and M_{21}) and positivity (M_{30} and M_{12}) in the range of 1-5% when the flow goes from upstream to centre while it decreases in the range of 2-6% when the flow goes from upstream to downstream. This implies that sediment transport rate increases at the centre portion and then decreases at the downstream portion as observed from Reynolds stress profiles. But for the case of 5 mm upstream-10 mm downstream (Figure 4.5a, 4.5b and 4.5c), the positive values of M_{30} and M_{12} and the negative values of M_{03} and M_{21} increases in the range of 4-8% as the flow occurs from upstream 5mm portion towards the centre portion and 5-10% as the flow goes from upstream portion towards the downstream 10 mm diameter portion. The presence of lesser vegetation density at the downstream portion leads to more sediment transport rate at the downstream section.

4.6 Quadrant Analysis

Stress contributions to Reynolds stress for different vegetation pattern corresponding to flow depth are shown in figure 4.6 and 4.7. The figures are plotted for no-seepage, 10% seepage and 15% seepage at the three measurement location. The difference between sweep and ejection (*Q4-Q2*) is also calculated where the negative value infers that ejection event is dominant while its positive value implies that sweep action dominates.

It is observed that in the flow region above the vegetation, the flow is dominated by ejection events for no-seepage case but equal contribution of ejection and sweep for lower flow region. With 10% seepage, the difference between ejection and sweep lies closer to zero for upper flow region inferring almost equal contribution of sweep and ejection and the contribution of sweep event is increased. Accordingly with 15% seepage, sweep event has slightly higher contribution comparing to ejection event. It is observed that the application of seepage enhances the sweep event since the flux is occurring in the downward direction.

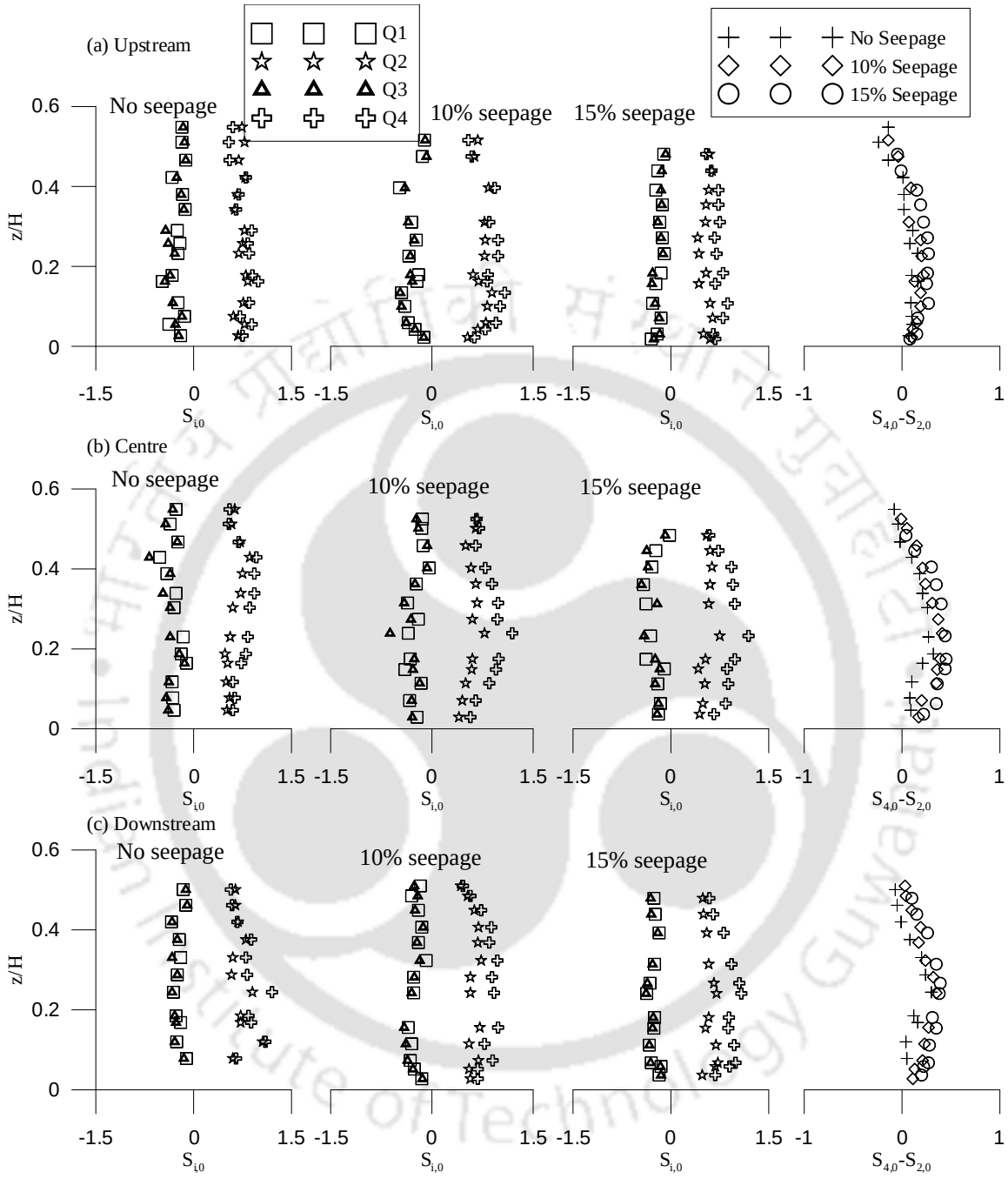

Figure 4.6 Profiles showing fractional stress contribution to Reynolds stress of 5mm diameter upstream and 10 mm diameter downstream

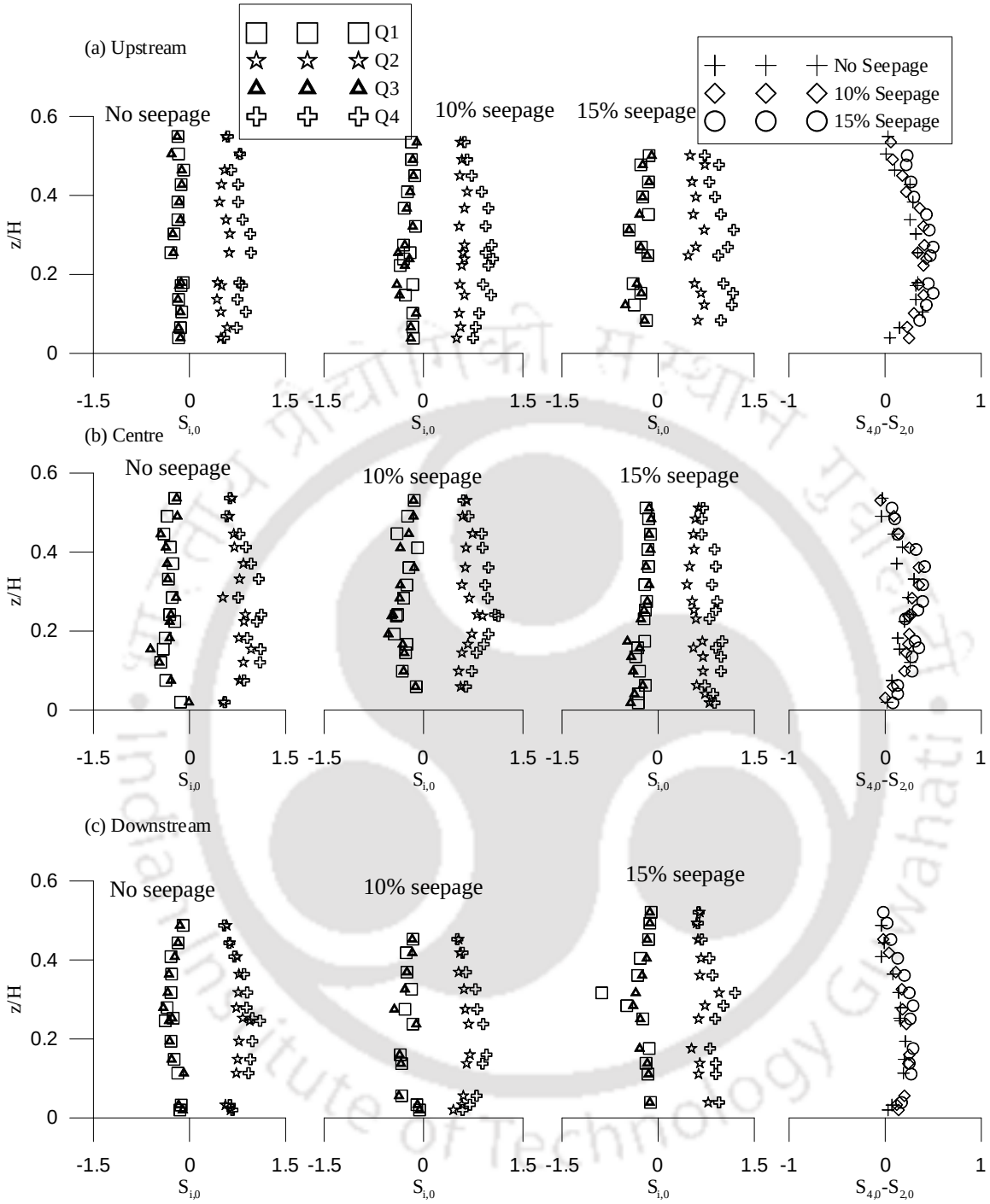

Figure 4.7 Profiles showing fractional stress contribution to Reynolds stress of 10mm diameter upstream and 5 mm diameter downstream

With the application of seepage, sweep action comes to play a dominant role in the lower flow region, difference between sweep and ejection being higher for increasing seepage percentage.

The difference between the sweep and ejection increases in the range of 3-5% for 10% seepage as compared to no-seepage and 2-4% for 15% seepage as compared to 15% seepage.

For the case of 5mm diameter upstream-10 mm diameter downstream (Figure 4.6a, 4.6b and 4.6c), the difference in the sweep and ejection events increases in the value of 3-6% as the flow travels from upstream 5mm diameter towards the centre section and 4-8% from centre towards downstream. More sweep events means more inrush of flow and hence more negative values of M_{03} and positive values of M_{30} are achieved. While for 10mm diameter upstream-5mm diameter downstream, the difference between the sweep events and ejection events is increased in the 2-5% as the flow occurs from upstream towards the centre. An interesting feature is observed for this case where a reduction in the difference between the sweep and ejection is observed in the range of 4-7% when the flow goes from upstream to downstream. This means that the presence of more vegetation density at the downstream portion reduces the occurrence of more sweep event ultimately reducing the sediment transport.

4.7 Drag Coefficient

The measurement of drag force because of vegetation stems directly is a difficult task using appropriate devices. Therefore, it is calculated from the horizontally averaged momentum equation (Nepf and Vivoni, 2000; Nezu and Sanjou, 2008). The momentum equation for steady and uniform 2D open channel flow with homogenous vegetation stems is given below:

$$\frac{\partial}{\partial y}\left(\left(\left(-u'w'\right)+\left(-U''W''\right)\right)+\upsilon\frac{\partial U}{\partial y}\right)=-gI_e-f_{Fx}-f_{Vx} \qquad (4.1)$$

Where I_e is the energy gradient, $\left(-U''W''\right)$ is the dispersive stress term, f_{Vx} is the viscous drag force and f_{Fx} is the form drag force. I_e can be calculated from

$$u_* = \sqrt{\mathrm{gI}_e(H-h_d)} \qquad (4.2)$$

The friction velocity is generally defined as the maximum value of Reynolds stress near the vegetation top, $\left(u'w'\right)_{z=h_d}=u_*^2$. The viscous drag and dispersive stress are assumed to be

negligibly small as compared to stem drag and hence after neglecting these terms, equation (4.1) becomes

$$\frac{\partial}{\partial y}\left(\frac{-u'w'}{u_*^{\,2}}\right) = -\frac{1}{H-h_d} - \frac{f_{Fx}}{u_*^{\,2}} \tag{4.3}$$

The form drag is given by:

$$f_{Fx} = -\frac{1}{2} C_D.a.U^2 \tag{4.4}$$

Where a is the projected plant area per unit volume and U is the time averaged velocity. For cylindrical shape vegetation models, it is estimated as given below:

$$a = \frac{d_v}{s_v^{\,2}} \tag{4.5}$$

where d_v is the vegetation diameter and s_v is the vegetation spacing. Now, the final equation for C_D calculation is:

$$\frac{\partial}{\partial y}\left(\frac{-u'w'}{u_*^{\,2}}\right) = \frac{1}{2} C_D.a.\left(\frac{U}{u_*}\right)^2 - \frac{1}{H-h_d} \tag{4.6}$$

The values of C_D for different vegetation pattern are calculated and plotted in figure 4.8. The value of C_D increases near the bed as was observed by Nepf and Vivoni (2000) which reflects the importance of viscous effects. The observed values of C_D near the bed lie ≤ 3, which agree well with the literature (Nepf and Vivoni, 2000). But, C_D diminishes near the vegetation top as observed by Nepf and Vivoni (2000) and explained that the decrease in the value is attributed to a relaxation of form drag as the flow bleeds around the free end. The average value of C_D for different vegetation diameters when placed at upstream and downstream are plotted against the percentage of seepage. It is observed that 5mm diameter flexible stems when placed at downstream has the highest value of C_D as compared to other cases. This implies that the flow condition in this vegetation pattern has more drag and resists the flow more in the downstream section as is observed from the results of velocity profiles shown above. Because of more drag, sediment transport is less which results in lower value of Reynolds stress.

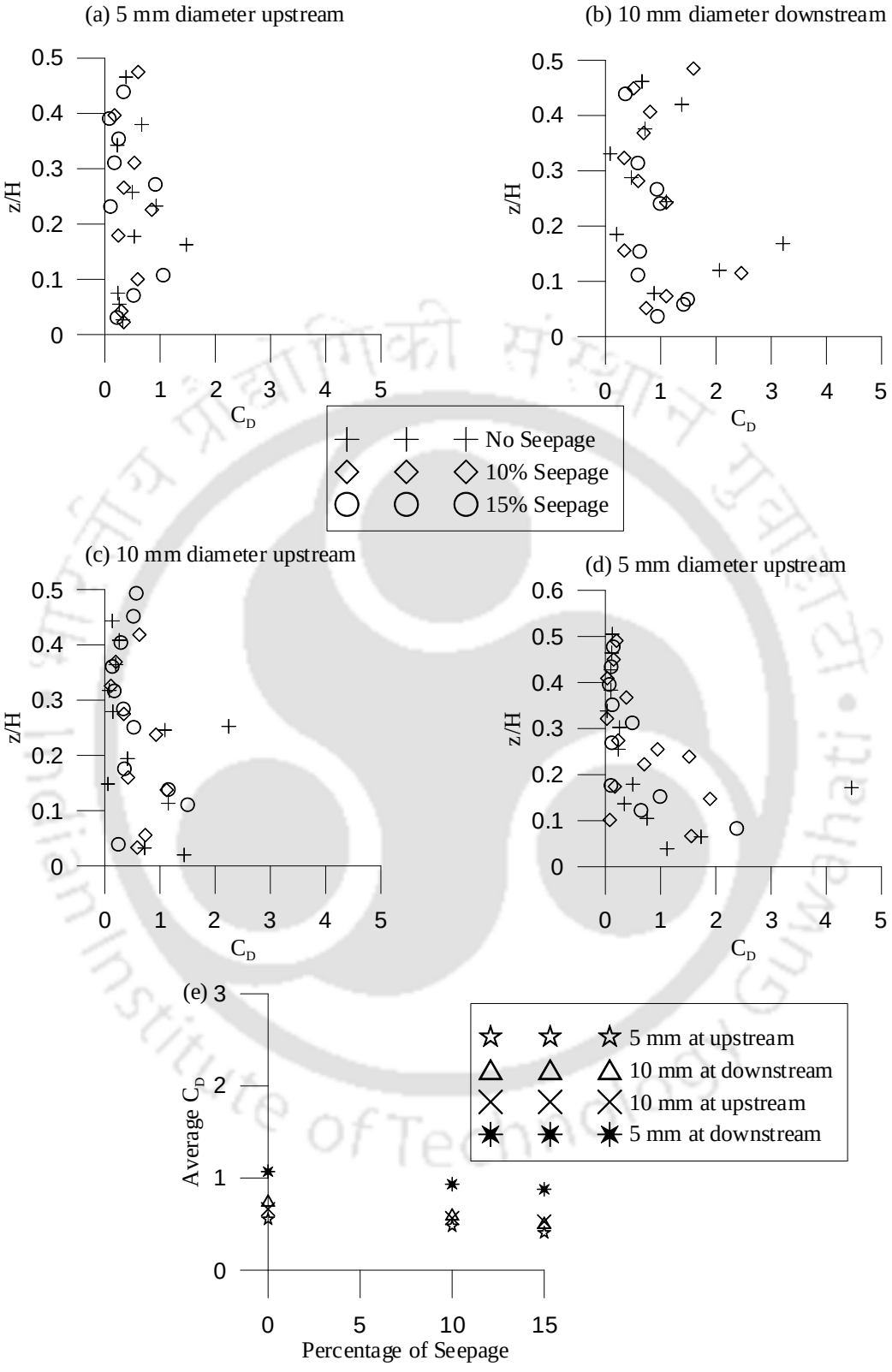

Figure 4.8 Drag Coefficient of different vegetation pattern (a, b, c, d) and average C_D (e) for no-seepage, 10% seepage and 15% seepage

The effect of downward seepage on C_D is also studied. For all the cases, C_D decreases with increase in downward seepage percentage, which means that the downward force owing to seepage is stronger than the vegetation drag which leads to more sediment transport.

4.8 Conclusions

The present study focusses on the experimental investigation of the drag and turbulent characteristics of mixed vegetation densities under downward seepage condition in a mobile-bed flume. The type of vegetation used for the study was flexible vegetation which was simulated by flexible rubber stems of two different diameters of 10 mm and 5 mm. The vegetation densities were fixed with respect to the vegetation diameter (Vegetation density of 10 mm d_v =120 stems/m^2 and vegetation density of 5 mm d_v = 430 stems/m^2). The flow depth was kept more than the vegetation so that the vegetation was under fully submerged condition. The experiments were conducted for no-seepage, 10% seepage and 15% seepage. Different results showing distributions of velocity profiles, Reynolds stress, turbulence intensities, third order moments, stress contributions and drag coefficient for no-seepage, 10% seepage and 15% seepage at different sections i.e. upstream, centre and downstream improve our knowledge in understanding the flow characteristics in a vegetated channel with downward seepage. From the velocity distributions, it is observed that the application of seepage shows the existence of higher velocity zone near the bed. An inflection point occurs near the top of the vegetation. Velocity increases in the range of 7-10% with the application of 10% seepage as compared to no seepage and 3-5% for 15% seepage than the velocity for 10% seepage. The maximum value of Reynolds stress and turbulent intensities occur near the inflection point in the velocity profile. The maximum exchange of mass and momentum between the upper non-vegetated layer and lower vegetated layer occurs near the vegetation top as is evident from the achievement of maximum Reynolds stress near the top of the vegetation. The maximum Reynolds stress near the vegetation top is increased to a value of 5-10% from no seepage to 10% seepage and 3-8 % from 10% seepage to 15% seepage. The presence of high vegetation density at the downstream section reduces the flow velocity and Reynolds stress which is an important finding for river restoration project. Moment analysis was carried out for getting a virtual information regarding contribution of velocity fluctuations, in terms of flux and diffusion, to turbulent production. The increase in the negativity of M_{03} and M_{21} near the bed with the downward seepage implies that inrush of flow is occurring in the region and the flow coming

towards the bed is again carried away by the flow in the flow direction which is observed from positive values of M_{30} and M_{12}.The contribution of velocity fluctuations to Reynolds stress or bursting phenomenon was studied by carrying out quadrant analysis. In the presence of downward seepage, sweep action dominates in the whole region and the difference in the contribution between sweep and ejection increases with increase in seepage percentage. The high vegetation density placed at the downstream portion of the test section reduces the flux transport in the streamwise as well as downward direction as observed by the reduction in the dominance of sweep event over ejection event from quadrant analysis which leads to less sediment transport in the portion. The drag coefficient was also calculated for investigating the resistance of flow imposed by the vegetation stems when placed at different sections (upstream and downstream). It is found that high density vegetation when placed at downstream section has the highest value of C_D. The change in the average drag coefficient with seepage was also studied and found that the value of C_D decreases with increase in seepage percentage.

5 Hydrodynamics of seepage affected channel with vegetation bundles[iv]

5.1 Introduction

In order to evaluate the effect of vegetation on global resistance, it would be necessary to consider the different typologies of vegetation and their natural characteristics, as shape and stiffness of branches and leaves, or shape and stiffness of trunk. Some investigations have approached the definition of drag considering also the presence of leaves and branches (Fathi Maghadam and Kouwen, 1997; James *et al*, 2004; Järvelä 2004; Järvelä, 2005; Righetti and Armanini, 2002; Stone and Shen, 2002; Wilson *et al* 2005), but generally only for the case of submerged vegetation. Other authors have considered also the flexibility of linearly elastic stems in the value of the drag coefficient (Babovic and Keijzer, 2000; Li and Xie, 2011), but only by numerical modeling. Drag coefficient is frequently used as a parameter for representing the flow resistance (Stone and Shen, 2002; Thompson *et al*, 2004, Armanini *et al*, 2005). Stem drag coefficient depends on a number of factors like stem height, diameter, spacing, distribution patterns and density. Li and Shen (1973) theoretically investigated the relations among stem drag coefficient and stem staggering patterns and reported that stem staggering patterns had great influence on flow resistance by affecting the stem drag coefficient. Fenzl (1962) using inflexible thin wire rods conducted an extensive laboratory studies to evaluate flow resistance including vegetal drag coefficient and proposed several empirical formulae to evaluate drag coefficient. However, these empirical formulae have limitation in their applicability since they were developed with considerations of lower values of area concentrations up to 0.81% only. Kouwen *et al* (1969) conducted a laboratory study using polyethylene plastic strips to simulate vegetation. They developed some empirical formulae to compute channel average velocity which is used to estimate drag coefficient. Similar to Fenzl (1962), these formulae have limitations that they were developed without considerations of large

[iv] Devi, T. B., & Kumar, B. (2016). Experimentation on submerged flow over flexible vegetation patches with downward seepage. *Ecological Engineering*, *91*, 158-168.

number of values of roughness area concentrations. Nepf (1999) developed a model to describe the drag, turbulence and diffusion for flow through emergent vegetation and covered the natural range of vegetation density and stem Reynolds numbers to extend the cylinder-based model for vegetative resistance by including the dependence of the drag coefficient, stem density and highlight the importance of mechanical diffusion in vegetated flows. Experimental measurements have been assessed to characterize the flow phenomenon in a natural channel with vegetation patches. Profiles of velocity, Reynolds stress and Turbulence intensities are presented. Quadrant and moment analysis are also evaluated and observed for the present study.

5.2 Velocity

The presence of an inflection point near the top of the vegetation stem is observed because of the difference in velocity in the upper flow region and the lower flow region (Poggi *et al*, 2004; Carollo *et al*, 2005; Chen *et al*, 2011; Nepf, 2012b). From figure 5.1, it is observed that velocity for no seepage for both the spacing is reduced near the top of the deflected vegetation patch height and then starts increasing as observed by previous investigators for sparse vegetation density (Righetti, 2008; Chen *et al*, 2011; Siniscalchi *et al*, 2012; Li *et al*, 2014). Variation in velocity in the vegetation patch region is attributed to the local effect imposed by the presence of vegetation patch. The near bed velocity for both the spacing at 8.5 m is higher (8-16%) as compared to the subsequent downstream sections, 7 m and 5.5 m. This means that the presence of vegetation patch increases the roughness or resistance of the flume thereby reducing the flow velocity. The effect of vegetation spacing on flow velocity can also be observed. Vegetation spacing of 15 cm has a higher velocity (8-12%) as compared to 10 cm spacing which implies that smaller vegetation spacing (or more vegetation density) provides more resistance to the flow. Velocity profiles for different seepage percentages are also plotted correspondingly. It is known that downward seepage shifts the velocity downwards because of which a higher velocity is achieved in the near bed region (Dey and Nath, 2009; Cao and Chiew, 2013). In the present study, the effect of seepage in a vegetation patch zone is studied. Irrespective of the patch pattern and spacing, a higher velocity zone exists in the lower flow region or the near bed region (Figure 5.1).The near bed velocity increases on an average value of 8 % with the application of 10% seepage. It is also observed that in the lower flow region the velocity for 15% seepage case is slightly higher, with an average

increasing value of 15%, than the velocity for no seepage. However, the velocity at the upstream 8.5 m is always higher than the downstream 5.5 m section irrespective of the application of downward seepage.

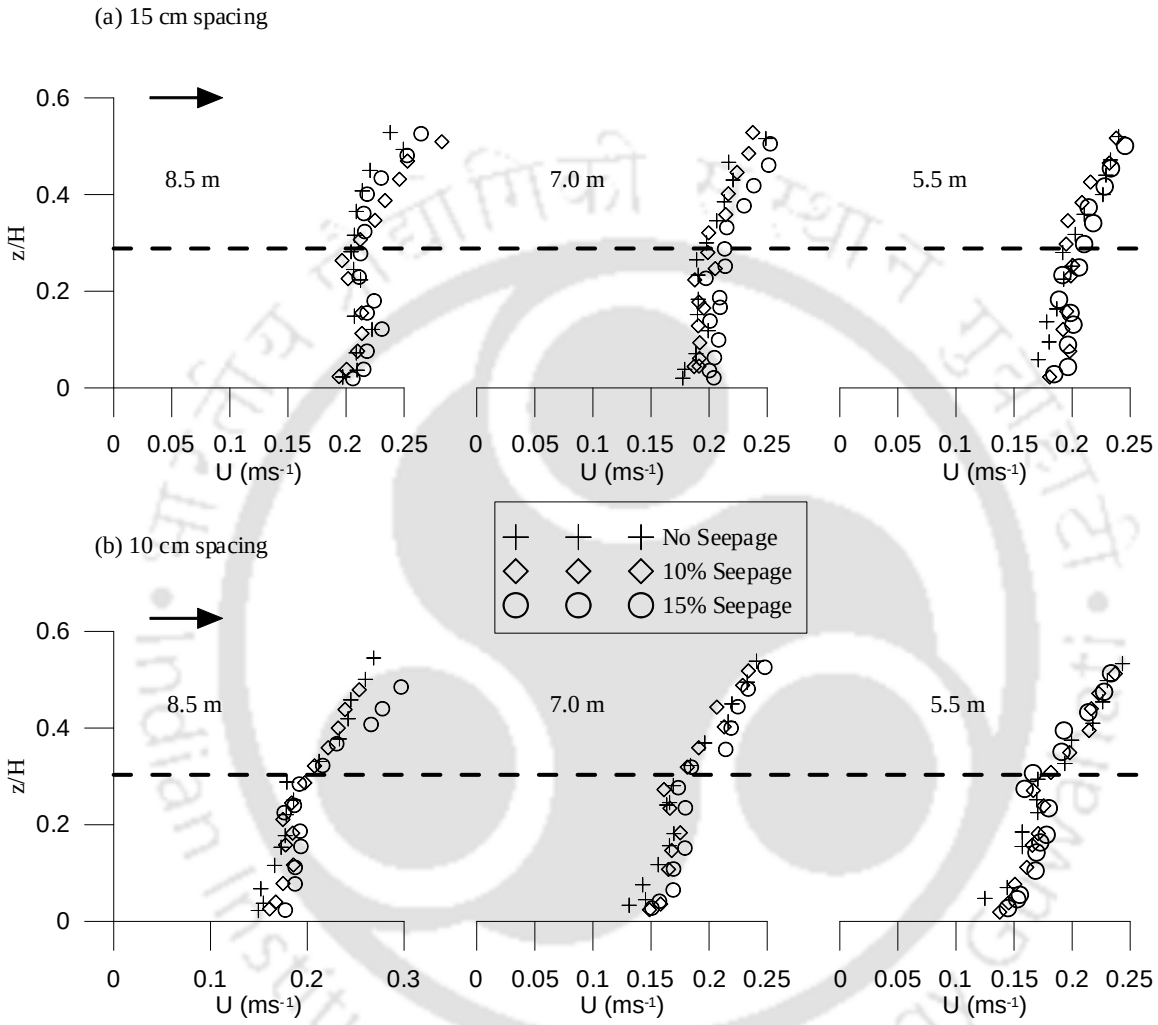

Figure 5.1 Velocity profiles plotted against flow depth at three different measurement locations for no-seepage, 10% seepage and 15% seepage (a) vegetation spacing of 15 cm (b) vegetation spacing of 10 cm (Dashed line shows the height of the deflected vegetation top)

5.3 Reynolds stress

The flow velocity fluctuations lead to exchange of momentum in the flow region which is expressed by the Reynolds stress. It is therefore an important parameter in evaluating the soil erosion and sediment transportation.

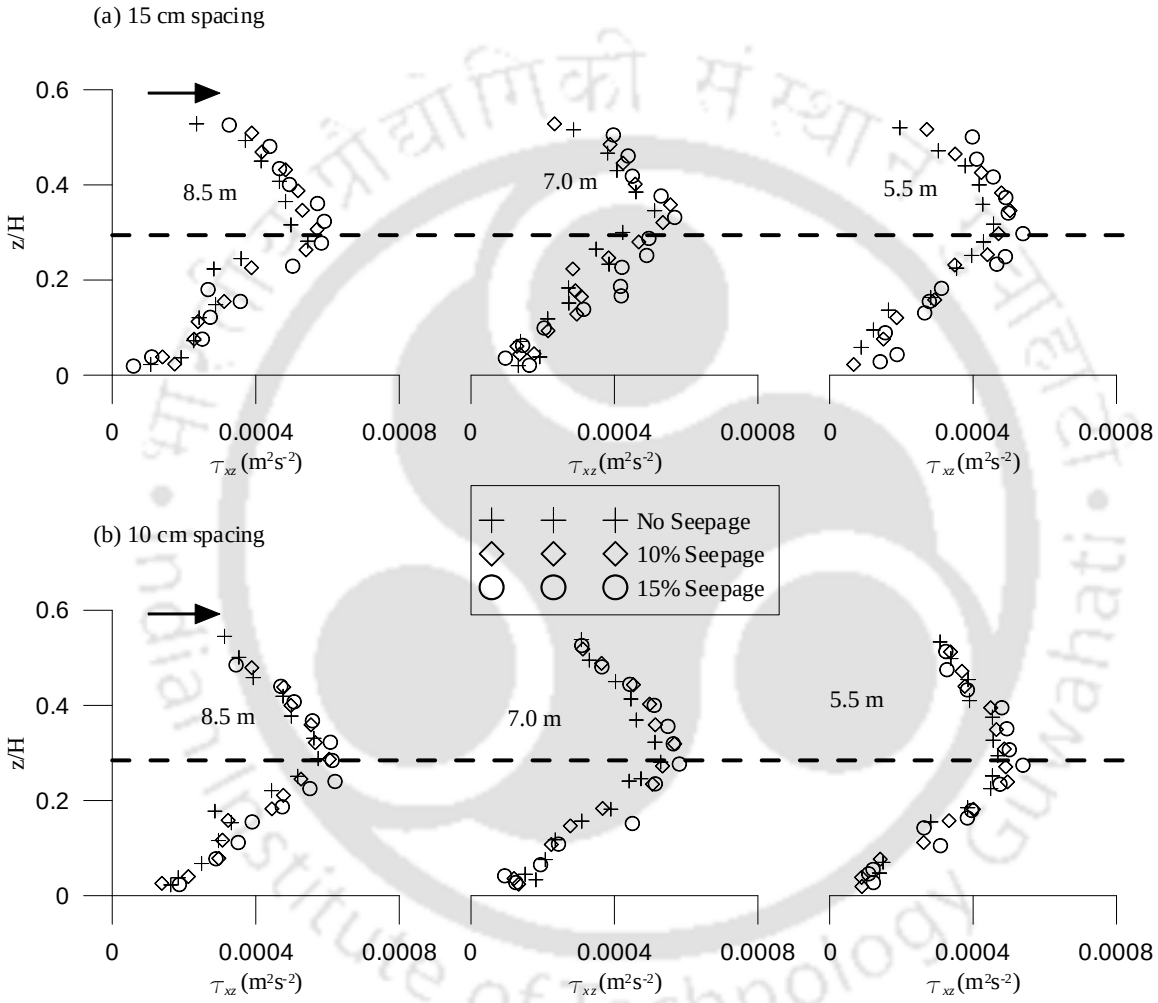

Figure 5.2 Reynolds stress profiles plotted against flow depth at three different measurement locations for no-seepage, 10% seepage and 15% seepage (a) vegetation spacing of 15 cm (b) vegetation spacing of 10 cm

Reynolds stress for 8.5 m, 7 m and 5.5 m are plotted against the flow depth for 15 cm and 10 cm spacing (Figure 5.2). It is observed that Reynolds stress is increased from the water surface towards the location where vegetation is present and reached a maximum value near the top of the

vegetation. After attaining a maximum value near the top of the vegetation, it decreases towards the bed. The Reynolds stress distribution for all the cases has a sharp peak near the vegetation patch edge which implies that the primary turbulence production is contributed by the vegetation stems. This leads to occurrence of more momentum exchange near the top of the vegetation patch. Additionally, the diminishing nature of Reynolds stress is attributed to the fact that the farther the location from the top of the vegetation, the smaller is the turbulence generated by the vegetation patch stems. Thus, vertical distribution of Reynolds stresses is calculated in order to describe the momentum diffusion mechanism. An important observation is that the maximum Reynolds stress at the same location of upstream 8.5 m is more than downstream 5.5 m by a value of 19% and 22% for 15 cm spacing and 10 cm spacing respectively. It is also observed that the maximum Reynolds stress for 15 cm spacing is lower (2-7%) compared to 10 cm spacing.

Figure 5.2 also shows different distributions of Reynolds stress of different vegetation patch spacing for no-seepage, 10% seepage and 15% seepage. It is known that the downward seepage increases the shear stress which leads to more sediment transport as compared to no-seepage (Dey and Nath, 2010). In all the profiles, with the increase in seepage percentage, an increase in shear stress is achieved. The maximum Reynolds stress near the vegetation patch top is increased in the range of 4-9% from no-seepage to 10% seepage and 7-18% from no seepage to 15% seepage. This reiterates that application of downward seepage increases the Reynolds stress thereby increasing bed material transport. Reynolds stress for both 10% and 15% seepage at the upstream 8.5 m is reduced in the range of 10-20 % when the flow reached the downstream 5.5 m. Consequently, it means that in spite of increase in Reynolds stress with the application of downward seepage, vegetation patch reduces the Reynolds stress as the flow goes downstream.

5.4 Turbulence Intensities

Turbulence intensities in the streamwise and vertical directions, σ_u and σ_w, are plotted for no-seepage, 10% seepage and 15% seepage and shown in figure 5.3. Streamwise and vertical turbulence intensities for different spacing of staggered pattern are presented. The turbulence occurring near the vegetation patch top increases the vertical as well as streamwise turbulence intensities.

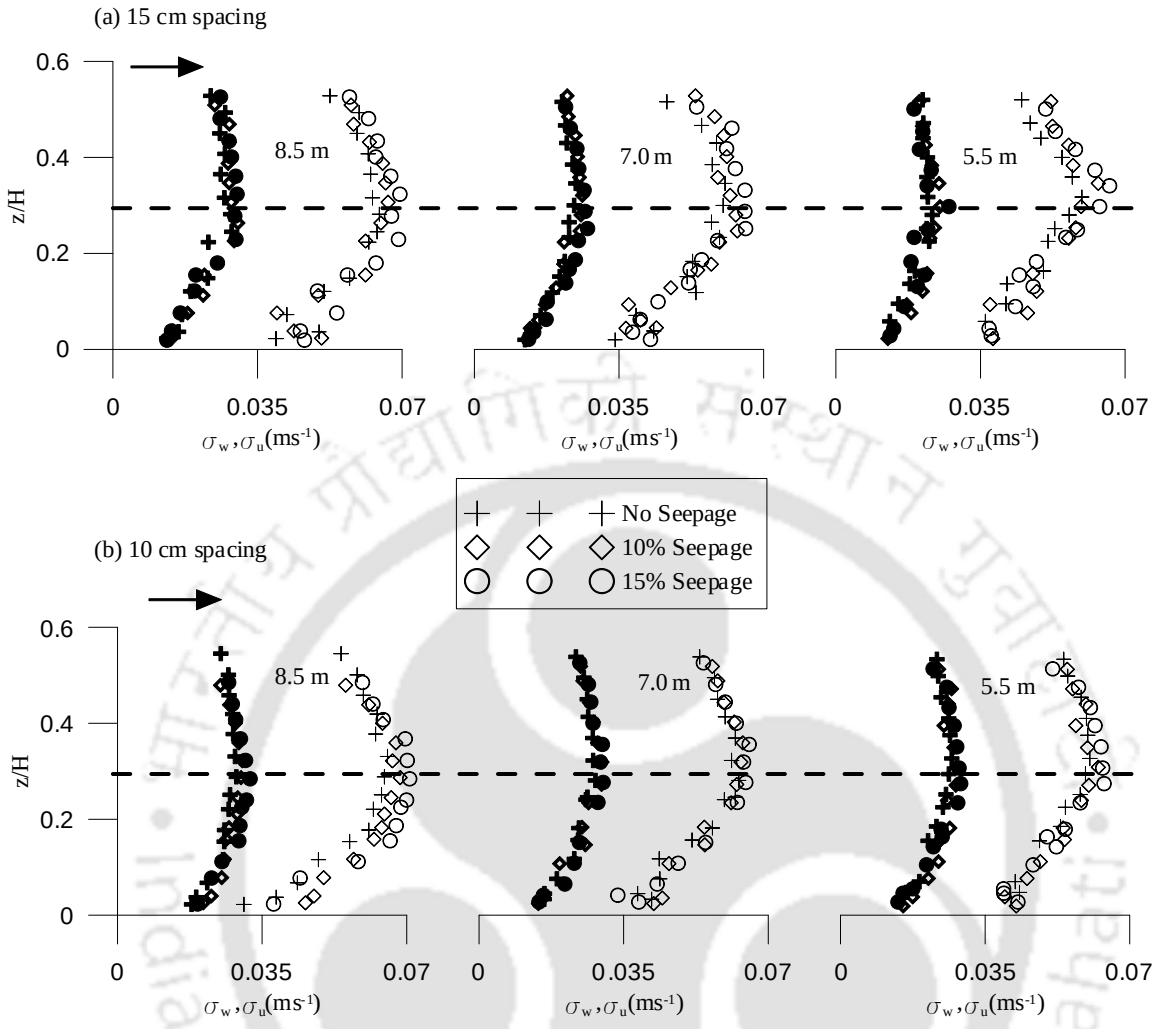

Figure 5.3 Streamwise and vertical turbulence intensities profiles plotted against flow depth at three different measurement locations for no-seepage, 10% seepage and 15% seepage (a) vegetation spacing of 15 cm (b) vegetation spacing of 10 cm, σ_u (+, ◇ ,○) σ_w (✚,◆,●)

All the profiles show maximum value near the top of the vegetation patch. The presence of the inflection point in the velocity profile and the maximum turbulence intensity lie in close approximation (Carollo *et al*, 2002; Velasco *et al*, 2003). The turbulence intensities at the upstream 8.5 m is reduced in the range of 5-9% as the flow reached 5.5 m. From the results of the turbulence intensities, it can be deduced that the intensity of velocity fluctuations occur at the starting portion of the vegetation patch zone decreases at the ending of the vegetation zone implying that the turbulence production is reduced because of the presence of vegetation patch.

Additionally, it is observed that 15 cm centre-centre spacing has got slightly lower turbulence intensities than 10 cm centre-centre spacing. The flow is slightly more sheared for 10 cm centre-centre than 15 cm centre-centre which is shown by higher value of Reynolds stress. 15 cm spacing has approximately 3-9% less intensities values as compared to 10 cm spacing. The effect of seepage is also studied. As observed, downward seepage increases the shear stress and hence with increase in downward seepage percentage, the flow is more sheared which leads to more turbulence intensities. For 10% and 15% seepage also, turbulence intensities for both the spacing are more, achieving an average increase value of 11%, as compared to no-seepage case.

5.5 Third order moments

Third order correlations of velocity fluctuations (M_{30}, M_{03}, M_{12} and M_{21}) for no-seepage, 10% seepage and 15% seepage at three measurement location of 15 cm spacing are shown in figure 5.4 below. For no seepage, M_{30} has positive values near the bed which changes to negative values with increasing depth and the maximum positive occurs below the vegetation. This implies that the $\overline{u'u'}$ flux occurs in the flow direction and the presence of vegetation top obstructs the flux. With the application of seepage, it is known that seepage increases the shear stress which means that more sediment particles get transported in the flow direction. M_{30} achieves a higher positive value near the bed at 10% and 15% seepage percentages as compared to no-seepage case. This means that the transport of flux in the flow direction is more with the application of seepage.

In the case of M_{03}, it has negative values near the bed and positive values with increase in depth which indicates that the $\overline{w'w'}$ flux is in downward direction. With the application of downward seepage, the negativity of M_{03} increases which is justifiable with the fact that downward flow is occurring from seepage. More negative value is observed below the vegetation zone.

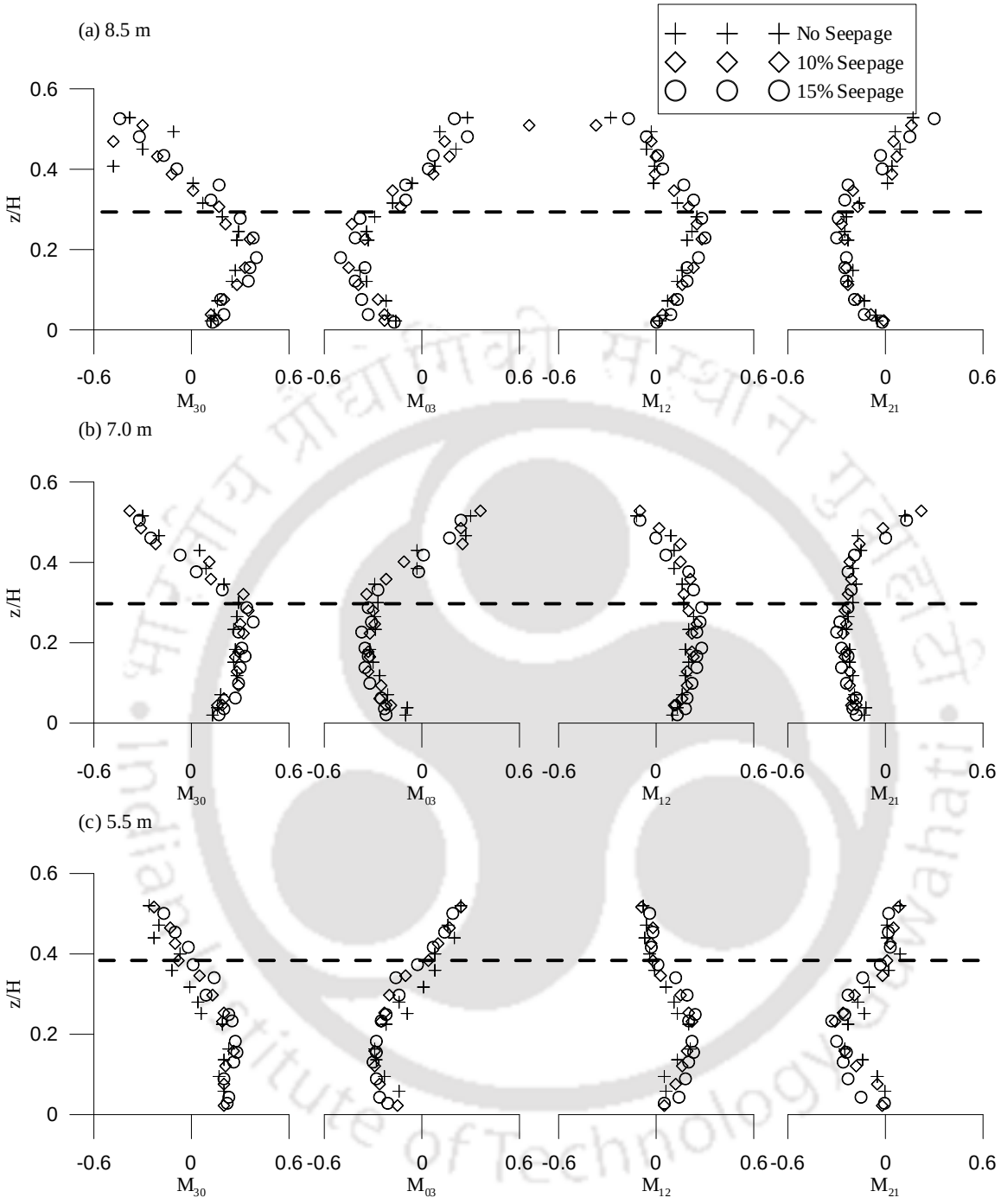

Figure 5.4 Third order moments plotted against flow depth at three different measurement locations for no-seepage, 10% seepage and 15% seepage (a) upstream (b) centre (c) downstream (15 cm vegetation spacing)

M_{12} and M_{21} define the turbulent advection of the normal Reynolds stresses. For 10% seepage and 15% seepage, these two correlations tend to deviate from zero value. M_{12} started to have positive values near the bed and the positive nature increases with increase in downward seepage percentage. M_{21} also has negative values near the bed and increases with increase in seepage percentage. M_{12} being positive near the bed and M_{21} being negative near the bed indicates that the $\overline{w'w'}$ diffusion propagates in the flow direction and $\overline{u'u'}$ diffusion occurs in the downward direction respectively.

The negative values of M_{03} and M_{21} near the bed infer that inrush of flow is occurring in the region and the flow coming towards the bed is again carried away by the flow in the flow direction which is observed from positive values of M_{30} and M_{12}

5.6 Quadrant analysis

Stress contributions to Reynolds stress for different vegetation pattern and spacing corresponding to flow depth are shown in figure 5.5. The figures are plotted for no-seepage, 10% seepage and 15% seepage at 8.5m, 7.0 m and 5.5 m of 15 cm spacing. The difference between ejection and sweep is also calculated. The difference between sweep and ejection (*Q4-Q2*) is also calculated where the negative value infers that ejection event is dominant while its positive value implies that sweep action dominates.

The flow regions dominated by ejection events are analogous with negative values of M_{30} and positive values of M_{03} while sweep events are associated with positive values of M_{30} and M_{03} (Righetti, 2008; Dey and Nath, 2009). For no seepage, flow region above vegetation patch at 8.5 m and 7.0 m has achieved almost equal contribution of ejection and sweep while the flow region below the vegetation patch or near bed region is dominated by sweep event. But, at 5.5 m, the whole flow region has got equal contribution of sweep and ejection. The dominance of sweep event in the near bed region is not considerable because of which lower Reynolds stress is achieved in this section as compared to 8.5 m and 7 m.

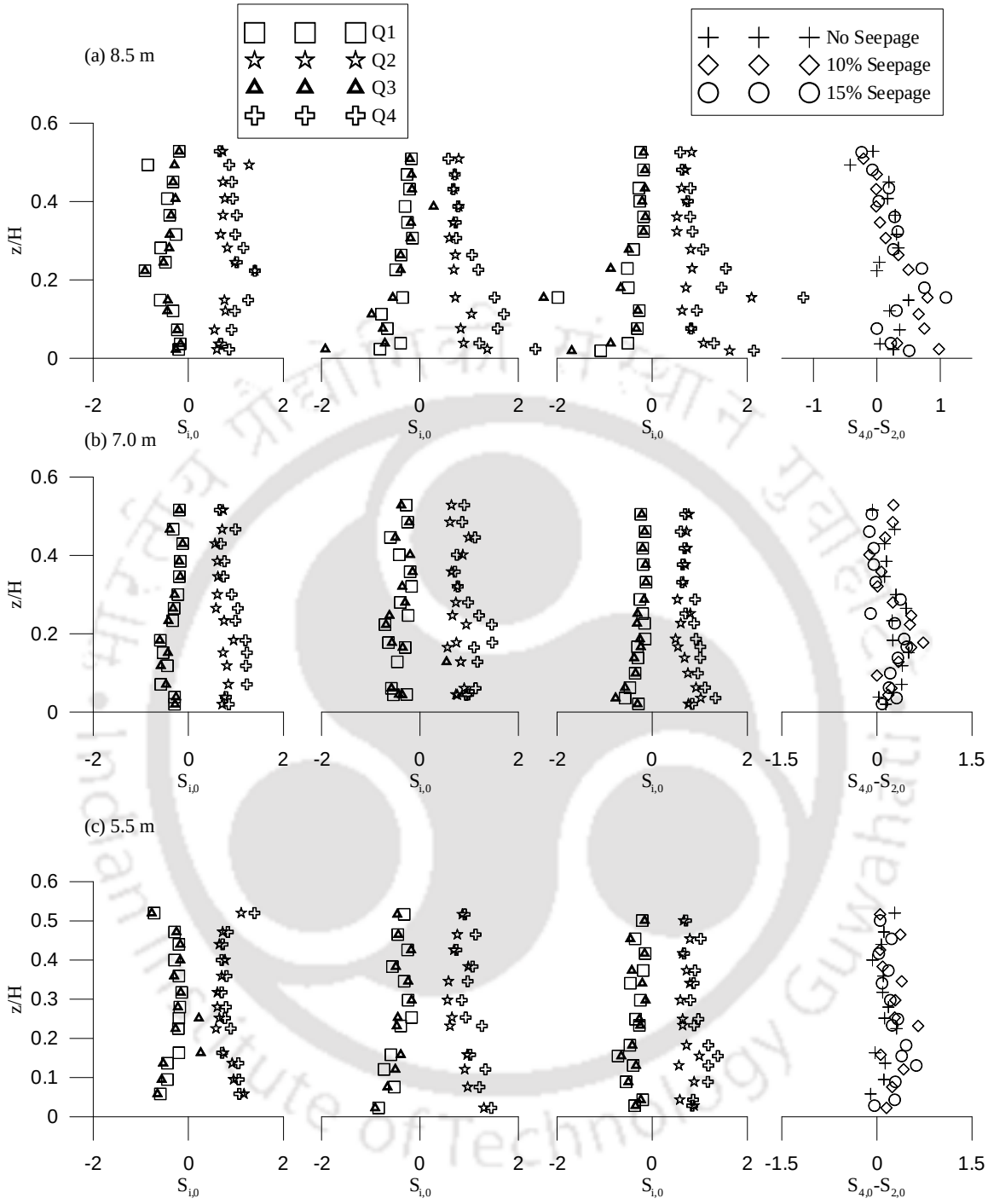

Figure 5.5 Stress contributions plotted against flow depth at three different measurement locations for no-seepage, 10% seepage and 15% seepage (a) upstream (b) centre (c) downstream (15 cm vegetation spacing)

From the profiles of difference in sweep and ejection ($S_{4,0}$-$S_{2,0}$) against the flow depth, it can be observed that the value lies close to zero for the flow above vegetation which means equal contribution of sweep and ejection. With the application of seepage, sweep action comes to play a dominant role in the lower flow region, difference between sweep and ejection being higher for increasing seepage percentage. The profiles of 10% and 15% are higher than no seepage which infers that downward seepage triggers more sweep event compared to ejection event and thus Reynolds stress increases leading to more sediment transport.

5.7 Drag Coefficient

Vegetative drag has a pronounced effect on flow velocities and thus it affects the flow resistance and therefore any flow expressions in vegetated open channel must consider this drag. The values of C_D for different vegetation patch spacing are calculated and plotted in figure 5.6.

Drag coefficient of flexible vegetation is a depth-dependent parameter, as the rigidity and thickness of the plants are decreasing with the plant's length from the roots to the upper part of the plant. The observed values of C_D for no seepage near the bed lie closer to 2, which agree well with the literature (Nepf and Vivoni, 2000). The values of C_D decreases near the vegetation patch top and then increases as flow depth decreases. The increase in the value of C_D reflects the importance of viscous effects (Nepf and Vivoni, 2000). The diminishing nature of C_D near the vegetation patch top is attributed to a relaxation of form drag as the flow bleeds around the free end (Nepf and Vivoni, 2000).

Table 5.1 shows the average drag coefficient for different vegetation spacing and seepage conditions. It is observed that vegetation spacing also plays an important role in influencing the flow conditions. The average C_D value for no seepage is 0.79 for 15 cm spacing and 0.87 for 10 cm spacing. This implies that smaller vegetation patch spacing (or higher vegetation density) provides more resistance to flow because of which lower velocity is achieved. Because of more drag, sediment transport is less which results in lower value of Reynolds stress.

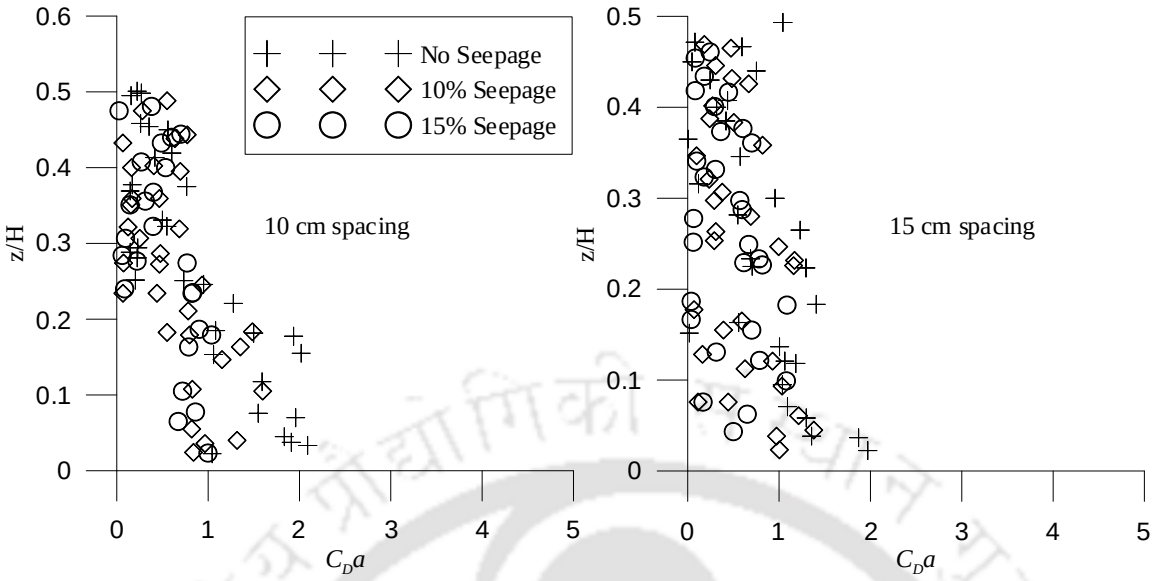

Figure 5.6 Drag coefficient plotted against flow depth at three different measurement locations for no-seepage, 10% seepage and 15% seepage (a) vegetation spacing of 15 cm (b) vegetation spacing of 10 cm

Table 5.1 Average drag coefficient for different vegetation spacing and seepage conditions

Vegetation spacing (s_v)	Seepage conditions	Average C_D
15 cm	0% (No seepage)	0.79
15 cm	10% Seepage	0.58
15 cm	15% Seepage	0.47
10 cm	0% (No seepage)	0.87
10 cm	10% Seepage	0.64
10 cm	15% Seepage	0.52

The effect of downward seepage on C_D is also studied. For both the vegetation spacing, C_D decreases with the application of downward seepage, which means that downward seepage pulls the vegetation patch towards the bed thereby lowering the roughness. The downward force owing to seepage is stronger than the vegetation drag which leads to attainment of more Reynolds stress

with seepage as compared to no seepage resulting in more sediment transport. The average C_D for 10 % seepage are 0.58 (15 cm spacing) and 0.64 (10 cm spacing) and for 15% seepage are 0.47 (15 cm spacing) and 0.52 (10 cm spacing).

5.8 Conclusions

Flow structures of fully submerged flexible vegetation patches in a staggered pattern with two different spacing are analyzed in a flume incorporating the effect of downward seepage. Experimental results demonstrate that the velocities measured at the upstream vegetation patch section is 8-16% more than the downstream vegetation patch section thereby meaning that the presence of increases the roughness or resistance of the flume thereby reducing the flow velocity. The effect of the change in vegetation spacing on flow velocity is also observed and found that low vegetation spacing offers more resistance to flow because of which a reduction in the range of 8-12% is achieved. Downward seepage increases the near-bed velocity of no seepage case by an average value of 8% and 15% for 10% and 15% seepage respectively. However, the velocity at the upstream 8.5 m is always higher than the downstream 5.5 m section irrespective of the application of downward seepage. Reynolds stress distribution shows a maximum value near the vegetation top highlighting the importance of turbulence generated near the vegetation stems. When the flow enters the vegetation patch zone, higher Reynolds stress is achieved because of the flow contraction eroding the upstream vegetation patch section but it decreases (19% and 22% for 15 cm spacing and 10 cm spacing) as the flow reaches the downstream vegetation patch section. This implies that the upstream vegetation patch section acts like an erosion barrier for the downstream vegetation patch section. Downward seepage increases the maximum Reynolds stress near the vegetation patch top by 4-9% from no-seepage to 10% seepage and 7-18% from no seepage to 15% seepage. Vegetation patch continues to act like an erosion control measure with downward seepage also as it reduces the maximum Reynolds stress by 10-20% as the flow reaches the downstream vegetation patch section. The turbulence intensities at the upstream 8.5 m are reduced in the range of 5-9% as the flow reached 5.5 m. From the results of the turbulence intensities, it can be deduced that the intensity of velocity fluctuations occur at the starting portion of the vegetation patch zone decreases (5-9%) at the ending of the vegetation zone implying that the turbulence generation is reduced because of the presence of vegetation. For 10% and 15%

seepage also, turbulence intensities for both the spacing increases by an average value of 11%, as compared to no-seepage case. Third order moments show that the negative values of M_{03} and M_{21} near the bed implies that flow is coming towards the bed and the flow coming towards the bed is transported in the flow direction which is observed from positive values of M_{30} and M_{12}. Downward seepage aggravates the flux transport in downward direction and diffusion in the streamwise direction leading to more sediment transport. Different stress contributions towards Reynolds stress are evaluated through quadrant analysis which divides the whole contribution in four quadrants. Quadrant analysis shows that sweep and ejection provides more contribution than outward and inward interactions. The flow region above the vegetation patch has got almost equal contribution of ejection and sweep. The dominance of sweep can be observed in the near bed region which increases with the application of downward seepage. Drag coefficient is decreased near the vegetation patch top as observed by Nepf and Vivoni (2000) and is more near the bed region because of which a lower velocity region is achieved in the vegetation patch zone.

6 An experimental study of flow through natural vegetation[v,vi]

6.1 Introduction

Recent investigations have been featuring the role of aquatic vegetation as improving water quality by removing nutrients from and releasing oxygen to the water column (Wilcock *et al*, 1999; Schulz *et al*, 2003; Zhu *et al*, 2016), promoting habitat diversity by creating a diversity of flow regimes (Kemp *et al*, 2000; Crowder and Diplas, 2002), stabilizing the river bed and channel morphologies (Braudrick *et al*, 2009; Chao *et al*, 2009; Li and Millar, 2010) and inducing sediment deposition and retention (Abt *et al*, 1994; López and García, 1998; Lee and Shih, 2004; Cotton *et al*, 2006; Gurnell *et al*, 2006). Realizing the importance of vegetation, it has been regarded as river system engineers which not only responds to their physical environment but also modifies it thereby controlling aquatic and riparian ecosystem structure and function as well as river morphodynamics (Jones *et al*, 1994; Gurnell, 2014). Therefore, vegetation can be regarded as the key element to investigate interconnections between ecological, hydrodynamic and biomechanical aspects of physical processes developing at different scales. A large number of researches have been carried out for investigating the flow characteristics in a vegetated channel. De Lima (2015) studied the flow patterns around two neighboring patches of emergent vegetation and observed that flow distribution is influenced by interaction between neighboring vegetation patches and suggest that this may create feedbacks that influence the evolution of vegetated landscapes. Folkard (2011) presented the analyses of results from laboratory flume experiments in which flow within gaps in canopies of flexible, submerged aquatic vegetation simulations is investigated. Okamoto and Nezu (2013) investigated the spatial evolution of coherent motions considering a finite length rigid vegetation patch and examined the transition from boundary-layer flow upstream of the patch to mixing-layer-type flow within the patch. Pang *et al* (2013) investigated the turbulence structure

[v] Devi, T. B., & Kumar, B. (2016). Flow characteristics in an alluvial channel covered partially with submerged vegetation. *Ecological Engineering*, *94*, 478-492.

[vi] Devi,T.B. & Kumar, B. Flow characteristics in a fully covered submerged natural vegetation with downward seepage. *Canadian Journal of Civil Engineering* (Accepted)

and flow field of shallow water with a submerged eel grass patch and found that turbulent intensity increases from the water surface to the canopy, then decreases to the plant root. Vegetation produces drag and thus has a hydraulic impact on flow carrying capacity. The hydraulic resistance produced by vegetation depends on many factors, including the vegetation stem size, plant height, vegetation density and flow depth. Vegetation produces drag and thus has a hydraulic impact on flow carrying capacity. The hydraulic resistance produced by vegetation depends on many factors, including the vegetation stem size, plant height, vegetation density and flow depth. James *et al* (2006) developed a hypothetical model of vegetation-influenced flow for identifying the most significant variable for determination of flow resistance.

6.2 Fully submerged

6.2.1 Velocity

The presence of vegetation in a channel affects the flow characteristics. The transition from sand bed to the vegetated bed leads to the development of a new boundary layer. Figure 6.1 shows the distribution of streamwise component of velocity at the free upstream (0.5 m upstream of the vegetation zone), centre (centre of the vegetation zone) and free downstream (0.5 m downstream of the vegetation zone) sections. The flow velocity (no seepage) in the free upstream of the vegetation zone follows a logarithmic velocity profile (Figure 6.1) as observed by Chen and Chiew (2004). For fitting the data points to the logarithmic law of the wall, the time averaged velocity, U and the vertical distance, z are scaled by the shear velocity, u_* and d_{50} such that $u^+=U/u_*$ and $z^+=z/d_{50}$. More detail information regarding the fitting can be found in Deshpande and Kumar (2016b). The fitting of the log law is shown in Figure 6.1. The non-dimensional expression of the log law is:

$$\frac{U}{u_*}=\frac{1}{k}\ln\left(\frac{z^+ + \Delta z^+}{\chi^+}\right) \tag{6.1}$$

where $z^+ = z/d_{50}$, $\Delta z^+ = \Delta z/d_{50}$, Δz is the depth of the virtual bed below the bed surface, $\chi^+ = z_0/d_{50}$, z_0 is the zero velocity level and k is the von Karman's constant.

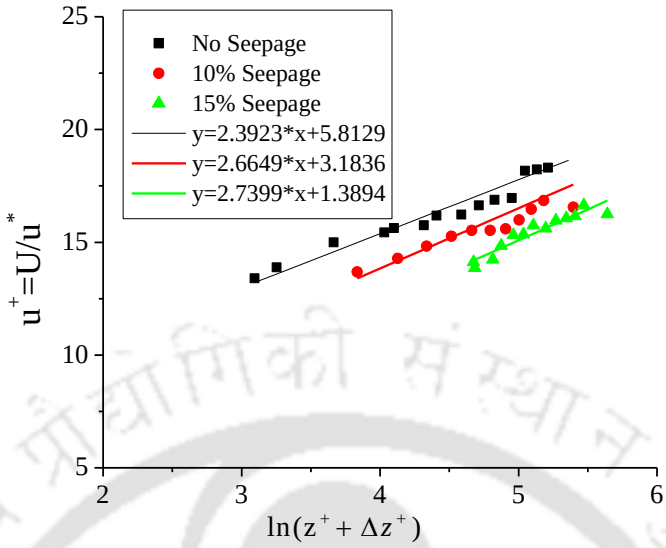

Figure 6.1 Velocity distribution at the free upstream showing the fit of logarithmic law

The values of von Karman's constant for no seepage, 10% seepage and 15% seepage are 0.41, 0.37 and 0.36 respectively. The value of von Karman's constant for no seepage condition is found to be in good agreement with the universal value (0.40). Because of the application of downward seepage, the channel bed transports the sediment particles and therefore achieve a lower value of von Karman's constant. The depth of virtual bed level and zero velocity level for no seepage are 2.92 mm and 0.04 mm; 4.18 mm and 0.13 mm for 10% seepage and 5.85 mm and 0.69mm for 15% seepage. The increase in the value of virtual bed level and zero velocity level with the application of downward seepage is attributed to the exposure of sediment particles on the bed surface to an increased velocity. But the presence of vegetation modifies the velocity profile which is similar to the profile as observed by Righetti (2008), Chen *et al* (2011) and Li *et al* (2014). For each of the velocity distributions, vegetation height is found to influence the flow characteristics; flow velocity is reduced near the vegetation top.

As seen from figure 6.2, for the region above the vegetation, the flow is fully developed and decreases toward the vegetation region. The vegetation stems provide resistance to flow and hence velocity is lower in the lower vegetation layer as compared to the upper free surface layer. The

presence of downward seepage brings to a change in flow discharge and momentum transfer and hence the velocity distribution is modified.

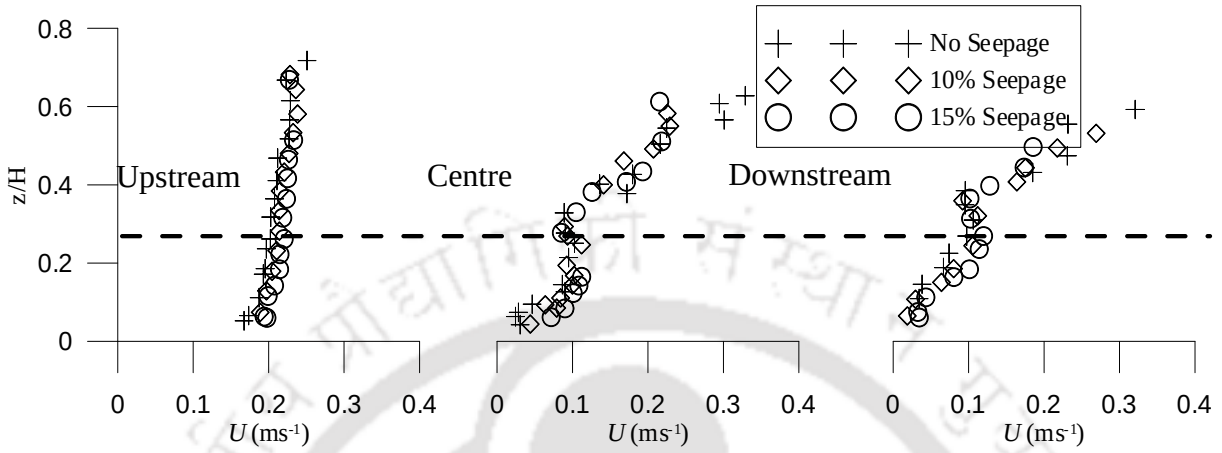

Figure 6.2 Velocity distribution at the upstream, centre and downstream of vegetation section for no seepage, 10% seepage and 15% seepage (Dashed line shows the top of vegetation)

It is known that when downward seepage occurs in a channel, the velocity profile shifts downwards because of which the velocity near the bed increases (Chen and Chiew, 2004; Cao and Chiew, 2013). From figure 6.2, it can be seen that the presence of seepage leads to an increase in velocity near the bed, when 10% and 15% seepage percentages are applied, as compared to no-seepage case. At all the measurement sections, the velocity for 10% seepage case is more than the no seepage case and the velocity is again increased at 15% seepage case.

6.2.2 Reynolds Stresses

Maximum Reynolds stress occurs near the bed for upstream free-vegetation zone highlighting the importance of channel bed in turbulence production but for the centre of the vegetation zone, the position of maximum Reynolds stress is no longer the channel bed. The difference in velocity just above and below the vegetation layer causes momentum exchange at the interface or top of the vegetation which leads to the formation of shear layer. Oscillations are produced near the top of the vegetation because of the shear layer. These oscillations help in exchanging mass and momentum between the lower or vegetated layer and upper or surface layer. Thus, the maximum value of Reynolds stresses in the vegetation zone occurs near the top of the vegetation. Figure 6.3 shows different distributions of Reynolds stress at three different streamwise or streamwise

distances (upstream, centre and downstream). The value of Reynolds stress is increased from the water surface towards the top of the vegetation and achieved a maximum value near the top of the vegetation. After attaining a maximum value near the top of the vegetation, it decreases towards the bed. The oscillation at the top of the vegetation leads to the creation of more turbulence. This in turn leads to occurrence of more momentum exchange near the top of the vegetation and ultimately results in more Reynolds stress at that location. The oscillation in the downside of the vegetated layer is obstructed by the vegetation stems. This implies that the value of Reynolds stress is decreased as the location moves away from the top of the vegetation. The increase in Reynolds stress in the vegetation zone is attributed to the phenomenon of local erosion and deposition occurring because of the presence of vegetation.

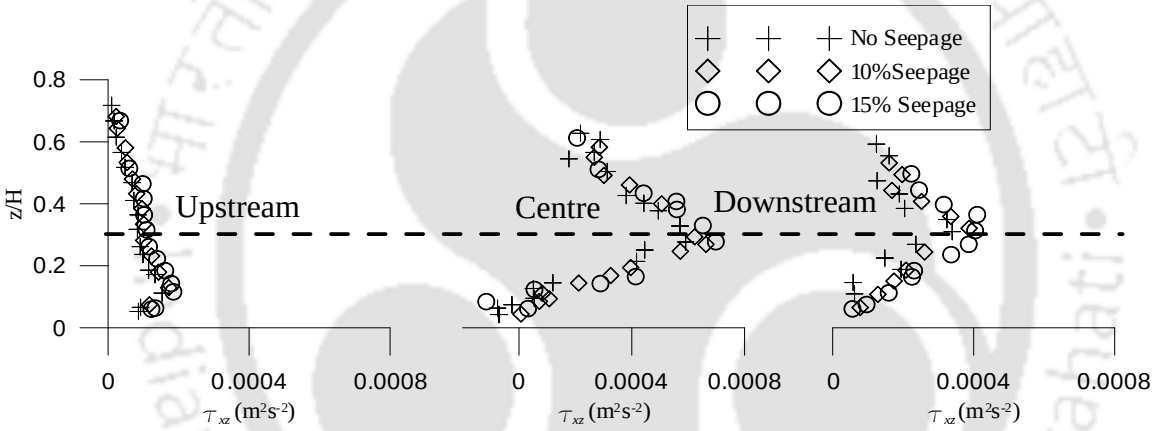

Figure 6.3 Reynolds stress distribution at the upstream, centre and downstream of vegetation section for no seepage, 10% seepage and 15% seepage

When water is drawn through the bed because of the application of downward seepage, it leads to a change in boundary shear stresses. It is already found from previous studies (Maclean 1991; Rao *et al* 1994; Chen and Chiew 2004; Patel et. al. 2015; Deshpande and Kumar 2016b) that presence of downward seepage increases the bed shear stress thereby increasing the sediment movement or transport. In the present study also, it is found that downward seepage increases the maximum Reynolds stress at no seepage by a percentage increase of 19% (average value for upstream, centre and downstream) for 10% seepage and average of 38% for 15% seepage as compared to no seepage. A noteworthy point is that even with the application of downward seepage the maximum Reynolds stress at the centre of the vegetation zone is always higher than the downstream measurement location (an average approx. value of 15%) which signifies that vegetation is still

effective in reducing the Reynolds stress highlighting the importance of using vegetation as a part of river restoration programme.

6.2.3 Turbulence Intensity

Turbulence intensity is generally calculated to obtain information regarding contribution of fluctuating components of velocity to the turbulence production.

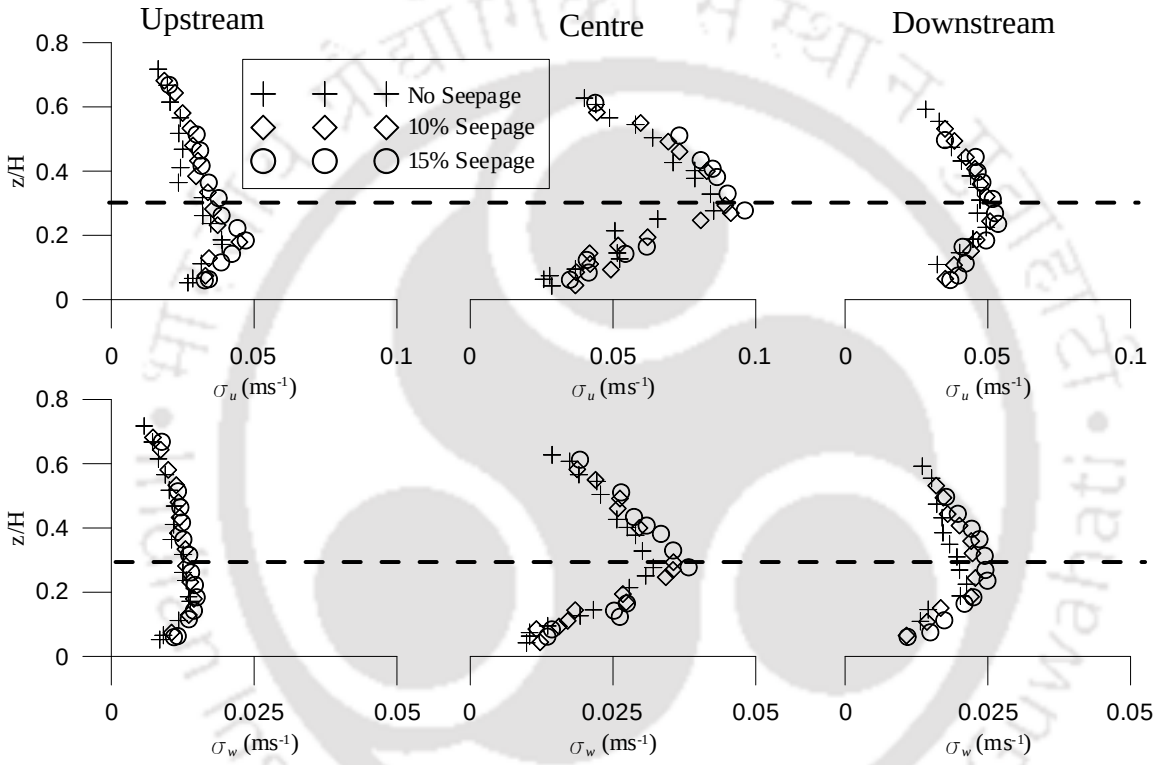

Figure 6.4 Turbulent intensities distribution at the upstream, centre and downstream of vegetation section for no seepage, 10% seepage and 15% seepage

The turbulence intensities in the centre and downstream of the vegetation zone have a maximum value near the top of the vegetation which is different from the case of upstream free-vegetation zone where the maximum value of turbulent intensities lies near the bed (Figure 6.4). The flow is highly sheared near the top of the vegetation and hence a maximum value of turbulence intensity is noted. Vertical turbulence intensities also exhibit similar behaviour as streamwise turbulence intensities but in terms of magnitude vertical turbulence intensities are nearly one-third of the streamwise turbulence intensities.

As observed, downward seepage increases the shear stress and hence with increase in downward seepage percentage, the flow is more sheared which leads to more turbulence intensities. For 10% and 15% seepage also, turbulence intensities are more, achieving an average increase value of 16% for 10% seepage and 27% for 15% seepage as compared to no-seepage case.

6.2.4 Moment Analysis

The study of the third order correlation of velocity fluctuations are generally carried out to derive virtual information on contribution of velocity fluctuations, in terms of flux and diffusion, to the turbulent coherent structures. Third order correlations of velocity fluctuations (M_{30}, M_{03}, M_{12} and M_{21}) for no-seepage, 10% seepage and 15% seepage at upstream, centre and downstream are shown in figure 6.5. For the upstream section which is free of vegetation, M_{30} and M_{12} start with small positive values near the bed, changing over to negative values for $z/H \geq 0.06$ which implies that the bed-load transport influences M_{30} and M_{12} by changing the $\overline{u'u'}$-flux and the $\overline{w'w'}$-diffusion to the streamwise direction. At $z/H > 0.06$, the $\overline{u'u'}$-flux and the $\overline{w'w'}$ -diffusion occur against the streamwise direction and become pronounced with increasing z/H. M_{03} and M_{21} in mobile-bed flows are negative near the bed ($z/H \leq 0.06$) and positive for $z/H > 0.06$ which suggests that the $\overline{w'w'}$-flux and the $\overline{u'u'}$-diffusion are in downward direction in the near-bed flow zone for the mobile-bed case. For the centre of the vegetation zone, M_{30} has maximum positive values near the vegetation top which changes to negative values with increasing depth. This implies that the $\overline{u'u'}$ flux occurs in the flow direction for the vegetation zone which denotes the occurrence of shear layer near the vegetation top (Nezu and Sanjou 2008; Righetti 2008). With increase in seepage percentage, there is an increase in the positive values of M_{30} near the bed. In the case of M_{03}, it has negative values near the bed, having maximum negative value near the top of the vegetation. With the application of downward seepage, the negativity of M_{03} increases which is justifiable with the fact that downward flow is occurring because of seepage.

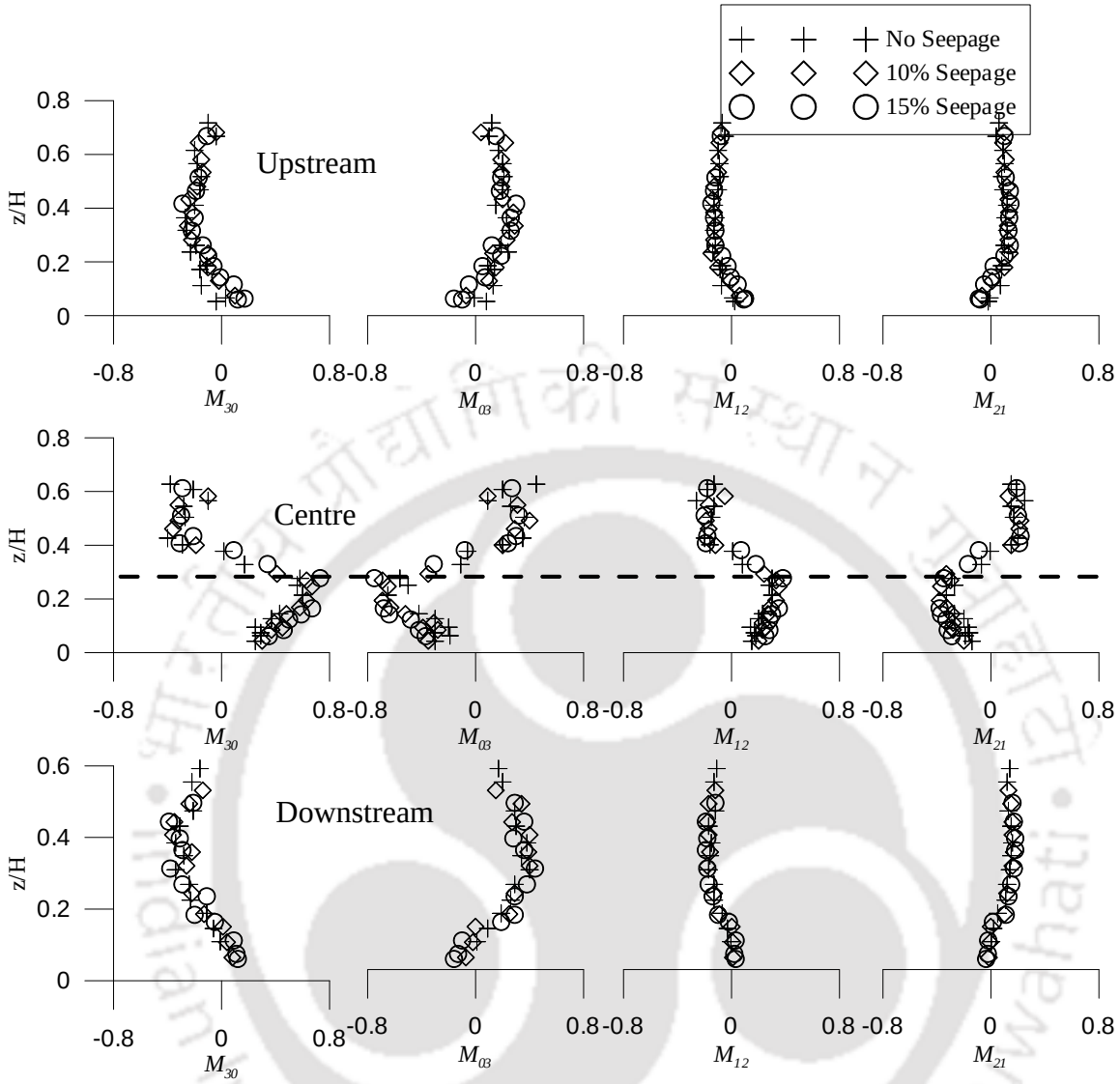

Figure 6.5 Third order moments distribution at the upstream, centre and downstream of vegetation section for no seepage, 10% seepage and 15% seepage

M_{12} and M_{21} define the turbulent advection of the normal Reynolds stresses. M_{12} starts to have positive values near the bed and the positive nature increases with increase in downward seepage percentage. M_{21} also has negative values near the bed and increases with increase in seepage percentage. M_{12} being positive near the bed and M_{21} being negative near the bed indicates that the $\overline{w'w'}$ diffusion propagates in the streamwise direction and $\overline{u'u'}$ diffusion occurs in the downward direction respectively.

The negative values of M_{03} and M_{21} near the bed infer that inrush of flow is occurring in the region and the flow coming towards the bed is again carried away by the flow in the streamwise direction which is observed from positive values of M_{30} and M_{12}. Thus, it can be inferred from the results that the downward seepage appears to decrease the upward flux and the vertical transport of $\overline{u'u'}$ while it increases the streamwise flux and streamwise transport of $\overline{w'w'}$ flux.

6.2.5 Integral Scales of flow

Coherent structures of the turbulent flow are related to the initiation of bed features, which form because of the dominance of turbulent sweep events in the near-bed region (Gyr and Schmid 1989). The mechanism behind the sediment transport in a vegetated channel can be conferred through changes in time and integral length scales after the application of downward seepage. In order to describe the changes in the bed transport condition after the application of seepage, time scale and integral length scale are calculated for the near-bed velocity of the no seepage and 10% seepage runs. Integral time scale and length scale are determined in the near-bed region using the 120 s time series collected at z/H= 0.11 above the bed. An integral time scale indicates the large eddy turnover time at a given point, and an integral length scale suggests the characteristic eddy size in the flow.

These eddies are associated with the transfer of momentum and turbulent kinetic energy in the flow. The Eulerian integral time scale E_T is defined as

$$E_T = \int_0^{k'} R(t)dt \qquad (6.2)$$

where $R(t)$ is the auto-correlation function, dt is the lag distance between consecutive auto-correlation functions, and k' is the time at which $R(t)$ started to oscillate about zero (Tennekes and Lumley 1972). Autocorrelation is calculated using linear interpolation to convert the time series into regularly spaced events. Around 24,000 samples of instantaneous velocities were collected in 120 s to minimize the error in the calculation of integral scales of flow. Value of k' was determined on the basis of autocorrelation at which $R(t) \approx 0.01$ where lag time is 0.01 s.

Eulerian integral length scale is calculated using Taylor's (1935) approximation, with the following equation:

$$E_L = E_T U \tag{6.3}$$

where U is time mean velocity at a particular point.

Table 6.1 Integral time and length scales for no seepage, 10% seepage and 15% seepage

Location	No Seepage			10% Seepage			15% Seepage		
	U (m/s)	E_T (s)	E_L (m)	U (m/s)	E_T (s)	E_L (m)	U (m/s)	E_T (s)	E_L (m)
Upstream	0.1736	0.5479	0.0947	0.1889	0.6605	0.1248	0.1941	0.7210	0.1399
Centre	0.0244	0.7440	0.0181	0.044	0.8820	0.0388	0.0517	0.9840	0.0509
Downstream	0.0344	0.4181	0.0143	0.0396	0.5340	0.0211	0.0433	0.6279	0.0272

Integral time scale and length scale are calculated and represented in Table 6.1. E_T and E_L vary between 0.4181 s - 0.7440 s and 0.0143-0.0947 m for no seepage, 0.5340-0.8820 s and 0.0211-0.1248 m for 10% seepage and 0.6279-0.9840 s and 0.0272-0.1399 m for 15% seepage. E_T and E_L are also plotted against the flow depth for no seepage, 10% seepage and 15% seepage (Figure 6.6). These scales have the maximum value near the top of the vegetation reflecting the occurrence of more momentum exchange as observed from Reynolds stress. Another aspect is that the eddy length and large eddy turnover time are increased with downward seepage which shows that the eddy size increases corresponding to higher momentum and energy transfer and less destruction of turbulent motions. This shows that values of E_T and E_L are increased in the seepage runs as compared to the no seepage runs. Thus, eddy length and large eddy turnover time are increased significantly with downward seepage. Increased eddy size in the near-bed region corresponds to higher momentum and energy transfer and less destruction of turbulent motions. Thus higher levels of turbulence prevail near the bed with an increased eddy size, which results in higher Reynolds stresses with downward seepage.

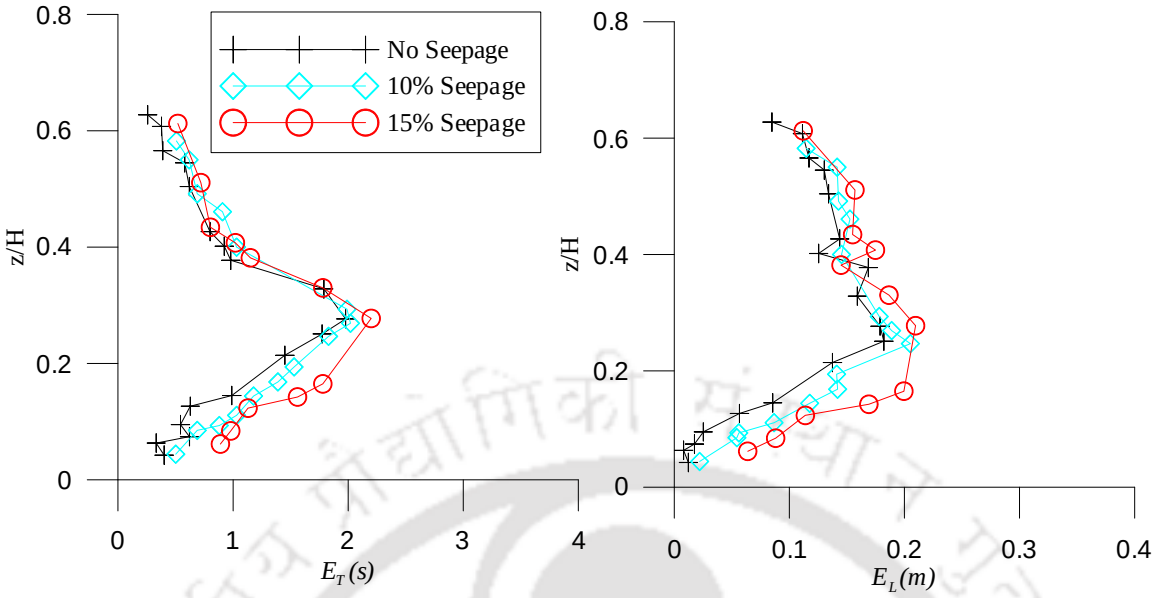

Figure 6.6 Time and Length scales plotted against the flow depth for the centre of the vegetation zone

6.2.6 Drag coefficient

The values of C_D for different seepage cases are calculated and plotted in figure 6.7. Drag coefficient of flexible vegetation is a depth-dependent parameter, as the rigidity and thickness of the plants are decreasing with the plant's length from the roots to the upper part of the plant. The effect of downward seepage on C_D is also studied. The drag coefficient for no seepage is 2.30, for 10% seepage is 1.971 and for 15% seepage is 1.631. This indicates that C_D decreases with the application of downward seepage. Therefore, downward seepage reduces the roughness or resistance offered by the vegetation by pulling the vegetation towards the bed and consequently an increase in velocity with downward seepage is also noted.

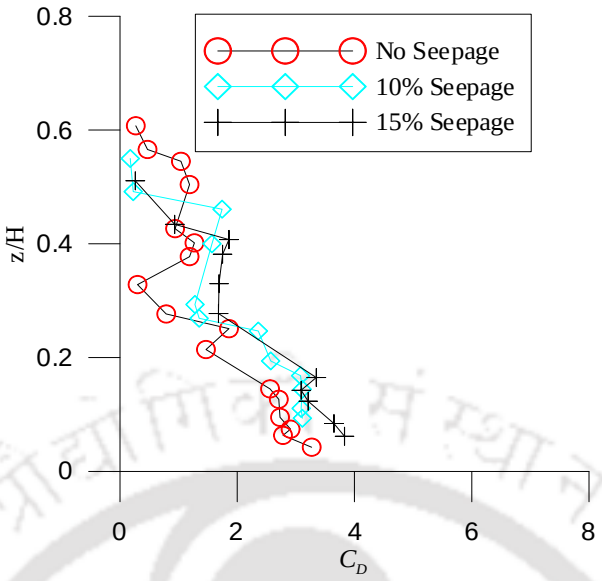

Figure 6.7 Drag coefficient for the centre of the vegetation zone

From the above experimental results, it can be summarized that the presence of vegetation in a mobile bed channel affects the flow characteristics. A velocity reduction is found near the top of the vegetation. The presence of downward seepage in a natural channel leads to an increase in velocity in the vegetation zone, Reynolds stress and turbulent intensities. However, the important finding of the present study is that even though downward seepage increases all these flow characteristics at all locations, these flow characteristics decreases at the downstream of the vegetation zone which means that vegetation can act as one of the measures for river restoration projects.

6.2.7 Conclusions

Laboratory experiments were conducted for investigation on a permeable channel covered fully with submerged flexible *Oryza sativa* (rice) stems. Experiments were conducted considering the downward seepage occurring at the permeable boundaries of natural channel. Measurements were done at the upstream free-vegetation zone, centre of the vegetation zone and downstream free-vegetation zone to study the change in flow conditions as flow occurs in a vegetated channel. Results from velocity profiles show that velocity is reduced in the vegetated region which exhibits the importance of vegetation in reducing the velocity. The near bed velocity increases on average

value 14% and 20% with the application of 10% seepage and 15% seepage as compared to no seepage. It is noted that vegetation is still effective in resisting the flow irrespective of the application of downward seepage by achieving a lower velocity at the end of the vegetation zone. Reynolds stress and turbulent intensity profiles show that the maximum value occurs near the vegetation top for vegetated region while for the upstream it lies near the bed denoting the region of turbulence generation. The occurrence of higher Reynolds stress and turbulence intensities at the centre of vegetation zone is attributed to the local effect induced by vegetation stems. The maximum Reynolds stress and turbulent intensities in the vegetation zone is higher than the downstream free vegetation zone which means that vegetation acts as a barrier in reducing the Reynolds stress and turbulent intensities by attaining a lower maximum Reynolds stress and turbulent intensities at the downstream end. The increase in Reynolds stress and turbulent intensities with the application of downward seepage is noted. Results from third order moments exhibit that M_{30} achieves a higher positive value near the bed at 10% and 15% seepage percentages as compared to no-seepage case which means that the transport of flux in the flow direction is more with the application of seepage. The increase in the negativity of M_{03} with 10% and 15% seepage states that vertical flux transport is occurring in downward direction. Results from integral scales explore that eddy length and large eddy turnover time increase with downward seepage as compared to no seepage. The length scale and time scale increases with increase in percentage of seepage which infers that an increase in eddy size is observed which results in higher Reynolds stresses with downward seepage. Drag coefficient decreases with increase in the percentage of seepage.

6.3 Partly covered

6.3.1 Velocity

The difference in the flow velocity in the upper flow region and lower flow region in a vegetated zone leads to the presence of an inflection point near the top of the vegetation (Poggi *et al*, 2004; Carollo *et al*, 2005; Chen *et al*, 2011; Nepf, 2012b). Figure 6.8 shows the reduction in flow velocity (no seepage case) near the top of the vegetation for the vegetated section as observed by Righetti (2008), Chen *et al* (2011), Siniscalchi *et al* (2012) and Li *et al* (2014). The flow velocity in the vegetated section is reduced as the flow goes downstream which implies that the vegetation increases the roughness as the flow goes downstream which is an important observation for using vegetation patch as a velocity reduction mattress. The flow velocity variations along streamwise sections of vegetation, interface and unvegetation regions are evaluated to investigate the effects of vegetation on flow velocity distribution in partially vegetated channel. Because of the presence of vegetation, more water is forced to flow along the unvegetated region causing the increase of velocities this region. It is also observed that the existence of vegetation considerably reduces the flow velocity in the vegetated area as the flow goes downstream while the flow velocity in the unvegetated area increases as the flow goes downstream. This shows that the reduced velocity in the vegetated region is deflected towards the unvegetated region. The difference between the flow velocities at the free-upstream and free-downstream is observed, the presence of vegetation reduces the flow velocity at the free downstream. Comparing the average flow velocities of the vegetated region and unvegetated region, the average flow velocities of vegetated section and interface section are 0.1927 m/s for no seepage, 0.1934 m/s for 10% seepage and 0.1971 m/s for 15% seepage. These velocities are 40% lower than the average flow velocities in the unvegetated region.

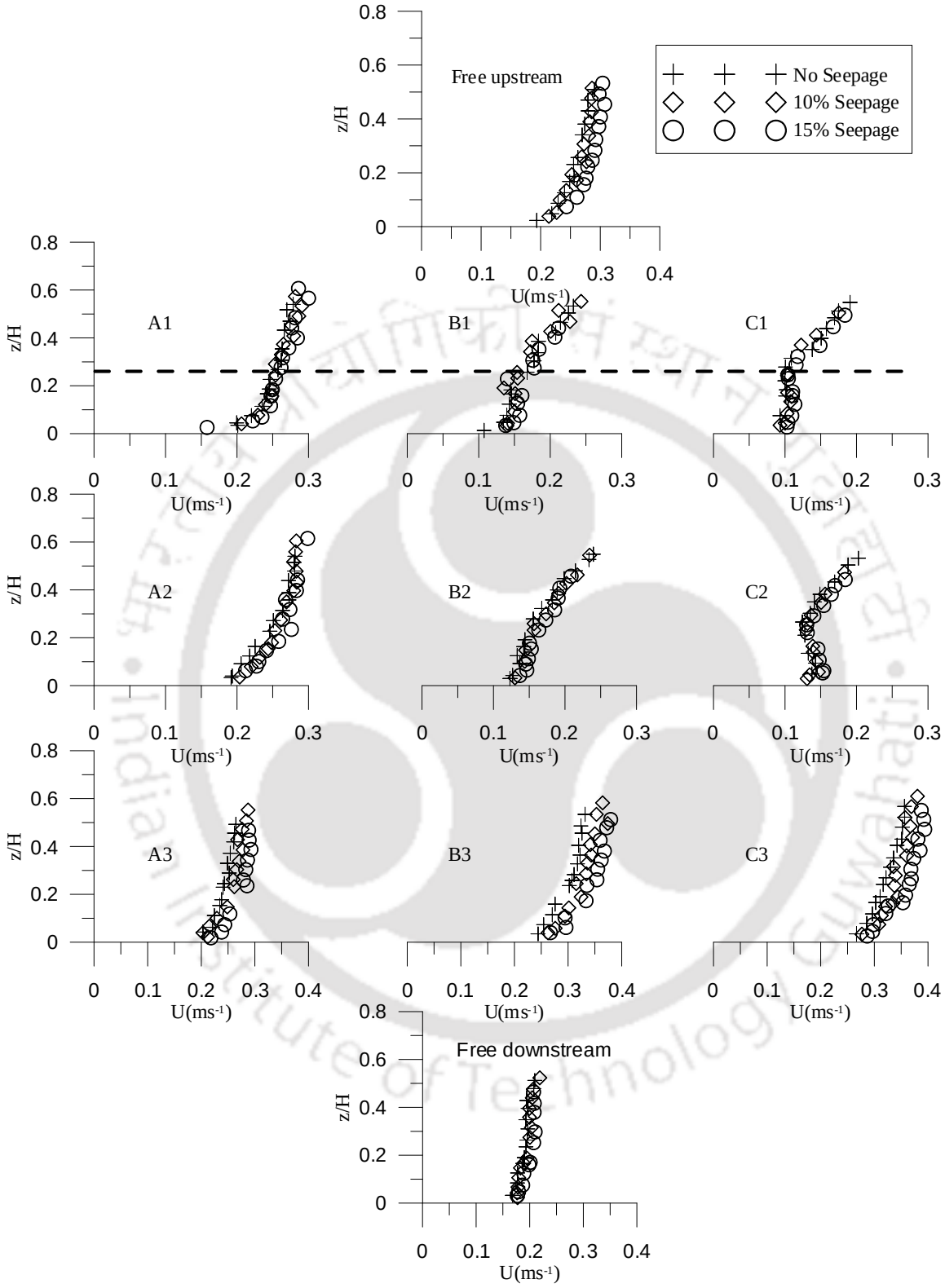

Figure 6.8 Velocity profiles at different measurement locations for no-seepage, 10% seepage and 15% seepage (the average deflected vegetation height lies at approx. z/H=0.27)

Velocity profiles for different seepage percentages are also plotted correspondingly. It is known that downward seepage shifts the velocity downwards because of which a higher velocity is achieved in the near bed region (Dey and Nath, 2009; Cao and Chiew, 2013). Irrespective of the measurement location, a higher velocity zone exists in the lower flow region or the near bed region (Figure 6.8). The near bed velocity increases on an average value of 10 % with the application of 10% seepage. It is also observed that in the lower flow region the velocity for 15% seepage case is slightly higher, with an average increasing value of 12%, than the velocity for no seepage. It is noted that the velocity at A1 and B1 are always higher than C1 even with seepage also which means that inspite of downward seepage application, vegetation is still effective in resisting the flow and hence velocity at C1 is always lower. However for unvegetated section, the flow at the downstream (C3) is always higher than A3 and B3. This shows that for seepage cases also, the velocity reduced in the vegetated region is diverted in the unvegetated region.

6.3.2 Reynolds stress

The Reynolds stress distribution helps to estimate the shear velocity in evaluating the bed resistance to the flow (Afzalimehr and Dey, 2009). Thus, vertical distribution of Reynolds stresses are calculated inorder to describe the momentum diffusion mechanism. Because of the non-uniformity of water flow, the Reynolds stress distribution is complex for partially vegetated channel (Zhang *et al*, 2015b). The Reynolds stresses are determined for the partially vegetated channel corresponding to no seepage, 10% seepage and 15% seepage. From figure 6.9, the difference in the position of maximum stress for vegetated region and unvegetated region can be observed. For vegetated region, maximum Reynolds stress occurs near the vegetation top while for the unvegetated region, it occurs near the bed. Because of the difference in the velocity above the vegetation and below the vegetation, a shear layer is formed near the top of the vegetation which leads to the occurrence of more momentum exchange at this region. This implies that the primary source of turbulence generation in the vegetated region is dominated by the turbulence near the vegetation top while for the unvegetated region, it is dominated by the turbulence near the channel bed.

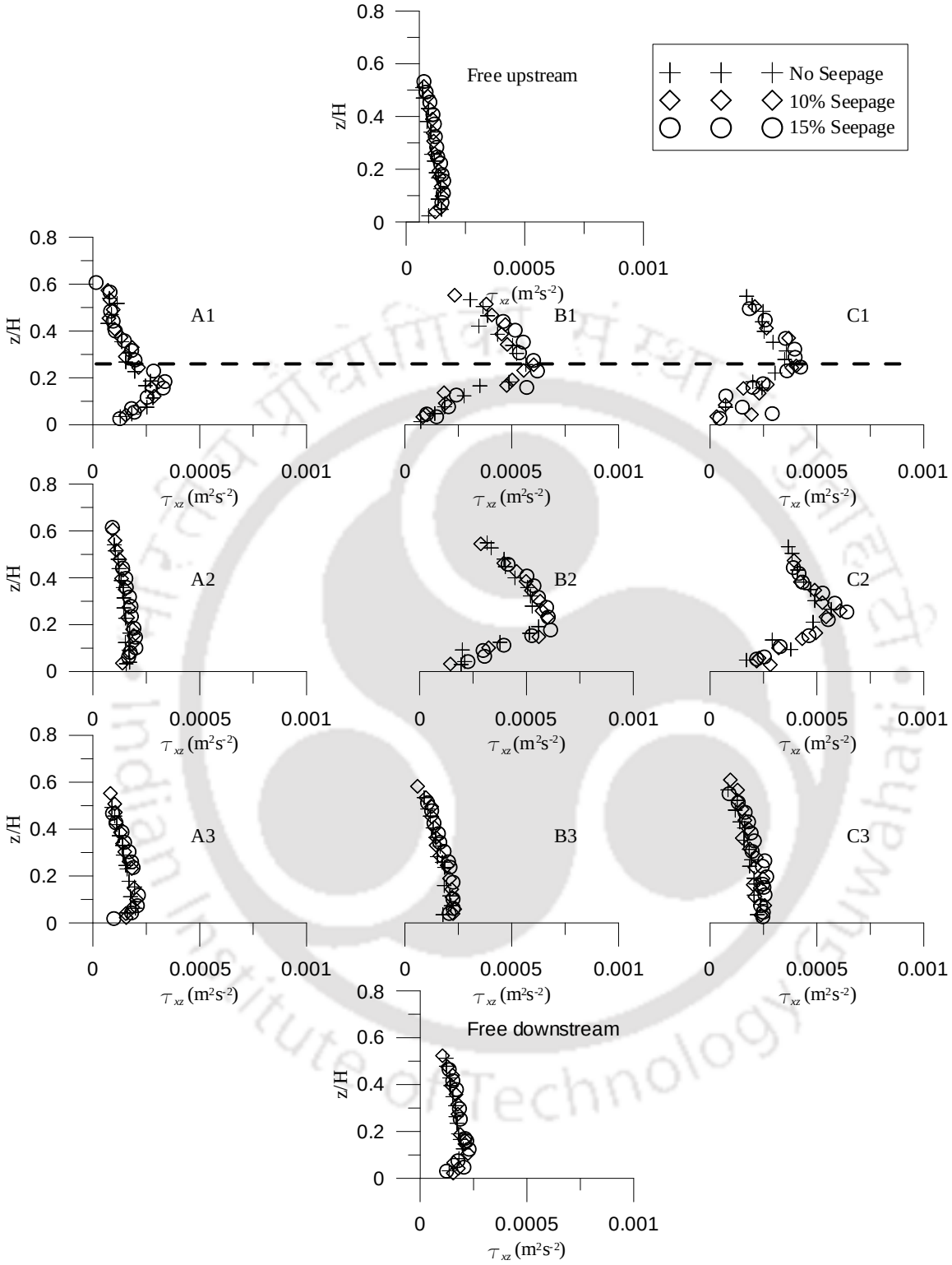

Figure 6.9 Reynolds stress profiles at different measurement locations for no-seepage, 10% seepage and 15% seepage

Except for A1 and A2, which are the locations for starting of the vegetation zone, other locations of A and B have the maximum Reynolds stress near the vegetation top. While for the unvegetated section, all the profiles have maximum value near the bed. The Reynolds stress in vegetated section shows decline tendency along the channel i.e. C1 has a lower Reynolds stress than B1.This means that the flow passing downstream in the vegetation zone is resisted by the vegetation. This reduction is important for the reduction of soil erosion in a vegetation based river channel. The maximum Reynolds stress at B2 and C2 are almost similar to B1 and C1. For the unvegetated section, the values of Reynolds stresses are relatively low. Higher value of maximum Reynolds stress is achieved for vegetated region as compared to the unvegetated region because of the local effect of erosion and deposition around the vegetation. It is also noteworthy to mention that for no seepage, the centre of the vegetation region, B1, has 38% higher value of maximum Reynolds stress comparing to the end of vegetation region, C1 which means that vegetation reduces the momentum diffusion at C1 and thus reducing sediment transport. While for the interface section, C2 has about 25% higher value of maximum Reynolds stress than B2 which implies that higher lateral flow and momentum exchange occurs in this transition zone between vegetated and unvegetated area as the flow goes downstream. This leads to the achievement of higher value of maximum Reynolds stress (39%) for free downstream as compared to free upstream. For the unvegetated section, maximum Reynolds stress occurring at C3 is higher as compared to A3 and B3 which means that the Reynolds stress reduced in the vegetation section is deflected towards the unvegetated zone. Thus for a partially vegetated channel, the more the reduction in Reynolds stress in the vegetation section, the more the increase in Reynolds stress in the unvegetated region.

Figure 6.9 also shows different distributions of Reynolds stress of different vegetation spacing for no-seepage, 10% seepage and 15% seepage. It is known that the downward seepage increases the shear stress which leads to more sediment transport as compared to no-seepage (Dey and Nath, 2009). In all the profiles, with the increase in seepage percentage, an increase in the value of maximum Reynolds stress is achieved. The maximum Reynolds stress near the vegetation top is increased in the range of 6-12% from no-seepage to 10% seepage and 9-17% from no seepage to 15% seepage. This reiterates that application of downward seepage increases the Reynolds stress thereby increasing bed material transport. Reynolds stress for both 10% and 15% seepage at B1 is reduced in the range of 13-18 % when the flow reached the downstream C1. Consequently, it

means that despite of increase in Reynolds stress with the application of downward seepage; vegetation still reduces the Reynolds stress as the flow goes downstream.

6.3.3 Turbulent Intensities

The turbulence intensity is generated by the variation of instantaneous velocity at a point, which can be influenced by the magnitude of the velocity, vegetation and bed roughness etc. σ_u and σ_w are the turbulence intensities in streamwise and vertical directions. σ_u and σ_w are plotted for no-seepage, 10% seepage and 15% seepage and shown in figure 6.10 and 6.11 below. Maximum turbulent intensities occur where there is maximum turbulence generation which implies that at B1, C1, B2 and C2 has the highest turbulent fluctuations near the vegetation top while the remaining locations have the highest fluctuations near the channel bed. The maximum turbulence intensities at the centre of the vegetation zone, B1 is reduced by an average value of 10% as the flow reaches C1. From the results of the turbulence intensities, it can be deduced that the intensities of velocity fluctuations occur at the centre of the vegetation zone decreases at the end of the vegetation zone implying that the turbulent fluctuations is reduced because of the presence of vegetation. Higher lateral flow and momentum exchange occurring in the transition zone between vegetated and unvegetated area is transported downstream and thus a higher value is achieved at the downstream C2 comparing to B2. Additionally, for unvegetated section, the lateral flow occurring at the transition zone is again deflected towards the unvegetated region and the turbulent fluctuations suppressed by the vegetation is transported in the unvegetated region causing more turbulent intensity at the downstream.

As observed, with the increase in the percentage of downward seepage, the flow is more sheared leading to the attainment of more turbulence intensities. For 10% and 15% seepage also, turbulence intensities for all the locations are more, achieving an average increase value of 15% as compared to no-seepage case.

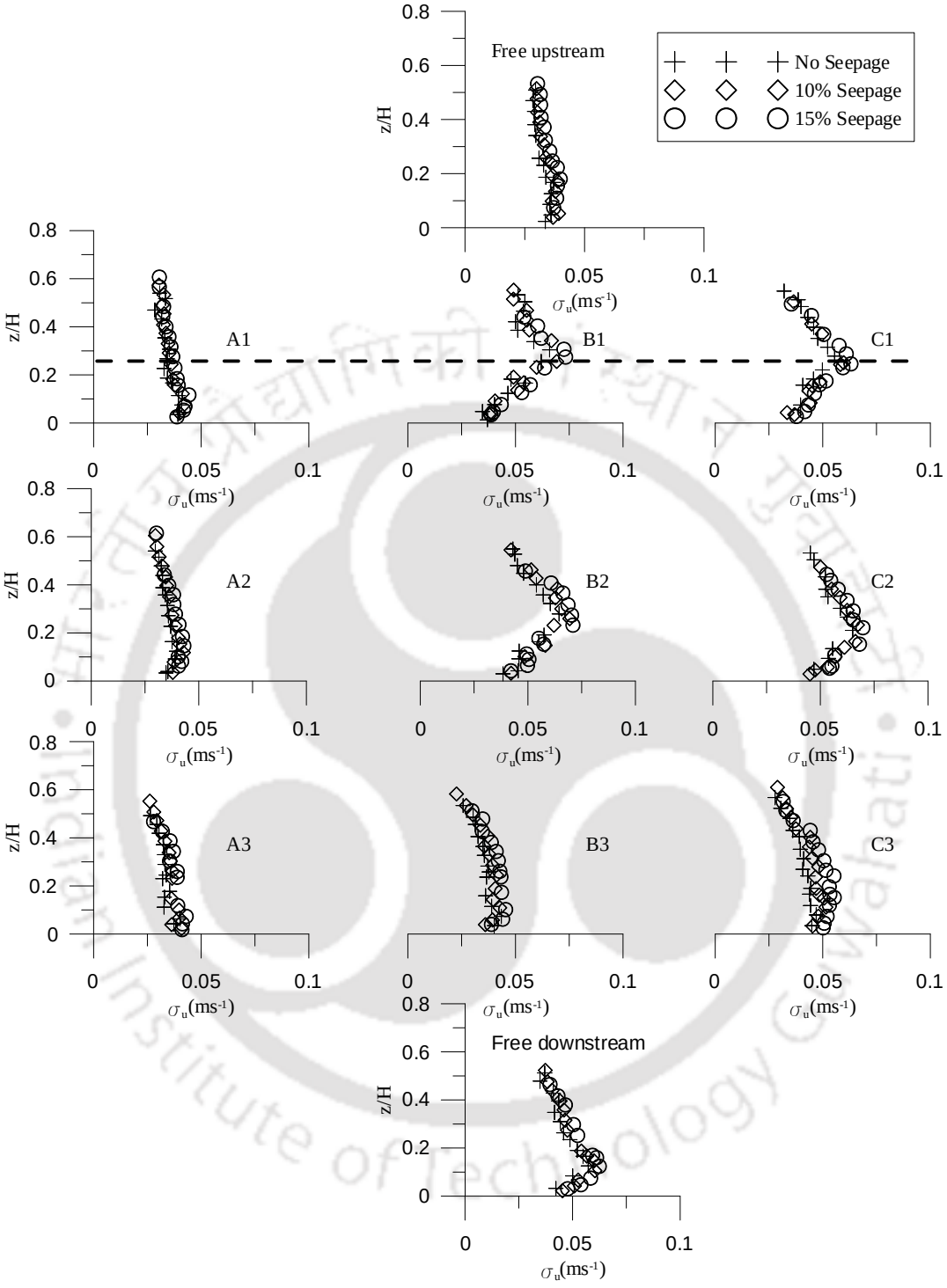

Figure 6.10 Streamwise turbulent intensity profiles at different measurement locations for no-seepage, 10% seepage and 15% seepage

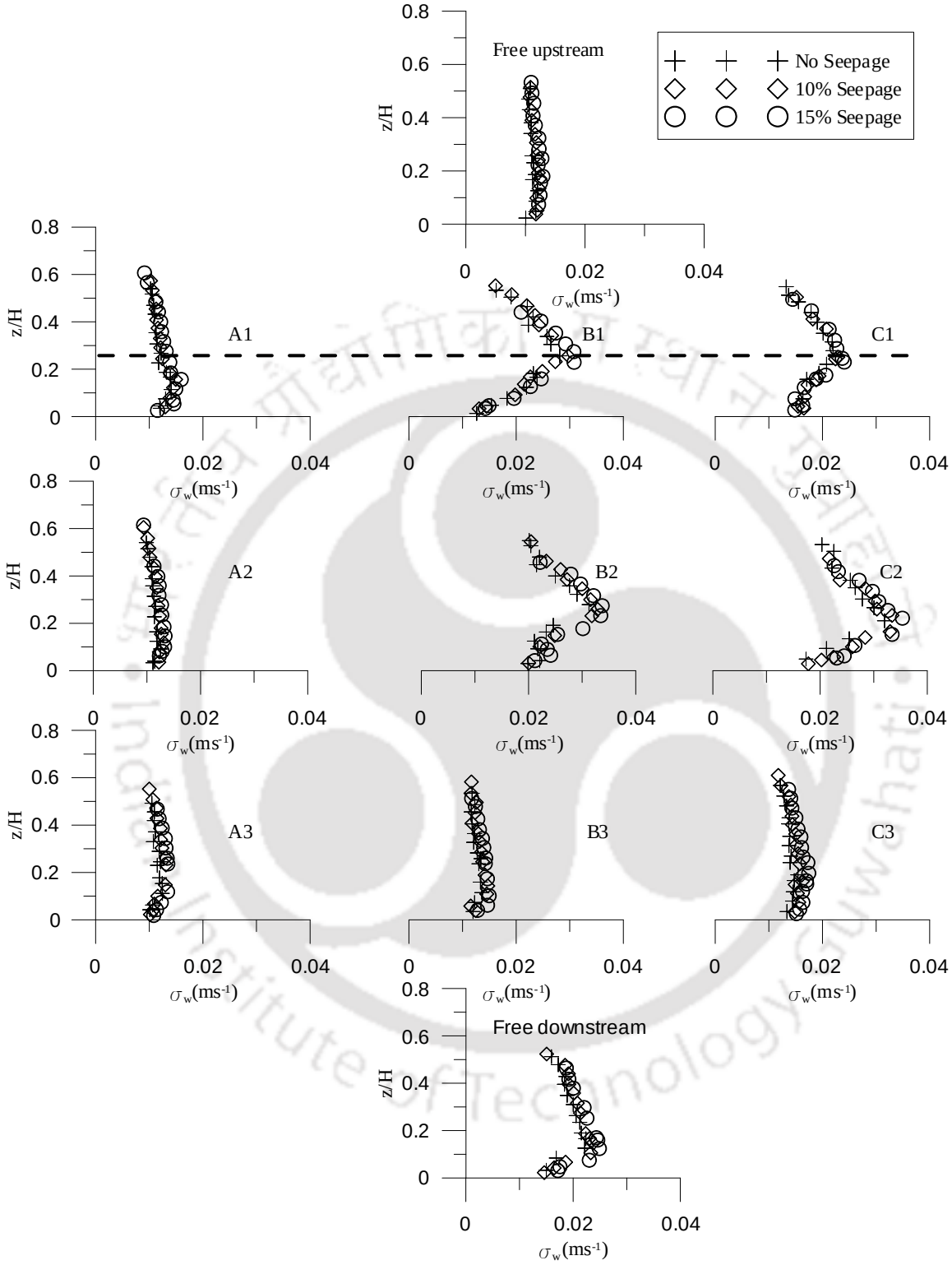

Figure 6.11 Vertical turbulent intensity profiles at different measurement locations for no-seepage, 10% seepage and 15% seepage

In all the profiles, the maximum turbulent intensities in the vegetation zone is higher than the unvegetated region leading to localized erosion and deposition occurring around the vegetation stems.

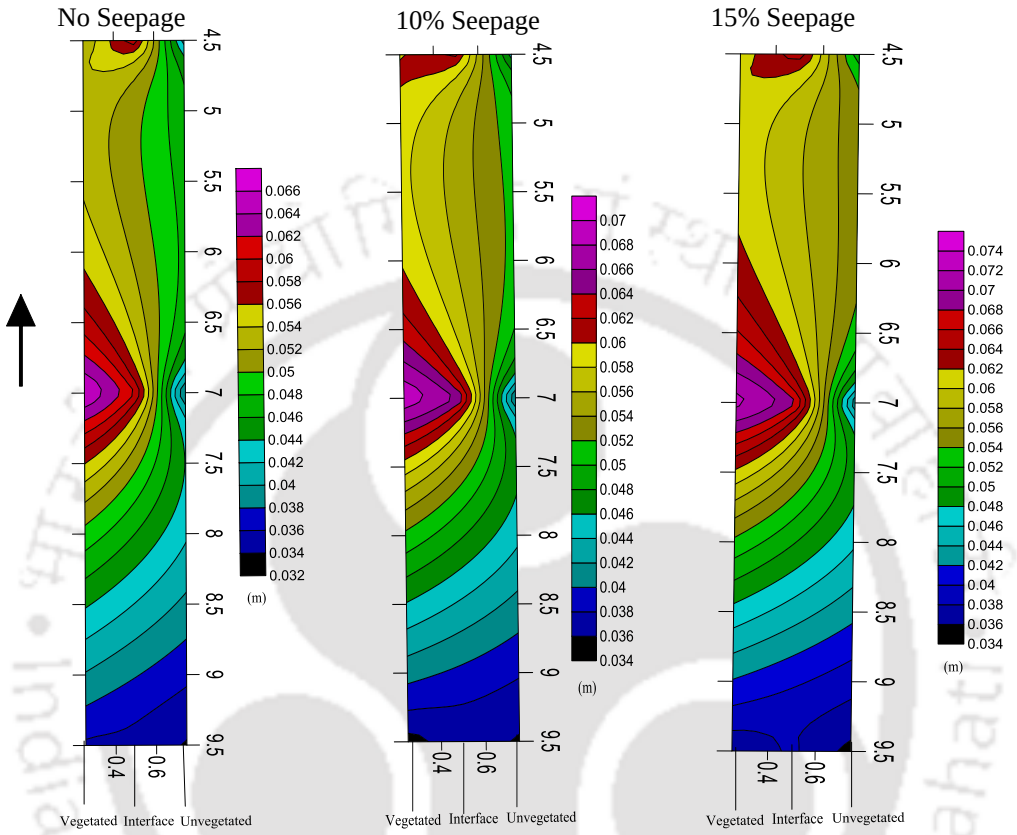

Figure 6.12 Distribution of streamwise turbulent intensities (σ_u) at different measurement sections for no-seepage, 10% seepage and 15% seepage (All dimensions in metre)

Figure 6.12 and 6.13 also show the contour profiles of distribution of turbulent intensities in the test section (x-y plane) for a particular flow depth z/H=0.28 (near the top of the vegetation). From the contour profiles, σ_u and σ_w have maximum turbulent intensities at the middle of the vegetated test section (A-section). The upstream test section is marked by weak turbulent fluctuations at the entry of the vegetation zone. The turbulent intensities increase for unvegetated section as the flow goes downstream while it is opposite for vegetated section which implies that the presence of vegetation impairs the fluctuation coming with the flow thus protecting the downstream section against erosion. The diversion of higher turbulent fluctuations from the vegetated section towards the unvegetated section is also observed and therefore may cause erosion in this region.

The application of downward seepage also follows the same pattern as of no seepage with the only difference in the magnitude. The downward seepage increases the turbulent fluctuation which leads to more sediment transport. However, an important observation for vegetated section is that the presence of vegetation is still effective in impairing the turbulent fluctuations as the flow goes downstream.

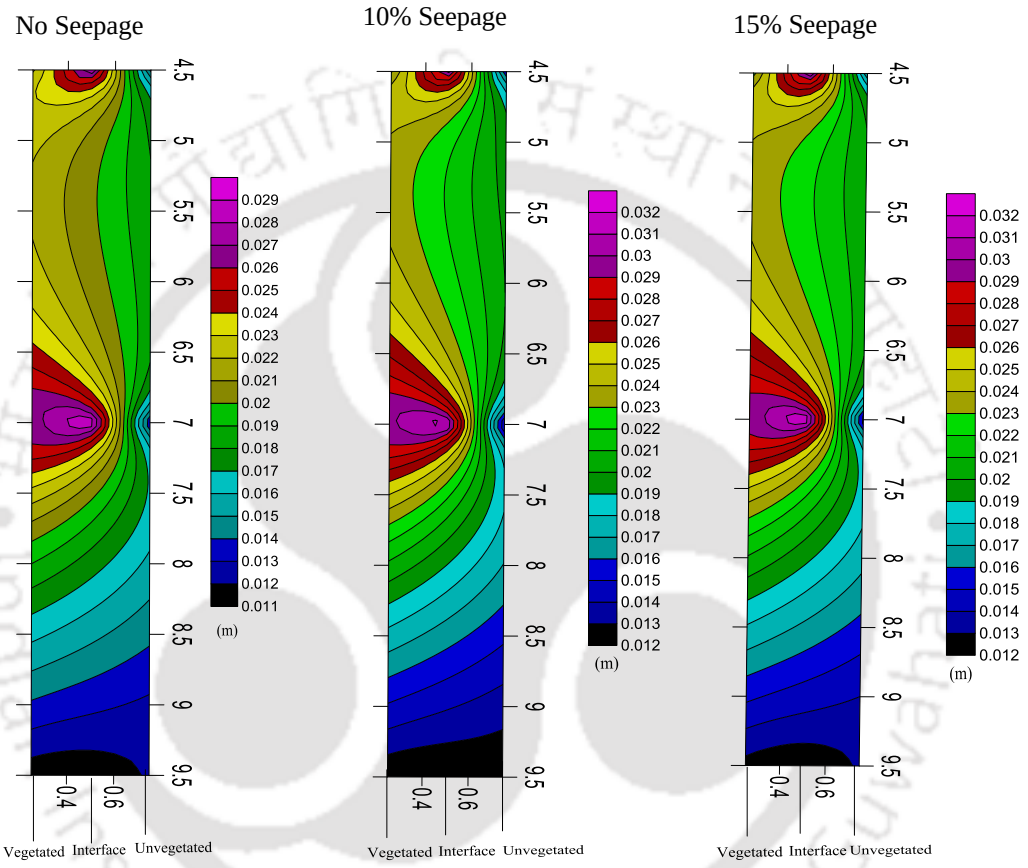

Figure 6.13 Distribution of vertical turbulent intensities (σ_w) at different measurement sections for no-seepage, 10% seepage and 15% seepage (All dimensions in metre)

6.3.4 Moments

Third order correlations of velocity fluctuations (M_{30}, M_{03}, M_{12} and M_{21}) for no-seepage, 10% seepage and 15% seepage at B1, B2 and B3 are shown in figure 6.14 below. The difference in the flux transport in the vegetated and unvegetated regions is observed.

For B1 and B2, M_{30} and M_{12} have negative values near the water surface which changes to positive values with decreasing depth and the maximum positive occurs below the top of the vegetation. This implies that the $\overline{u'u'}$ flux and $\overline{w'w'}$ diffusion propagate in the flow direction. With the application of seepage, it is known that seepage increases the shear stress which means that more sediment particles get transported in the flow direction. M_{30} and M_{12} achieve a higher positive value near the bed at 10% and 15% seepage percentages as compared to no-seepage case. This means that the transport of flux in the flow direction is more with the application of seepage. M_{03} and M_{21} start with negative values near the bed and positive values with increase in depth which indicates that the $\overline{w'w'}$ flux and $\overline{u'u'}$ diffusion are in downward direction. With the application of downward seepage, the negativity of M_{03} *and* M_{21} increase which is justifiable with the fact that downward flow is occurring from seepage. More negative value is observed below the vegetation zone.

For B3, M_{30} and M_{12} have negative values near the water surface and have values close to zero in the near bed region. This implies that the occurrence of $\overline{u'u'}$ flux and $\overline{w'w'}$ diffusion against the flow direction near the water surface decreases closer to the bed. M_{30} *and* M_{12} achieve a higher positive value near the bed at 10% and 15% seepage percentages as compared to no-seepage case. This means that the transport of flux in the flow direction in the near bed region is more with the application of seepage thus causing more sediment movement. M_{03} and M_{21} start with values closer to zero in the near bed and positive values with increase in depth which indicates that the $\overline{w'w'}$ flux and $\overline{u'u'}$ diffusion are in downward direction. With the application of downward seepage, the negativity of M_{03} *and* M_{21} increase. Achievement of more flux transport in the vegetated section is attributed to the local effect of erosion and deposition occurring in the vegetation zone.

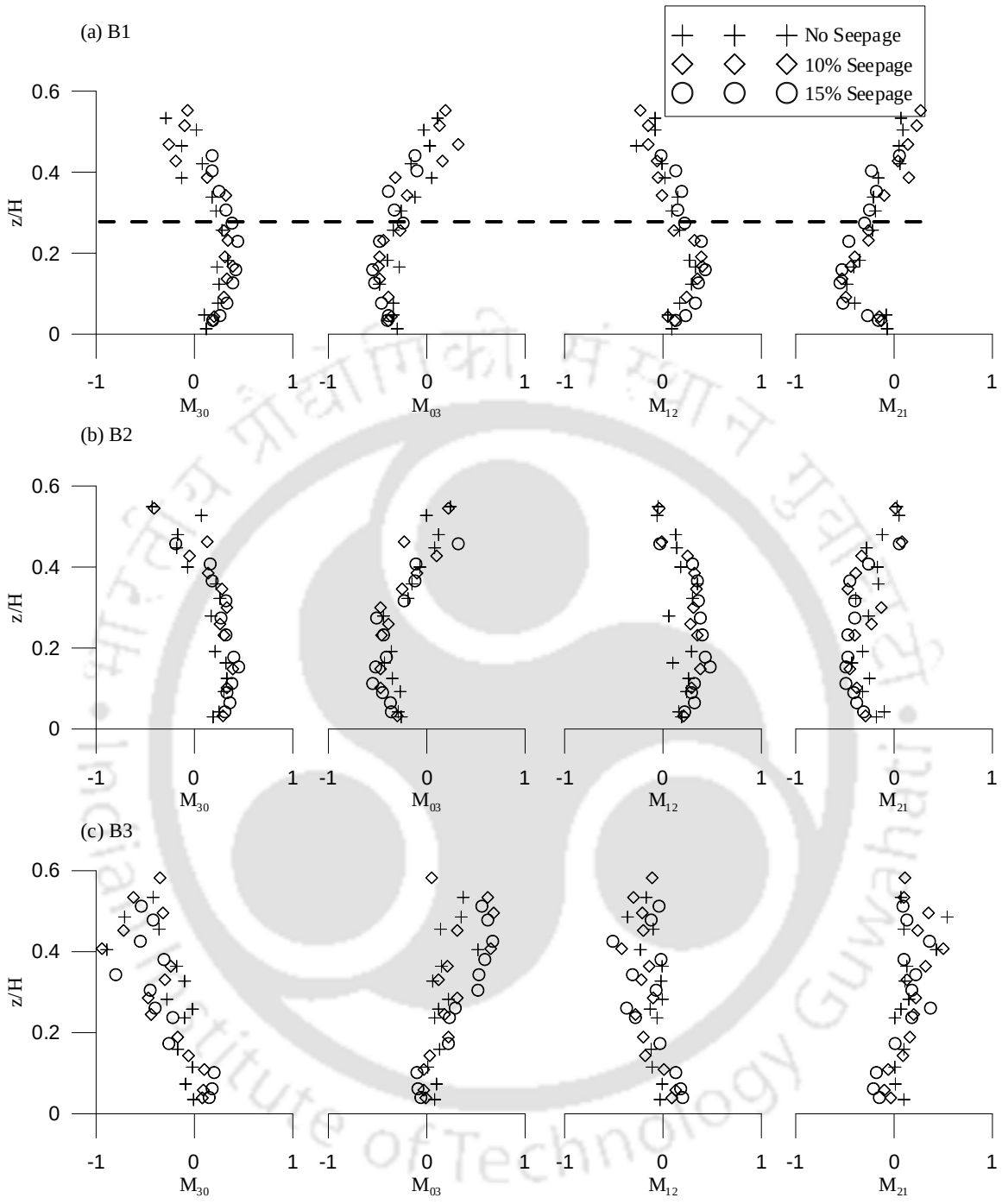

Figure 6.14 Third order moments at the measurement locations B1, B2 and B3 for no-seepage, 10% seepage and 15% seepage

6.3.5 Quadrant analysis

Quadrant analysis is carried out to study the contribution of different velocity fluctuations to Reynolds stress at a point. The summation of stress contributions to Reynolds stress equals 100% or 1 (Raupach, 1981). For example, the contributions of outward interaction, ejection, inward interaction and sweep at location A2 are 27%, 66%, 30% and 91% (for z/H=0.34, no seepage). Stress contributions to Reynolds stress for B1, B2 and B3 corresponding to flow depth are shown in figure 6.15.

Sweep and ejection events play an important role in stress contribution to Reynolds stress as compared to inward and outward interactions. In all the profiles, inward and outward interaction events have almost equal contribution. The flow regions dominated by ejection events are analogous with negative values of M_{30} and positive values of M_{03} while sweep events are associated with positive values of M_{30} and negative values of M_{03} (Righetti, 2008; Dey and Nath, 2010).

For no seepage, flow region above vegetation top at B1 has achieved almost equal contribution of ejection and sweep while the flow region below the vegetation top or near bed region is dominated by sweep event. For 10% seepage, at some regions above the vegetation top, the flow is dominated by sweep event while the region below the vegetation top is dominated by sweep event. However at 15% seepage, the whole flow region is dominated by sweep event. This implies that downward seepage triggers more sweep event compared to ejection event and thus Reynolds stress increases leading to more sediment transport. At B2 location, the lower flow region is dominated by sweep event which denoted higher momentum transfer at this transition or interface zone. For B3 location also, sweep and ejection events contribute almost equally to Reynolds stress.

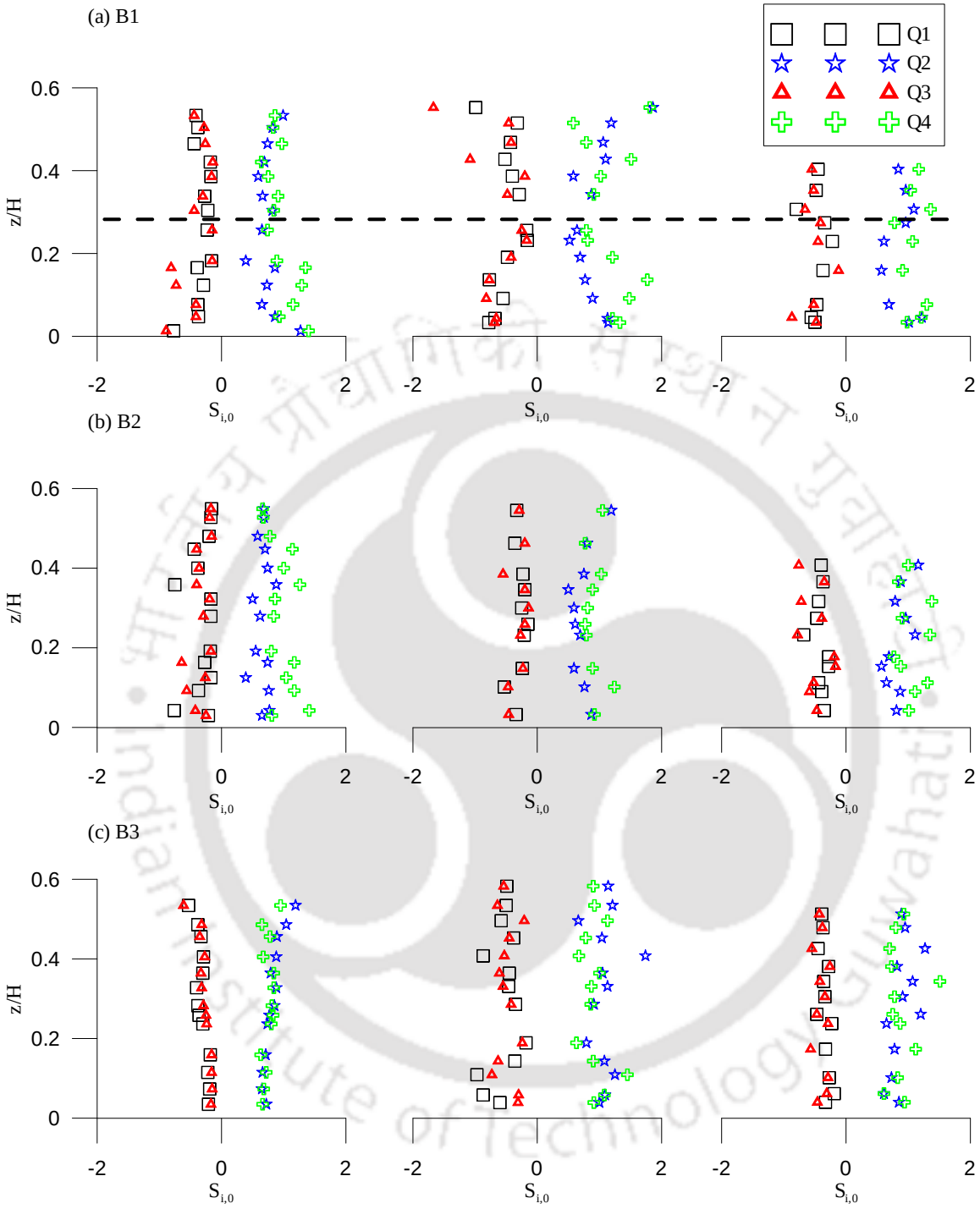

Figure 6.15 Stress contributions at the measurement locations B1, B2 and B3 for no-seepage, 10% seepage and 15% seepage

6.3.6 Drag coefficient

The study of flow characteristics around the vegetation requires provision of drag coefficient as it is one of the important parameters for defining vegetation characteristics and is the key to understand the vertical distribution of velocity.

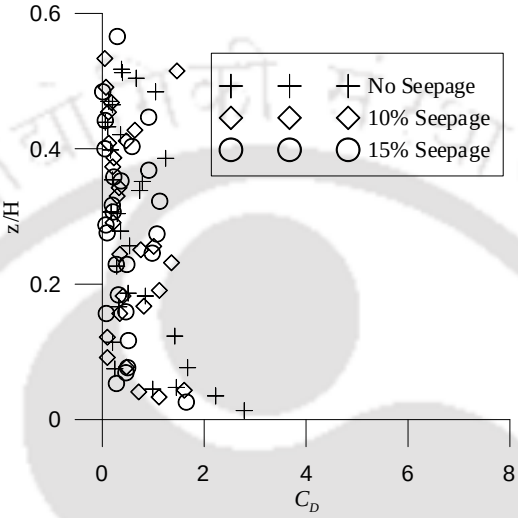

Seepage Condition	Average C_D
No Seepage	0.692
10% Seepage	0.542
15% Seepage	0.468

Figure 6.16 Drag coefficient for no-seepage, 10% seepage and 15% seepage

The values of C_D for different seepage cases are calculated and plotted in figure 6.16. Drag coefficient of flexible vegetation is a depth-dependent parameter, as the rigidity and thickness of the plants are decreasing with the plant's length from the roots to the upper part of the plant. The effect of downward seepage on C_D is also studied. The drag coefficient for no seepage is 0.692, for 10% seepage is 0.542 and for 15% seepage is 0.468. This indicates that C_D decreases with the application of downward seepage. Therefore, downward seepage reduces the roughness or resistance offered by the vegetation by pulling the vegetation towards the bed and consequently an increase in velocity with downward seepage is also noted.

6.3.7 Integral Scales of flow

The mechanism behind the sediment transport in a partially vegetated channel can be conferred through changes in time and integral length scales after the application of downward seepage. In order to describe the changes in the bed transport condition after the application of seepage, time scale and integral length scale are calculated for the near-bed velocity of the no seepage, 10% seepage and 15% seepage runs.

Table 6.2 Integral scales of flow for no seepage, 10% seepage and 15% seepage at different measurement locations

Location	No seepage			10% Seepage			15% Seepage		
	E_T (s^{-1})	U (ms^{-1})	E_L (m)	E_T (s^{-1})	U (ms^{-1})	E_L (m)	E_T (s^{-1})	U (ms^{-1})	E_L (m)
A1	0.191	0.199	0.038	0.218	0.206	0.045	0.225	0.222	0.050
A2	0.414	0.134	0.055	0.449	0.140	0.063	0.479	0.149	0.071
A3	0.388	0.093	0.036	0.413	0.105	0.043	0.455	0.110	0.050
B1	0.156	0.218	0.034	0.188	0.221	0.041	0.214	0.226	0.048
B2	0.189	0.193	0.036	0.286	0.203	0.058	0.348	0.212	0.074
B3	0.334	0.126	0.042	0.394	0.130	0.051	0.438	0.136	0.060
B4	0.208	0.137	0.028	0.280	0.146	0.041	0.344	0.152	0.052
B5	0.198	0.167	0.033	0.228	0.176	0.040	0.278	0.179	0.050
C1	0.167	0.203	0.034	0.205	0.212	0.043	0.232	0.238	0.055
C2	0.185	0.244	0.045	0.223	0.262	0.058	0.295	0.267	0.067
C3	0.205	0.266	0.054	0.259	0.276	0.071	0.287	0.286	0.082

E_T and E_L vary between 0.156-0.388 s and 0.028-0.055 m for no seepage, 0.188-0.449 s and 0.041-0.071 m for 10% seepage and 0.214-0.479 s and 0.048-0.082 m for 15% seepage (Table 6.2). This shows that values of E_T and E_L are increased in the seepage runs as compared to the no seepage runs. Thus higher levels of turbulence prevail near the bed with an increased eddy size, which results in higher Reynolds stresses with downward seepage. E_T and E_L are also plotted against the flow depth for no seepage, 10% seepage and 15% seepage (Figure 6.17). These scales have the maximum value near the top of the vegetation reflecting the occurrence of more momentum

exchange as observed from Reynolds stress. Another aspect is that the eddy length and large eddy turnover time are increased significantly with downward seepage which shows that the eddy size increases corresponding to higher momentum and energy transfer and less destruction of turbulent motions.

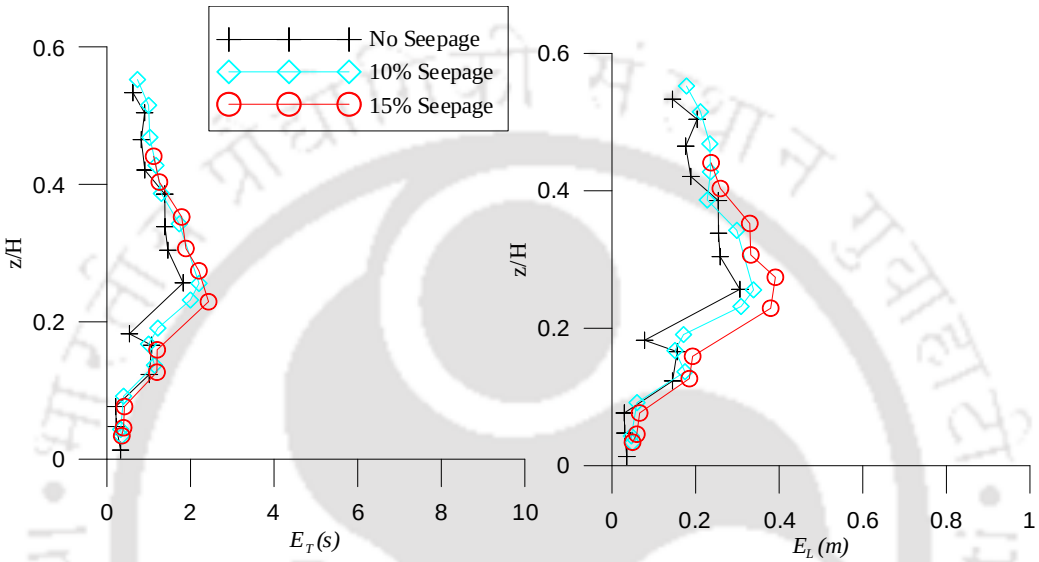

Figure 6.17 E_T and E_L for no-seepage, 10% seepage and 15% seepage (at the centre of the vegetation section, B1)

Based on previous investigations, it was found that vegetation in various arrays and configurations can modify the flow and turbulence structure and then influence sediment transport and stream morphology (Afzalimehr and Dey, 2009; Neary *et al* 2012). According to Nepf (2012a) the scour patterns similar to that observed around piers occurred at the scale of individual stems while transition in bed forms, from migrating dunes to a fixed pattern of scour associated with individual plants occurred in the unvegetated area. Most previous studies observe enhanced deposition in regions of vegetation, with greater deposition observed in regions of higher stem density (Bos *et al* 2007). However, some recent studies have also noted regions of erosion that develop at the edges of vegetation, because, as flow is diverted away from the vegetation (Bouma *et al* 2007, Rominger *et al* 2010). The redistribution of flow also produces spatial patterns in sediment transport condition, with fine grain sediment and organic matter accumulating within patches, where velocity is reduced, and coarse grain sediment left between the patches, where velocity is

enhanced (Sand-Jensen and Madsen 1992). The degree of sediment redistribution is a function of the stem density within the vegetated area (Sharpe and James 2006, Mudd *et al* 2010). Van Katwjk et al (2010) observed that sparse patches of vegetation are associated with sandification, a decrease in fine particles and organic matter, which is most likely attributed to higher levels of turbulence within the sparse patch, relative to adjacent bare regions. If the stem density is sufficiently low, so that the velocity within the patch remains high, turbulence generation within the wakes of individual stems increases the turbulence levels within the patch (Nepf 1999), which inhibits deposition (Zong and Nepf 2012). Further, Chen et al (2012) observed that the deposition of fine material is limited to a region where both the mean and turbulent velocities are depressed. As recognized by the researchers in the field, there are many interactional factors affecting the flow, vegetation, erosion, and sediment processes (Zhang and Dai, 2009).

A proper understanding regarding the sediment transport process is important for planning of river restoration projects. For understanding the flow characteristics in a partially vegetated channel, it is important to retrieve information from the sediment transport conditions. It is known that vegetation helps in protecting erosion but the main point lies in exploring the flow and sediment transport conditions in the unvegetated region of a partially vegetated channel.

Figure 6.18 shows sediment transport pattern in the unvegetated region, where y=0 indicates the edge of the vegetation patch. It is noted that the depth of erosion increases with the application of downward seepage as compared to no seepage. For no seepage, erosion is more on the half portion of the unvegetated section while the other half portion has negligible or very weak (0.3-2 mm) erosion at the upstream section (x= 9.5 - 6.5 m) and erosion of 2-6 mm occurs at x=6.5 -3.5 m and y=4 m-16 m. For 10% seepage, highest erosion takes place in the region y=30-35m while for 15% seepage, highest erosion regions occur in spots. The presence of vegetation may force the water flowing from the vegetated region towards the unvegetated region and it seems as if the forcing intensity increases as the flow goes downstream. The high flow velocity in the unvegetated region may cause soil erosion and sediment transport. It is found that flow velocity in the unvegetated region increases as the flow goes downstream and this occurrence of higher velocity at C3 as compared to A3 leads to more erosion of sediment particles thus attaining a higher erosion depth as the flow goes downstream. It is noted that more erosion occurs for 15% seepage as compared

to no seepage and 10% seepage which is in agreement with the increase of Reynolds stress with increase in seepage.

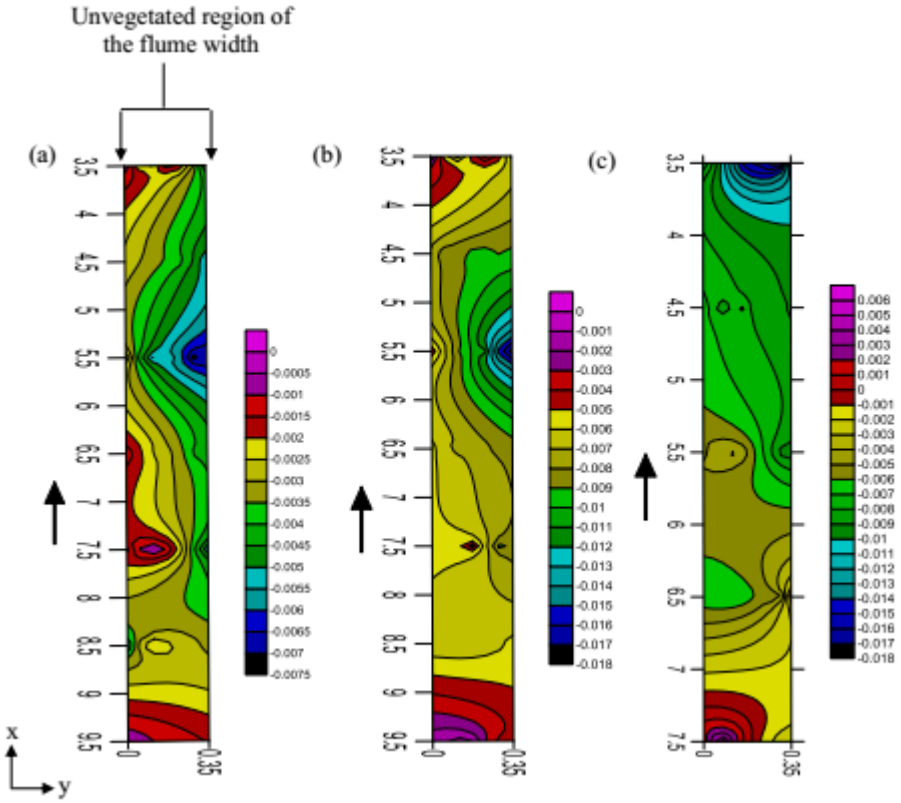

Figure 6.18 Sediment transport conditions at the unvegetated portion of 5 m test section (a) No seepage (b) 10% seepage (c) 15% seepage (All dimensions in metre)

6.3.8 Conclusions:

The present study highlights the experimental investigation on a channel covered partially with submerged flexible *Oryza sativa* (rice) stems. Experiments were conducted considering the downward seepage occurring at the permeable boundaries of natural channel. Results from velocity profiles demonstrate that velocity is reduced in the vegetated region which exhibits the importance of vegetation in reducing the velocity. An interesting feature is that the reduced velocity in the vegetated region seems to be deflected towards the unvegetated region and therefore a higher velocity is achieved in the unvegetated region. The near bed velocity increases on average value 10 % and 17% with the application of 10% seepage and 15% seepage. It is noted that vegetation is still effective in resisting the flow irrespective of the application of downward seepage by achieving a lower velocity at the end of the vegetation zone. Therefore, the presence

of vegetation may be used as a measure to reduce soil erosion and improve bank stability. Reynolds stress and turbulent intensity profiles show that the maximum value occurs near the vegetation top for vegetated region while the rest lie near the bed denoting the region of turbulence generation. The occurrence of higher Reynolds stress and turbulence intensities at the downstream end of the transition zone and unvegetated zone is attributed to the occurrence of lateral flow and higher momentum transfer at the junction of vegetated region and unvegetated region. The maximum Reynolds stress and turbulent intensities in the vegetation zone is higher than the unvegetated region leading to local sediment movement around the vegetation stems. It is also observed that vegetation acts as a barrier in reducing the Reynolds stress and turbulent intensities by attaining a lower maximum Reynolds stress and turbulent intensities at the end of the vegetation zone. However an increase in the maximum Reynolds stress and turbulent intensities are achieved at the downstream end of the unvegetated region. Results from third order moments exhibit that M_{30} achieves a higher positive value near the bed at 10% and 15% seepage percentages as compared to no-seepage case which means that the transport of flux in the flow direction is more with the application of seepage. The increase in the negativity of M_{03} with 10% and 15% seepage states that vertical flux transport is occurring in downward direction. Quadrant analysis shows that sweep and ejection events play a major role in stress contribution to Reynolds stress. For the vegetated section, the dominance of sweep event in the whole flow region at 15% seepage is observed which is related with more positive values of M_{30} and more negative values of M_{03}.The application of downward seepage reduces the roughness of the vegetation which is shown by the reduction in C_D value with increase in seepage percentage as compared to no seepage. This reduction in C_D leads to the achievement of higher velocity with increase in the percentage of downward seepage. Results from integral scales explore that eddy length and large eddy turnover time increase with downward seepage as compared to no seepage. The length scale and time scale increases with increase in percentage of seepage which infers that an increase in eddy size is observed which results in higher Reynolds stresses with downward seepage. The presence of vegetation forces the flow from the vegetation zone towards the unvegetated region leading to the occurrence of erosion in the unvegetated region. More erosion takes place with the application of downward seepage as compared to no seepage and the erosion depth increases as the flow goes downstream in the unvegetated region.

7 Conclusions and future recommendations

The present study was carried out for studying the flow characteristics in a vegetated channel using artificial vegetation as well as natural vegetation. The effect of vegetation height, vegetation spacing and pattern of placing vegetation were considered for investigating the change in flow characteristics. The main objective of this study lies in incorporating the effect of downward seepage and exploring the flow characteristics in a vegetated channel. Experiments were conducted for no-seepage, 10% seepage and 15% seepage. Important conclusions are drawn from the present study which is presented below:

7.1 Flow characteristics in a channel covered with uniformly distributed vegetation

- The position of inflection point in the velocity profile lies in close approximation with the position of maximum Reynolds stress and turbulent intensities even with downward seepage. The inflection point in the velocity profile occurs near the top of the vegetation.
- The decrease in vegetation spacing or increase in vegetation density leads to reduction of flow velocity and increase in Reynolds stress and turbulent intensities leading to more localized sediment transport for both no seepage as well as seepage cases.
- Placing of vegetation in uniform pattern leads to occurrence of more flow velocity than staggered pattern because of the presence of free stream region in between the vegetation element for both no seepage as well as seepage cases.
- Increase in the percentage of downward seepage increases the flow velocity, Reynolds stress and turbulent intensities.
- Application of downward seepage increases the flux transport in the downward direction and then carried the sediments along the flow direction, therefore highlighting the dominance of sweep event over ejection event.
- The study of the change in the flow characteristics along the flow direction shows that the presence of vegetation is effective in protecting the downstream region even with the presence of downward seepage which is an important finding for river restoration programme.

7.2 Effect of mixed vegetation densities on flow structure

- The presence of higher vegetation density at the downstream section reduces the flow velocity and Reynolds stress which is an important finding for river restoration project.
- The high density vegetation placed at the downstream portion of the test section reduces the flux transport in the streamwise as well as downward direction and therefore a reduction in the dominance of sweep event over ejection event from quadrant analysis which leads to less sediment transport in the portion.
- High density vegetation when placed at downstream section has the highest value of C_D meaning more resistance to flow.
- The average value of C_D decreases with downward seepage.

7.3 Hydrodynamics of seepage affected channel with vegetation bundles

- Higher Reynolds stress is achieved at the upstream vegetation section because of the flow contraction eroding the upstream vegetation patch section but it decreases as the flow reaches the downstream vegetation patch section which implies that upstream vegetation patch section acts like an erosion barrier for the downstream vegetation patch section.
- Irrespective of the application of downward seepage, the flow velocity, maximum Reynolds stress and turbulent intensities are reduced at the downstream vegetation section which highlights the importance of vegetation as erosion control measure.
- Dominance of sweep event can be observed in the near bed region which increases with the application of downward seepage.
- The value of C_D increases near the bed and decreases near the vegetation top even with seepage. Higher value of C_D is achieved for lesser vegetation spacing providing more resistance to flow.

7.4 Experimental study of flow through natural vegetation

- Presence of vegetation modifies the universal logarithmic velocity distribution.

- More value of Reynolds stress and turbulent intensities are occurred near the vegetation top for the vegetation region as compared to free stream where there is no vegetation which depicts the occurrence of localized erosion and deposition in the vegetation zone.
- For partially covered vegetation, higher Reynolds stress and turbulence intensities at the downstream end of the transition zone and unvegetated zone is attributed to the occurrence of lateral flow and higher momentum transfer at the junction of vegetated region and unvegetated region.
- Maximum value of length and time scales near the top of the vegetation which infers the occurrence of more momentum exchange as observed from Reynolds stress.
- Length scale and time scale increases with increase in percentage of seepage which denotes an increase in the size of eddy therefore resulting in higher Reynolds stresses with downward seepage.
- Presence of vegetation forces the flow from the vegetation zone towards the unvegetated region leading to the occurrence of erosion in the unvegetated region.

7.5 Recommendations for future work

The present research leaves a wide scope for the future investigators to explore many other aspects of vegetated open channels. The flow characteristics in the present study were determined with limited data of flow discharges and depths. Vegetation can vary considerably in shape and size, more research is necessary to understand how the vegetative length scales influence the flow and resistance characteristics. Various vegetation characteristics like height, thickness, vegetation placing patterns and density of vegetation can be used to have a more detailed study. In the present study, only two seepage percentages were used, 10% and 15% downward seepage. Flow through vegetation is highly three-dimensional in nature. Therefore, more research is needed in which the velocity and turbulence characteristics are examined in all three flow directions. Various seepage percentage can also be applied and study the change in flow conditions. The present research work was focused on the flow characteristics but there is a need to study the sediment transport related with the presence of stems and on a new rational approach to predict the sediment transport capacity both in vegetated and unvegetated beds, which may be extended for no seepage as well as seepage cases. Effect of boundary and side wall shear stress on flow hydraulics in vegetated

open channels need to be studied in the future research. The structure of vortex formation around the vegetation are not well understood and should be examined in more detail. The effect of wake formation behind the roughness element on flow resistance and velocity profile also needs an elaborate study. The vegetative rough floodplain can be studied for compound channel with main channel of different roughness. The work can also be extended for meandering and nonprismatic channel with vegetation. Since there is a growing interest in erosion and sediment control practices, the importance of vegetation in effectively reducing mean velocity and induce sediment deposition must be explored.

References

Abt, S. R., Clary, W. P., & Thornton, C. I. (1994). Sediment deposition and entrapment in vegetated streambeds. *Journal of Irrigation and Drainage Engineering*, *120*(6), 1098-1111.

Afzalimehr, H., and Dey, S. (2009). Influence of bank vegetation and gravel bed on velocity and Reynolds stress distributions. *International Journal of Sediment Research*, 24 (2), 236–246.

ANCID (2006). Australian Irrigation Water Provider Benchmarking Data Report for 2004-2005, *Australian National Committee on Irrigation and Drainage*, Canberra.

Anwar, H. O. (1996). Velocity profile in shallow coastal waters. *Journal of Hydraulic Engineering*, *122*(4), 220-223.

Armanini, A., & Righetti, M. (1998). Resistenza al moto in alvei vegetati a scabrezza eterogenea. *Proc., 26th Convegno di Idraulica e Costruzioni Idrauliche*, 3-14.

Armanini, A., Righetti, M., & Grisenti, P. (2005). Direct measurement of vegetation resistance in prototype scale. *Journal of Hydraulic Research*, *43*(5), 481-487.

Babovic, V., & Keijzer, M. (2000). Genetic programming as a model induction engine. *Journal of Hydroinformatics*, *2*(1), 35-60.

Baiamonte, G., & Ferro, V. (1997). The influence of roughness geometry and Shields parameter on flow resistance in gravel-bed channels. *Earth Surface Processes and Landforms*, *22*(8), 759-772.

Baptist, M. J., Babovic, V., Rodríguez Uthurburu, J., Keijzer, M., Uittenbogaard, R. E., Mynett, A., & Verwey, A. (2007). On inducing equations for vegetation resistance. *Journal of Hydraulic Research*, *45*(4), 435-450.

Bos, A. R., Bouma, T. J., de Kort, G. L., & van Katwijk, M. M. (2007). Ecosystem engineering by annual intertidal seagrass beds: sediment accretion and modification. *Estuarine, Coastal and Shelf Science*, *74*(1), 344-348.

Bouma, T. J., Van Duren, L. A., Temmerman, S., Claverie, T., Blanco-García, A., Ysebaert, T., & Herman, P. M. J. (2007). Spatial flow and sedimentation patterns within patches of epibenthic structures: Combining field, flume and modelling experiments. *Continental Shelf Research*, *27*(8), 1020-1045.

Braudrick, C. A., Dietrich, W. E., Leverich, G. T., & Sklar, L. S. (2009). Experimental evidence for the conditions necessary to sustain meandering in coarse-bedded rivers. *Proceedings of the National Academy of Sciences*, *106*(40), 16936-16941.

Brunke, M., & Gonser, T. O. M. (1997). The ecological significance of exchange processes between rivers and groundwater. *Freshwater biology*, *37*(1), 1-33.

Cao, D., & Chiew, Y. M. (2013). Suction effects on sediment transport in closed-conduit flows. *Journal of Hydraulic Engineering*, *140*(5), 04014008.

Carollo, F. G., Ferro, V. I. T. O., & Termini, D. (2005). Flow resistance law in channels with flexible submerged vegetation. *Journal of Hydraulic Engineering*, *131*(7), 554-564.

Carollo, F. G., Ferro, V., & Termini, D. (2002). Flow velocity measurements in vegetated channels. *Journal of Hydraulic Engineering*, *128*(7), 664-673.

Carpenter, S. R., & Lodge, D. M. (1986). Effects of submersed macrophytes on ecosystem processes. *Aquatic botany*, *26*, 341-370.

Chao, W. A. N. G., YU, J. Y., WANG, P. F., & GUO, P. C. (2009). Flow structure of partly vegetated open-channel flows with eelgrass. *Journal of Hydrodynamics, Ser. B*, *21*(3), 301-307.

Chen, S. C., Kuo, Y. M., & Li, Y. H. (2011). Flow characteristics within different configurations of submerged flexible vegetation. *Journal of Hydrology*, *398*(1), 124-134.

Chen, X., & Chiew, Y. M. (2004). Velocity distribution of turbulent open-channel flow with bed suction. *Journal of Hydraulic Engineering*, *130*(2), 140-148.

Chen, Y. C., & Kao, S. P. (2011). Velocity distribution in open channels with submerged aquatic plant. *Hydrological Processes*, *25*(13), 2009-2017.

Chen, Z., Ortiz, A., Zong, L., & Nepf, H. (2012). The wake structure behind a porous obstruction and its implications for deposition near a finite patch of emergent vegetation. *Water Resources Research*, *48*(9).

Cheng, N. S. (2011). Representative roughness height of submerged vegetation. *Water Resources Research*, *47*(8).

Chow, V.T. (1959). Open channel hydraulics. *McGraw-Hill Book Co.,* Singapore, pp. 680, ISBN 0-07-085906-X.

Corenblit, D., Tabacchi, E., Steiger, J., & Gurnell, A. M. (2007). Reciprocal interactions and adjustments between fluvial landforms and vegetation dynamics in river corridors: a review of complementary approaches. *Earth-Science Reviews*, *84*(1), 56-86.

Cotton, J. A., Wharton, G., Bass, J. A. B., Heppell, C. M., & Wotton, R. S. (2006). The effects of seasonal changes to in-stream vegetation cover on patterns of flow and accumulation of sediment. *Geomorphology*, *77*(3), 320-334.

Crowder, D. W., & Diplas, P. (2002). Vorticity and circulation: spatial metrics for evaluating flow complexity in stream habitats. *Canadian Journal of Fisheries and Aquatic Sciences*, *59*(4), 633-645.

Darby, S. E. (1999). Effect of riparian vegetation on flow resistance and flood potential. *Journal of Hydraulic Engineering*, *125*(5), 443-454.

De Lima, P. H., Janzen, J. G., & Nepf, H. M. (2015). Flow patterns around two neighboring patches of emergent vegetation and possible implications for deposition and vegetation growth. *Environmental Fluid Mechanics*, *15*(4), 881-898.

Deshpande, V., & Kumar, B. (2016a). Advent of sheet flow in suction affected alluvial channels. *Environmental Fluid Mechanics*, *16*(1), 25-44.

Deshpande, V., & Kumar, B. (2016b). Turbulent flow structures in alluvial channels with curved cross-sections under conditions of downward seepage. *Earth Surface Processes and Landforms*, 41, 1073-1087.

Dey, S., & Nath, T. K. (2009). Turbulence characteristics in flows subjected to boundary injection and suction. *Journal of Engineering Mechanics*, *136*(7), 877-888.

Dey, S., Das, R., Gaudio, R., & Bose, S. K. (2012). Turbulence in mobile-bed streams. *Acta Geophysica*, *60*(6), 1547-1588.

Edgar, G. J. (1990). The influence of plant structure on the species richness, biomass and secondary production of macrofaunal assemblages associated with Western Australian seagrass beds. *Journal of Experimental Marine Biology and Ecology*, *137*(3), 215-240.

Fairbanks, J. D. (1998). Velocity and turbulence characteristics in flows through rigid vegetation (*Doctoral dissertation, Virginia Polytechnic Institute & State University*).

Fathi-Maghadam, M., & Kouwen, N. (1997). Nonrigid, nonsubmerged, vegetative roughness on floodplains. *Journal of Hydraulic Engineering*, *123*(1), 51-57.

Fenzl, R. N. (1962). *Hydraulic resistance of broad shallow vegetated channels* (Doctoral dissertation, University of California).

Ferro, V. (2006). La sistemazione dei bacini idrografici-seconda edizione. McGraw–Hill, Milano, Italy (in Italian)

Ferro, V., & Giordano, G. (1990). Esperienze sulle resistenze al moto in alvei di tipo montano. Riesame critico e nuove acquisizioni [in Sicilia]. *Rivista di Ingegneria Agraria*.

Ferro, V., & Giordano, G. (1992). Valutazione sperimentale delle resistenze al moto in alvei con vegetazione rigida sul fondo in condizioni di macroscabrezza. *Quad. Idronom. Montana*, *11*(12), 163-181.

Finnigan, J. J. (1979). Turbulence in waving wheat. *Boundary-Layer Meteorology*, *16*(3), 181-211.

Folkard, A. M. (2011). Flow regimes in gaps within stands of flexible vegetation: laboratory flume simulations. *Environmental Fluid Mechanics*, *11*(3), 289-306.

Gao, W., & Shaw, R. H. (1989). Observation of organized structure in turbulent flow within and above a forest canopy. In *Boundary Layer Studies and Applications* (pp. 349-377). Springer Netherlands.

Ghisalberti, M., & Nepf, H. (2006). The structure of the shear layer in flows over rigid and flexible canopies. *Environmental Fluid Mechanics*, *6*(3), 277-301.

Ghisalberti, M., & Nepf, H. (2009). Shallow flows over a permeable medium: the hydrodynamics of submerged aquatic canopies. *Transport in porous media*, *78*(2), 309-326.

Ghisalberti, M., & Nepf, H. M. (2002). Mixing layers and coherent structures in vegetated aquatic flows. *Journal of Geophysical Research: Oceans*, *107*(C2).

Goring, D. G., & Nikora, V. I. (2002). Despiking acoustic Doppler velocimeter data. *Journal of Hydraulic Engineering*, *128*(1), 117-126.

Gourlay, M. R. (1970). Discussion of 'Flow retardance in vegetated channels' by N. Kouwen, TE Unny, and HM Hill. *J Irrig Drain Eng*, *96*(3), 351-357.

Gurnell, A. (2014). Plants as river system engineers. *Earth Surface Processes and Landforms*, *39*(1), 4-25.

Gurnell, A. M., Van Oosterhout, M. P., De Vlieger, B., & Goodson, J. M. (2006). Reach-scale interactions between aquatic plants and physical habitat: River Frome, Dorset. *River Research and Applications*, *22*(6), 667-680.

Gyr, A., & Schmid, A. (1989). The different ripple formation mechanism.*Journal of Hydraulic Research*, *27*(1), 61-74.

Huai, W. X., Han, J., Zeng, Y. H., An, X., & Qian, Z. D. (2009). Velocity distribution of flow with submerged flexible vegetations based on mixing-length approach. *Applied mathematics and mechanics*, *30*, 343-351.

Huthoff, F., Augustijn, D., & Hulscher, S. J. (2007). Analytical solution of the depth-averaged flow velocity in case of submerged rigid cylindrical vegetation. *Water resources research*, *43*(6).

Ikeda, S., & Kanazawa, M. (1996). Three-dimensional organized vortices above flexible water plants. *Journal of Hydraulic Engineering*, *122*(11), 634-640.

Inoue, E. (1963). On the turbulent structure of airflow within crop canopies. *J. Meteor. Soc. Japan*, *41*, 317-326.

Ishikawa, Y., Mizuhara, K., & Ashida, M. (2000). Drag force on multiple rows of cylinders in an open channel. *Grant-in-aid research project report, Kyushu Univ, Fukuoka, Japan*.

Jadhav, R. S., & Buchberger, S. G. (1995). Effects of vegetation on flow through free water surface wetlands. *Ecological Engineering*, *5*(4), 481-496.

James, C. S., & Makoa, M. J. (2006, December). Conveyance estimation for channels with emergent vegetation boundaries. In *Proceedings of the Institution of Civil Engineers-Water Management* (Vol. 159, No. 4, pp. 235-243). Thomas Telford Ltd.

James, C. S., Birkhead, A. L., Jordanova, A. A., & O'sullivan, J. J. (2004). Flow resistance of emergent vegetation. *Journal of Hydraulic Research*, *42*(4), 390-398.

Järvelä, J. (2002). Flow resistance of flexible and stiff vegetation: a flume study with natural plants. *Journal of Hydrology*, *269*(1), 44-54.

Järvelä, J. (2004). Determination of flow resistance caused by non-submerged woody vegetation. *International Journal of River Basin Management*, *2*(1), 61-70.

Järvelä, J. (2005). Effect of submerged flexible vegetation on flow structure and resistance. *Journal of Hydrology*, *307*(1), 233-241.

Jones, C. G., Lawton, J. H., & Shachak, M. (1994). Organisms as ecosystem engineers. In *Ecosystem management* (pp. 130-147). Springer New York.

Jones, J. B., & Mulholland, P. J. (1999). *Streams and ground waters*. Academic Press.

Kadlec, R. H. (1995). Overview: surface flow constructed wetlands. *Water Science and Technology*, *32*(3), 1-12.

Katul, G., Wiberg, P., Albertson, J., & Hornberger, G. (2002). A mixing layer theory for flow resistance in shallow streams. *Water Resources Research*, *38*(11).

Kemp, J. L., Harper, D. M., & Crosa, G. A. (2000). The habitat-scale ecohydraulics of rivers. *Ecological Engineering*, *16*(1), 17-29.

Kinzli, K. D., Martinez, M., Oad, R., Prior, A., & Gensler, D. (2010). Using an ADCP to determine canal seepage loss in an irrigation district. *Agricultural water management*, *97*(6), 801-810.

Klopstra, D., Barneveld, H. J., Van Noortwijk, J. M., & Van Velzen, E. H. (1996). Analytical model for hydraulic roughness of submerged vegetation. In *Proceedings of the Congress-International Association for Hydraulic Research (pp. 775-780). Local organizing committee of the XXV Congress.*

Kothyari, U. C., Hashimoto, H., & Hayashi, K. (2009a). Effect of tall vegetation on sediment transport by channel flows. *Journal of Hydraulic Research*, *47*(6), 700-710.

Kothyari, U. C., Hayashi, K., & Hashimoto, H. (2009b). Drag coefficient of unsubmerged rigid vegetation stems in open channel flows. *Journal of Hydraulic Research*, *47*(6), 691-699.

Kouwen, N. (1988). Field estimation of the biomechanical properties of grass. *Journal of Hydraulic Research*, *26*(5), 559-568.

Kouwen, N. (1992). "Modern approach to design of grassed channels." *J. Irrigation and Drain. Engg*., 118(5), 733-743.

Kouwen, N. N., & Li, R. M. (1980). Biomechanics of vegetative channel linings. *Journal of the Hydraulics Division*, *106*(ASCE 15464).

Kouwen, N., Li, R. M., & Simons, D. B. (1981). Flow resistance in vegetated waterways. *Transactions of the ASAE*, *24*(3), 684-0690.

Kouwen, N., Unny, T. E., & Hill, H. M. (1969). Flow retardance in vegetated channels. *Journal of the Irrigation and Drainage Division*, *95*(2), 329-344.

Kowobari, T. S., Rice, C. E., & Garton, J. E. (1972). Effect of roughness elements on hydraulic resistance for overland flow. *Transactions of the ASAE*, *15*(5), 979-0984.

Krogstad, P. Å., & Kourakine, A. (2000). Some effects of localized injection on the turbulence structure in a boundary layer. *Physics of Fluids (1994-present)*, *12*(11), 2990-2999.

Kubrak, E., Kubrak, J., & Kiczko, A. (2015). Experimental Investigation of Kinetic Energy and Momentum Coefficients in Regular Channels with Stiff and Flexible Elements Simulating Submerged Vegetation. *Acta Geophysica*, *63*(5), 1405-1422.

Kutija, V., & Thi Minh Hong, H. (1996). A numerical model for assessing the additional resistance to flow introduced by flexible vegetation. *Journal of Hydraulic Research*, *34*(1), 99-114.

Lee, H. Y., & Shih, S. S. (2004). Impacts of vegetation changes on the hydraulic and sediment transport characteristics in Guandu mangrove wetland. *Ecological Engineering*, *23*(2), 85-94.

Li, C. W., & Xie, J. F. (2011). Numerical modeling of free surface flow over submerged and highly flexible vegetation. *Advances in Water Resources*, *34*(4), 468-477.

Li, R. M., & Shen, H. W. (1973). Effect of tall vegetations on flow and sediment. *Journal of the hydraulics division*, *99*(hy5).

Li, S. S., & Millar, R. G. (2011). A two-dimensional morphodynamic model of gravel-bed river with floodplain vegetation. *Earth Surface Processes and Landforms*, *36*(2), 190-202.

Li, Y., Wang, Y., Anim, D. O., Tang, C., Du, W., Ni, L., & Acharya, K. (2014). Flow characteristics in different densities of submerged flexible vegetation from an open-channel flume study of artificial plants. *Geomorphology*, *204*, 314-324.

Liu, D., Diplas, P., Fairbanks, J. D., & Hodges, C. C. (2008). An experimental study of flow through rigid vegetation. *Journal of Geophysical Research: Earth Surface*, *113*(F4).

López, F., & García, M. (1998). Open-channel flow through simulated vegetation: Suspended sediment transport modeling. *Water resources research*, *34*(9), 2341-2352.

López, F., & García, M. H. (2001). Mean flow and turbulence structure of open-channel flow through non-emergent vegetation. *Journal of Hydraulic Engineering*, *127*(5), 392-402.

Lü, S. Q. (2008). *Experimental Study on Suspended Sediment Distribution in Flow with Rigid Vegetation* (Doctoral dissertation, Ph. D. Dissertation. Hohai University, Nanjing (in Chinese)).

Lu, S. S., & Willmarth, W. W. (1973). Measurements of the structure of the Reynolds stress in a turbulent boundary layer. *Journal of Fluid Mechanics*, *60*(03), 481-511.

Maclean, A. G. (1991). Bed shear stress and scour over bed-type river intake. *Journal of Hydraulic Engineering*, *117*(4), 436-451.

Maclean, A. G., & Willetts, B. B. (1986). Measurement of boundary shear stress in non-uniform open channel flow. *Journal of Hydraulic Research*, *24*(1), 39-51.

Mars, M., Kuruvilla, M., and Goen, H. (1999). The role of submergent macrophyte *triglochin huegelii* in domestic greywater treatment. *Ecol. Eng.*, 12 (1), 57-66.

Marsh, N. A., Western, A. W., & Grayson, R. B. (2004). Comparison of methods for predicting incipient motion for sand beds. *Journal of hydraulic engineering*, *130*(7), 616-621.

Martin, C. A., & Gates, T. K. (2014). Uncertainty of canal seepage losses estimated using flowing water balance with acoustic Doppler devices. *Journal of Hydrology*, *517*, 746-761.

Meire, D. W., Kondziolka, J. M., & Nepf, H. M. (2014). Interaction between neighboring vegetation patches: Impact on flow and deposition. *Water Resources Research*, *50*(5), 3809-3825.

Miller, M. C., McCave, I. N., & Komar, P. (1977). Threshold of sediment motion under unidirectional currents. *Sedimentology*, *24*(4), 507-527.

Monin, A. S., & Yaglom, A. M. (2013). *Statistical fluid mechanics, volume II: Mechanics of turbulence* (Vol. 2). Courier Corporation.

Mudd, S. M., D'Alpaos, A., & Morris, J. T. (2010). How does vegetation affect sedimentation on tidal marshes? Investigating particle capture and hydrodynamic controls on biologically mediated sedimentation. *Journal of Geophysical Research: Earth Surface*, *115*(F3).

Musleh, F. A., & Cruise, J. F. (2006). Functional relationships of resistance in wide flood plains with rigid unsubmerged vegetation. *Journal of hydraulic engineering*, *132*(2), 163-171.

Neary, V. S., Constantinescu, S. G., Bennett, S. J., & Diplas, P. (2011). Effects of vegetation on turbulence, sediment transport, and stream morphology. *Journal of Hydraulic Engineering*, *138*(9), 765-776.

Nehal, L., & Ming, Y. Z. (2005). Study on the flow of water through non-submerged vegetation.

Nepf, H. M. (1999). Drag, turbulence, and diffusion in flow through emergent vegetation. *Water resources research*, *35*(2), 479-489.

Nepf, H. M. (2012a). "Flow and transport in regions with aquatic vegetation." *Annual Review of Fluid Mechanics*, 44, 123-142.

Nepf, H. M. (2012b). Hydrodynamics of vegetated channels. *Journal of Hydraulic Research*, *50*(3), 262-279.

Nepf, H. M., & Vivoni, E. R. (2000). Flow structure in depth-limited, vegetated flow. *Journal of Geophysical Research: Oceans*, *105*(C12), 28547-28557.

Nepf, H., & Ghisalberti, M. (2008). Flow and transport in channels with submerged vegetation. *Acta Geophysica*, *56*(3), 753-777.

Neumeier, U. R. S., & Amos, C. L. (2006). The influence of vegetation on turbulence and flow velocities in European salt-marshes. *Sedimentology*, *53*(2), 259-277.

Nezu, I., & Sanjou, M. (2008). Turburence structure and coherent motion in vegetated canopy open-channel flows. *Journal of hydro-environment research*, *2*(2), 62-90.

Nikora, V. (2010). Hydrodynamics of aquatic ecosystems: an interface between ecology, biomechanics and environmental fluid mechanics. *River Research and Applications*, *26*(4), 367-384.

Okamoto, T. A., & Nezu, I. (2009). Turbulence structure and "Monami" phenomena in flexible vegetated open-channel flows. *Journal of Hydraulic Research*, *47*(6), 798-810.

Okamoto, T. A., & Nezu, I. (2010). Flow resistance law in open-channel flows with rigid and flexible vegetation. *River flow 2010*, 261-268.

Okamoto, T. A., & Nezu, I. (2013). Spatial evolution of coherent motions in finite-length vegetation patch flow. *Environmental fluid mechanics*, *13*(5), 417-434.

Okamoto, T. A., Nezu, I., & Ikeda, H. (2012). Vertical mass and momentum transport in open-channel flows with submerged vegetations. *Journal of Hydro-environment Research*, *6*(4), 287-297.

Palmer, V. J. (1945). A method for designing vegetated waterways. *Agricultural Engineering*, *26*(12), 516-520.

Pang, C. C., Wu, D., Lai, X. J., Wu, S. Q., & Wang, F. F. (2014). Turbulence structure and flow field of shallow water with a submerged eel grass patch. *Ecological Engineering*, *69*, 201-205.

Patel, M., Deshpande, V., & Kumar, B. (2015). Turbulent characteristics and evolution of sheet flow in an alluvial channel with downward seepage. *Geomorphology*, *248*, 161-171.

Petryk, S., & Bosmajian III, G. (1975). Analysis of flow through vegetation. *Journal of the Hydraulics Division*, *101*(ASCE# 114517 Proceeding).

Pierobon, E., Castaldelli, G., Mantovani, S., Vincenzi, F., & Fano, E. A. (2013). Nitrogen removal in vegetated and unvegetated drainage ditches impacted by diffuse and point sources of pollution. *CLEAN–Soil, Air, Water*, *41*(1), 24-31.

Poggi, D., Porporato, A, Ridolfi, L., Albertson, J., and Katul, G. (2004a). The effect of vegetation density on canopy sub-layer turbulence. *Bound. Lay. Met.* 111(3), 565-587.

Pollen, N., and Simon, A. (2005). Estimating the mechanical effects of riparian vegetation on stream bank stability using a fiber bundle model. *Water Resour. Res.*, 41(7).

Pope, S. B. (2001). Turbulent flows. Cambridge University Press, Cambridge.

Prinos, P. (1995). Bed-suction effects on structure of turbulent open-channel flow. *Journal of Hydraulic Engineering*, *121*(5), 404-412.

Ramakrishna Rao, A., Subrahmanyam, V., Thayumanavan, S., & Namboodiripad, D. (1994). Seepage effects on sand-bed channels. *Journal of irrigation and drainage engineering*, *120*(1), 60-79.

Rao, A. R., & Sitaram, N. (1999). Stability and mobility of sand-bed channels affected by seepage. *Journal of Irrigation and Drainage Engineering*, *125*(6), 370-379.

Rao, A. R., & Sreenivasulu, G. (2009). Design of plane sand-bed channels affected by seepage. *Periodica Polytechnica. Civil Engineering*, 53(2), 81.

Rao, A. R., Sreenivasulu, G., & Kumar, B. (2011). Geometry of sand-bed channels with seepage. *Geomorphology*, *128*(3), 171-177.

Raupach, M. R. (1981). Conditional statistics of Reynolds stress in rough-wall and smooth-wall turbulent boundary layers. *Journal of Fluid Mechanics*, *108*, 363-382.

Raupach, M. R., Antonia, R. A., & Rajagopalan, S. (1991). Rough-wall turbulent boundary layers. *Applied Mechanics Reviews*, *44*(1), 1-25.

Righetti, M. (2008). Flow analysis in a channel with flexible vegetation using double-averaging method. *Acta Geophysica*, 56(3), 801-823.

Righetti, M., & Armanini, A. (2002). Flow resistance in open channel flows with sparsely distributed bushes. *Journal of Hydrology*, *269*(1), 55-64.

Rominger, J. T., Lightbody, A. F., & Nepf, H. M. (2010). Effects of added vegetation on sand bar stability and stream hydrodynamics. *Journal of Hydraulic Engineering*, *136*(12), 994-1002.

Sand-Jensen, K. A. J., & VindbÆK Madsen, T. O. M. (1992). Patch dynamics of the stream macrophyte, Callitriche cophocarpa. *Freshwater Biology*, *27*(2), 277-282.

Schulz, M., Kozerski, H. P., Pluntke, T., & Rinke, K. (2003). The influence of macrophytes on sedimentation and nutrient retention in the lower River Spree (Germany). *Water Research*, *37*(3), 569-578.

Sharpe, R. G., & James, C. S. (2006). Deposition of sediment from suspension in emergent vegetation. *Water Sa*, *32*(2), 211-218.

Shen, H. W. (1973). Flow resistance over short simulated vegetation and various tall simulated vegetation groupings on flow resistance and sediment yield. *Environmental Impact on Rivers* (Rivers MechanicsIII, Fort Collins, Colo).

Shi, Z., Pethick, J. S., Burd, F., & Murphy, B. (1996). Velocity profiles in a salt marsh canopy. *Geo-Marine Letters*, *16*(4), 319-323.

Simões, F. J., & Wang, S. S. Y. (1997). Three-Dimensional Modeling of Compound Channels with Vegetated Flood Plains. In *Environmental and Coastal Hydraulics: Protecting the Aquatic Habitat* (pp. 809-814). ASCE.

Siniscalchi, F., Nikora, V. I., & Aberle, J. (2012). Plant patch hydrodynamics in streams: Mean flow, turbulence, and drag forces. *Water Resources Research*, *48*(1).

Sreenivasulu, G., Kumar, B., & Rao, A. R. (2011). Variation of stream power with seepage in sand-bed channels. *Water SA*, *37*(1), 115-119.

Stephan, U., & Gutknecht, D. (2002). Hydraulic resistance of submerged flexible vegetation. *Journal of Hydrology*, *269*(1), 27-43.

Stone, B. M., & Shen, H. T. (2002). Hydraulic resistance of flow in channels with cylindrical roughness. *Journal of hydraulic engineering*, *128*(5), 500-506.

Sumer, B. M., Kozakiewicz, A., Fredsøe, J., & Deigaard, R. (1996). Velocity and concentration profiles in sheet-flow layer of movable bed. *Journal of Hydraulic Engineering*, *122*(10), 549-558.

Takemura, T., & Tanaka, N. (2007). Flow structures and drag characteristics of a colony-type emergent roughness model mounted on a flat plate in uniform flow. *Fluid Dynamics Research*, *39*(9), 694-710.

Tang, H., Yan, J., & Lu, S. (2007). Advances in research on flows with vegetation in river management. *Advances in Water Science*, *18*(5), 792.

Tanino, Y., & Nepf, H. M. (2008). Lateral dispersion in random cylinder arrays at high Reynolds number. *Journal of Fluid Mechanics*, *600*, 339-371.

Tanino, Y., and Nepf, H. (2008). Lateral dispersion in random cylinder arrays at high Reynolds number. *J. Fluid Mech.* 600, 339-371.

Tanji, K.K., and Kielen, N.C. (2002). Agricultural drainage water management in arid and semi-arid areas. *In: Irrigation Drainage Paper* 61, FAO, Rome.

Temple, D. M. (1982). Flow retardance of submerged grass channel linings. *Transactions of the ASAE*, *25*(5), 1300-1303.

Tennekes, H., & Lumley, J. L. (1972). *A first course in turbulence*. MIT press.

Termini, D. (2015). Flexible vegetation behaviour and effects on flow conveyance: experimental observations. *International Journal of River Basin Management*, *13*(4), 401-411.

Thompson, A. M., Wilson, B. N., & Hansen, B. J. (2004). Shear stress partitioning for idealized vegetated surfaces. *Transactions of the ASAE*, *47*(3), 701.

Tsujimoto, T. (1999). Fluvial processes in streams with vegetation. *Journal of hydraulic research*, *37*(6), 789-803.

Tsujimoto, T., Shimizu, Y., Kitamura, T., & Okada, T. (1992). Turbulent open-channel flow over bed covered by rigid vegetation. *Journal of Hydroscience and Hydraulic Engineering*, *10*(2), 13-25.

Turker, U., Yagci, O., and Kabdasli, M. (2006). Analysis of coastal damage of a beach profile under the protection of emergent vegetation. *Ocean Engineering*, 33, 810-828.

Turner, I. L. (1995). Simulating the influence of groundwater seepage on sediment transported by the sweep of the swash zone across macro-tidal beaches. *Marine Geology*, *125*(1), 153-174.

Van Katwijk, M. M., Bos, A. R., Hermus, D. C. R., & Suykerbuyk, W. (2010). Sediment modification by seagrass beds: muddification and sandification induced by plant cover and environmental conditions. *Estuarine, Coastal and Shelf Science*, *89*(2), 175-181.

Velasco, D., Bateman, A., Redondo, J. M., & DeMedina, V. (2003). An open channel flow experimental and theoretical study of resistance and turbulent characterization over flexible vegetated linings. *Flow, turbulence and combustion*, *70*(1-4), 69-88.

Wang, C., & Wang, C. (2010). Turbulent characteristics in open-channel flow with emergent and submerged macrophytes. *Advances in Water Science*, *21*(6), 816-822.

Wang, C., Wang, C., & Wang, Z. (2010). Effects of submerged macrophytes on sediment suspension and NH sub (4)-N release under hydrodynamic conditions. *Journal of hydrodynamics*, *22*(6), 810-815.

Watters, G. Z., & Rao, M. V. (1971). Hydrodynamic effects of seepage on bed particles. *Journal of the Hydraulics Division*, *97*(3), 421-439.

Wessels, W. P. J., & Strelkoff, T. S. Established Surge in An Impervious Vegetation Bed. *Journal of the Irrigation and Drainage Division*, *94*(1), 1-22.

Wilcock, R. J., Champion, P. D., Nagels, J. W., & Croker, G. F. (1999). The influence of aquatic macrophytes on the hydraulic and physico-chemical properties of a New Zealand lowland stream. *Hydrobiologia*, *416*, 203-214.

Willetts, B. B., & Drossos, M. E. (1975). Local erosion caused by rapid forced infiltration. *Journal of the Hydraulics Division*, *101*(ASCE# 11796 Proceeding).

Wilson, C. A. M. E., Stoesser, T., & Bates, P. D. (2005). *Modelling of open channel flow through vegetation* (pp. 395-428). John Wiley and Sons: Chichester, UK.

Wilson, C. A. M. E., Stoesser, T., Bates, P. D., & Pinzen, A. B. (2003). Open channel flow through different forms of submerged flexible vegetation. *Journal of Hydraulic Engineering*, *129*(11), 847-853.

Wu, F. C., Shen, H. W., & Chou, Y. J. (1999). Variation of roughness coefficients for unsubmerged and submerged vegetation. *Journal of Hydraulic Engineering*, *125*(9), 934-942.

Wu, F. S. (2007). Flow resistance of flexible vegetation in open channel. *J. Hydraul. Eng*, *38*, 283-287.

Yagci, O., & Kabdasli, M. S. (2008). The impact of single natural vegetation elements on flow characteristics. *Hydrological processes*, *22*(21), 4310-4321.

Yalin, M. S. (1972). Mechanics of sediment transport. Pergamon Press,Oxford,298.

Yang, W., & Choi, S. U. (2010). A two-layer approach for depth-limited open-channel flows with submerged vegetation. *Journal of Hydraulic Research*, *48*(4), 466-475.

Zhang, H., & Dai, L. (2009, January). Surface runoff and its erosion energy in a partially continuous system: an ecological hydraulic model. In *ASME 2009 International Mechanical Engineering Congress and Exposition* (pp. 575-583). American Society of Mechanical Engineers.

Zhang, H., Wang, Z., Dai, L., & Xu, W. (2015b). Influence of Vegetation on Turbulence Characteristics and Reynolds Shear Stress in Partly Vegetated Channel. *Journal of Fluids Engineering*, *137*(6), 061201.

Zhang, Y., Lai, X., & Jiang, J. (2015a). The impact of plant morphology on flow structure: comparative analysis of two types of submerged flexible macrophyte. *Hydrological Sciences Journal*, 61(12), 2226-2236.

Zhu, T., Cao, T., Ni, L., He, L., Yi, C., Yuan, C., & Xie, P. (2016). Improvement of water quality by sediment capping and re-vegetation with Vallisneria natans L.: A short-term investigation using an in situ enclosure experiment in Lake Erhai, China. *Ecological Engg*., *86*, 113-119.

Zong, L., & Nepf, H. (2012). Vortex development behind a finite porous obstruction in a channel. *Journal of Fluid Mechanics*, *691*, 368-391.

Appendix A

Turbulence Characteristics of Vegetated Channel with downward Seepage[vii]

Introduction

The fluctuation of stream wise and vertical velocity u' and w' are the random quantities in open channel flow whose mean value of the product $u'w'$ yields the Reynolds stress $-\rho\overline{u'w'}$ where ρ is the density of water. Due to this reason, in a flowing fluid $-\rho\overline{u'w'}$ is nonzero implies that u' and w' are correlated quantities. The theoretical analysis of this random quantities u' and w' are well explained by the simple one sided exponential distribution of probability function. The Probability Distribution Functions (PDFs) are derived from a truncated universal Gram Charlier (GC) series expansion based on the exponential or Laplace type distributions for turbulent velocity fluctuations. The knowledge of Probability density function (PDF) of these quantities helps in understanding the associated turbulent bursting phenomenon (Nakagawa and Nezu, 1977; Afzal *et al*, 2009). The non-Gaussian behaviour of velocity fluctuations were considered for deriving a GC series expansion for the joint PDFs of velocity fluctuations by inverting a Gaussian based characteristic function (Feriet and Kampe, 1966; Antonia and Atkinson, 1973; Nakagawa and Nezu, 1977). Bose and Dey (2010) derived a theoretical expression, highlighting the importance of skewness and kurtosis, for PDFs of velocity fluctuations, Reynolds stress and conditional Reynolds stress from GC series expansion based on exponential distributions and validated with the experimental observations.

Probability Distribution Functions

In open channel flow, production of turbulence at near bed region is due to flow over the bed. The two dimensional instantaneous velocities (u, w) at a point can be decomposed in terms of time averaged part (U, W) and fluctuation part (u',w') by applying Reynolds decomposition in the way

[vii] Devi, T. B., Sharma, A., & Kumar, B. Turbulence Characteristics of Vegetated Channel with downward Seepage. *Journal of Fluids Engineering*.

$(u,w) = (U,W) + (u',w')$. Bose and Dey (2010) and Dey *et al*(2012) show that velocity fluctuation (u',w') follows the Gram Charlier (GC) series based on exponential distribution at which u' and w' is normalized as $\hat{u} = u'/\sigma_u$ and $\hat{w} = w'/\sigma_w$ where, σ_u and σ_w are the stream wise and vertical turbulence intensity respectively. Bose and Dey (2010) has given the probability density function (PDF) for stream wise and vertical velocity fluctuation as explained in the following form of equations

$$P_{\hat{u}}(\hat{u}) = \left[\begin{array}{l} \frac{1}{2} + \frac{1}{4}C_{10}\hat{u} - \frac{1}{16}C_{20}(1+|\hat{u}|-\hat{u}^2) - \frac{1}{96}C_{30}\hat{u}(3+3|\hat{u}|-\hat{u}^2) \\ + \frac{1}{768}C_{40}(9+9|\hat{u}|-3\hat{u}^2-6|\hat{u}|^3+\hat{u}^4)+..... \end{array}\right] \exp(-|\hat{u}| \quad (1)$$

$$P_{\hat{w}}(\hat{w}) = \left[\begin{array}{l} \frac{1}{2} + \frac{1}{4}C_{01}\hat{w} - \frac{1}{16}C_{02}(1+|\hat{w}|-\hat{w}^2) - \frac{1}{96}C_{03}\hat{w}(3+3|\hat{w}|-\hat{w}^2) \\ + \frac{1}{768}C_{04}(9+9|\hat{w}|-3\hat{w}^2-6|\hat{w}|^3+\hat{w}^4)+..... \end{array}\right] \exp(-|\hat{w}|) \quad (2)$$

where, $C_{10} = M_{10}$, $C_{20} = \frac{1}{2}M_{20} - 1, C_{30} = \frac{1}{6}M_{30} - 2M_{10}, C_{40} = \frac{1}{24}M_{40} - \frac{3}{2}M_{20} + 2$ (3)

$$C_{01} = M_{01}\ C_{02} = \frac{1}{2}M_{02} - 1,\ C_{03} = \frac{1}{6}M_{03} - 2M_{01},\ C_{40} = \frac{1}{24}M_{40} - \frac{3}{2}M_{20} + 2 \quad (4)$$

where, $M_{j0} = \int_{-\alpha}^{\alpha} \hat{u}^j P_{\hat{u}}(\hat{u})\,\mathrm{d}\hat{u}$, $M_{0k} = \int_{-\alpha}^{\alpha} \hat{w}^j P_{\hat{w}}(\hat{w})\,\mathrm{d}\hat{w}$ (Bose and Dey 2010). As a result, the coefficient C_{j0} and C_{0k} is to be estimated from the experimental data. The theoretical curves for PDF s of $P_{\hat{u}}(\hat{u})$ and $P_{\hat{w}}(\hat{w})$ can be estimated by using the relative frequency $f_{\hat{u}}(\hat{u})$ and $f_{\hat{w}}(\hat{w})$ of the random variables û and ŵ which was determined from the experimental data at a given flow depth z. The moments, m_{j0} and m_{0k} were estimated by approximating $P_{\hat{u}}(\hat{u})$ and $P_{\hat{w}}(\hat{w})$ by $f_{\hat{u}}(\hat{u})$ and $f_{\hat{w}}(\hat{w})$ respectively and the integrals were evaluated by a composite Simpson's rule. In this way, the C_{j0} and C_{0k} were estimated by using Equation (3) and (4) and the PDFs are computed to yield the theoretical curves for $P_{\hat{u}}(\hat{u})$ and $P_{\hat{w}}(\hat{w})$. Two points on a vertical line were selected for the study of PDFs $P_{\hat{u}}(\hat{u})$ and $P_{\hat{w}}(\hat{w})$. They are at near the bed (z=0.03H) and within the outer layer (z=0.53H).

Reynolds stress is defined by $\tau_{xz} = -\rho\overline{u'w'}$ hence $-\frac{\tau_{xz}}{\rho}$ is the mean value of product of random variable *u'w'* due to which the PDFs of τ_{xz} depends upon the joint PDFs of *u'* and *w'*. In order to study the PDFs of τ_{xz}, dimensionless random variable $\hat{\tau} = \hat{u}\hat{w}$ is considered. Based on this consideration, Bose and Dey (2010) derived the PDFs of $\hat{\tau}$ as:

$$\begin{aligned} P_{\hat{\tau}}(\hat{\tau}) &= K_0(2\tau_1) - \frac{1}{8}(C_{20}+C_{02})(1-\tau_1^2)K_0(2\tau_1) \\ &+ \frac{1}{4}C_{11}\hat{\tau}K_0(2\tau_1) + \frac{1}{64}C_{22}\left[(1-\tau_1^2+\tau_1^4)K_0(2\tau_1) - 2\tau_1^3K_1(2\tau_1)\right] \\ &- \frac{1}{96}(C_{31}+C_{13})\hat{\tau}(3-\tau_1^3)\left[K_0(2\tau_1)+\tau_1K_1(2\tau_1)\right] \\ &+ \frac{1}{384}(C_{40}+C_{04})\left[(9-9\tau_1^2+\tau_1^4)K_0(2\tau_1) - 2\tau_1^3K_1(2\tau_1)\right] + \ldots\ldots \end{aligned} \tag{5}$$

where $\tau_1 = (|\hat{\tau}|)^{0.5}$, K_0 and K_1 are the Bessel function of order 0 and 1 respectively. The coefficient in the above expression can be found out by the following moments

$$\begin{aligned} \int_{-\infty}^{\infty} \hat{\tau}P_{\hat{\tau}}(\hat{\tau})d\hat{\tau} &= C_{11} + \frac{11}{8}(C_{31}+C_{13}) \\ \int_{-\infty}^{\infty} \hat{\tau}^2P_{\hat{\tau}}(\hat{\tau})d\hat{\tau} &= 4 + 4(C_{20}+C_{02}) + \frac{25}{4}C_{22} \\ \int_{-\infty}^{\infty} \hat{\tau}^3P_{\hat{\tau}}(\hat{\tau})d\tau &= 144C_{11} + 7407(C_{31}+C_{13}) \end{aligned} \tag{6}$$

Where $C_{20} = \frac{1}{2}M_{20} - 1$, $C_{02} = \frac{1}{2}M_{02} - 1$, $C_{40} = \frac{1}{24}M_{40} - \frac{3}{2}M_{20} + 2$, $C_{40} = \frac{1}{24}M_{40} - \frac{3}{2}M_{20} + 2$

The theoretical curves for PDFs of $P_{\hat{\tau}}(\hat{\tau})$ is estimated by using the relative frequency $f_{\hat{\tau}}(\hat{\tau})$ by replacing $P_{\hat{\tau}}(\hat{\tau})$ of the random variables $\hat{u}\hat{w}$ which was determined from the experimental data at a given flow depth *z*.

The fractional contribution from each bursting events to the production of total Reynolds stress is represented by the random variable $\hat{\tau} = \langle \hat{u}\hat{w} \rangle_{Qi}$ where *i* corresponds to the appropriate quadrant. The PDFs of events *Q1, Q2, Q3* and *Q4* are denoted by $P_1(\hat{\tau})$, $P_2(\hat{\tau})$, $P_3(\hat{\tau})$ and $P_4(\hat{\tau})$ respectively which follows that

$$P_1(\hat{\tau}) + P_2(\hat{\tau}) + P_3(\hat{\tau}) + P_4(\hat{\tau}) = P_{\hat{\tau}}(\hat{\tau}) \tag{7}$$

Bose and Dey (2010) has shown that the expression for $P_1(\hat{\tau})$ and $P_4(\hat{\tau})$ is the same as that given by equation (8). For $\hat{\tau} < 0$, $P_1(\hat{\tau})$=0, the distribution of Q1 is one sided and remaining on the positive side while for $\hat{\tau} > 0$, $P_4(\hat{\tau})$=0, the distribution of Q4 is one sided and remaining on the negative side.

$$\begin{aligned} P_1(\hat{\tau} > 0) = P_4(\hat{\tau} < 0) &= \frac{1}{2} P_{\hat{\tau}}(\hat{\tau}) + \frac{1}{4}(C_{10} - C_{01})\tau_1 K_1(2\tau_1) \\ &- \frac{1}{96}(C_{30} - C_{03})\tau_1 \left[\tau_1 K_0(2\tau_1) + (4 - \tau_1) K_1(2\tau_1)\right] \\ &+ \frac{1}{32}(C_{21} - C_{12})\tau_1 \left[\tau_1 K_0(2\tau_1) + (1 - \tau_1^2) K_1(2\tau_1)\right] + ... \end{aligned} \tag{8}$$

In the similar way, Bose and Dey (2010) has shown that the expression for $P_2(\hat{\tau})$ and $P_3(\hat{\tau})$ is the same as that given by equation (9). For $\hat{\tau} > 0$, $P_2(\hat{\tau})$=0, the distribution of Q2 is one sided and remaining on the negative side while for $\hat{\tau} < 0$, $P_3(\hat{\tau})$=0, the distribution of Q3 is one sided and remaining on the positive side $\hat{\tau}$.

$$\begin{aligned} P_2(\hat{\tau} < 0) = P_3(\hat{\tau} > 0) &= \frac{1}{2} P_{\hat{\tau}}(\hat{\tau}) - \frac{1}{4}(C_{10} - C_{01})\tau_1 K_1(2\tau_1) \\ &+ \frac{1}{96}(C_{30} - C_{03})\tau_1 \left[\tau_1 K_0(2\tau_1) + (4 - \tau_1) K_1(2\tau_1)\right] \\ &- \frac{1}{32}(C_{21} - C_{12})\tau_1 \left[\tau_1 K_0(2\tau_1) + (1 - \tau_1^2) K_1(2\tau_1)\right] + ... \end{aligned} \tag{9}$$

The summation of expression $P_1(\hat{\tau}), P_2(\hat{\tau}),\ P_3(\hat{\tau})$ and $P_4(\hat{\tau})$ given by the above equation satisfies equation (7). The coefficient in the above expression (8) and (9) is given by

$$\int_0^{\infty} \hat{\tau} P_1(\hat{\tau}) d\hat{\tau} = \frac{1}{2}\int_0^{\infty} \hat{\tau} P_{\hat{\tau}}(\hat{\tau}) d\hat{\tau} + \frac{1}{4}(C_{10} - C_{01}) - \frac{3}{32}(C_{21} - C_{12}) \qquad (10)$$

The coefficient is calculated from the experimentally determined relative frequencies $f_1(\hat{\tau})$ and $f_{\hat{\tau}}(\hat{\tau})$ of $\hat{\tau}$.

Results

Figure 1 shows $P_{\hat{u}}(\hat{u})$ and $P_{\hat{w}}(\hat{w})$ distributions at near the bed and within the outer layer. The coefficient C_{j0} and C_{0k} are tabulated in Table 1.Experimental observation of $P_{\hat{u}}(\hat{u})$ and $P_{\hat{w}}(\hat{w})$ are in reasonable agreement with the computed curves, implying that $P_{\hat{u}}(\hat{u})$ and $P_{\hat{w}}(\hat{w})$ can be represented by GC series expansion based on exponential distribution.

Table 1 Coefficient for the computation of $P_{\hat{u}}(\hat{u})$ *and* $P_{\hat{w}}(\hat{w})$

Case		C_{10}	C_{01}	C_{20}	C_{02}	C_{30}	C_{03}	C_{40}	C_{04}
Plain bed	z=0.03H	-3.9E-05	-0.0004	-0.5	-0.5	0.011	-0.016	0.61	0.65
	z=0.53H	-0.0002	-0.0006	-0.5	-0.5	-0.026	0.13	0.66	0.636
No Seepage	z=0.03H	-0.0005	0.0044	-0.5	-0.5	-0.027	-0.0031	0.677	0.654
	z=0.53H	-0.0015	0.0004	-0.5	-0.5	0.0462	-0.028	0.615	0.62
10% Seepage	z=0.03H	-0.0002	-0.001	-0.5	-0.5	-0.007	0.26	0.61	0.61
	z=0.53H	0.0008	-0.0015	-0.5	-0.5	0.071	0.0314	0.634	0.635
15% Seepage	z= 0.03H	-8.9E-05	-0.0017	-0.5	-0.5	0.043	-0.077	0.631	0.633
	z= 0.53H	0.00025	0.0007	-0.5	-0.5	-.00057	-.021	0.62	0.66

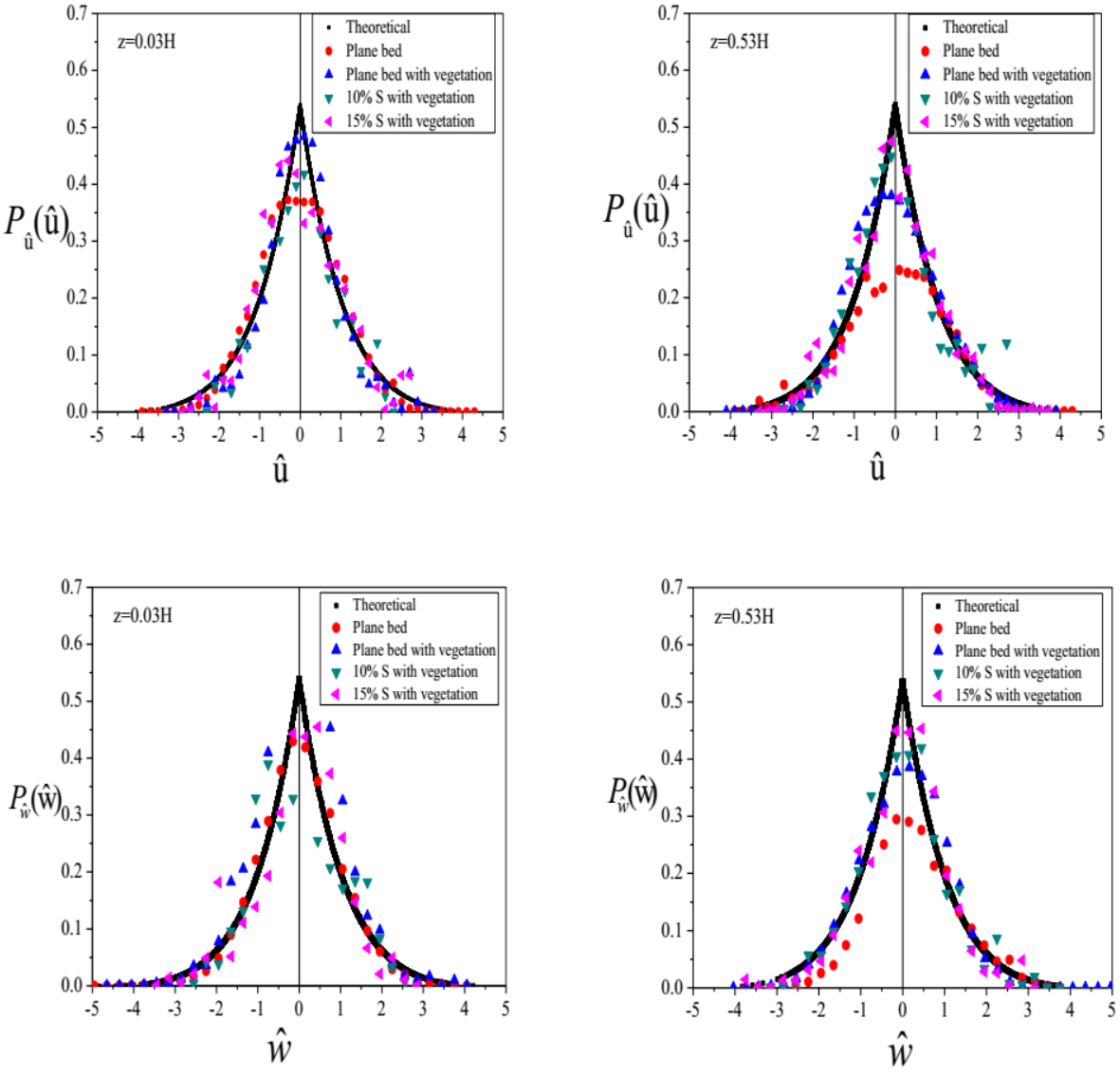

Figure 1 Comparisons of computed $P_{\hat{u}}(\hat{u})$ *and* $P_{\hat{w}}(\hat{w})$ *with experimental data for all cases*

The computed $P_{\hat{u}}(\hat{u})$ and $P_{\hat{w}}(\hat{w})$ distributions are sharply peaked at zero velocity fluctuations that is not observed in case of experimentally estimated PDFs distributions because of the absence of relative frequencies of such narrow ranges in the histogram. The results pointed that PDFs distribution for velocity fluctuations follow the GC series expansion based on exponential distributions for plane bed as well as seepage cases irrespective of the presence of the vegetation. Since vegetation stems induce larger drag forces, shear-generated turbulence is reduced due to the inhibition of momentum exchange by the stems surface area for which PDF distribution for velocity fluctuations in plane bed without vegetation and plane bed with vegetation is different.

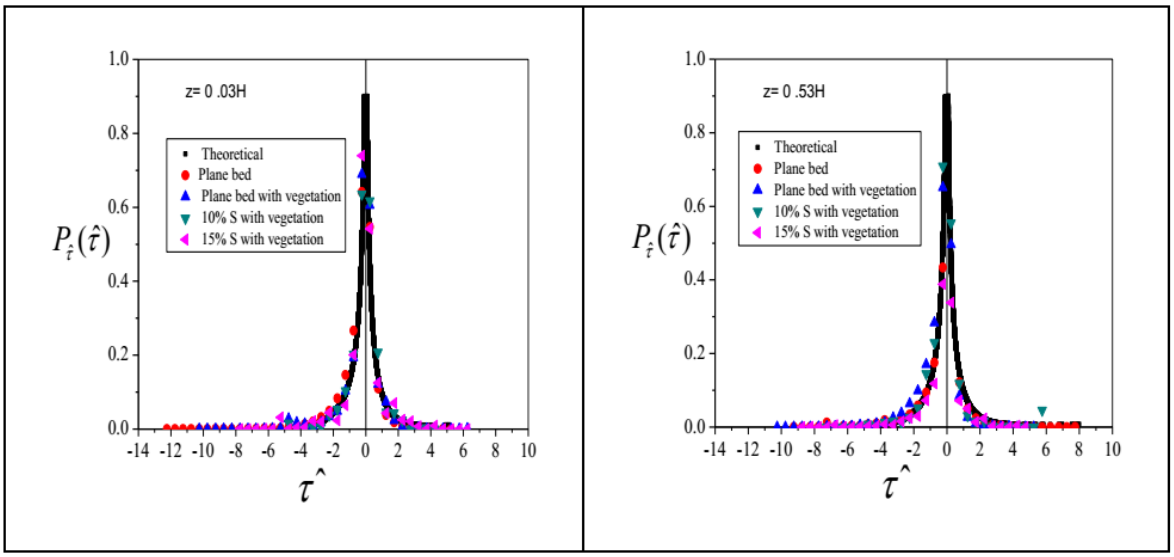

Figure 2 Comparisons of computed $P_{\hat{\tau}}(\hat{\tau})$ *with experimental data for all cases*

Table 2 Coefficient for the computation of $P_{\hat{\tau}}(\hat{\tau})$

Case		C_{11}	C_{13}	C_{31}	C_{22}
Plain bed	$z = 0.03H$	-0.40	0.59	0.616	0.313
	$z = 0.53H$	-0.284	0.376	0.342	0.40
No-Seepage	$z = 0.03H$	-0.27	0.383	0.4	0.318
	$z = 0.53H$	-0.51	0.794	0.796	0.353
10% Seepage	$z = 0.03H$	-0.1	0.146	0.168	0.2
	$z = 0.53H$	-0.13	0.238	0.316	0.392
15% Seepage	$z = 0.03H$	-0.15	0.23	0.207	0.348
	$z = 0.53H$	-0.208	0.272	0.34	0.318

The required parameters are calculated using equation (6) to yield the theoretical expression for $P_{\hat{\tau}}(\hat{\tau})$ given by equation (5). Figure 2 compares the computed and observed $P_{\hat{\tau}}(\hat{\tau})$ distributions at near the bed (z=0.03H) and within the outer layer (z=0.53H). The values of coefficient are tabulated in Table 2. Figure 2 indicates that the experimental calculated $P_{\hat{\tau}}(\hat{\tau})$ shows satisfactory agreement with the computed curves implying that derivation of $P_{\hat{\tau}}(\hat{\tau})$ using the GC series expansion based on the exponential distribution being applicable to mobile bed flows as well as seepage case.

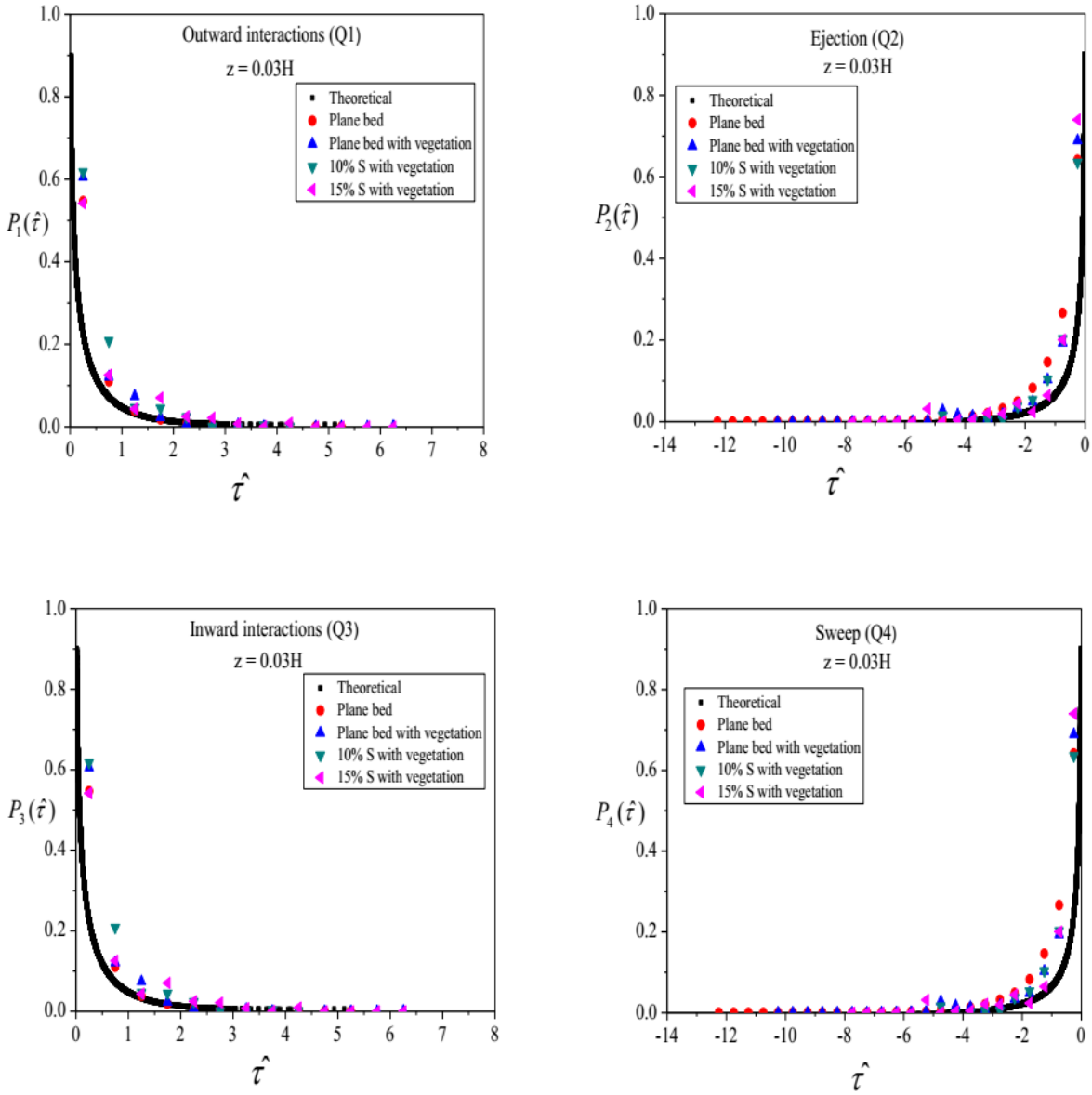

Figure 3 Comparisons of computed $P_i(\hat{\tau})$ *with experimental data at z= 0.03H for all cases*

Figures 3 and 4 compare the computed $P_i(\hat{\tau})$ with those measured for all cases at z=0.03H and 0.53H. It is found that the conditional Reynolds stress corresponding to ejections (Q2) and sweeps (Q4) can be well represented by the exponential based Gram Charlier distribution while outward interaction (Q1) and inward interactions (Q3) have a departure from computed distribution.

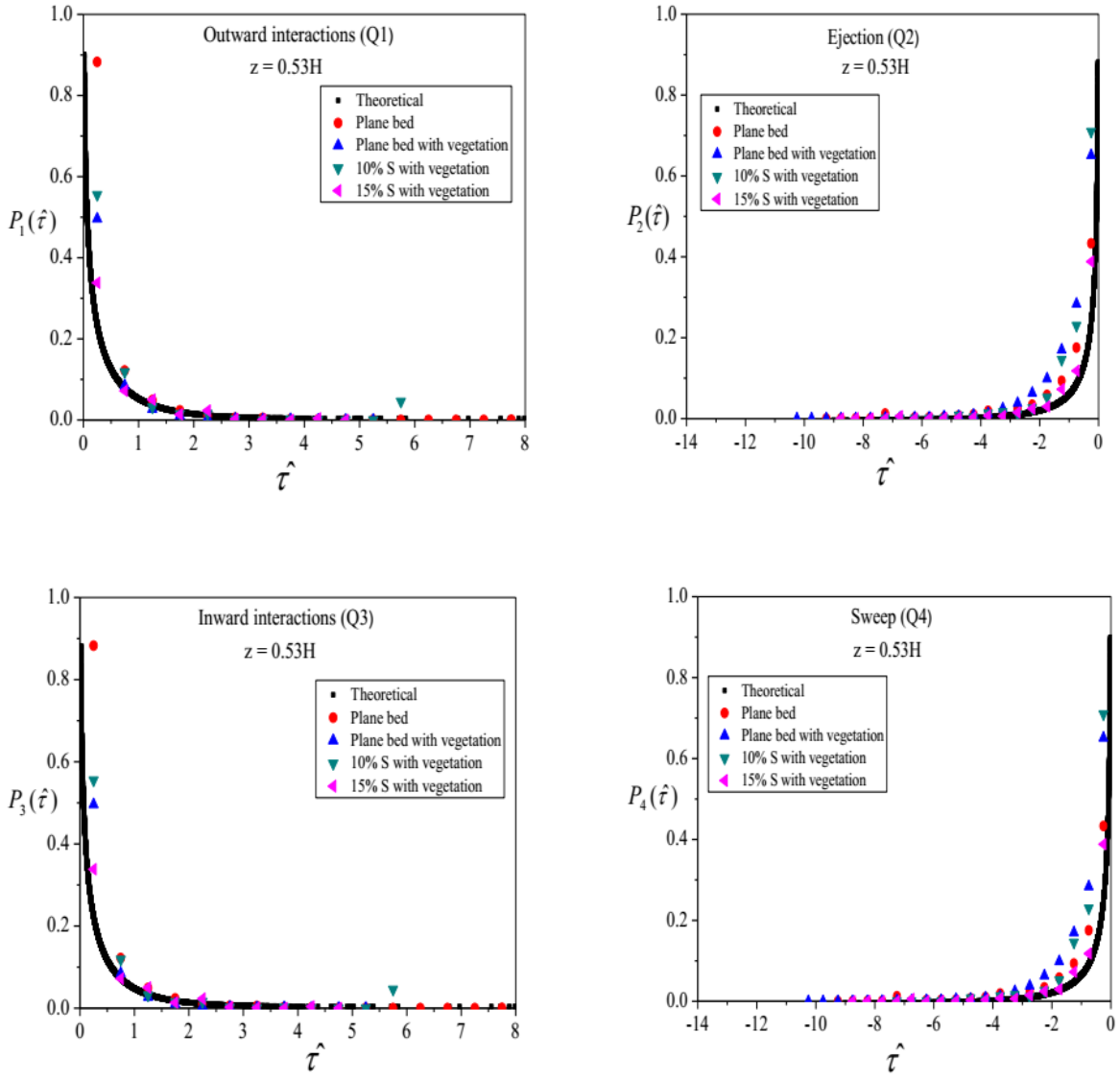

Figure 4 Comparisons of computed $P_i(\hat{\tau})$ *with experimental data at z= 0.53H for all cases*

Conclusions

The universal PDF distributions of velocity fluctuations and Reynolds stress in flows over vegetative channel for plane bed without vegetation, plane bed, 10%S and 15%S cases with vegetation follow Gram Charlier series expansion based on exponential distribution. The universal PDF distribution of conditional RSS are also compared with the experimental observation and found reasonable agreement for RSS corresponding to Q2 and Q4 while a slight departure is observed for Q1 and Q3 which may be due to weaker events.

References

Afzal, B., Faruque, M. A., & Balachandar, R. (2009). Effect of Reynolds number, near-wall perturbation and turbulence on smooth open-channel flows. *Journal of Hydraulic Research*, *47*(1), 66-81.

Antonia, R. A., & Atkinson, J. D. (1973). High-order moments of Reynolds shear stress fluctuations in a turbulent boundary layer. *Journal of Fluid Mechanics*, *58*(03), 581-593.

Bose, S. K., & Dey, S. (2010). Universal probability distributions of turbulence in open channel flows. *Journal of Hydraulic Research*, *48*(3), 388-394.

Dey, S., Das, R., Gaudio, R., & Bose, S. K. (2012). Turbulence in mobile-bed streams. *Acta Geophysica*, *60*(6), 1547-1588.

Feriet, D. E., & Kampe, J. (1966). *The Gram-Charlier approximation of the normal law and the statistical description of homogenous turbulent flow near statistical equilibrium. David Taylor Model Basin Report 2013. Naval Ship Research and Development Center, Washington, DC.*

Nakagawa, H., & Nezu, I. (1977). Prediction of the contributions to the Reynolds stress from bursting events in open-channel flows. *Journal of fluid mechanics*, *80*(01), 99-128.

Appendix B

Studies on emergent flow over vegetative channel bed with downward seepage[viii]

Introduction

In rivers, aquatic vegetation was historically considered only as a source of flow resistance, and vegetation was frequently removed to enhance flow conveyance and reduce flooding. The vegetation along the bed of rivers plays an important role on the hydrodynamic behavior, on the ecological equilibrium and on the characteristics of the river (Wilcock *et al*, 1999; Mars *et al*, 1999; Rowinski and Kubrak, 2002; Pollen and Simon, 2005; Turker *et al*, 2006). To better understand and protect these systems, the study of vegetation hydrodynamics has been integrated with other disciplines, such as biology (Hurd, 2000; Koch, 2001; Huang *et al*, 2011), fluvial geomorphology (Bennett *et al*, 2002; Tal and Paola, 2007), landscape ecology (Larsen and Harvey, 2011), and geochemistry (Clarke 2002; Harvey *et al*, 2003).

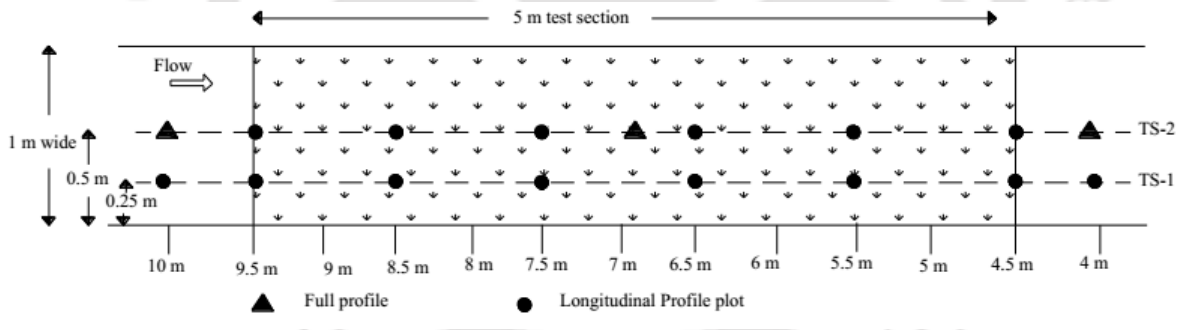

Figure 1 Plan view of the test section with measurement locations

Schnauder (2004) proved that the frontal area (or momentum absorbing area) decreased as a result of vegetation bending. O'Hare *et al* (2007) used five different macrophytes from a lowland river to consider the drag and reconfiguration. The vegetation changed shape and bend with the increasing velocity, which in turn reduced the flow rate. Hui *et al* (2010) considered single leafy

[viii] Devi, T.B., Sharma,A., & Kumar, B. (2016). Studies on emergent flow over vegetative channel bed with downward seepage. *Hydrological Sciences Journal* (Accepted)

shrub and three mixed communities (including shrub-grass, shrub-reed and reed-grass community) in their experiment to find out the effects of ecological factors (diameter and flexibility) and vegetation community composition on the drag coefficient related with vegetation.

Results

Velocity profiles of longitudinal plot (Figure 2) show that velocity is decreased from 10 m, which is 0.5m upstream of the vegetation zone, to 9.5m where placing of vegetation starts. The presence of vegetation causes some changes in velocities locally behind vegetation elements. This local effect of the presence of vegetation has caused variation in the velocity along the vegetated portion of the channel as the flow is forced around the vegetation. Similar results are also observed in Shucksmith *et al* (2010).

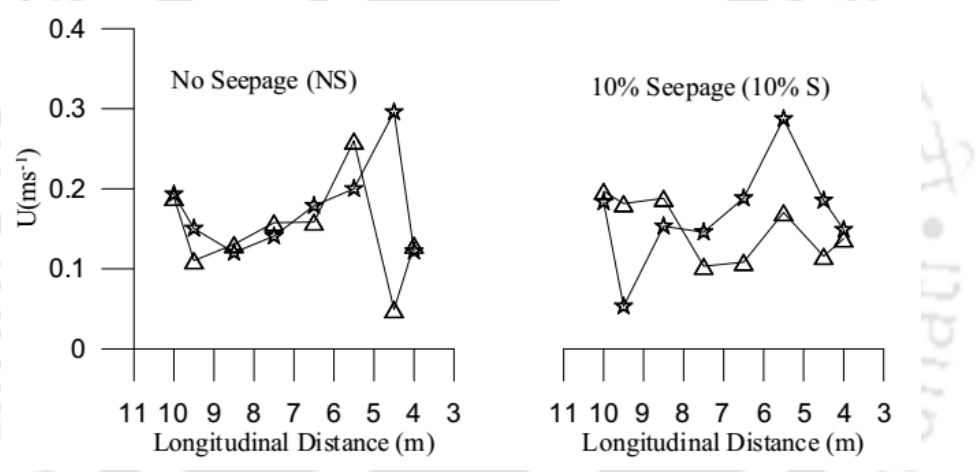

Figure 2 Velocity profiles for no seepage and 10% seepage plotted along eight longitudinal sections

An interesting feature is that the downstream free zone i.e. 4m has lower velocity as compared to the upstream free zone i.e. 10 m. For the case of no-seepage, the velocity for both the transverse sections, TS1 and TS2, at 10 m is reduced by about 46% and 58% as the flow reached 4m. Even for the seepage case also, the velocity for TS1 and TS2 at 10 m is approximately 43% and 23% higher as compared to the velocity at 4 m. Results from velocity profiles show that velocity decrease outside the vegetation zone at the downstream section which reveals that emergent vegetation increases the roughness and friction resistance of the flume by the leaves and stems and thus reduce the flow velocity.

Longitudinal profile of Reynolds stress is shown in the Figure 3. At 10m or 0.5m upstream of the vegetation zone, Reynolds stress values seldom change at TS1 and TS2 with small values close to zero indicating that there is not much turbulence outside the vegetation zone. However, Reynolds stress in the vegetation zone (9.5-4.5m) changed greatly at both TS1 and TS2. It can be inferred that flow velocities induce strong fluctuation in the flume when met the vegetation as observed by Shucksmith *et al* (2010).

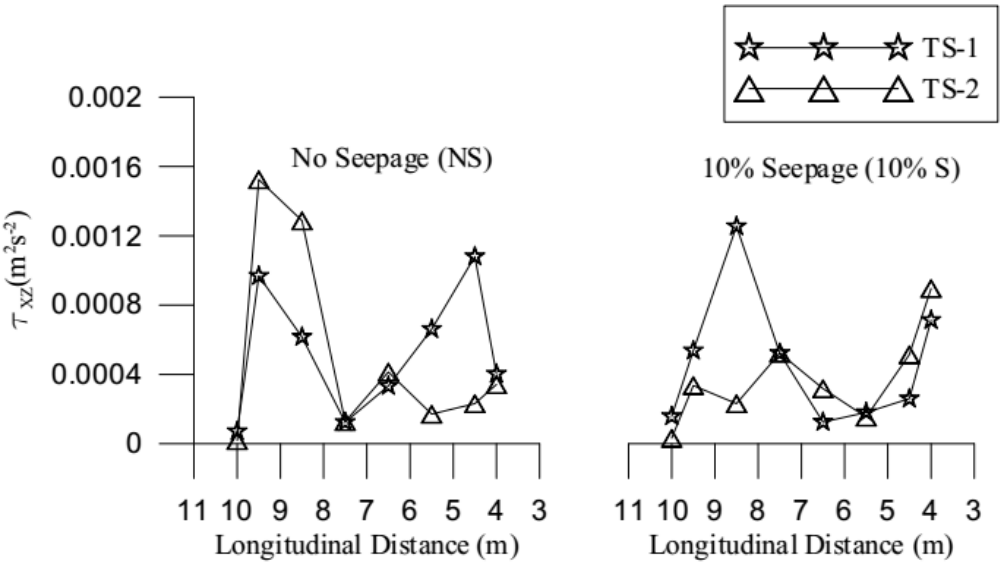

Figure 3 Reynolds stress profiles for no seepage and 10% seepage plotted along eight longitudinal sections

The Reynolds stress plotted against flow depth is smaller than the Reynolds stress plotted for longitudinal distances in vegetated cases (average longitudinal Reynolds stress ~ 4.78 X 10^{-4} m^2/s^2 (no-seepage) and 3.22 X 10^{-4} m^2/s^2 (10% seepage), average Reynolds stress along flow depth ~1.68X 10^{-4} m^2/s^2 (no-seepage) and 2.33 X 10^{-4} m^2/s^2 (10% seepage), similar to the findings of Nepf, (1999) and Shucksmith *et al* (2010). This is because the stem wakes generate non-isotropic turbulence; that is, the vertical orientation of the plant stems generates longitudinal rather than vertical stem wakes. Higher Reynolds stress is achieved at the starting of the vegetation zone where contraction in flow occurs because of the presence of vegetation elements. It was noted that higher Reynolds stress is achieved in the range of 9.5 m- 8.5 m. This is the region where maximum bed material transport occurs. The maximum Reynolds stress occurring at the starting of the vegetation zone is reduced in the range of 40-78% as the flow reaches downstream portion except for TS1 case which may be because of wall effect. It can be concluded that Reynolds stresses generated

large fluctuations at the starting of the vegetation zone and then decreases towards the downstream area which means that flow velocities induce large strong fluctuations in the flume when met the vegetation zone and then decreases towards the downstream region. Because of the effect of fluctuations in the velocity, Reynolds stress accounts for turbulent fluctuations in the flow. Reynolds stress is produced by the velocity fluctuations and can lead to considerable turbulent intensities.

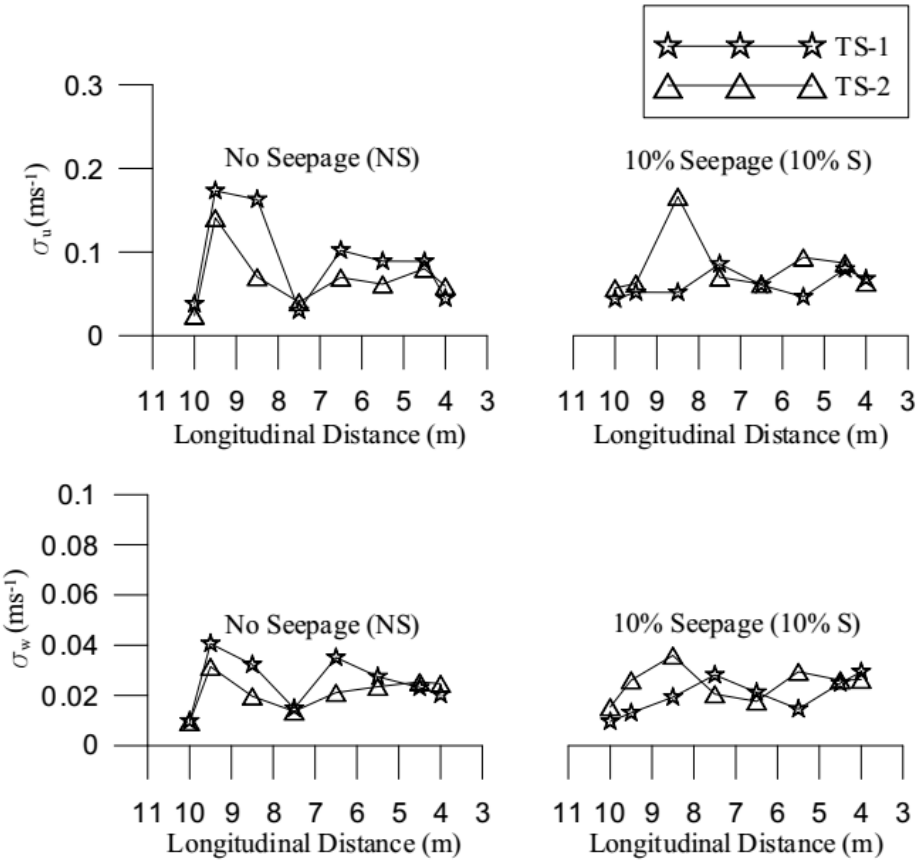

Figure 4 Turbulence Intensities (σ_u and σ_w) profiles for no seepage and 10% seepage plotted along eight longitudinal sections

Turbulence intensities also show a decreasing trend from upstream to downstream (Figure 4). σ_u of no-seepage case has a reduction of about 48% and 43% turbulence intensities for TS1 and TS2 respectively as the flow goes from starting to ending of the vegetation zone. For TS2, σ_u of 10% seepage is also reduced by about 47% when the flow goes from starting to ending of the vegetation zone. Similarly, it is observed for σ_w of no-seepage that σ_w decreases approximately by 21% and

43% from starting to ending of the vegetation zone for the measurement location TS2 and TS1 respectively. For the case of 10% seepage, σ_w at the starting of the vegetation zone decreases by a value of about 21% when the flow reaches the downstream vegetation region. The change in turbulence intensities in the vegetation zone is attributed to the local effect induced by the vegetation stems. From the results of the turbulence intensities, it can be deduced that the intensity of velocity fluctuations occur at the starting portion of the vegetation zone and then decreases at the ending of the vegetation zone implying that the turbulence production is reduced because of the presence of vegetation. It is observed that at locations 10 m and 4m, the turbulence intensities seldom change for TS-1 and TS-2 and most of the values are less than 0.1.

Conclusions

Results from longitudinal profile show that velocity for no-seepage case and 10% seepage at the upstream free zone before the vegetation zone starts is reduced by an average amount of 42% (approximately) when the flow reaches the downstream free zone, 0.5 m downstream of the vegetation zone. It is also observed that higher Reynolds stress occurs at the starting of the vegetation section thereby meaning that maximum bed material transport occurs in this region. The maximum Reynolds stress occurring at the starting of vegetation zone is reduced by an average value of 60% (approximately) as the flow reaches downstream portion except for TS1 case which may be because of wall effect. It can be concluded from the results of longitudinal profile that vegetation reduces the flow velocity, Reynolds stress, turbulence intensities which means that vegetation can be used as an effective tool for erosion control.

References

Bennett, S. J., Pirim, T., & Barkdoll, B. D. (2002). Using simulated emergent vegetation to alter stream flow direction within a straight experimental channel. *Geomorphology*, *44*(1), 115-126.

Clarke, S. J. (2002). Vegetation growth in rivers: influences upon sediment and nutrient dynamics. *Progress in Physical Geography*, *26*(2), 159-172.

Harvey, J. W., Conklin, M. H., & Koelsch, R. S. (2003). Predicting changes in hydrologic retention in an evolving semi-arid alluvial stream. *Advances in Water Resources*, *26*(9), 939-950.

Huang, I., Rominger, J., & Nepf, H. (2011). The motion of kelp blades and the surface renewal model. *Limnology and Oceanography*, *56*(4), 1453-1462.

Hui, E. Q., Hu, X. E., Jiang, C. B., & ZHU, Z. D. (2010). A study of drag coefficient related with vegetation based on the flume experiment. *Journal of Hydrodynamics, Ser. B*, *22*(3), 329-337.

Hurd, C. L. (2000). Water motion, marine macroalgal physiology, and production. *Journal of Phycology*, *36*(3), 453-472.

Koch, E. W. (2001). Beyond light: physical, geological, and geochemical parameters as possible submersed aquatic vegetation habitat requirements. *Estuaries*, *24*(1), 1-17.

Larsen, L. G., & Harvey, J. W. (2011). Modeling of hydroecological feedbacks predicts distinct classes of landscape pattern, process, and restoration potential in shallow aquatic ecosystems. *Geomorphology*, *126*(3), 279-296.

Mars, M., Kuruvilla, M., and Goen, H. (1999). The role of submergent macrophytes *triglochin huegelii* in domestic greywater treatment. *Ecol. Eng.*, 12 (1), 57-66.

O'Hare, M. T., Hutchinson, K. A., & Clarke, R. T. (2007). The drag and reconfiguration experienced by five macrophytes from a lowland river. *Aquatic Botany*, *86*(3), 253-259.

Pollen, N., & Simon, A. (2005). Estimating the mechanical effects of riparian vegetation on stream bank stability using a fiber bundle model. *Water Resources Research*, *41*(7).

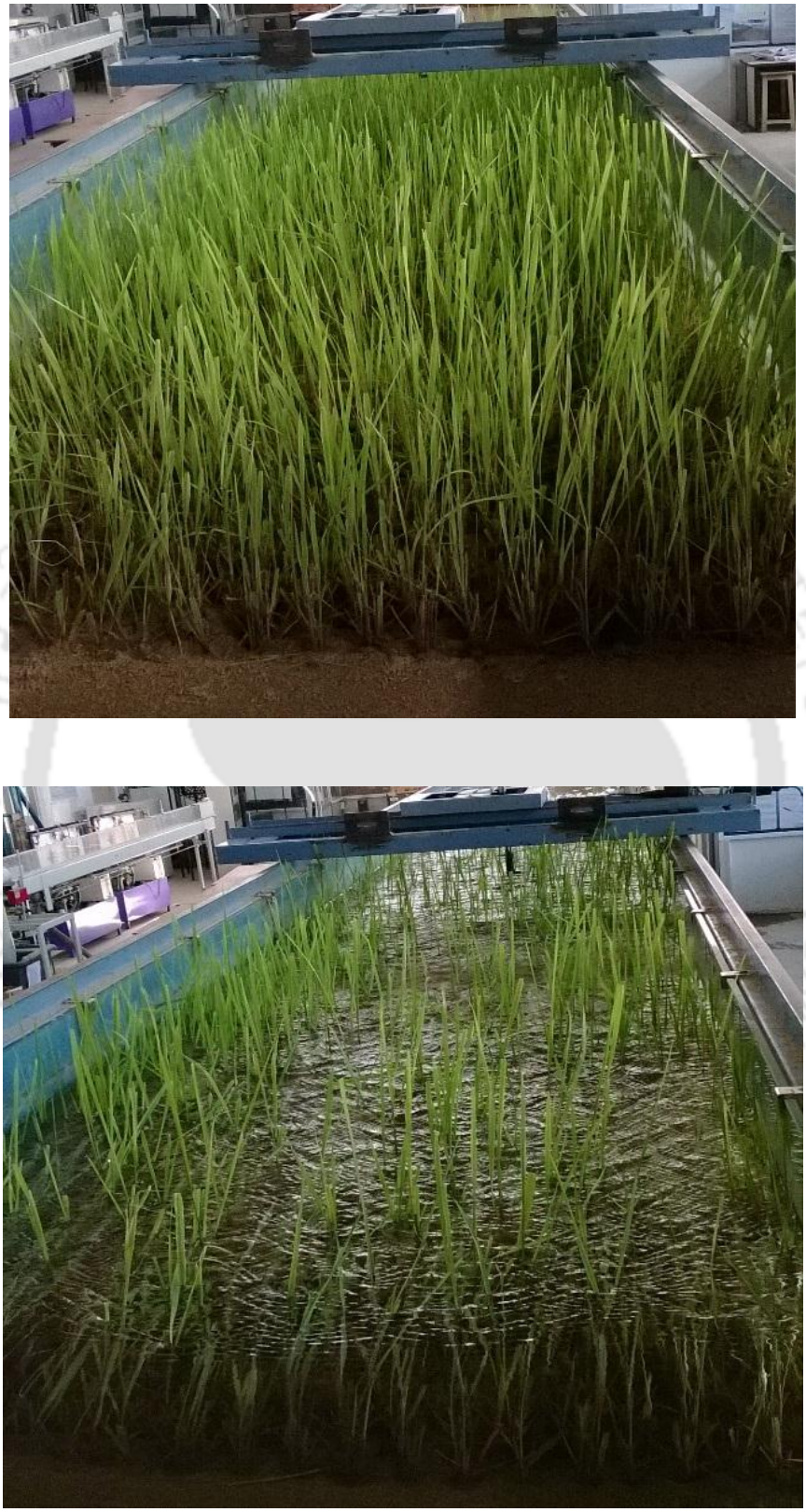

Photographs for experiments on emergent vegetation